Vol. 2: 201–205, 2008
doi: 10.3354/ab00051

AQUATIC BIOLOGY
Aquat Biol

Printed June 2008
Published online June 19, 2008

THEME SECTION

Bioturbation in aquatic environments: linking past and present

Idea and coordination: **Martin Solan, Liam G. Herringshaw**

CONTENTS

Benthic bioturbation in the past, present and future

Liam G. Herringshaw[1,*], Martin Solan[2]

[1]Geology & Petroleum Geology, School of Geosciences, Meston Building, University of Aberdeen, Aberdeen AB24 3UE, UK
[2]Oceanlab, University of Aberdeen, Main Street, Newburgh, Aberdeenshire AB41 6FL, UK

Understanding how ecosystems function at present is critical to any assessment of how they functioned in the past and of how they will function in the future. The geological record provides the dataset by which previous periods of environmental change can be examined and their consequences assessed. Ecological research, particularly predictive studies of ecosystem functioning, should therefore consider both modern and ancient case studies. Integrating research on bioturbation (the mixing of sediment by living organisms) with studies of trace fossils (ichnology) can provide a wealth of new information for aquatic biologists, ecologists, sedimentologists and palaeontologists. Bioturbation studies enable quantification of the behaviour of benthic organisms, their impact upon the environment, and their response to environmental change. In sedimentary rocks, ichnology may be the only means of assessing the organisms and ecosystems of the past. However, as noted by Meysman et al. (2006, p. 688), there is often 'a rather slow transfer of ideas' between workers in the

*Email: l.herringshaw@abdn.ac.uk

two fields. Our aim in this Theme Section is to illustrate some of the many interesting topics in current bioturbation research for both modern and ancient eras, stimulate cross-disciplinary discussion, and highlight potentially fruitful areas of collaboration.

Impacts of bioturbation on aquatic environments

Bioturbation changes preserved in the rock record enable the recognition of 3 significant events in the evolution of aquatic ecosystems: the colonization of infaunal habitats in shallow marine settings, the colonization of the deep sea, and the colonization of freshwater environments. Infaunal activity was negligible in the Precambrian, but the Cambrian radiation of marine invertebrates led to a 'substrate revolution' (Bottjer et al. 2000). Through burrowing, feeding, ventilatory and locomotory behaviour, infauna altered biochemical and diagenetic reactions profoundly, and facilitated a radical redistribution of sediment particles and pore water across the sediment–water interface. Whilst the impact of bioturbation is species-specific and context dependent (e.g. Solan & Kennedy 2002), it directly alters key ecosystem processes, including organic matter remineralisation and decomposition, nutrient cycling, pollutant release, sediment resuspension and microbial activity (see, inter alia, Rhoads 1974, Aller 1982, Krantzberg 1985). As bioturbating organisms evolved, a temporally and spatially dynamic mosaic of microenvironments was created, enabling the exploitation of new ecospace and the development of more complex and diverse benthic communities. Understanding and quantifying the mechanisms of bioturbation are therefore of primary importance for disentangling organism–sediment interactions as they relate to the provision and long-term sustainability of ecosystem function.

Restricted primarily to shallow marine environments during the Cambrian, complex, diverse bioturbation became prevalent in deep marine settings by the early Ordovician (Orr 2001). This offshore transition is attributed to an increasing competition for space and resources in shallow marine environments (Orr 2001) that led to the displacement of some groups of tracemakers (see also Crimes et al. 1992, Crimes 2001). Full details of the transition remain to be worked out, with deep marine strata of late Cambrian and early Ordovician age requiring further ichnological investigation, but the interpretation of its causes is generally accepted. The ecological and environmental effects of bioturbation in these deep marine environments have seen far less study, despite recognition that benthic biodiversity plays a key role in ecological and biogeochemical processes at a global scale (e.g. Danovaro et al. 2008).

The history of bioturbation in freshwater settings is less well understood than in marine environments, not least because trace fossils are comparatively uncommon in lacustrine and fluvial deposits (particularly the latter). The colonization of brackish water environments probably began in the Ediacaran (Buatois et al. 2005), but evidence of bioturbation in truly freshwater settings is lacking prior to the Cambro-Ordovician (see Buatois & Mángano 2007). Furthermore, these Early Palaeozoic freshwater traces are epifaunal trackways from the margins of lakes (e.g. Johnson et al. 1994) and rivers (e.g. Wright et al. 1995). Traces recording the first freshwater infauna are much rarer, and their age less well constrained. The ichnotaxa described from fluvial channels and inter-dune ponds in the Tumblagooda Sandstone of Australia are probably late Silurian in age (Trewin & McNamara 1995), but palaeomagnetic data has been used to suggest that the sediments were deposited in the Ordovician (Schmidt & Hamilton 1990). Whichever age is correct, these domichnia (dwelling burrows) are the oldest freshwater examples known, but resolution of the geochronology is critical to establishing when such substrates were first colonized by infaunal organisms. The early evolution of terrestrial ecosystems is incompletely understood, and future ichnological studies have the potential to provide many new insights.

Effects of environmental change on bioturbation

The effects of biodiversity loss on bioturbation are beginning to be recognised (Solan et al. 2008, this Theme Section), but little is known about how bioturbation processes are affected by progressive species loss under realistic extinction scenarios (Solan et al. 2004). Five major extinctions are recognized in the Phanerozoic: the late Ordovician, late Devonian, end-Permian, late Triassic, and end-Cretaceous events. The nature of these events was determined primarily using body fossils, and only recently have researchers begun examining the intervals for ichnological changes. Parameters such as burrow size and bioturbation depth can be used as proxies for ecological stress; Twitchett & Barras (2004) highlighted the value of such measurements in determining the ecological aftermath of extinction events. In stratigraphic successions of sufficiently high resolution, the same approach could be applied to the onset and duration of extinctions. There is a noticeable paucity of work on the late Ordovician and late Devonian events; most research so far has focused on the end-Permian and end-Cretaceous extinctions. Herringshaw & Davies (2008, this Theme Section) have studied ichnological changes in the late Ordovician of the Welsh Basin, but more work needs to

be conducted over a much broader geographical area, and for all extinction intervals. In terms of predicting future change, research into extinctions driven by intrinsic mechanisms such as eustatic sea level change (rather than extrinsic events such as meteorite impacts) could be especially informative.

Anthropogenic stresses, including overfishing, habitat destruction and pollution are amongst the most immediate threats to the persistence of sediment-dwelling invertebrates in present day coastal and deep-sea benthic habitats. However, knowledge of the effects of species loss on human welfare is limited by a lack of fine-scale data for these systems. Few biodiversity–ecosystem function protocols actually include the environmental context surrounding an extinction event, or the specific cause of extinction. Instead, investigators opt for a design that assumes random biodiversity loss as a consequence of an unspecified forcing, despite the wealth of information accessible from the palaeoecological community. Recent work indicates that the effect of extinction on ecosystem processes depends on the type of extinction driver (Solan et al. 2004) and whether or not species have identical extinction risks (Gross & Cardinale 2005). Thus, a disconnection exists between the representation of biodiversity loss scenarios in experimental systems and the context in which biodiversity–ecosystem process relations are moderated in the real world and under stress. A better understanding of these links is critical for underpinning marine conservation initiatives and policy decisions regarding the sustainability of natural marine resources in the face of the major challenges posed by global environmental change.

Bioturbation and behaviour

One of the intractable problems facing ichnologists is assigning trace fossils to the organisms that produced them. Studies of analogous structures produced by extant taxa, however, are useful for establishing a plausible list of candidates, and the likely behaviour of the trace-maker. Gingras et al. (2008, this Theme Section) have examined traces produced by shallow marine organisms, enabling their comparison with trace fossils from similar environments. Their results show that we can be fairly confident about the origin of some trace fossils, but also that similar structures can be produced by different taxa behaving in very different ways. Traces morphologically equivalent to the ichnogenus *Gyrolithes*, for example, are produced by worms anchoring themselves to the seabed, and by ramp-building shrimps (Gingras et al. 2008). This highlights the risk of interpreting trace fossils definitively, but further studies of this kind can provide greater clarity.

For ecologists and ichnologists interested in lacustrine bioturbation, the problems are arguably greater. Compared with marine environments, modern lakes are inhabited by significantly fewer burrowing organisms. Lakes are also subject to major seasonal and regional variations, and lacustrine facies are scarce in the rock record. White & Miller (2008, this Theme Section) note that bioturbation in lakes has seen little research, and studies comparing modern traces with the ichnological record are especially scarce. There are also terminological issues: the intrinsic variability of lakes makes the broadly constant terms of marine ecology and geology difficult to apply, and many limnological (and some oceanographic) terms are defined biologically, such as the littoral zone. In marine environments, this is described commonly as the part of the shoreline that is exposed at low tide and submerged at high tide, though it is also defined using the distribution of key plant and animal taxa (see e.g. Lewis 1961). In lakes, however, it is defined as the zone to which light penetrates sufficiently for macrophytes to photosynthesize, typically measured as 1% of the surface light intensity (see e.g. Loeb et al. 1983). This definition cannot be applied satisfactorily to lacustrine strata, as light penetration levels are almost impossible to determine in the rock record, whilst macrophytes are rarely fossilized *in situ*. Instead, the grain size and sedimentary structures are used to assess the energy regime under which sediments were deposited, with coarser material indicating a more proximal setting. Resolving this dichotomy is difficult, but comparisons of trace fossils with bioturbation in modern lakes may enable identification of assemblages diagnostic of particular lake zones. Work of this nature has begun, but only 2 trace fossil assemblages (ichnofacies) have been recognized thus far, both of which can occur in a variety of freshwater sub-environments (see Buatois & Mángano 2007).

Bioturbation depth over time and space

The mean global depth of marine bioturbation was calculated by Boudreau (1994) to be 98 ± 45 mm (mean ± SD), a value revised only very slightly (to 97 mm) by later modelling (Boudreau 1998). New work by Teal et al. (2008, this Theme Section) produces a value of 57.5 ± 56.7 mm, but illustrates how variable the available data are, regionally and bathymetrically, observing that 'we have reasonable estimates of bioturbation for only a limited set of conditions and regions of the world' (Teal et al. 2008, p. 207). This probably applies to ichnology also, with European and North American trace fossils having been studied for far longer than those of Asia, Africa and South America.

The importance of time scales should also be emphasized. Measurements of bioturbation are tracer-dependent, so different tracer longevities will give different results, particularly if areas are subject to bioturbation 'events' separated by many years. Maire et al. (2008, this Theme Section) review the different methods currently available to assess sediment reworking by benthic infauna using living organisms, and Meysman et al. (2008, this Theme Section) provide guidance on which method is most appropriate for short-term bioturbation studies. In such experiments, the integration of bioturbation events over time may influence the interpretation of natural mixing processes at short time scales, a problem that is also highly relevant to the extended time-series data on bioturbation in the rock record. Ichnofabrics preserved in sedimentary rocks, for example, are often a time-averaged record of the activity of more than one community (Ekdale et al. 1984, Pickerill 1992, McIlroy 2004), but it is possible to identify ichnofabrics formed by a single community or succession of closely similar communities (Ekdale et al. 1984, McIlroy 2004). With a suitable quantity of data, variations in mean mixed depth over geological timescales would therefore be a potential avenue of exploration. For the prediction of ecosystem responses to biodiversity loss at the present day, variations in bioturbation depth during previous extinction events could also be utilized. Boudreau (1994, 1998) argued that the mean mixed depth in modern oceans is effectively independent of variations in water depth and sedimentation rate (but see Middelburg et al. 1997). This was probably not the case in the early Palaeozoic, as deep marine environments in the Cambrian had lower ichnological diversity and more limited colonization than post-Cambrian equivalents (Orr 2001), but its applicability to later Palaeozoic, Mesozoic and Cenozoic strata has yet to be investigated.

LITERATURE CITED

Aller RC (1982) The effects of macrobenthos on chemical properties of marine sediment and overlying water. In: McCall PL, Tevesz MJS (eds) Animal–sediment relations: the biogenic alteration of sediments. Top Geobiol 2: 53–102

Bottjer DJ, Hagadorn JW, Dornbos SQ (2000) The Cambrian substrate revolution. Geol Soc Am Today 10:1–7

Boudreau BP (1994) Is burial velocity a master parameter for bioturbation? Geochim Cosmochim Acta 58: 1243–1249

Boudreau BP (1998) Mean mixed depth of sediments: the wherefore and the why. Limnol Oceanogr 43:524–526

Buatois LA, Mángano MG (2007) Invertebrate ichnology of continental freshwater environments. In: Miller W (ed) Trace fossils: concepts, problems, prospects. Elsevier, Amsterdam, p 285–323

Buatois LA, Gingras MK, MacEachern J, Mángano MG and others (2005) Colonization of brackish-water systems through time: evidence from the trace-fossil record. Palaios 20:321–347

Crimes TP (2001) Evolution of the deep-water benthic community. In: Zhuravlev AY, Riding R (eds) The ecology of the Cambrian radiation. Columbia University Press, New York, p 275–297

Crimes TP, Garcia Hidalgo JF, Poire DG (1992) Trace fossils from the Arenig flysch sediments of Eire and their bearing on the early colonisation of the deep seas. Ichnos 2:61–77

Danovaro R, Gambi C, Dell'Anno A, Corinaldes C and others (2008) Exponential decline of deep sea ecosystem functioning linked to benthic biodiversity loss. Curr Biol 18: 1–8

Ekdale AA, Bromley RG, Pemberton SG (1984) Ichnology: trace fossils in sedimentology and stratigraphy. SEPM Short Course 15, Society of Economic Palaeontologists and Mineralogists, Tulsa, OK

Gingras MK, Dashtgard SE, MacEachern JA, Pemberton SG (2008) Biology of shallow marine ichnology: a modern perspective. Aquat Biol 2:255–268

Gross K, Cardinale BJ (2005) The functional consequences of random vs. ordered species extinctions. Ecol Lett 8: 409–418

Herringshaw LG, Davies NS (2008) Bioturbation levels during the end-Ordovician extinction event: a case study of shallow marine strata from the Welsh Basin. Aquat Biol 2:279–287

Johnson EW, Briggs DEG, Suthren RJ, Wright JL, Tunnicliff SP (1994) Non-marine arthropod traces from the subaerial Ordovician Borrowdale Volcanic Group, English Lake District. Geol Mag 131:395–406

Krantzberg G (1985) The influence of bioturbation on physical, chemical, and biological parameters in aquatic environments: a review. Environ Pollut Ser A Ecol Biol 39: 99–102

Lewis JR (1961) The littoral zone on rocky shores: A biological or physical entity? Oikos 12:280–301

Loeb SL, Reuter JE, Goldman CR (1983) Littoral zone production of oligotrophic lakes: the contributions of phytoplankton and periphyton. In: Wetzel RG (ed) Periphyton of freshwater ecosystems. Dr. W. Junk Publishers, Den Haag, p 161–167

Maire O, Lecroart P, Meysman F, Rosenberg R, Duchêne JC, Grémare A (2008) Quantification of sediment reworking rates in bioturbation research: a review. Aquat Biol 2: 219–238

McIlroy D (2004) Some ichnological concepts, methodologies, applications and frontiers. In: McIlroy D (ed) The application of ichnology to palaeoenvironmental and stratigraphic analysis. Spec Pub 228, Geol Soc London Publishing House, Bath, p 3–27

Meysman FJR, Middelburg JJ, Heip CHR (2006) Bioturbation: a fresh look at Darwin's last idea. Trends Ecol Evol 21: 688–695

Meysman FJR, Malyuga VS, Boudreau BP, Middelburg JJ (2008) Quantifying particle dispersal in aquatic sediments at short time scales: model selection. Aquat Biol 2:239–254

Middelburg JJ, Soetaert K, Herman PKJ (1997) Empirical relationships for use in global diagenetic models. Deep-Sea Res I 44:327–344

Orr PJ (2001) Colonization of the deep-marine environment during the early Phanerozoic. Geol J 36:265–278

Pickerill RK (1992) Carboniferous nonmarine invertebrate ichnocoenoses from southern New Brunswick, eastern Canada. Ichnos 2:21–35

Rhoads DC (1974) Organism–sediment relations on the muddy sea floor. Oceanogr Mar Biol Annu Rev 12:263–300

Schmidt PW, Hamilton PJ (1990) Palaeomagnetism and the age of the Tumblagooda Sandstone, Western Australia. Aust J Earth Sci 37:381–385

Solan M, Kennedy R (2002) Observation and quantification of *in situ* animal–sediment relations using time-lapse sediment profile imagery (t-SPI). Mar Ecol Prog Ser 228: 179–191

Solan M, Cardinale BJ, Downing AL, Engelhardt KAM, Ruesink JL, Srivastava DS (2004) Extinction and ecosystem function in the marine benthos. Science 306: 1177–1180

Solan M, Batty P, Bulling MT, Godbold JA (2008) How biodiversity affects ecosystem processes: implications for ecological revolutions and benthic ecosystem function. Aquat Biol 2:289–301

Teal LR, Bulling MT, Parker ER, Solan M (2008) Global patterns of bioturbation intensity and the mixed depth of marine soft sediments. Aquat Biol 2:207–218

Trewin NH, McNamara KJ (1995) Arthropods invade the land: trace fossils and palaeoenvironments of the Tumblagooda Sandstone (?late Silurian) of Kalbarri, Western Australia. Trans R Soc Edinb 85:177–210

Twitchett RJ, Barras CG (2004) In: McIlroy D (ed) The application of ichnology to palaeoenvironmental and stratigraphic analysis. Spec Pub 228, Geol Soc London Publishing House, Bath, p 397–418

White DS, Miller MF (2008) Benthic invertebrate activity in lakes: linking present and historical bioturbation patterns. Aquat Biol 2:269–277

Wright JL, Quinn L, Briggs DEG, Williams SH (1995) A subaerial arthropod trackway from the upper Silurian Clam Bank Formation of Newfoundland. Can J Earth Sci 32:304–313

Vol. 2: 207–218, 2008
doi: 10.3354/ab00052

AQUATIC BIOLOGY
Aquat Biol

Printed June 2008
Published online June 19, 2008

Contribution to the Theme Section 'Bioturbation in aquatic environments: linking past and present'

OPEN ACCESS

Global patterns of bioturbation intensity and mixed depth of marine soft sediments

L. R. Teal[1,2,*], M. T. Bulling[1,3], E. R. Parker[2], M. Solan[1]

[1]Oceanlab, University of Aberdeen, Main Street, Newburgh, Aberdeenshire AB41 6AA, UK
[2]CEFAS, Pakefield Road, Lowestoft, Suffolk NR33 0HT, UK
[3]University of York, Environmental Department, Heslington, York YO10 5DD, UK

ABSTRACT: The importance of bioturbation in mediating biogeochemical processes in the upper centimetres of oceanic sediments provides a compelling reason for wanting to quantify *in situ* rates of bioturbation. Whilst several approaches can be used for estimating the rate and extent of bioturbation, most often it is characterized by calculating an intensity coefficient (D_b) and/or a mixed layer depth (L). Using measures of D_b (n = 447) and L (n = 784) collated largely from peer-reviewed literature, we have assembled a global database and examined patterns of both L and D_b. At the broadest level, this database reveals that there are considerable gaps in our knowledge of bioturbation for all major oceans other than the North Atlantic, and almost universally for the deep ocean. Similarly, there is an appreciable bias towards observations in the Northern Hemisphere, particularly along the coastal regions of North America and Europe. For the assembled dataset, we find large discrepancies in estimations of L and D_b that reflect differences in boundary conditions and reaction properties of the methods used. Tracers with longer half-lives tend to give lower D_b estimates and deeper mixing depths than tracers with shorter half-lives. Estimates of L based on sediment profile imaging are significantly lower than estimates based on tracer methods. Estimations of L, but not D_b, differ between biogeographical realms at the global level and, at least for the Temperate Northern Atlantic realm, also at the regional level. There are significant effects of season irrespective of location, with higher activities (D_b) observed during summer and deeper mixing depths (L) observed during autumn. Our evaluation demonstrates that we have reasonable estimates of bioturbation for only a limited set of conditions and regions of the world. For these data, and based on a conservative global mean (±SD) L of 5.75 ± 5.67 cm (n = 791), we calculate the global volume of bioturbated sediment to be >20 700 km^3. Whilst it is clear that the role of benthic invertebrates in mediating global ecosystem processes is substantial, the level of uncertainty at the regional level is unacceptably high for much of the globe.

KEY WORDS: Bioturbation · Sediment mixed depth · Bioturbation coefficient · Global analysis · Tracer · Sediment profile imaging

INTRODUCTION

The seabed is the most extensive habitat on the planet, occupying >75% of the Earth's surface. Most marine sediments are cohesive muds that are replete with complex biogeochemical cycles, which are critical for the marine ecosystem. Benthic macrofauna bioturbate and bioirrigate the upper centimetres of marine sediments, significantly increasing the depth of the mixed layer, the recycling of nutrients, and the flux of materials from the sediment to the water column. Accurate measurements of bioturbation rates are crucial in determining how faunal-induced fluid and particle redistribution affects the properties of the sediment profile. Given the vast area of marine sediments across the globe and the importance of bioturbators in mediating ecosystem processes, there are numerous studies measuring bioturbation values worldwide. To-

*Email: l.teal@abdn.ac.uk

gether, these form a valuable repository of information on global patterns of bioturbation intensity and the mixed depth of marine soft sediments (see e.g. Boudreau 1994, 1998, Middelburg et al. 1997).

Studies investigating the rate and extent of bioturbation have generally adopted modelling techniques that allow the distribution and exchange rates of pore water solutes, or sediment particles, across the sediment–water interface to be quantified and compared. Bioturbation is characterized numerically by determining a mixed layer depth (L), over which sediment mixing most frequently occurs, and/or a bioturbation coefficient (D_b) (for review, see Meysman et al. 2003). D_b is defined as the rate at which the variance of particle location changes over time, where the variance is a measure of the spread of particles in a tracer profile and is proportional to the velocity of the diffusing particle (Crank 1975), thus providing a convenient descriptor of the intensity of bioturbation. Both L and D_b can be determined by measuring the vertical distribution of a tracer through the sediment profile. Tracers commonly used for bioturbation experiments include naturally occurring, particle reactive radionuclides and artificial tracers such as glass beads, fluorescent sediment particles (luminophores), metal-doped sediment and isotopically labelled algae (Mahaut & Graf 1987, Wheatcroft et al. 1994, Blair et al. 1996, Gerino et al. 1998, Sandnes et al. 2000, Berg et al. 2001, Green et al. 2002, Forster et al. 2003). Incorporation of the tracer into the sediment by faunal activity results in a vertical tracer profile that is either: (1) smooth and exponential in decline, in which case faunal-mediated particle movements approximate diffusional mixing, or (2) more complex, resulting from discrete burrowing events, in which case particles are displaced by the fauna in a series of 'non-local' movements. Mathematical models appropriate to the form of the tracer profile are applied, and a D_b coefficient can be estimated (for an overview, see Meysman et al. 2003, 2008, this Theme Section). L can also be determined from tracer profiles, or, when using alternative methods such as sediment profile imaging (SPI; Rhoads & Cande 1971), can be measured directly from the sediment profile.

Despite methodological differences (Gerino et al. 1998), some analyses of published D_b and L values have been used to determine empirical relationships between parameters used in diagenetic models and water depth (Boudreau 1994, 1998, Middelburg et al. 1997). Such empirical relationships can enable predictions to be made about biogeochemical rates and processes in oceanic sediments where data are still limited or absent. In a rudimentary analysis of >200 datapoints, for example, Boudreau (1994) found a significant correlation between D_b and sedimentation rate (ω), both of which decrease with increasing water depth (Middelburg et al. 1997). Conversely, no apparent relationships between L and ω or L and water depth were found. In fact, L exhibited a well-defined world-wide mean (±SD) of 9.8 ± 4.5 cm (Boudreau 1994), which was later shown to result from the feedback between the food dependence of bioturbation and the decay of that resource (Trauth et al. 1997, Boudreau 1998, Smith & Rabouille 2002). In this case, the independence of L would indicate that considerable confidence can be placed in using an average L in sediment modelling (Boudreau 1994), although we recognize that the factors influencing L are likely to be numerous and interact with one another.

This contribution builds on that of Boudreau (1994, 1998) by extending the database of L and D_b. Our objectives were to: (1) examine the relationship between measured estimates of bioturbation and the method of determination, (2) determine the influence of season, water depth and location on D_b and L, (3) identify areas of high and low D_b and L, (4) highlight regions or benthic habitats that have been poorly researched, and (5) refine the global estimate of bioturbated sediment. In so doing, we wish to summarise the present knowledge of bioturbation at the global level and, after taking into account biases in the data, recommend areas of future research.

METHODS

Global database. Global data on L and D_b were collated from peer-reviewed literature. Data were retrieved from the 'ISI Web of Knowledge' using the 'Science Citation Index Expanded' and 'Social Sciences Citation Index' databases. A 'general search' using the search term *bioturbation* in the titles and key words of all document types, in all languages, was performed for the publication years 1970 to 2006. All published sources were manually searched for values of L and/or D_b, and, where available, additional information was gathered on the geographical position of the study (latitude, longitude), water depth, sedimentation rates (ω), type of tracer used (hereafter method) and month of year the measurement was taken. Additional D_b and L values were added from the publications cited in Boudreau (1994), and further estimates of L were obtained from the sediment profile imaging literature. Much of the latter includes monitoring studies that document localized benthic impacts. As our focus was to determine representative estimates of bioturbation, only reference sites furthest away from any anthropogenic impact (as defined by the study authors), or sites acknowledged as having no discernable anthropogenic impact, were used. In addition, we determined additional values for L from previously unpublished SPI surveys (n = 31; for sources, see

'Acknowledgements'). In SPI images, the depth of L is delineated using the vertical colour transition (from brown to olive green/black) that occurs within the sediment profile (Fenchel 1969, Lyle 1983). This coloration is dictated by the redox state (ferrous or ferric) of the dominant electron acceptor iron (Lovley & Phillips 1986), such that regions of high reflectance (brown) in an image represent the oxidised bioturbated sediment and can be delineated using standard threshold analysis. For all unpublished SPI surveys, L was determined using a custom-made, semi-automated macro that runs within ImageJ (Version 1.38), a Java-based public domain program developed at the USA National Institutes of Health (available at http://rsb.info.nih.gov/ij/index.html). Including all sources of information, the total database included >2000 studies. After eliminating publications that lacked the data required and including data from studies that investigated multiple locations, the refined database included 791 individual values of L and 454 individual values of D_b from 130 publications and the additional SPI analyses.

Generation of a global map. All points (latitude and longitude) were plotted on a global map (Fig. 1) using ArcView GIS (v3.3). When the precise location of a study was not provided, latitude and longitude coordinates were estimated from the available information reported in each study using Google Earth (http://earth.google.com/). To account for regional differences in environmental conditions, Bailey's oceanic regions (Bailey 1998) and Spalding's coastal regions (Spalding et al. 2007) were combined to ensure complete global coverage. Within these regions, there are 2 oceanic levels (domains and ecoregions) and 3 coastal levels (realms, provinces and ecoregions). Using GIS, each datapoint was linked to its corresponding domain and ocean ecoregion or, in coastal areas, the corresponding realm, province and coastal ecoregion.

An estimate of the area of the global ocean floor was generated using ETOPO2v2 (2006; available from the US National Geophysical Data Center www.ngdc.noaa.gov/). Several digital databases of seafloor elevations contribute to this database on a 2′ latitude–longitude grid (1′ of latitude = 1 n mile = 1852 m). The resolution of the gridded data varies from true 2′ intervals for the Atlantic, Pacific and Indian Ocean floors and all land masses to 5′ for the Arctic Ocean floor.

Statistical analysis. The inherent biases in the data (Table 1) made the statistical analyses potentially imbalanced, with some independent variables poorly represented. We therefore removed from each analysis all independent variables with <5 datapoints. Sedimentation rate was excluded from the analysis, as few studies included estimates. As a significant portion of

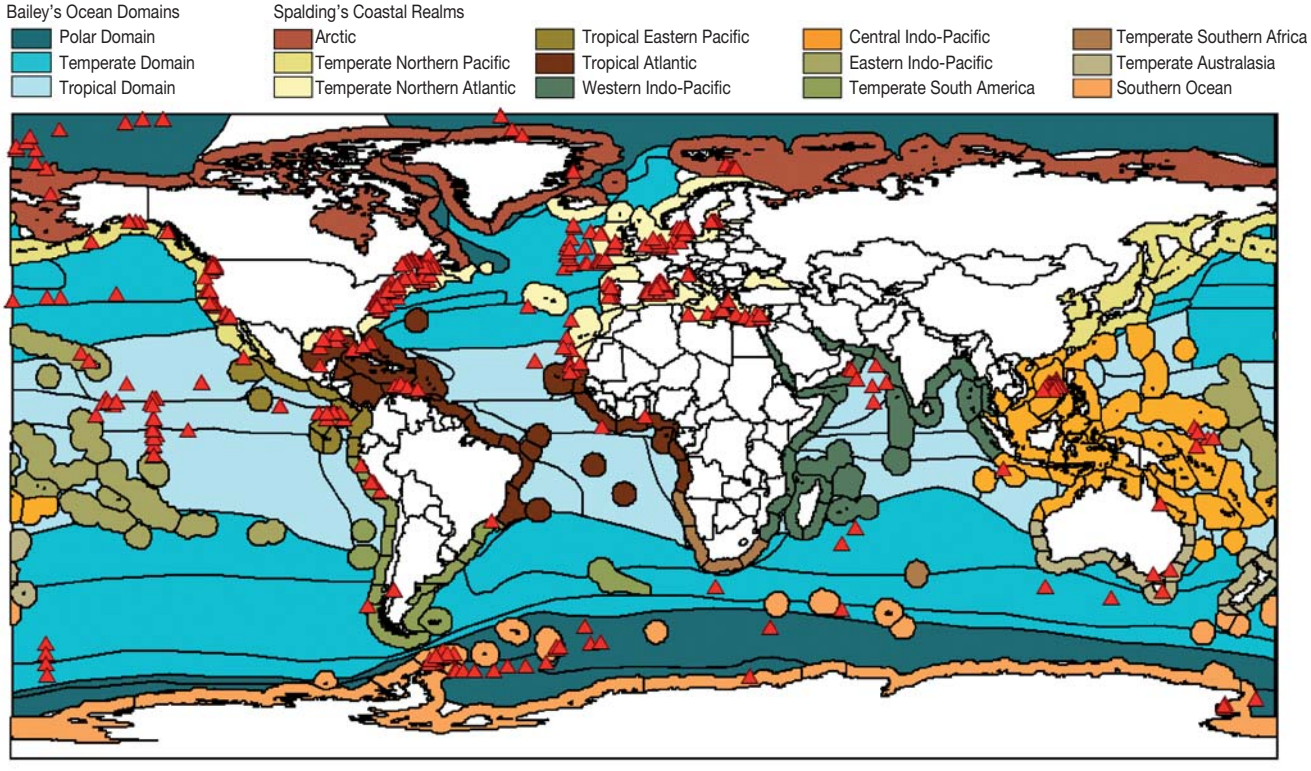

Fig. 1. World map showing ocean domains and coastal realms (coloured areas), ocean and coastal ecoregions (black borders), and locations where D_b and/or L values have been measured (red triangles)

Table 1. Summary of the bioturbation database. Number of observations for mixing depth (L) and mixing intensity (D_b), by Bailey's ocean domains and Spalding's coastal realms (see Fig. 1), as well as by method. Methods with <10 datapoints (^{134}Cs, ^{137}Cs, ^{18}O, ^{32}Si, ^{7}Be, ^{226,228}Ra, tektites, organic C, glass beads, X-ray) are included in 'Other'. SPI: sediment profile imaging

	L	D_b
Region		
Polar Domain	26	16
Temperate Domain	31	32
Tropical Domain	33	63
Arctic	3	2
Temp. N. Pacific	87	97
Temp. N. Atlantic	497	170
Trop. E. Pacific	–	8
Trop. Atlantic	33	29
W. Indo-Pacific	15	12
Central Indo-Pacific	24	1
E. Indo-Pacific	3	2
Temp. S. America	14	10
Temp. S. Africa	–	–
Temp. Australasia	3	1
Southern Ocean	16	8
Method		
^{14}C	15	2
^{210}Pb	307	275
^{234}Th	36	102
Chl *a*	1	18
^{239,240}Pu	12	16
Luminophores	13	13
SPI	358	1
Colour	19	–
Other	27	24

datapoints (32% in the case of D_b, 59% in the case of L; Table 1) represented the Temperate Northern Atlantic realm, we performed a global analysis on all data followed by an analysis using only data from the Temperate Northern Atlantic realm. At the global level, the largest divisions (Spalding's realms + Bailey's domains, hereafter referred to collectively as 'regions') were used to ensure sufficient data were present to enable comparisons. For analyses within the regional level, we adopted Spalding's ecoregions (hereafter referred to as 'subregions'). Latitude and longitude were potential independent variables, but were excluded from the analyses because: (1) there was distinct clustering in the distribution of the data; (2) they do not necessarily describe a set gradient of environmental conditions; and (3) such clines are not continuous, as they are disrupted by landmasses and oceanographic features, such as large-scale current flows. Water depth was treated as a continuous independent variable. Method included 18 levels (^{210}Pb, ^{14}C, ^{234}Th, ^{239,240}Pu, ^{134}Cs, ^{137}Cs, ^{18}O, ^{32}Si, ^{7}Be, ^{226,228}Ra, Tektites, organic C, chl *a*, glass beads, luminophores, colour, X-ray, SPI) and was treated as a nominal independent variable. As the distribution of data between methods was uneven (Table 1), methods with <10 observations were grouped together into a separate category (Other) in order to maximize the number of data available for the model, but this grouping was not compared directly to specific methods.

As our analyses include data from both the Northern and Southern Hemispheres, where calendar months do not correspond to the same season, the seasonal offset was corrected by classifying each study into 1 of 4 seasons (spring, summer, autumn and winter). Spring included studies that took place between April and June in the Northern Hemisphere (NH) or October and December in the Southern Hemisphere (SH). Summer included studies that took place during July to September (NH) or January to March (SH); autumn, during October to December (NH) or April to June (SH); and winter, during January to March (NH) or July to September (SH). Due to latitudinal variations in seasonal timing, the scheme is not representative of any specific location.

In the global and Temperate Northern Atlantic realms, both dependent variables (L and D_b) followed a highly skewed distribution with many small values. We assessed the use of generalized linear modelling using a Poisson or quasi-Poisson link, but highly skewed distributions remained in the residuals due to strong over-dispersion. We therefore cube root-transformed L and D_b (less severe transformations were insufficient). For both the global and the Temperate Northern Atlantic realm analysis, the first step was a linear regression model for both L and D_b, with season and method as nominal independent variables, and water depth as a continuous independent variable. We tested for potential regional (or, within the Temperate Northern Atlantic realm models, subregional) effects by producing a linear mixed model with random regional effects. Comparison with the original linear model was carried out using the likelihood ratio test. If the random effect was found to be significant at the 0.05 level, the random structure in the model was retained. At this stage, for some of the models, the diagnostic residual plots indicated heteroscedasticity due to the inherent heterogeneity of variance within independent variables. If this was the case, we produced models using the generalized least squares (GLS) extension. GLS allows the introduction of a range of variance–covariate structures (see Table 5.1 in Pinheiro & Bates 2000) that model the variance structure. These models were compared with the equivalent model without the GLS extension using Akaike's information criterion (AIC) and examination of plots of residuals versus fitted values. The model with the most-appropriate random structure was then

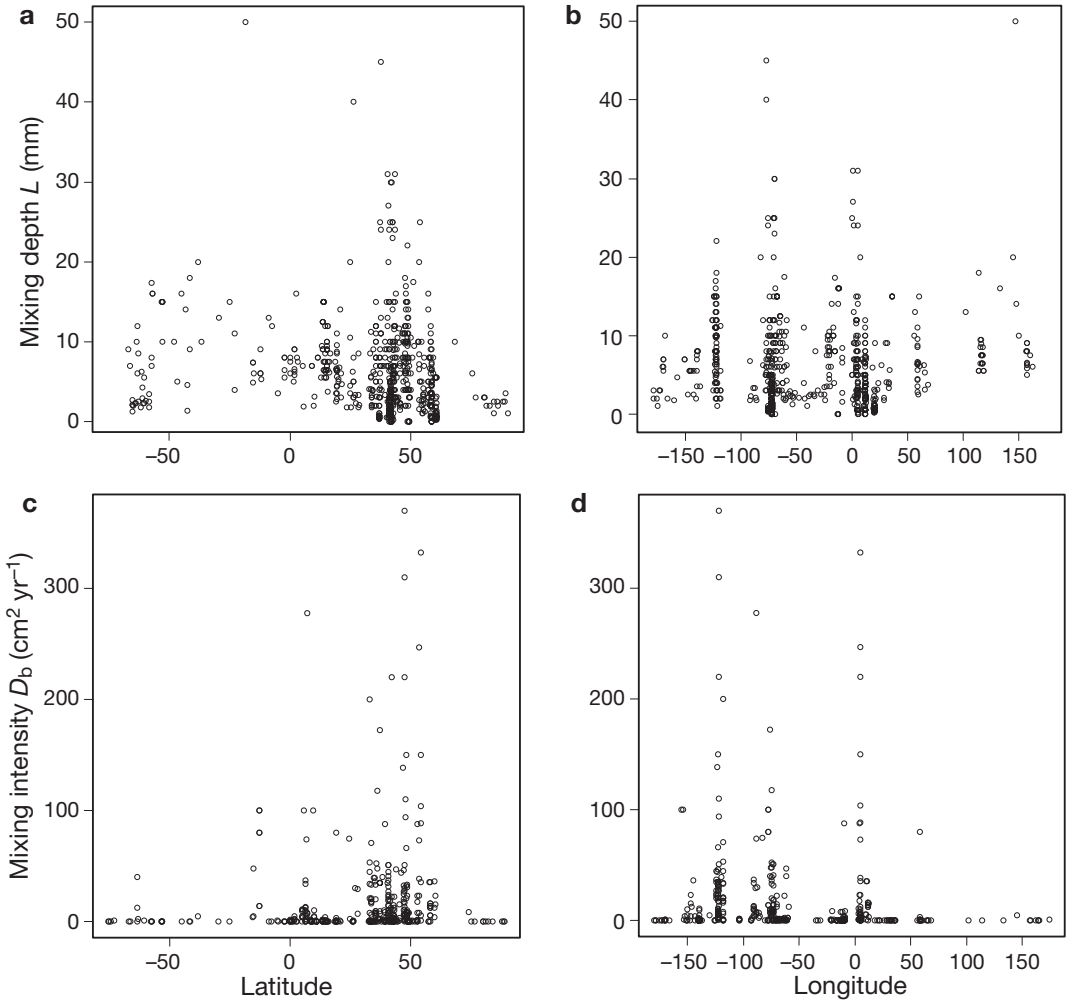

Fig. 2. Global patterns of bioturbation expressed as (a,b) mixing depth (L) and (c,d) mixing intensity (D_b) for (a,c) latitude and (b,d) longitude

used as a starting point for determining the most-appropriate fixed structure. This was done by applying a backward selection process using the likelihood ratio test obtained by maximum likelihood estimation. The numerical output of the minimal adequate model was obtained using restricted maximum likelihood (REML) (Faraway 2006, West et al. 2007). All analyses were performed using the 'nlme' package (v3.1; Pinheiro et al. 2006) in the 'R' statistical and programming environment (R Development Core Team 2005).

RESULTS

The database included 791 measurements of L and 454 measurements of D_b. The greater numbers of mixing depth data were largely attributable to the inclusion of SPI, which generally does not provide an estimate of D_b (but see Solan et al. 2004). At the broadest level, the global coverage of bioturbation estimates was reasonable, but highly clustered (Fig. 1). The data revealed a strong bias towards the Northern Hemisphere and, in particular, coastal regions thereof. Remote locations such as the Central Pacific and Antarctic were represented by a limited number of studies often based on a single cruise or research campaign (e.g. ANDEEP; Diaz 2004, Howe et al. 2004, 2007). In terms of latitude and longitude, data were available from 89.98° N to 75.20° S and from 174.00° E to 179.76° W. Over 88% of the data, however, emanated from studies in the Northern Hemisphere, particularly along the coasts of North America and Europe (Figs. 1 & 2). No obvious patterns or trends were observed in either L or D_b from north to south (Fig. 2a,c) or from east to west (Fig. 2b,d).

For water depth, estimates of bioturbation (L and D_b) ranged from the intertidal zone (0 m, n = 8) down to 5654 m (Yang et al. 1986), although the data were highly skewed towards shallower waters (mean ± SD = 1133 ± 1630 m, median = 100 m, n = 917). Most esti-

mates of bioturbation (L and D_b) were from the shelf (<200 m) or coastal regions (n = 510), with fewer from bathyal (n = 174) or abyssal (n = 223) depths. No estimates of hadal bioturbation were available. Seasonal information was difficult to collate as observation dates were missing in 47% of the studies. Of those studies that did include dates, 79% took place in spring or summer.

Regional and methodological biases within the data are shown in Table 1. For L, regions that were not well represented (n < 5) include the Arctic, Eastern Indo-Pacific and Temperate Australasia. Measurements were missing for the Tropical Eastern Pacific. The vast majority of L data was from the Temperate Northern Atlantic realm, which includes the North American east coast and European coastal waters. This was reflected in the large range of L values at approximately 50° N, 0° W and 75° W (Fig. 2a,b).

Although slightly less pronounced, a similar pattern in the distribution of data existed for D_b. As with L, there were no obvious patterns or trends with latitude or longitude, and the large range of D_b values around 50° N, and in the Western Hemisphere, corresponded to where most data have been collected. Although D_b values were present for all regions, data were sparse (n < 5) in the Arctic, Central Indo-Pacific, Eastern Indo-Pacific and Temperate Australasia. Whereas SPI and ^{210}Pb were by far the most common methods used to measure L (Table 1), comprising 45 and 39% of the mixing depth data, respectively, most D_b values were calculated from models on ^{210}Pb (61%) and ^{234}Th (22%) tracer profiles.

Global analysis

Mixing depth (L)

The simplest model adequate for the analysis of mixing depth (n = 300) was a linear mixed effects model incorporating 3 single terms (method, season and water depth). The maximal subset of data included 4 levels of method (^{210}Pb, ^{234}Th, luminophores, SPI) and all 4 seasons. Region was included as a random factor as it contributed significantly to the model (L-ratio = 82.06, df = 1, p < 0.0001). The variance–covariate terms were season and water depth. Method had the greatest influence on L (L-ratio = 94.69, df = 4, p < 0.0001), followed by season (L-ratio = 31.10, df = 3, p < 0.0001) and water depth (L-ratio = 3.94, df = 1, p = 0.047), which was only marginally significant. The data were not strong enough to investigate interactions between the single terms.

The depth of L was dependent on the type of tracer used, a finding consistent with that of others (e.g. Gerino et al. 1998). The 2 most-common methods used to calculate L were ^{210}Pb tracers and SPI, although values of L were significantly lower when estimated with SPI (coefficient = –0.757, df = 286, p < 0.0001; Fig. 3a). Estimates of L based on ^{234}Th were also significantly lower than those based on ^{210}Pb (coefficient = –0.528, df = 286, p = 0.0001). Luminophore tracers provided estimates of L that were marginally lower than those based on ^{210}Pb (coefficient = –0.389, df = 286, p = 0.047) and marginally higher than those based on ^{234}Th (coefficient = 0.139, df = 286, p = 0.534) and SPI (coefficient = 0.368, df = 286, p = 0.050).

The timing of each bioturbation study with respect to season was also influential in determining the depth of L. Mixing depths were greatest in the autumn relative to all other seasons (Fig. 3b, p < 0.001 in all cases). Summer values of L were shallower than those determined in the spring (coefficient = –0.133, df = 286, p = 0.001). We found no evidence that mixing depths determined in winter were different to any other season; however, the low numbers of data (n = 15) for winter made this conclusion tentative.

In contrast to the findings of Boudreau (1994), we found that water depth had a significant and positive effect on mixing depth (coefficient = 9.25×10^{-5}, df = 286, p = 0.0498). However, the coefficient is so small that it is unlikely to be ecologically relevant.

Bioturbation intensity (D_b)

The minimum adequate model for the analysis of D_b (n = 140) was a linear regression with a GLS extension incorporating 3 single terms (method, season and water depth). The maximal subset of data included 4 levels of method (^{210}Pb, ^{234}Th, chl *a*, luminophores) and all 4 seasons. There was no significant effect of region

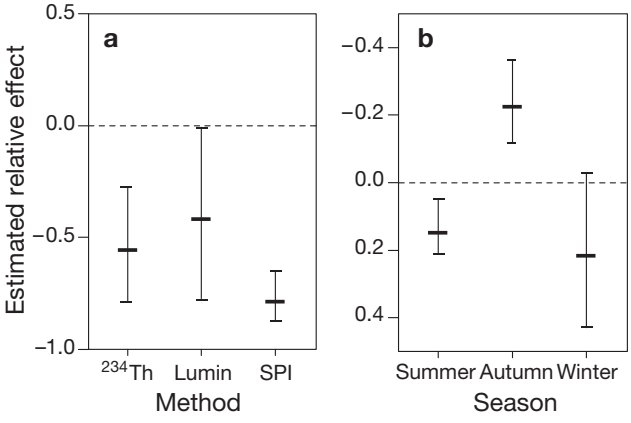

Fig. 3. Estimated relative effect of (a) method and (b) season for the global analysis of mixing depth (L); (a) relative to ^{210}Pb (dashed line); (b) relative to spring (dashed line). Error bars show 95% CI. Lumin: luminophores

as a random factor (L-ratio = 0.53, df = 1, p = 0.466), so it was removed from the model. Season was the only necessary variance–covariate term. Method had the greatest influence on D_b (L-ratio = 64.747, df = 3, p < 0.0001), followed by season (L-ratio = 18.12, df = 3, p < 0.001) and water depth (L-ratio = 15.50, df = 1, p < 0.0001). As for *L*, the data for D_b was not strong enough to investigate interactions between the single terms.

Estimates of D_b determined using ^{210}Pb were lower than those based on ^{234}Th (coefficient = –0.735, df = 139, p < 0.0001), chl *a* (coefficient = –1.391, df = 139, p < 0.0001), or luminophores (coefficient = –1.277, df = 139, p = 0.0001) (Fig. 4a). Of the latter 3 methods, ^{234}Th-based D_b values were significantly lower than those based on chl *a* (coefficient = –0.656, df = 139, p < 0.001), whilst luminophore-based D_b values were equivalent to those estimated using ^{234}Th (coefficient = –0.542, df = 139, p = 0.095) and chlorophyll *a* (coefficient = 0.1134, df = 139, p = 0.735).

Whereas the greatest depth of *L* occurred in the autumn, the highest D_b value was recorded in summer, declining through autumn, winter and spring (Fig. 4b). Both summer and autumn D_b values were significantly higher than values obtained in the spring (coefficient = 0.664, df = 139, p < 0.0001 and coefficient = 0.412, df = 139, p = 0.005, respectively). As with *L*, we found no evidence that D_b values were higher in the winter; this was also most likely due to the low quantity of data (n = 17) available.

The values for D_b were significantly and negatively affected by water depth (coefficient = -1.61×10^{-4}, df = 139, p < 0.0001). However, as with *L*, the coefficient was so small that it was likely to be ecologically irrelevant; the effect of water depth over the maximum depth range in the ocean (~11 000 m) would amount to <1.8 cm^2 yr^{-1}.

Temperate Northern Atlantic realm analysis

Mixing depth (*L*)

The minimum adequate model for the analysis of mixing depth within the Temperate Northern Atlantic realm (n = 237) was a linear mixed effects model incorporating 3 single terms (method, season and water depth) and subregion as a random factor (L-ratio = 4.461, df = 1, p = 0.035). The maximal subset of data included 3 levels of method (^{210}Pb, luminophores, SPI) and all seasons. Only season was required as a variance–covariate term. Method had the greatest influence on *L* (L-ratio = 55.76, df = 2, p < 0.0001), followed by season (L-ratio = 16.79, df = 3, p < 0.0001) and water depth (L-ratio = 6.91, df = 1, p = 0.009). The data was not strong enough to investigate interactions between the single terms.

As with the global model, the depth of *L* was dependent on the type of tracer used and the season in which the study was taken (Fig. 5). Closer examination of the model coefficients revealed that the inter-level differences in the values of *L* for method and season were broadly consistent with the findings of the global model. Values of *L* based on ^{210}Pb were significantly higher than those estimated with SPI (coefficient = 0.678, df = 225, p < 0.0001) and were marginally higher than those estimated with luminophores (coefficient = 0.389, df = 225, p = 0.055; Fig. 5a). Estimates of *L* based on luminophores are marginally higher than those based on SPI (coefficient = 0.368, df = 225, p = 0.044).

In terms of season, a pattern of estimated effect similar to the global model was predicted from the Temperate Northern Atlantic model (compare Figs. 3b & 5b). The lowest values of *L* occurred in the winter

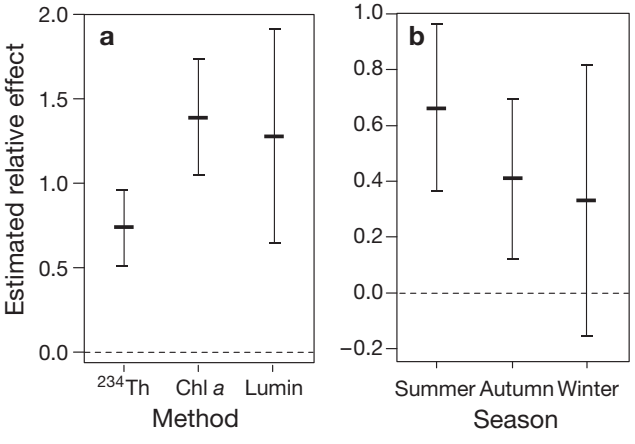

Fig. 4. Estimated relative effect of (a) method and (b) season for the global analysis of mixing intensity (D_b); (a) relative to ^{210}Pb (dashed line); (b) relative to spring (dashed line). Error bars show 95% CI. Lumin: luminophores

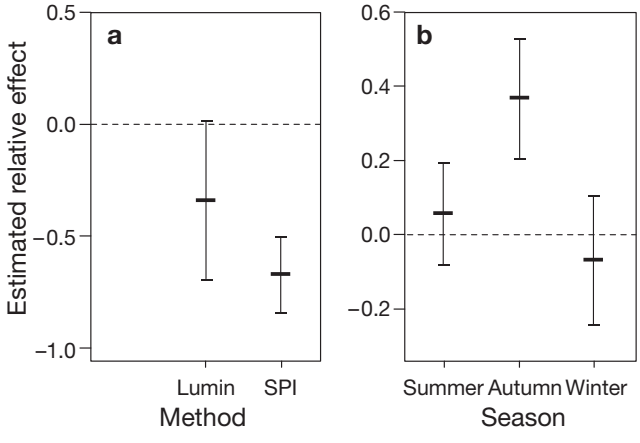

Fig. 5. Estimated relative effect of (a) method and (b) season on analysis of mixing depth (*L*) in the Temperate Northern Atlantic realm; (a) relative to ^{210}Pb (dashed line); (b) relative to spring (dashed line). Error bars show 95% CI. Lumin: luminophores

and increased through the spring and summer before reaching a maximum in the autumn (Fig. 5b). Examination of the model coefficients revealed that values of L measured in the autumn were significantly greater than those obtained in the spring (coefficient = 0.354, df = 225, p = 0.0001), summer (coefficient = 0.292, df = 225, p < 0.001) and winter (coefficient = 0.418, df = 225, p = 0.0001).

In contrast to the global analysis of L, water depth showed a positive effect on mixing depth (coefficient = 1.65×10^{-4}, df = 225, p = 0.008), but as highlighted earlier, the ecological relevance of such a small effect is highly debatable and should be discounted.

Bioturbation intensity (D_b)

The minimum adequate model for bioturbation intensity (D_b) within the Temperate Northern Atlantic realm (n = 78) was a linear regression with a GLS extension incorporating 2 single terms (method and season). The maximal subset of data included 4 levels of method (^{210}Pb, ^{234}Th, chl *a*, luminophores) and all seasons. There was no significant effect of region as a random factor (L-ratio < 0.0001, df = 1, p = 0.9999), and the variance–covariate term was depth. Method had a greater influence on D_b (L-ratio = 31.93, df = 3, p < 0.0001) than season (L-ratio = 18.47, df = 3, p = 0.0004). As with the previous analyses, the data were not strong enough to investigate interactions between the single terms.

Overall, the patterns of D_b observed in the Temperate Northern Atlantic corresponded closely to those observed for the global analysis (Fig. 6), although there was less certainty in the results due to the reduction in data. Nevertheless, estimates of D_b determined using ^{210}Pb were significantly lower than those based on chl *a* (coefficient = –1.375, df = 78, p < 0.0001) and luminophores (coefficient = –1.275, df = 78, p = 0.001), but not those based on ^{234}Th (coefficient = –0.331, df = 78, p = 0.08) (Fig. 6a). Of the latter 3 methods, ^{234}Th-based D_b values were significantly lower than those based on chl *a* (coefficient = –1.044, df = 78, p < 0.0001) or luminophores (coefficient = –0.944, df = 78, p = 0.010). Chl *a* and luminophore-based D_b values were equivalent to one another (coefficient = 0.099, df = 78, p = 0.805).

The highest D_b was recorded in summer, declining through autumn, winter and spring (Fig. 6b). However, the summer D_b values were only significantly higher than values obtained in the spring (coefficient = 0.838, df = 78, p < 0.0001), a finding most likely due to the expanded confidence limits caused by the reduced dataset.

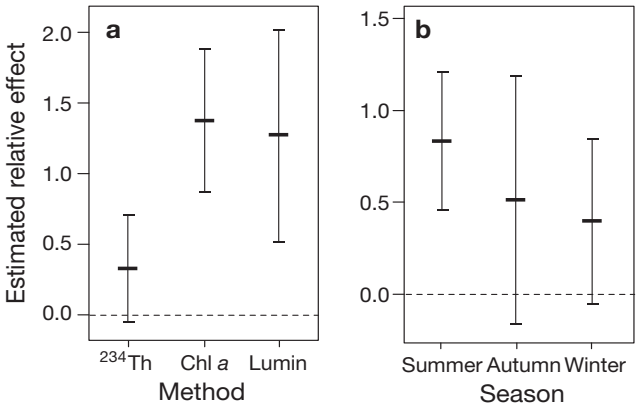

Fig. 6. Estimated relative effect of (a) method and (b) season on analysis of mixing intensity (D_b) in the Temperate Northern Atlantic realm; (a) relative to ^{210}Pb (dashed line); (b) relative to spring (dashed line). Error bars show 95% CI. Lumin: luminophores

Regional patterns

When comparing the global and Temperate Northern Atlantic realm analyses, broadly similar outcomes were determined for both L and D_b. We interpret this to indicate that the North Atlantic bias in the data governs the outcome of the global model, rather than suggesting that the same effects are dominant over different scales. The complex nature of the global and regional models for L and D_b, however, made it difficult to estimate patterns at a global level, although it was possible to determine relative differences using the raw data used within the models. In doing so, we found that the deepest values for L were recorded in Temperate South America ($\bar{x}$ = 6.4 ± 2.7 cm, n = 10), whilst the shallowest values of L were located in the Temperate ($\bar{x}$ = 0.8 ± 1.8 cm, n = 5) and Polar ($\bar{x}$ = 2.3 ± 0.3 cm, n = 6) domains and in the Southern Ocean ($\bar{x}$ = 2.8 ± 1.3 cm, n = 12). Bioturbation intensities follow the same pattern, with the highest mean (±SD) D_b recorded in Temperate South America ($\bar{x}$ = 35.90 ± 40.78 cm^2 yr^{-1}, n = 7) and the lowest in the Temperate domain ($\bar{x}$ = 0.8 ± 2.3 cm^2 yr^{-1}, n = 12). It should be noted, however, that our formal analyses only identified significant effects of Region for L and not for D_b. Of the data used in the models, the Temperate Northern Atlantic realm had the highest number of datapoints for both L (n = 256) and D_b (n = 87) and had a mean (±SD) L of 3.9 ± 5.0 cm and D_b of 23.00 ± 50.17 cm^2 yr^{-1}.

Within the Temperate Northern Atlantic realm, the highest mean (±SD) L ($\bar{x}$ = 24.00 ± 8.22 cm, n = 5) was observed in the Gulf of Maine, whilst the lowest was recorded in the Baltic Sea ($\bar{x}$ = 0.9 ± 0.7 cm, n = 40). The North Sea had the highest number of datapoints (n=135) and a mean (±SD) L of 2.7 ± 2.3 cm. The highest D_b ($\bar{x}$ = 59.01 ± 86.85 cm^2 yr^{-1}, n = 21) was observed in the North Sea, whilst the lowest D_b ($\bar{x}$ = 1.7 ± 3.4 cm^2 yr^{-1}, n = 5) occurred in the Celtic Sea.

DISCUSSION

A global database of bioturbation intensity and sediment mixing depths has been collated and analysed despite an inherent bias in the data and the inconsistencies between studies in recording information necessary for an integrative analysis. An important component missing from the dataset is information on the faunal assemblages dominant at the study sites, which is often poorly documented, absent, or focused on a particular species. The lack of information on faunal characteristics is not overly surprising as a large proportion of the studies in our database have a geological focus. Whilst data are numerous in areas that are either more accessible or near regions of high research density (e.g. Temperate Northern Atlantic realm), the Arctic, Central Pacific and most tropical regions lack sufficient data to make a credible position statement. Nevertheless, our results demonstrate broadly that methodology and season have clear effects on both D_b and L and that water depth, although significant in our models, is unlikely to be of ecological importance over the range of depths so far studied (<6000 m).

Whilst our findings are consistent with previous, less statistically sophisticated analyses that used much smaller datasets (e.g. Boudreau 1994, 1998, Middelburg et al. 1997, Gerino et al. 1998), our analyses differ in that they fully incorporate the heteroscedasticity inherent in the data—caused by biogeographic regions—using a mixed modelling framework. The inclusion of biogeographic regions in this way has revealed spatial differences in bioturbation at subregional and regional scales that have not been detected previously. Such regional differences contradict the view that a global average of L is sufficient for sediment modelling purposes (Boudreau 1994), whilst reinforcing the argument that mixing depth reflects the supply and availability of food, rather than the activity of benthos per se (Trauth et al. 1997, Boudreau 1998, Smith & Rabouille 2002, Niggerman et al. 2007; but see Johnson et al. 2007). The Temperate South American realm, for example, includes extremely productive areas of coastal upwelling and has both the deepest mixing depth and highest intensity of bioturbation (Gutierrez et al. 2000). In contrast, the Temperate domain includes a greater proportion of less productive waters and supports a low level of mixing intensity, with correspondingly shallow mixing depths.

Despite strong evidence for regional effects, there is little evidence for latitudinal or longitudinal effects on bioturbation. Intuitively, such trends are to be expected for both L and D_b, as both of these are linked to attributes of the fauna (species richness, biomass, abundance, functional groups) that vary along geographical clines (e.g. Rex et al. 2000, Roy et al. 2000, Attrill et al. 2001, Cusson & Bourget 2005, Ormond et al. 2005). Similar trends have also been documented with depth (e.g. Rex et al. 2006), but our data showed only weak evidence that D_b or L follow suit. The lack of evidence for such trends is not, however, surprising given the limited quantity and sparse geographical spread of the available data.

Perhaps the most important findings of the present study are the large discrepancies in estimates of both D_b and L between methods, raising critical questions over the validity and comparability of alternative techniques. Earlier studies (e.g. Smith et al. 1993, Pope et al. 1996, Gerino et al. 1998, Hughes et al. 2005) compared D_b coefficients obtained from different naturally occurring tracers within a specific region and, consistent with the findings presented here, concluded that the rates of bioturbation measured are commonly tracer dependent. For radionuclide tracers, for example, Smith et al. (1993) demonstrated that there is an inverse relationship between the half-life of the tracer used (^{210}Pb, ^{234}Th, ^{228}Th and ^{32}Si) and the observed mixing coefficient, indicating that the longer the period over which mixing effects are accumulated, the smaller the measured bioturbation intensity. Based on these findings, Smith et al. (1993) proposed that the characteristic time scale of a continuous-supply tracer (the time frame within which 95% of the tracer activity is likely to have entered deep-sea sediments) is approximately equal to 5 times its half-life. Thus, ^{210}Pb, which has a half-life of 22.3 yr, will record mixing events over ~100 yr, whereas ^{234}Th (half-life of 24 d) will illustrate mixing events over only ~120 d. There is, however, a more parsimonious explanation for the apparent tracer dependency observed between D_b values. The biodiffusion model is the default descriptor for biogenic reworking of sediments, but using such a model on short-lived radionucleotide profiles, or artificial tracers observed over a short duration (days), often violates the underlying assumptions of the model and will produce erroneous mixing coefficients (Reed et al. 2006). The relationship between D_b values and tracer half-life can, therefore, relate to use of the incorrect model, highlighting the unreliability of D_b values obtained from short-lived tracers.

The different time scales over which tracers operate will also affect the measured mixing depth, depending on how frequently deep mixing occurs and how fast a tracer decays relative to the rate and depth of mixing. Hughes et al. (2005) found that ^{210}Pb estimates of L in the Rockall Trough (NW of Scotland) were, on average, shallower than those measured by Thomson et al. (2000) using ^{14}C profiles at the same site. Unlike ^{14}C, estimates of L based on ^{210}Pb also varied significantly within the site, indicating that ^{14}C (half-life of 5730 yr) was recording deep mixing events that occur infre-

quently, perhaps only once in every 100 to 1000 yr. The discrepancy between ^{14}C and ^{210}Pb has, however, been refuted by other studies that have obtained mixing depths that are in good agreement with one another and which approximate well to the sediment mixed layer (Nozaki et al. 1977, Peng & Broecker 1979, Henderson et al. 1999). Model predictions from the analyses here show a similar discrepancy between ^{210}Pb and ^{234}Th, where deep mixing events occurring on greater time scales are more likely to be integrated using ^{210}Pb, resulting in deeper mixing depths. Shallower mixing depths can also be an artefact of tracer decay rate because, as is often the case when using ^{234}Th, the tracer may disappear before reaching the mixing depth, especially in areas where deep mixing events occur frequently. Similarly, our analyses show that studies using other types of tracers (e.g. luminophores and chl *a*) that integrate over even shorter time scales (days) will generally result in higher D_b and shallower L. Whilst criticism over model selection may be valid in some cases (Reed et al. 2006), particles associated with chl *a*, for example, can also be affected substantially by the differential reworking of the sediment profile resulting from selective particle feeding. Particles that are low in excess density and/or have organic coatings (i.e. younger particles) are selected 10 to 100 times more often than surrounding sediment particles, increasing their mixing rate by the same order of magnitude (Smith et al. 1993). For some methods, however, particle displacement may be under-represented.

The low values of L obtained using sediment profile imaging (relative to those obtained with particulate tracers) were a striking outcome of our analyses. In SPI images, the lower limit of mixing depth is delineated using colour, which correlates well with the transition between the oxic and anoxic layers of sediment (see e.g. Rosenberg et al. 2001, Diaz & Trefy 2006) that is, in turn, influenced directly by infaunal bioturbation. Thus, being essentially biogeochemical profiles, SPI images are likely to reflect the rate of bioirrigation (and sediment permeability) rather than particle movement. Determining such a gradient can be a complex process, however, particularly in oligotrophic or deep areas where the colour change is less pronounced. Furthermore, differences in camera technology (e.g. sensor, colour response, flash position and intensity) and the sophistication of image analysis systems make direct comparisons between data obtained with different cameras difficult. Due to the different behaviour of tracers within the sediment and the discrepancy between mixing depths derived with SPI, methods used for assessing bioturbation intensities and sediment mixing depths need to be selected carefully based on their appropriateness for the objectives of the study, the processes in question and the time scales over which they operate. An equally cautious approach needs to be adopted when selecting models to fit the tracer profiles to ensure mixing coefficients are estimated appropriately (Reed et al. 2006).

Considering the characteristic time scales of some tracers, it is somewhat surprising to detect a strong effect of season on L and D_b. Had more data been available, it is likely that the inclusion of a method × season interaction term in our models would have emphasized the importance of tracer dependency. This was not possible due to the dataset having a strong bias towards summer months and the low number of studies that provided a definitive study date. Nevertheless, seasonal differences are evident, and, although L is not appreciably dependant on D_b (Boudreau 1994), there are many seasonal processes that would affect both L and D_b simultaneously, such as plankton blooms and changes in species activity, abundance and biomass. Our analyses reveal a seasonally related change in L, but this lags behind that of D_b and may be affected more by seasonal increases in infaunal biomass or abundance that occur later in the year and lead to deeper burrowing events, than by bioturbation intensity per se.

Whilst its importance for habitat quality (Pearson & Rosenberg 1978) and other ecosystem processes (e.g. Emmerson et al. 2001) is well known and has been well documented at local scales, bioturbation has seldom been considered on a global scale. Although we have assembled the most extensive database to date, significant gaps in our knowledge remain, hindering a derivation of global relations between variables that are needed to parameterize global diagenetic models of bioturbation. Taken as a whole, our analyses indicate a global mean (±SD) D_b of 19.98 ± 42.64 $cm^2\ yr^{-1}$ (n = 454) and L of 5.75 ± 5.67 cm (n = 791). Based on a conservative estimate of ocean area of 360 million km^2, the global volume of bioturbated sediment is 20 700 km^3, a quantity approximately 8.5 times the volume of Mount Everest or that would bury the entire metropolitan area of London under 13 km of sediment. Nevertheless, this estimate is small relative to the global mean (±SD) L of 9.7 ± 4.5 cm (n = 200) calculated by Boudreau (1994). His estimate, however, did not include any measurements of L by SPI, which underestimates particle movement and therefore lowers the global mean. Recalculation of L for the present dataset reveals a global mixing depth of 2.52 ± 2.46 cm (n = 381) based on SPI or 8.37 ± 6.19 cm (n = 403) based on particle tracer methods, raising the global estimate of bioturbated sediment to 30 132 km^3. Changes in bioturbation at this scale are likely to have far-reaching consequences for global cycles. Our focus was to provide a representative global estimate for sediments unaffected by human activity, but a large fraction

(41%) of the oceans have already been strongly affected by multiple anthropogenic drivers (Halpern et al. 2008). Comparison of the distribution of our datapoints with a global map of human impact on the world's oceans (loc. cit.) shows that much of our knowledge on bioturbation stems from areas that are most impacted. Given that the advent of complex bioturbation is one of the most significant events in the evolution of marine ecosystems (Seilacher & Pflüger 1994), the question of how much the world's bioturbation has already been reduced and what effect any further loss may have on the function of the marine ecosystem remains an open empirical question.

Acknowledgements. The authors gratefully acknowledge K. E. Dyson, J. A. Godbold and L. M. Murray for their assistance with extracting data from the literature. We thank B. Boudreau (Dalhousie University, Canada), J. D. Germano (Germano and Associates, USA), R. J. Diaz (Virginia Institute of Marine Sciences, USA) and S. Creevan (Aquafact International, Ireland) for providing additional data, D. R. Green (University of Aberdeen, UK) for GIS guidance, R. G. Bailey (USDA Forest Service, USA) and M. Spalding (The Nature Conservancy, UK) for providing GIS shapefiles and 3 anonymous reviewers for helpful comments. This contribution is supported by a University of Aberdeen 6th Century scholarship (awarded to L.T.) and CEFAS, Lowestoft (DP204).

LITERATURE CITED

Attrill MJ, Stafford R, Rowden AA (2001) Latitudinal diversity patterns in estuarine tidal flats: indications of a global cline. Ecography 24:318–324

Bailey RG (1998) Ecoregions: the ecosystem geography of the oceans and continents. Springer, New York

Berg P, Rysgaard S, Funch P, Sejr MK (2001) Effects of bioturbation on solutes and solids in marine sediments. Aquat Microb Ecol 26:81–94

Blair NE, Levin LA, DeMaster DJ, Plaia G (1996) The short-term fate of fresh algal carbon in continental slope sediments. Limnol Oceanogr 4:1208–1219

Boudreau B (1994) Is burial velocity a master parameter for bioturbation? Geochim Cosmochim Acta 58:1243–1249

Boudreau B (1998) Mean mixed depth of sediments: the wherefore and the why. Limnol Oceanogr 43:524–526

Crank J (1975) The mathematics of diffusion. Oxford University Press, Oxford

Cusson M, Bourget E (2005) Global patterns of macroinvertebrate production in marine benthic habitats. Mar Ecol Prog Ser 297:1–14

Diaz RJ (2004) Biological and physical processes structuring deep-sea surface sediments in the Scotia and Weddell Seas, Antarctica. Deep-Sea Res II 51:1515–1532

Diaz RJ, Trefy JH (2006) Comparison of sediment profile image data with profiles of oxygen and Eh from sediment cores. J Mar Syst 62:164–172

Emmerson MC, Solan M, Emes C, Paterson DM, Raffaelli D (2001) Consistent patterns and the idiosyncratic effects of biodiversity in marine ecosystems. Nature 411:73–77

ETOPO2v2 (2006) 2-minute Gridded Global Relief Data (ETOPO2v2). US Department of Commerce, National Oceanic and Atmospheric Administration, National Geophysical Data Center. Available at: www.ngdc.noaa.gov/mgg/fliers/06mgg01.html

Faraway JJ (2006) Extending the linear model with R. Generalized linear, mixed effects and non-parametric regression models. Chapman & Hall/CRC and Taylor & Francis Group, Boca Raton

Fenchel T (1969) The ecology of marine microbenthos. IV. Structure and function of the benthic ecosystem its chemical and physical factors and the microfauna communities with special reference to the ciliated protozoa. Ophelia 6:1–182

Forster S, Khalili A, Kitlar J (2003) Variation of nonlocal irrigation in a subtidal benthic community. J Mar Res 61: 335–357

Gerino M, Aller RC, Lee C, Cochran JK, Aller JY, Green MA, Hirschberg D (1998) Comparison of different tracers and methods used to quantify bioturbation during a spring bloom: 234-thorium, luminophores and chlorophyll *a*. Estuar Coast Shelf Sci 46:531–547

Green MA, Aller RC, Cochran JK, Lee C, Aller JY (2002) Bioturbation in shelf/slope sediments off Cape Hatteras, North Carolina: the use of ^{234}Th, Chl-*a*, and Br^- to evaluate rates of particle and solute transport. Deep-Sea Res II 49:4627–4644

Gutierrez D, Gallardo VA, Mayor S, Neira C and others (2000) Effects of dissolved oxygen and fresh organic matter on the bioturbation potential of macrofauna in sublittoral sediments off Central Chile during the 1997/1998 El Niño. Mar Ecol Prog Ser 202:81–99

Halpern BS, Walbridge S, Selkoe KA, Kappel CV and others (2008) A global map of human impact on marine ecosystems. Science 319:948–952

Henderson GM, Lindsay FN, Slowey NC (1999) Variation in bioturbation with water depth on marine slopes: a study on the Little Bahamas Bank. Mar Geol 160:105–118

Howe JA, Shimmield TM, Diaz R (2004) Deep-water sedimentary environments of the northwestern Weddell Sea and South Sandwich Islands, Antarctica. Deep-Sea Res II 51:1489–1514

Howe JA, Wilson CR, Shimmield TM, Diaz RJ, Carpenter LW (2007) Recent deep-water sedimentation, trace metal and radioisotope geochemistry across the Southern Ocean and northern Weddell Sea, Antarctica. Deep-Sea Res II 54: 1652–1681

Hughes DJ, Brown L, Cook GT, Cowie G and others (2005) The effects of megafaunal burrows on radiotracer profiles and organic composition in deep-sea sediments: preliminary results form two sites in the bathyal north-east Atlantic. Deep-Sea Res I 52:1–13

Johnson NA, Campbell JW, Moore TS, Rex MA, Etter RJ, McClain CR, Dowell MD (2007) The relationship between the standing stock of deep-sea macrobenthos and surface production in the western North Atlantic. Deep-Sea Res I 54:1350–1360

Lovley DR, Phillips EJP (1986) Organic matter mineralisation with reduction of ferric iron in anaerobic sediments. Appl Environ Microbiol 51:683–689

Lyle M (1983) The brown-green colour transition in marine sediments: a marker of the Fe(III)–Fe(II) redox boundary. Limnol Oceanogr 28:1026–1033

Mahaut ML, Graf G (1987) A luminophore tracer technique for bioturbation studies. Oceanol Acta 10:323–328

Meysman FJR, Boudreau B, Middelburg JJ (2003) Relations between local, non-local, discrete and continuous models of bioturbation. J Mar Res 61:391–410

Meysman FJR, Malyuga VS, Boudreau BP, Middelburg JJ (2008) Quantifying particle dispersal in aquatic sediments at short time scales: model selection. Aquat Biol 2:239–254

Middelburg JJ, Soetaert K, Herman PKJ (1997) Empirical relationships for use in global diagenetic models. Deep-Sea Res I 44:327–344

Niggemann J, Ferdelman TG, Lomstein BA, Kallmeyer J, Schubert CJ (2007) How depositional conditions control input, composition, and degradation of organic matter in sediments from the Chilean coastal upwelling region. Geochim Cosmochim Acta 71:1513–1527

Nozaki YK, Cochran JK, Turekian KK, Keller G (1977) Radiocarbon and ^{210}Pb distribution in submersible-taken deep-sea cores from Project FAMOUS. Earth Planet Sci Lett 34:167–173

Ormond FGR, Gage JD, Angel MV (2005) Marine biodiversity. Patterns and processes. Cambridge University Press, Cambridge

Pearson TH, Rosenberg R (1978) Macrobenthic succession in relation to organic enrichment and pollution of the marine environment. Oceanogr Mar Biol Annu Rev 16:229–311

Peng TH, Broecker WS (1979) Rates of benthic mixing in deep-sea sediment as determined by radioactive tracers. Deep-Sea Res 11:141–149

Pinheiro JC, Bates DM (2000) Mixed-effects models in S and S-plus. Springer, New York

Pinheiro J, Bates D, DebRoy S, Sarkar D (2006) nlme: an R package for fitting and comparing Gaussian linear and nonlinear mixed-effects models. Available at: www.stats.bris.ac.uk/R/

Pope RH, DeMaster DJ, Smith CJ, Seltmann H Jr (1996) Rapid bioturbation in equatorial Pacific sediments: evidence from excess ^{234}Th measurements. Deep-Sea Res II 43: 1339–1364

R Development Core Team (2005) R: a language and environment for statistical computing. R Foundation for Statistical Computing, Vienna. Available at: www.R-project.org

Reed DC, Huang K, Boudreau BP, Meysmann FJR (2006) Steady-state tracer dynamics in a lattice-automaton model of bioturbation. Geochim Cosmochim Acta 70: 5855–5867

Rex MA, Stuart CT, Coyne G (2000) Latitudinal gradients of species richness in the deep-sea benthos of the North Atlantic. Proc Natl Acad Sci USA 97:4082–4085

Rex MA, Etter RJ, Morris JS, Crouse J and others (2006) Global bathymetric patterns of standing stock and body size in the deep-sea benthos. Mar Ecol Prog Ser 317:1–8

Rhoads DC, Cande S (1971) Sediment profile camera for *in situ* study of organism–sediment relations. Limnol Oceanogr 16:110–114

Rosenberg R, Nilsson HC, Diaz RJ (2001) Response of benthic fauna and changing sediment redox profiles over a hypoxic gradient. Estuar Coast Shelf Sci 53:343–350

Roy K, Jablonski D, Valentine JW (2000) Dissecting latitudinal diversity gradients: functional groups and clades of marine bivalves. Proc R Soc Lond B 267:293–299

Sandnes J, Forbes T, Hansen R, Sandnes B, Rygg B (2000) Bioturbation and irrigation in natural sediments, described by animal–community parameters. Mar Ecol Prog Ser 197: 169–179

Seilacher A, Pflüger F (1994) From biomats to benthic agriculture: a biohistoric revolution. In: Krumbein WE, Paterson DM, Stal LJ (eds) Biostabilisation of sediments. Bibliotheks- und Informationssystem (BIS), Carl von Ossietzky Universität, Oldenburg

Smith CR, Rabouille C (2002) What controls the mixed-layer depth in deep-sea sediments? The importance of POC flux. Limnol Oceanogr 47:418–426

Smith CR, Pope RH, DeMaster DJ, Magaard L (1993) Age-dependant mixing of deep-sea sediments. Geochim Cosmochim Acta 57:1473–1488

Solan M, Wigham BD, Hudson IR, Kennedy R and others (2004) *In situ* quantification of bioturbation using time-lapse fluorescent sediment profile imaging (f-SPI), luminophore tracers and model simulation. Mar Ecol Prog Ser 271:1–12

Spalding M, Fox H, Davidson N, Ferdana Z and others (2007) Marine ecoregions of the world: a bioregionalization of coast and shelf areas. Bioscience 57:573–583

Thomson J, Brown L, Nixon S, Cook GT, MacKenzie AB (2000) Bioturbation and holocene sediment accumulation fluxes in the north-east Atlantic (Benthic Boundary Layer Experiment sites). Mar Geol 169:21–39

Trauth MH, Sarnthein M, Arnold M (1997) Bioturbational mixing depth and carbon flux at the seafloor. Paleoceanography 12:517–526

West BT, Welch KB, Galecki AT (2007) Linear mixed models. A practical guide using statistical software. Chapman & Hall, New York

Wheatcroft RA, Olmez I, Pink FX (1994) Particle bioturbation in Massachusetts Bay: preliminary results using a new deliberate tracer technique. J Mar Res 52:1129–1150

Yang HS, Nozaki Y, Sakai H, Nagaya Y, Nakamura K (1986) Natural and man-made radionuclide distributions in northwest Pacific deep-sea sediments: rates of sedimentation, bioturbation and ^{226}Ra migration. Geochem J 20: 29–40

Submitted: January 3, 2008; Accepted: April 30, 2008

Proofs received from author(s): June 2, 2008

Vol. 2: 219–238, 2008
doi: 10.3354/ab00053

AQUATIC BIOLOGY
Aquat Biol

Printed June 2008
Published online June 19, 2008

Contribution to the Theme Section 'Bioturbation in aquatic environments: linking past and present'

OPEN ACCESS

Quantification of sediment reworking rates in bioturbation research: a review

Olivier Maire[1,*], Pascal Lecroart[2], Filip Meysman[3], Rutger Rosenberg[4], Jean-Claude Duchêne[5,6], Antoine Grémare[7]

[1]Oceanlab, University of Aberdeen, Newburgh, Aberdeenshire AB41 6AA, UK
[2]Université Bordeaux 1, CNRS, UMR 5805 EPOC, Avenue des Facultés, 33405 Talence, France
[3]Laboratory for Analytical and Environmental Chemistry, Vrije Universiteit Brussel (VUB), Pleinlaan 2, 1050 Brussel, Belgium
[4]Department of Marine Ecology, Göteborg University Kristineberg Marine Research Station, 45034 Fiskebäckskil, Sweden
[5]Université Pierre & Marie Curie-Paris 6, and [6]CNRS, UMR 7621, LOBB, Observatoire Oceanologique, 66651 Banyuls-sur-Mer, France
[7]Université Bordeaux 1, CNRS, UMR 5805 EPOC, Station Marine d'Arcachon, 2 rue du Professeur Jolyet, 33120 Arcachon, France

ABSTRACT: This review lists and discusses the different methods currently available to assess sediment reworking by benthic infauna. Direct methods are used to estimate the amount of sediment transported by infauna at the sediment–water interface during a given period of time. Particle-tracer methods are used to quantify the vertical distribution of particle tracers within the sediment column. Tracers are classified based on their mode of introduction at the sediment–water interface (i.e. whether they occur naturally or are deliberately introduced at the onset of the experiment). The main characteristics of each method, including modelling aspects, are presented, and their respective advantages and drawbacks are outlined with a particular emphasis on their accuracy, spatial (i.e. both horizontal and vertical) and temporal resolutions. Direct and particle-tracer methods assess different components of sediment reworking. Selection of the most appropriate approach depends on the specific question(s) to be answered, as well as other factors, including the behaviour of the organisms studied, the spatial and temporal scales considered, and whether the experiments are carried out *in situ* or under controlled laboratory conditions.

KEY WORDS: Sediment reworking · Bioturbation · Tracer · Radionuclides · Luminophores · Modelling · Particle dispersal

INTRODUCTION

The process of bioturbation, which involves both the dispersal of sediment particles (i.e. sediment reworking) and the transport of interstitial porewater (i.e. bioirrigation) by benthic organisms, is of global importance, as it occurs in most oxic sediments. Through various activities (mainly feeding, burrowing, locomotion and ventilation), benthic fauna modifies the physical, chemical and biological properties of the sediment (Rhoads 1974, Aller 1982, Lohrer et al. 2004). Bioturbation affects, in particular, fluxes of nutrients, oxygen, contaminants and pollutants, and more generally strongly influences the process of organic matter mineralization near the sediment–water interface (Lee & Swartz 1980, Aller 1982, Gilbert et al. 1995, Kristensen 2000, Furukawa et al. 2001). Accordingly, characterizing and quantifying bioturbation processes is of primary importance to unravel the tight and complex mechanisms that control benthic ecosystem functioning at different spatial and temporal scales. To date, a large variety of methods have been developed to assess bioturbation. In this review, we focus solely on those that are used to quantify particle dispersal. Common approaches are either based on the direct quantification of the amount of sediment reworked (direct methods) or on the fitting of mathematical models to vertical profiles of tracer concentrations (particle-tracer methods).

The choice of a method depends on the characteristics of the site and organisms that are studied, and on the scientific purpose. No consensus has been reached on a 'standard' method for the assessment of sediment re-

*Email: o.maire@abdn.ac.uk

working. For example, it is still a matter of discussion whether exotic tracer particles such as glass beads or luminophores are suitable to assess sediment reworking (Wheatcroft et al. 1994). Moreover, the most commonly used particle-tracer methods only provide a 1-dimensional (1D) assessment of sediment reworking (Maire et al. 2006). Another debate concerns the type of mathematical model that should be used to quantify sediment reworking from vertical tracer distributions (Meysman et al. 2003). Sediment reworking has most often been considered as analogous to diffusion, which assumes that displacements of individual particles are very frequent and occur randomly over very short distances (Boudreau 1986a). These assumptions are most often not met (Boudreau 1986a, Meysman et al. 2003), and this has led to the development of a series of models adapted to each main reworking mode (François et al. 1997, 2001) and to more generalized non-local transport models (Boudreau & Imboden 1987, Meysman et al. 2003, Maire et al. 2007a). Despite such developments, the biodiffusive model is still widely used, because of its simplicity and its ability to fit tracer profiles well. This striking contradiction between modelling theory and field practice has been referred to as the 'biodiffusion paradox' (Meysman et al. 2003).

The aims of this review are to (1) list the methods currently available to assess sediment reworking both *in situ* and during laboratory experiments; (2) discuss their main characteristics, including modelling aspects, relative advantages and drawbacks; and (3) present some new and promising approaches that allow for a more complete and/or accurate assessment of sediment reworking in relation to faunal activity.

DIRECT METHODS

Direct methods estimate the amount of sediment handled during a given period of time by (1) collecting the sediment brought up by organisms to the sediment–water interface (Rhoads 1963, 1967, Cadée 1976, Dobbs 1983, Hughes et al. 1996, Rowden et al. 1998, Berkenbusch & Rowden 1999) or (2) estimating the volume of sediment displaced using non-destructive techniques such as image analysis (Hollertz & Duchêne 2001, Lohrer et al. 2005) or laser telemetry (Maire et al. 2007b). Five main approaches have been developed to assess sediment displacement: direct-collection of castings, entrapment, levelling, microtopography, and image analysis (Table 1).

Direct collection of castings

The collection of sediment brought by organisms to the sediment–water interface was first introduced by

Table 1. Inventory of direct methods used to assess sediment reworking. SWI: sediment–water interface

Direct method	Spatial resolution Vertical	Horizontal	Temporal resolution	Advantages	Difficulties/Limitations	Characteristics of organisms	Source
Direct collection of castings	No	Low (cm to m)	Low (h to d)	• Simple and rapid Can be carried out on large sediment areas	• Separation between reworked and surrounding sediment	• Producing castings at the sediment surface	Cadée (1976), Bender & Davis (1984)
Entrapment	No	Low (cm to m)	Medium (min to h)	• No need to separate reworked from surrounding sediment	• Modify environmental conditions Potential bias linked to resuspension and sedimentation processes	• Sessile or discretely mobile	Rhoads (1967), Berkenbusch & Rowden (1999)
Levelling	No (dm to m)	Low (h to d)	Low	• Can be used *in situ*	• Potential bias linked to resuspension and sedimentation processes	• Large organisms inducing reworking of the SWI	Suchanek et al. (1986), Rowden et al. (1998)
Microtopography mapping	No	High (µm)	Medium (min to h)	• High spatial resolution	• Temporal resolution (depending on the covered sediment surface) Potential bias linked to resuspension and sedimentation processes	• Small discretely mobile organisms inducing reworking of the SWI	Maire et al. (2007b)
Image analysis	No	Medium (mm)	High (s)	• High temporal resolution	• Difficulty in tracking organism from the sediment surface	• Large bulldozer organisms living at the SWI	Hollertz & Duchêne (2001), Lohrer et al. (2005)

Davison (1891). Later, it was used, for example, by Cadée (1976) to estimate *in situ* sediment reworking by the lugworm *Arenicola marina*. Castings were collecting at low tide, and their amounts were standardized relative to immersion duration and sediment area. Direct collection assumes that all the sediment expelled at the sediment–water interface can be collected separately from the surrounding sediment. This often proves difficult, since a great proportion of reworked sediment may be unconsolidated and spread laterally (Cadée 1976, Bender & Davis 1984), which likely results in an underestimation of sediment reworking.

Entrapment

Entrapment consists of placing a trap (e.g. a piece of filter paper, aluminium foil, or a cylindrical tube) around the site of sediment expulsion (i.e. typically the opening of a burrow, a tube, or a siphon channel) (Fig. 1). After a known period of time, the trap is retrieved and the amount of collected (i.e. reworked) sediment is measured. This approach has been used for a large variety of benthic infauna, including polychaetes (Rhoads 1967, Nichols 1974, Kudenov 1982), bivalves (Rhoads 1963) and crustaceans (Berkenbusch & Rowden 1999), both *in situ* and during laboratory experiments. Sediment entrapment enables a more complete account of sediment reworking, including some of the unconsolidated faeces, pseudofaeces and burrow ejecta even if a portion of them can be lost through resuspension. The entrapment method is restricted to sessile or discretely motile organisms, and the presence of the trap may modify local environmental conditions such as hydrodynamics.

The 2 direct methods described above are exclusively based on the collection of sediment deposited at the sediment–water interface. These techniques are simple and straightforward, and, historically, they were the first to be used to estimate sediment reworking rates (Davison 1891, Rhoads 1963, 1967). Besides the technical drawbacks mentioned above, they do not allow for high-frequency measurements and do not provide any insights on where the sediment originates. Other direct methods involving sediment micro-topography mapping and image analysis have been recently developed to overcome these drawbacks (Table 1).

Levelling and microtopography mapping

Levelling consists of recording temporal changes in the height of the sediment–water interface during either laboratory (Rhoads 1967) or *in situ* experiments (Suchanek et al. 1986). The original sediment–water interface is used as a reference, and the sediment accumulated above this level is assumed to result from sediment reworking. This sediment can either be periodically collected and weighed (Rhoads 1967, Rowden et al. 1998), or its volume can be estimated from sequential measurements of the level of the sediment–water interface (Suchanek et al. 1986).

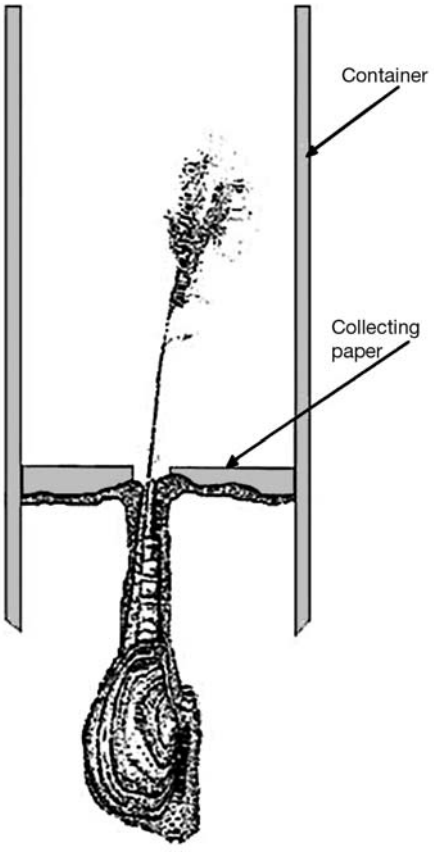

Fig. 1. Principle of the entrapment method. The volume of reworked sediment ejected at the sediment–water interface by the organism (for example *Yoldia limatula*; Bender & Davis 1984) is collected in a trap placed around the site of sediment rejection (modified from Rhoads 1963)

This approach has been recently improved by microtopography mapping. The amount of reworked sediment is then estimated through the assessment of temporal changes in microtopography of the sediment surface (Roy et al. 2002, 2005, Maire et al. 2007b) (Fig. 2). Two main techniques of data acquisition are used. (1) Projecting a laser line onto the sediment surface and comparing its position between successive images; this allows the mapping of sediment microtopography with a ca. 50 µm vertical and a high temporal resolution (Roy et al. 2002, 2005). (2) Using a laser telemeter mounted on 2 crossed step motor tables allowing for 2D displacements above the studied sediment surface (Maire et al. 2007b); this provides both high horizontal (200 µm) and vertical (15 µm) resolutions, and, thus, an accurate estimation

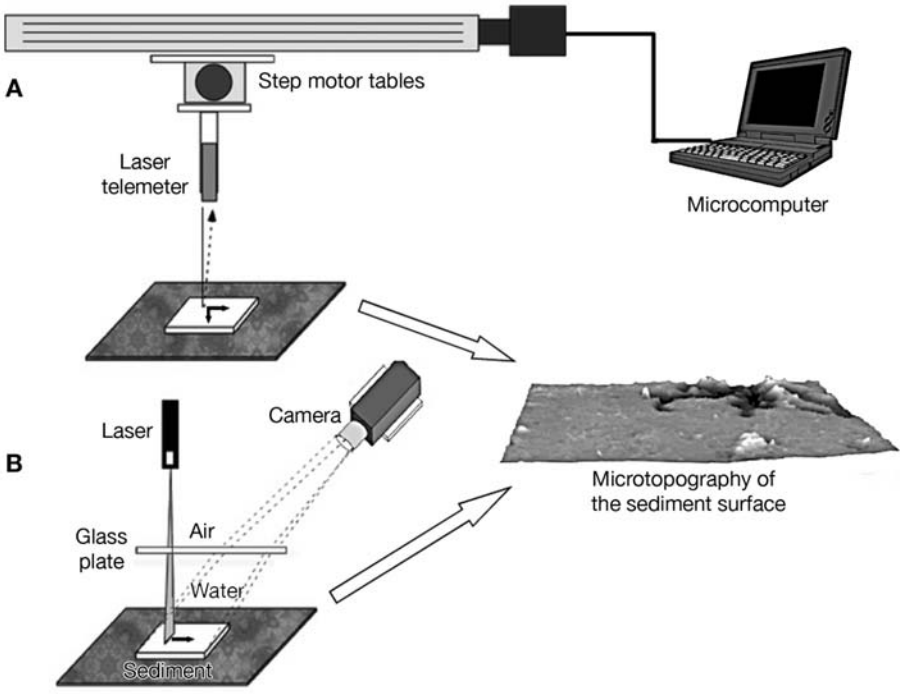

Fig. 2. Principle of the microtopography mapping method. The amount of reworked sediment is estimated through the assessment of temporal changes in the microtopography of the sediment surface. Successive microtopography mappings can be assessed: (A) using a laser telemeter mounted on 2 crossed step motor tables allowing for 2-dimensional displacements above the sediment surface (modified from Maire et al. 2007b) or (B) through the projection of a laser line onto the sediment surface. A glass plate placed at the air–water interface assures well-defined and constant refraction. An image of the projected laser line is recorded by a digital camera. The position of the laser line in the image is then determined, allowing for estimations of sediment surface elevations (modified from Roy et al. 2002)

of sediment reworking at the sediment–water interface between 2 successive scans (*SR*):

$$SR = \frac{\sum_{i,j} |\Delta LWSI|}{\Delta t} \quad (1)$$

where *i* and *j* correspond to the *x* and *y* coordinates in the sediment area, Δ*LWSI* represents the differences of levels of the sediment–water interface of the scanned area between 2 consecutive scans, and Δ*t* is the time interval between 2 consecutive scans.

The first technique is limited by the length of the laser line (typically 5 cm) and cannot provide microtopography measurements behind sediment mounds or within sharp pits. The main disadvantage of laser telemetry is the time required to run each scan (e.g. 67 min for a 64 cm^2 sediment surface; Maire et al. 2007b); this limits its temporal resolution. Moreover, when used during *in situ* experiments, levelling and microtopography mapping may result in erroneous estimations of sediment reworking, since reworked sediment may be transported out of the monitored area. Conversely, part of the sediment accumulated at the sediment–water interface may result from the sedimentation of resuspended material.

Surface image analysis

Surface image analysis involves the recording of the movements of benthic fauna at the sediment surface using a video sensor (Hollertz & Duchêne 2001, Lohrer et al. 2005) (Fig. 3). In each image, the position of the organism is automatically detected, and its coordinates within the image are recorded. At the end of the experiment, all coordinates, within successive images, are used to assess displacements. Sediment reworking rates (*SR*) are then computed as:

$$SR = \frac{(DT \times CS)}{\Delta t} \quad (2)$$

where *DT* is the distance travelled during a Δ*t* time interval, and *CS* is the cross section, i.e. the reworked area along the plane of locomotion.

This approach has been used for sea urchins both *in situ* (Lohrer et al. 2005) and during laboratory experiments (Hollertz & Duchêne 2001). Its main advantage is that it allows for the assessment of short-term temporal changes in sediment reworking (Hollertz & Duchêne 2001). In practice, its use is restricted to large organisms living immediately beneath the surface of the sediment, so that their movements can be tracked by monitoring the sediment–water interface. Moreover, it does not account for sediment reworking resulting from processes other than locomotion (e.g. feeding), which makes it particularly suitable for bulldozing organisms such as spatangoid sea urchins, where the ratio of sediment reworking caused by locomotion over that caused by feeding is between 60 and 150 (Hollertz & Duchêne 2001).

PARTICLE-TRACER METHODS

Particle-tracer methods were introduced to study the vertical component of sediment reworking. They are

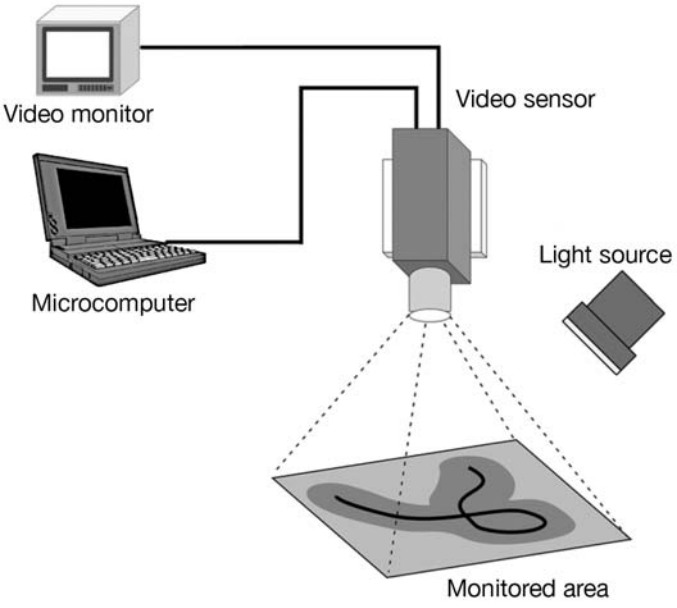

Fig. 3. Principle of the image analysis method. The position of the organism is automatically detected at the surface of the monitored sediment area, and its coordinates are recorded. At the end of the experiment, all coordinates, within successive images, are compiled to assess its displacements. The reworked volume of sediment is then estimated based on the linear track (i.e. the distance travelled during the time interval considered) and the cross section of the organism

based on the measurement of the vertical distribution of particle tracers within the sediment column. The underlying principle is that tracers initially deposited at the sediment–water interface, or placed at some horizon within the sediment column (see Gilbert et al. 2007), are displaced due to the action of benthic fauna. Sediment reworking coefficients are then computed using mathematical models that are fitted to the vertical tracer profile (Boudreau 1986a,b, Wheatcroft et al. 1990, François et al. 1997, 2001, Meysman et al. 2007) (Fig. 4).

Particle tracers are supposed to behave in the same way as sediment particles. The high diversity of particle-tracer methods focuses on: (1) type of tracers that differ in terms of stability, reactivity, association with sediment particles, and mode of introduction to the sediment–water interface, (2) recovery and quantification of the tracers, and (3) type of model used to infer sediment reworking coefficients.

Diversity and characteristics of particle tracers

Tracers can be classified depending on their mode of introduction at the sediment–water interface, irrespective of whether they are natural or deliberate, and whether they are non-conservative (initial mass of the tracer decreases over time as the tracer is degraded through chemical reactions within the sediment) or conservative (initial mass of the tracer remains constant over time) (Table 2).

Naturally occurring tracers

Radionuclides. During the last 3 decades, radionuclides have been the most widely used particle tracers to assess sediment reworking rates in aquatic environments (Krezoski et al. 1984, Sharma et al. 1987, Green et al. 2002). Some radionuclides occur naturally in the water column, such as ^{210}Pb, ^{234}Th, ^{228}Th, ^{32}Si, ^{14}C and ^{7}Be (Aller 1982). Most of them originate from atmospheric fallout. For example, ^{210}Pb is produced from ^{222}Rn decay in the atmosphere and by ^{226}Ra decay in the water column. ^{234}Th is produced by the decay of dissolved ^{238}U in the water column. ^{7}Be is produced by the interaction of cosmic rays with atmospheric constituents and delivered to the sea surface through wet and dry deposition. All are quickly scavenged from the water

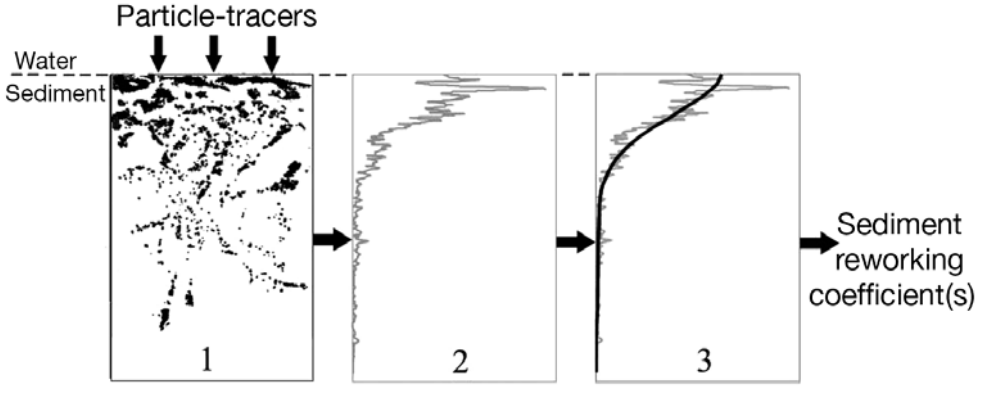

Fig. 4. Principle of particle-tracer methods. (1) Tracer particles deposited at the sediment–water interface are mixed within the sediment column due to infauna activity. (2) The vertical tracer profile is assessed using a tracer recovery method. (3) Sediment reworking coefficients are computed by fitting a mathematical model (black line) to the vertical profile (grey line)

Table 2. Inventory of particle tracers used to assess sediment reworking

Tracer	Temporal resolution	Advantages	Difficulties/Limitations	Source
Radionuclides	Medium–Low (mo to century)	• Naturally occurring in the field	• Preferential association with fine particles	Sharma et al. (1987), Green et al. (2002)
Chlorophyll *a*	Medium (mo)	• Naturally occurring in the field	• Positive selection of organic-rich particles	Sun et al. (1991), Gérino et al. (1998)
Microtektites	Low (centuries)	• Naturally occurring in the field	• Exotic particles Provide information on past sediment reworking	Glass (1969), Glass et al. (1973)
Heavy minerals	High (h to d)	• Can be used in coarse sediments	• High density	D'Andrea et al. (2004)
Isotopically labelled sediment particles	High (h to d)	• Pulse input allowing for sediment reworking assessment over short temporal scales	• Preparation of sediment particles before the experiments	White et al. (1987), Sandnes et al. (2000a)
Isotopically labelled organic matter	High (h to d)	• Pulse input allowing for sediment reworking assessment over short temporal scales	• Positive selection of organic-rich particles	Blair et al. (1996)
Metal doped sediment	High (h to d)	• Pulse input allowing for sediment reworking assessment over short temporal scales	• Possible desorption and re-adsorbtion	Wheatcroft et al. (1994), Olmez et al. (1994)
Glass beads	High (h to d)	• Pulse input allowing for sediment reworking assessment over short temporal scales	• Exotic particles	Berg et al. (2001)
Microtaggants	High (h to d)	• Pulse input allowing for sediment reworking assessment over short temporal scales	• Exotic particles	Wheatcroft (1991)
Luminophores	Very high (min to h)	• High frequency measurements Can be used with image analysis recovery methods	• Exotic particles	Mahaut & Graf (1987), Gérino (1990)

column by suspended particles, and transported to the sea floor, where they are rapidly incorporated and mixed into the sediment. Their vertical distribution within the sediment column depends on (1) external supply rates, (2) *in situ* production, (3) half-life, and (4) sediment reworking. When the values of the 3 first parameters are known, sediment reworking can be assessed based on vertical concentration profiles. Moreover, radionuclides with varied half-lives are suitable to mimic organic matter with different decay constants since, as pointed out by Aller (1982), the 2 types of decay have similar kinetics.

The main deliberate radionuclides used to assess sediment reworking rates in marine environments are radionuclides originating from nuclear testing such as ^{137}Cs (half-life 30.2 yr) and ^{241}Am (half-life 14.9 yr) (White et al. 1987, Thomson et al. 2000, Mulsow et al. 2002). They were first introduced into the marine environment in the 1950s and their concentrations peaked between 1963 and 1964 because of nuclear weapons testing (Callender & Robbins 1993). Because of their long half-lives, these radionuclides have been used to assess sediment reworking rates over decadal time scales (Sharma et al. 1987, Thomson et al. 2000). As opposed to natural radionuclides, which are continuously supplied to the sea floor, deliberate radionuclides are not characterized by steady-state distributions and can be considered a pulse input (Aller 1982).

Chlorophyll a. Chl *a* is a non-conservative tracer, and is thought to track the mixing of fresh organic matter. The concentration of chl *a* within the sediment column depends on its sedimentation and degradation rates, and on sediment reworking. Therefore, its use as a particle tracer for sediment reworking first requires knowledge about sedimentation and degradation rates and assumes that chl *a* can be considered as a particle-associated sedimentary component. The half-life of chl *a* is typically between 3 and 250 d, depending on redox conditions (about 23 d on average under oxic conditions) (Sun et al. 1991, 1993, Stephens et al. 1997, Gérino et al. 1998). Accordingly, the estimation of its degradation rate may prove difficult when bio-irrigators, introducing oxygen into the sediment, are present. Another drawback of chl *a* is that sediment reworking can be biased due to positive selection of chl *a* rich particles during feeding (Taghon 1982, Lopez & Levington 1987, Mahon & Dauer 2005). Moreover, the concentration of chl *a* is significantly affected during its transit through animals' guts (Abele-Oeschger & Theede 1991), which complicates its use in the case of non-local transport associated with feeding (e.g. conveyor belt feeders).

The distributions of chl *a* concentrations in the sediment column have nevertheless been used to assess sediment reworking on a few occasions (Sun et al. 1991, Gérino et al. 1998, Josefson et al. 2002).

Microtektites. Microtektites are small glass spheres (typical size range from 30 µm to 1 mm), which are deposited on the sea floor following meteorite showers. They are similar in density to sediment particles, but their rounded shape and transparent glassy appearance make them easy to distinguish and count under a dissecting microscope. Because their input to the sediment column is restricted in time, their subsequent vertical concentration profiles result from a balance between sediment reworking and sedimentation following the event (Glass et al. 1973). For example, microtektites derived from a meteorite encounter that occurred 700 000 yr ago have been used to infer sediment reworking in the deep Indian Ocean (Glass 1969, Glass et al. 1973). As for other exotic particles, the specific properties (shape, structure and chemical composition) of microtektites may modify their mixing behaviour compared to ambient sediment particles (Wheatcroft et al. 1994).

Pollen grains. Davis (1974) used pollen grains as a tracer to investigate the feeding and particle transport of tubificids inhabiting deep lake sediments. Specific pollen taxa (size range 20 to 120 µm) were selected based on their absence (or rareness) in the natural sediment and/or for specific features that make them easily recognizable. The use of pollen grains proved valuable to study feeding behaviour (e.g. depth of feeding, size of ingested particles, etc.), as well as vertical changes in particle transport. However, the approach also has several drawbacks: (1) identification and counting are tedious and time consuming, (2) pollen grains may be preferentially selected by organisms during feeding and (3) relatively rapid decomposition of the pollen particle (up to 30 % after 260 d) leads to an underestimation of the rate of particle transport.

Deliberately introduced tracers

Deliberately introduced tracers have been used both *in situ* and in the laboratory to assess the effects of environmental factors on sediment reworking (Gérino et al. 1994, Mugnai et al. 2003, Ouellette et al. 2004). Their main advantage is that they allow a direct quantification of sediment reworking over short temporal scales after the input of a tracer pulse at the sediment surface. However, the addition of deliberate tracers inevitably changes sediment conditions and thus could affect organism behaviour and sediment reworking.

Heavy mineral sand tracer. D'Andrea et al. (2004) used heavy mineral sand (garnet and magnetite) as particle tracers to assess sediment reworking in coarse sediments. Although this inert tracer could be suitable in sandy sediments, artefacts in the measurement of sediment reworking rates can nevertheless occur, since density significantly affects particle handling by benthic infauna (Jumars et al. 1982).

Isotopically labelled sediment particles. Natural sediment particles can be labelled with radioisotopic elements, classically ^{137}Cs (White et al. 1987) and ^{51}Cr (Hansen et al. 1999, Sandnes et al. 2000a,b). The vertical distribution of the tracer is monitored over time, and sediment reworking rates are calculated. This approach allows the assessment of short-term changes in sediment reworking.

Isotopically labelled organic matter. This method consists in labelling algae with ^{13}C or ^{14}C (Blair et al. 1996) and then assessing the vertical profile of these labels. As reported for chl *a*, bulk sediment reworking may be significantly overestimated because of the selectivity of organic-rich particles by benthic infauna (Taghon 1982, Lopez & Levington 1987).

Metal doped sediment particles. This technique is based on the thermal diffusion of noble metals (typically Au and Ag, which are naturally present only in trace amounts) into the mineral matrix of sediments (Wheatcroft et al. 1994). The technique does not affect the size and surface properties of sediment particles and only has a slight (<8 %) effect on their density (Olmez et al. 1994). One limitation is the possible desorption in pore water and subsequent re-adsorption. However, such processes have not been detected during experiments (Olmez et al. 1994).

Glass beads. Glass beads with a size representative of the average sediment grain size are also used as particle tracers (Shull & Yasuda 2001). In this sense, the method is similar to the microtektite method, but allows for short-term assessment of contemporary sediment reworking. The main shortcoming results from the exotic nature of the tracers, which have different surface properties from those of ambient sediment particles. These differences can be alleviated to some extent by the development of a biofilm on the surface of the beads prior to the experiments (Berg et al. 2001).

Microtaggants, luminophores and microspheres. Wheatcroft (1991) introduced the use of microtaggants, inert and non-toxic rough plastic particles with a size range of 50 to 125 µm and a specific gravity of 1.4 (similar to natural sediment particles). To facilitate their recovery, they are coated with blue paint, which makes microtaggants similar to luminophores (see below).

Mahaut & Graf (1987) introduced the use of luminophores. Luminophores are natural sediment particles that have been coated with a thin layer of UV fluorescent paint. Diameters of luminophores typically range between 10 and 500 µm, with a density of about 2.5 g cm^{-3}. Microspheres are UV fluorescent balls of polystyrene divinylbenzene or latex that have a much smaller size (down to 1 µm) and lower density (e.g. 1.05 g cm^{-3} for polystyrene microspheres) than luminophores (Gielazyn

et al. 1999, Ciutat et al. 2005). Because of their specific properties, the addition of microspheres does not modify initial sedimentary conditions. Their use is particularly interesting to investigate sediment reworking processes resulting mainly from feeding activity, since microspheres can be ingested together with surrounding sediment, and not on their own, even by the smallest species (Ciutat et al. 2005).

Usually, luminophore particles and microspheres are visually counted under a microscope, which can be tedious and time consuming (Mahaut & Graf 1987, Gérino 1990, François et al. 1999, Ciutat et al. 2005, Fernandes et al. 2006). However, image analysis techniques have been recently introduced to facilitate this operation (Gilbert et al. 2003, Solan et al. 2004, Maire et al. 2006). As for other exotic particles, some doubts remain as to whether some of the properties (size, density and fluorescent paint) may bias the assessment of sediment reworking due to differential manipulations by benthic infauna. It has also been reported that the coating may fill micro-crevices, which are important for bacterial attachment (Wheatcroft et al. 1994).

Particle-tracer recovery methods

The standard method for assessing the vertical distribution of particle tracers within the sediment column consists in collecting and slicing a sediment core, and, subsequently, quantifying the tracer within each sediment layer (Table 3). This procedure has been used *in situ* and *ex situ* with both natural (e.g. radionuclides) and deliberate (e.g. luminophores) tracers, either under steady-state (typically for natural radionuclides) or non-steady-state conditions (when the tracer is introduced as a pulse at the sediment surface) (Cochran & Aller 1979, Gérino et al. 1998, Turnewitsch et al. 2000, François et al. 2002, Mugnai et al. 2003, Schmidt et al. 2007). The thickness of each sediment layer is usually chosen between 0.5 and 1 cm in the upper most centimetres, and thereafter typically increases with depth. The amount of tracer within each sediment layer is estimated using a variety of techniques. Radionuclides and isotopically labelled particles are usually quantified using alpha or gamma spectrometry (Goldberg & Koide 1962, Thomson et al. 2000, Schmidt et al. 2007), while metal-doped sediment particles are analyzed using instrumentation neutron activation analysis (Wheatcroft et al. 1994, Olmez et al. 1994), and chl *a* using HPLC (Sun et al. 1991, Gérino et al. 1998). All visually distinguishable tracers, such as microtektites, glass beads, microtaggants and luminophores, are either classically counted under a dissecting microscope (Glass et al. 1973, Wheatcroft 1991, Blair et al. 1996, Madsen et al. 1997, Fernandes et al. 2006), or

Table 3. Inventory of tracer recovery methods used to assess vertical tracer profiles

	Spatial resolution Vertical	Horizontal	Temporal resolution	Advantages	Difficulties/Limitations of organisms	Characteristics	Source
Core slicing	Low (≥5 mm)	No	No	• Simple Can be carried out both *in* and *ex situ* with all particle tracers Initial information on tracer distribution in a 3D space	• Lack of a dynamic view Possible mixing of tracer particles during collection and slicing Low vertical resolution	• Inducing sediment reworking over relatively high vertical scales (>5 cm)	Cochran & Aller (1979), Gérino et al. (1998)
Image analysis	High (≤250 µm)	High (≤250 µm)	High (min to h)	• High spatial and temporal resolution	• Potential 'wall effect' Initial information on tracer distribution in a 2D space	• Small organisms, sessile or discretely mobile	Solan et al. (2004), Maire et al. (2006)

quantified using automated image acquisition and analysis techniques (Gilbert et al. 2003, Solan et al. 2004, Maire et al. 2006). The quantification of particle tracers within the sediment column can become difficult when their distribution is patchy or when the concentration approaches the detection limit. Overall, vertical profiles of radionuclides are widely used because of the sensitivity of the analytical method. Fornes et al. (2001), however, reported that the detection of short-lived radionuclides becomes difficult when the experimental duration approaches 5 times their half-lives.

Classical core slicing has several disadvantages including (1) lack of any dynamic view of sediment reworking, since cores are destroyed when assessing tracer profiles; (2) vertical resolution of tracer profiles is limited by the thickness of each sediment slice; (3) inability to assess sediment reworking at a spatial scale smaller than the whole experimental core (each slice is horizontally averaged); (4) possible mixing and carry-over between adjacent sediment layers during collection and slicing; and (5) no information about lateral particle transport. Methods using transparent thin aquaria or sediment profile imaging (SPI), combined with time-lapse photography, luminophore pulses and automated image analysis techniques, were recently introduced to overcome these drawbacks (Table 3). They result in high-frequency monitoring of luminophore displacements within a vertical plane of the sediment column. Using these approaches, Gilbert et al. (2003) and Solan et al. (2004) studied sediment reworking induced by natural benthic communities of the Swedish west coast, whereas Maire et al. (2006, 2007a) assessed the effects of food availability and temperature on sediment reworking by 2 closely related bivalves under laboratory conditions. A limitation of SPI and thin aquaria are potential wall effects. However, comparative measurements for thin aquaria showed that vertical tracer profiles derived from image analysis and classical slicing were similar (Maire et al. 2006). To our knowledge, this potential artefact has never been tested during *in situ* sediment profile imaging deployment. Moreover, as reported by Solan et al. (2004), SPI may induce an underestimation of sediment reworking, since some luminophores may be horizontally displaced away from the monitored sediment area.

Modelling

Types of sediment reworking models

There are 2 fundamental levels at which sediment reworking can be studied: the microscopic level of individual particles and the macroscopic level of the bulk sediment. These 2 levels have separate types of associated models. At the microscopic level, individual particles are displaced in discrete mixing events caused by various animal–sediment interactions, such as burrowing, ingestion/egestion, biodeposition and locomotion by epifauna (Solan & Wigham 2005). Accordingly, models at this level need to 'track' the trajectories of individual particles. Although the motion of each sediment particle is intrinsically deterministic, the interplay between particles and biological activity may be considered sufficiently complex, so that a particle's motion can be described as a stochastic process. The associated type of model is a random-walk model, which describes particle displacement in terms of consecutive random sediment reworking events. When an organism moves in the sediment, reshuffling of the sediment occurs, and particles are dislocated to a new position. In recent years, random walk models have gained considerable interest in sediment reworking theory, but mostly from a theoretical perspective (Boudreau 1989, Wheatcroft et al. 1990, Meysman et al. 2003, Meile & van Cappellen 2005).

One serious obstacle of random walk models is that they cannot be properly validated. This is because, with present experimental methods, it is not possible to track individual sediment particles. Moreover, the real interest of the sediment biogeochemist is to analyze tracer concentration profiles, which essentially characterize the 'averaged' behaviour of sediment particles. Accordingly, the relevant level of description is not that of the individual particle, but the macroscopic level of the sediment. The macroscopic models are termed continuum models, which describe how the concentration of tracer particles changes with time. Here, our prime interest is to discuss suitable tools for the analysis of tracer profiles, and, hence, only continuum models are further discussed; more details on random-walk models and their link to continuum models can be found in Meysman et al. (2003).

Two main types of continuum models are in use at present: (1) Local models are considered suitable to describe 'local transport', which includes sediment displacements that are spatially random, sufficiently frequent and occur over small spatial scales (Boudreau 1986a). (2) Non-local sediment reworking models are used for transport processes that lead to particle displacements between distant points or to directional transport of particles (Boudreau & Imboden 1987).

Biodiffusion model (local mixing)

The most widely implemented particle dispersal model is the biodiffusion model, which assumes that Ficks' law of diffusion is applicable and which de-

scribes particle dispersal by analogy with the diffusive heat transport (Goldberg & Koide 1962, Guinasso & Schink 1975, Meysman et al. 2003). If we consider vertical mixing over a depth layer of thickness L, the governing tracer equation becomes:

$$\frac{\partial C}{\partial t} = D_b \frac{\partial^2 C}{\partial x^2} - \omega \frac{\partial C}{\partial x} - \lambda C \quad (3)$$

where x represents the depth into the sediment, C is the concentration or activity of the selected tracer, D_b is the biodiffusion coefficient, ω is the burial velocity, t is time and λ the decay constant of the tracer.

In Eq. (3), the parameters D_b and ω are assumed not to depend on depth. Implicitly, Eq. (3) also requires that the porosity (ϕ) is constant with depth. Accordingly, this term drops from Eq. (3). The validity of these assumptions is discussed below. Suitable solutions of Eq. (3) are fitted to tracer depth profiles, and an optimal estimate for the biodiffusion coefficient D_b is obtained. For reactive tracers, D_b is typically deduced from the steady-state solution (Boudreau 1997):

$$C(x) = C_0 \exp\left(\frac{\omega - \sqrt{\omega^2 + 4D_b\lambda}}{2D_b} x \right) \quad (4)$$

where C_0 is the activity or concentration of the tracer at the sediment–water interface and λ is the decay constant of the tracer. To retain only C_0 and D_b as fitting parameters, suitable values of the burial velocity ω and the decay constant λ should be known *a priori*. In sedimentary environments dominated by sediment reworking (i.e. $\omega L/D_b \ll 1$), the advective term (ω) in Eq. (3) can be neglected. In other cases, ω should be independently determined, for example, by using the part of the tracer profile located just beneath the bioturbated layer that is unaffected by sediment reworking. A similar argument holds for the decay constant λ. Radioisotopes are popular tracers since their decay is tightly constrained (e.g. Crusius & Kenna 2007, Lecroart et al. 2007a). In the case of chl *a*, the decay constant is less well constrained, and should be introduced as an additional unknown parameter (e.g. Gérino et al. 1998). Fitting 2 parameters (D_b, λ) to a single tracer profile rather than one (D_b), however, introduces considerable uncertainty (see below).

For conservative tracers, D_b is typically deduced from the transient solution for an idealized pulse initial condition (Guinasso & Schink 1975). This pulse is an idealization of a unit layer of tracer particles added to the sediment–water interface. With the assumption of negligible burial velocity, this solution becomes:

$$C(x,t) = \frac{1}{\sqrt{\pi D_b t}} \exp\left(\frac{-x^2}{4D_b t} \right) \quad (5)$$

In this case, $C(x,t)$ represents the normalized tracer concentration relative to the initial input introduced at the sediment–water interface. This method has been applied to microtektites (e.g. Guinasso & Schink 1975) and luminophores (e.g. Gérino et al. 1998).

Non-local mixing

Non-local models are typically invoked when particular features in tracer profiles appear that cannot be explained by the classical biodiffusion analogy (Boudreau 1986b, Boudreau & Imboden 1987, Soetaert et al. 1996, François et al. 2002). For example, the presence of subsurface maxima in radiotracer profiles cannot be reproduced with the biodiffusion model (Soetaert et al. 1996, Shull 2001, Delmotte et al. 2007). Different modes of non-local transport have been described in the literature: upward conveyor, downward conveyor, regenerator and gallery diffusor (Fisher et al. 1980, Boudreau 1986b, Rice 1986, Robbins 1986, Smith et al. 1986, Soetaert et al. 1996, François et al. 1997, 2002). These reworking mechanisms correspond to different functional groups within macrobenthic communities (François et al. 1997). Note that non-local transport can be the dominant process in marine sediments. Along the ocean margin exchange (OMEX) transect, Soetaert et al. (1996) showed that between 8 and 86% of the total flux of radionuclides enters the sediment by non-local exchange.

Until now, non-local models have been 1-dimensional (1D) descriptions, except for the 2D models developed by François et al. (2001, 2002), which also incorporated lateral tracer transport. Up to now, 2D models have never been validated, due to the lack of appropriate experimental data.

Moreover, all non-local reworking mechanisms can be captured by the general non-local exchange formalism (Boudreau & Imboden 1987, Boudreau 1997, Meysman et al. 2003):

$$\frac{\partial C}{\partial t} = \int_0^L K(x,x';t) C(x',t) \mathrm{d}x' - \int_0^L K(x',x;t) C(x,t) \mathrm{d}x' \quad (6)$$

where $K(x,x')$ represents the exchange function and L is the depth of the (bioturbed) sediment layer. The 2 integral terms on the right-hand side describe the exchange between non-adjacent depth layers (they, respectively, represent the supply and removal of tracer from the depth layer centred at position x). These 2 terms are basically sink and source terms that need specification for different sediment environments. In other words, for each mode of non-local reworking, the exchange function K requires a suitable and explicit mathematical form.

In general, the exchange function K will be a function of a number of parameters. Like the biodiffusion coefficient, these parameters need adjustment when

fitting the non-local model solutions to the observed tracer profiles (Soetaert et al. 1996, François et al. 2002). This is often a challenging task, because non-local models are generally complex: they incorporate far more parameters than the single D_b of the biodiffusion model. The synchronous calibration of multiple parameters is numerically demanding and requires customized software, while fitted parameters often are poorly constrained (i.e. they have a large uncertainty associated). Accordingly, recent research efforts have focused on how to optimize model complexity (Meysman et al. 2006, Delmotte et al. 2007), and how to rigorously assess the uncertainty associated with calibrated parameters (Anderson et al. 2006). There are a number of ways to reduce model complexity by decreasing the number of calibrated model parameters. One way is to constrain parameter values *a priori* based on literature information. Another way is to use core imaging techniques to characterize parameters (Shull 2001), or to perform experiments with multiple tracers and sequentially calibrate parameters. See, for example, Delmotte et al. (2007) for a detailed case study of how to systematically constrain parameters in a model that describes head-down deposit feeding of tubificid oligochaetes.

Lattice-automaton sediment reworking models

Experimental techniques in sediment reworking research are frustrating in that they cannot address interactions between organisms and sediment at the microscale. For example, it is not possible to tag individual particles and follow their trajectories through the sediment. A new modelling approach developed by Choi et al. (2002) overcomes these problems. It is called lattice automaton bioturbation simulation (LABS), and basically constitutes a computer emulation of an actual sediment environment. In essence, LABS is composed of a 2D matrix of pixels, which can be designated as sediment particles, porewater, or organisms. Organisms move through the lattice as programmable entities, i.e. automatons, and follow certain rules that define organism displacement, particle ingestion, size and density distribution. These rules are designed to mimic the behaviour of benthic organisms such as subsurface deposit feeders. The activity of the virtual organisms (moving, feeding, burrowing, etc.) then creates particle dispersal. This allows all types of numerical sediment reworking simulations. For example, sediment particles can be virtually tagged with radioactive tracers of different half-lives (Boudreau et al. 2001, Reed et al. 2006). LABS is not a sediment reworking model in the sense of the previously discussed biodiffusion and non-local models. Rather than analyzing data, LABS is designed to *generate* synthetic tracer data. For example, the 2D distribution of the tracer particles within LABS can be laterally integrated, which results in 1D tracer profiles. These profiles can be subsequently analyzed by the classical models, i.e. the biodiffusion or non-local models discussed above. Accordingly, the purpose of LABS is not to replace existing models, but rather to provide a tool to investigate sediment reworking at the microscopic levels where data collection is impossible with current experimental techniques. LABS simulations allow the establishment of links between organism behaviour and classical sediment reworking parameters (Boudreau et al. 2001). One topic of great importance is to test when and where the biodiffusion model can be used to analyze tracer profiles (Reed et al. 2006).

DISCUSSION

Direct versus particle tracer methods

Direct methods, based on the collection of sediment conveyed by benthic infauna to the sediment surface (i.e. direct collection, entrapment and levelling) clearly suffer from a lack of accuracy (see Table 1). They account only for that portion of sediment reworking that results in a transfer of sediment particles to the sediment–water interface. Accordingly, they only provide a rough qualitative estimate of the rate of sediment reworking. This explains why they have been progressively abandoned. The recent development of surface image analysis, and more importantly of laser telemetry, provide a new generation of techniques with the potential for significant improvement. These approaches are non-destructive and require no sediment collection, nor any modification of the sediment–water interface. In addition, laser telemetry accounts for both particle excavation (i.e. transport of sediment from the surface to deeper level) as well as accumulation at the sediment–water interface, and allows the assessment of sediment reworking with a high spatial (on the micrometre order) resolution. Overall, laser telemetry and, to a lesser extent, surface image analysis constitute the most promising direct approaches to infer sediment reworking, even though these new techniques still require further testing and development.

As opposed to direct methods, tracer methods are based on the analysis of vertical tracer concentration profiles within the sediment column. Consequently, these 2 approaches provide an insight into different aspects of sediment reworking. Direct methods can account for both horizontal and vertical sediment reworking, provided that particles end up at (or in the

immediate vicinity of) the sediment–water interface. However, they do not allow a distinction between these 2 components. Conversely, particle-tracer methods assess only the vertical component of sediment reworking. The choice of a direct versus a particle-tracer method therefore depends on the mode of the sediment reworking, as well as the size, behaviour and position of the bioturbating organism (e.g. complexity of burrow structures). Direct methods can be appropriate for certain surface or sub-surface deposit feeders (Rowden et al. 1998, Hollertz & Duchêne 2001, Lohrer et al. 2005), whereas particle-tracer methods are appropriate for organisms inducing strong vertical displacement of sediment particles (e.g. gallery biodiffusors, conveyor belt deposit feeders) (François et al. 2002, Caradec et al. 2004, Ouellette et al. 2004, Maire et al. 2006).

There are also important discrepancies in the way sediment reworking is assessed through direct and particle-tracer methods. These discrepancies are linked to the existence of a modelling step in the particle-tracer method that is not present in the direct methods. Direct methods result in an evaluation of the amount of sediment reworked per unit of time (i.e. analogous to a flow), whereas particle-tracer methods result in a sediment reworking rate (i.e. biodiffusion coefficient [D_b], step length squared divided by resting time), which is computed through modelling. This makes any comparison between the 2 kinds of methods difficult with respect to the relationship between biological activity and sediment reworking. Maire et al. (2007b) used both direct (surface image analysis) and particle-tracer methods (with a biodiffusion model) for the deposit-feeding bivalve *Abra ovata*. They found a tight relationship between direct observation of siphon activity and sediment reworking assessed by direct methods (laser telemetry). The relationship was less clear when sediment reworking was assessed through particle tracer methods (luminophores coupled with 2D image acquisition) because (1) there were several types of activity inducing different kinds of luminophore displacement and (2) there was no correlation between the temporal scales associated with the measurement of bivalve activity and the computation of D_b. The choice between direct and particle tracer approaches, thus, also clearly relies on the ecological/biogeochemical question tackled.

Tracer characteristics and inherent limitations

As pointed out above, there is a large variety of particle tracer methods corresponding to different tracers and different tracer recovery methods. The choice of a particular tracer largely determines the time scale over which sediment reworking is assessed. The tracer recovery method mainly controls the spatial domain (1D, 2D) over which sediment reworking is studied. Each particle tracer has its inherent limitations. Microtektites, for example, have been used to assess sediment reworking in the deep Indian Ocean (Glass 1969). However, the use of microtektites is tightly limited by the number of meteorite showers that produces them. Moreover, this tracer only provides information on reworking in the period immediately following the encounter and assumes that both sediment reworking and sedimentation rates are constant during that period.

Chl *a* is not a tracer for mineral particles, but rather for the organic matter associated with these particles. Chl *a* is considered to be representative of the very labile fraction of sedimentary organic matter (Grémare et al. 1997). Therefore, its use as a tracer could be biased, because the quality of particulate organic matter affects biological processes involved in sediment reworking, most importantly feeding activity (Maire et al. 2006). This may explain why studies based on chl *a* typically result in higher sediment reworking rates than those based on radionuclides and luminophores (Gérino et al. 1998, Green et al. 2002). The same limitation applies to studies that use isotopically labelled organic matter (Blair et al. 1996). One way to overcome this selective-dispersal problem is to use natural sediment particles and label them with isotopes or metal. This method also leaves the density of particles unaltered relative to the bulk surrounding sediment. Isotope labelling and metal doping have, however, rarely been used (Olmez et al. 1994, Wheatcroft et al. 1994), possibly due to constraints in the preparation and analysis of the sediment. In contrast, the use of exotic particles such as luminophores and microspheres is much more widespread (Gérino 1990, François et al. 1999, Solan et al. 2004, Mermillod-Blondin et al. 2005, Fernandes et al. 2006, Maire et al. 2006). Luminophores are at present the most often used exotic particles for assessing sediment reworking. The primary practical limitation is the time required to count them. This same limitation also holds for glass beads and microtaggants. However, recent progress in image analysis now allows the automated identification and counting of luminophores under UV light (Gilbert et al. 2003, Solan et al. 2004, Maire et al. 2006). The main disadvantage of luminophores concerns their ability to mimic natural sediment particles. Luminophores have no organic coating and are covered with a fluorescent paint, and the (negative) effects of this on feeding and ingestion are unknown. Avoidance effects may result in an underestimation of the particle transport. Radionuclides are preferentially associated with fine particles that preclude their use in sandy and coarse sediments, because of the differential transport of fine particles through porewater advection. The counting

of radionuclides requires a substantial amount of sediment. The typical procedure involves the collection and slicing of sediment cores, which restrict the radionuclide approach to a 1D description of sediment reworking with a limited spatial resolution. Despite their respective drawbacks, luminophores and radionuclides are currently the most commonly employed tracers to quantify sediment reworking.

Spatial assessment of sediment reworking

A challenge in the study of sediment reworking is how to deal with spatial heterogeneity. As stated above, tracer methods have been mainly developed and applied to investigate the vertical (1D) component of sediment reworking. The standard approach to assess tracer concentration patterns remains core slicing. The homogenization of the tracer within each slice results in a smoothed vertical 1D profile, which helps to explain the 'biodiffusive paradox' (Maire et al. 2007a). Core slicing does not allow assessment of the horizontal component of sediment reworking, which requires the 2D mapping of particle tracer concentrations. Such 2D mappings have recently been achieved by using luminophores in combination with thin aquaria in the laboratory (Maire et al. 2006, 2007a,b) and sediment profile imagery of natural communities (Gilbert et al. 2003, Solan et al. 2004). However, no sediment reworking model has yet been applied to 2D sediment reworking. Maire et al. (2006) used a classic biodiffusive model to infer the horizontal heterogeneity of vertical sediment reworking and the influence of slice thickness on the computation of the sediment reworking rate. Gilbert et al. (2003) reduced the 2D luminophore distribution to a single sediment reworking coefficient (optical reworking coefficient) that encompasses both vertical and horizontal biological mixing. Wheatcroft (1991) applied a specific tracer injection method to calculate the horizontal component of the sediment reworking rate *in situ*.

From a methodological standpoint, a sound assessment of horizontal sediment reworking would require tracking of individual particle displacements. In spite of the technological advances in image analysis, this has not yet been achieved. One possibility is to increase image acquisition frequencies from 600 s (Maire et al. 2007b) to ca. 1 s (i.e. the current limit of sensors). Furthermore, the algorithm developed for the study of larval swimming (Duchêne & Nozais 1994, Duchêne & Queiroga 2001) and particle displacement along the tentacles of surface deposit feeders (Maire et al. 2007c) may prove efficient for tracking luminophores as well. Another possibility is to deposit luminophores in restricted areas rather than homogeneously spreading them over the entire experimental sediment surface. This way it would be possible to assess the horizontal component of their displacement from their original location. However, a fundamental obstacle is that the sediment matrix is not transparent, and image analysis can follow particles only within the 2D plane of the aquarium wall or SPI interface.

Ultimately, a full description of sediment reworking will have to be achieved in 3D. However, there is currently no method available for this purpose. Computer-assisted tomography (CAT-scan) is used to describe the 3D distribution of biogenic structures in sediment (Mermillod-Blondin et al. 2003, Dufour et al. 2005, Rosenberg et al. 2007). This method measures the density of elementary (sediment) cells called voxels. It can be used as a tracer method, if the tracer particles are slightly different in density from the surrounding sediment (Rosenberg et al. 2008). This new approach is promising, but still presents 2 difficulties: (1) Selective dispersal, as density differences between the tracer and the surrounding sediment may affect sediment reworking (see above). (2) Resolution, as the size of each voxel is currently much larger than that of individual tracer particles. Therefore, the average density within a voxel may actually correspond to a combination of materials of very different densities (e.g. water, sediment, tracer particles). Rosenberg et al. (2008) tried to resolve this resolution problem when using aluminium as a tracer to study the sediment reworking of an *Amphiura filiformis* community. They proposed to consider that voxels with a density compatible with the presence of aluminium indeed corresponded to reworked aluminium only if they were connected to the sediment–water interface through a continuous series of water and/or aluminium voxels (i.e. if those voxels were in direct contact with a biogenic structure). Rosenberg et al. (2007) recommended a similar criterion for the assessment of biogenic water. Nevertheless, this approach does not account for tracer particles that have been reworked away from biogenic structures, and its applicability is restricted to certain types of sediment reworking. More straightforward ways to resolve the difficulty could simply consist of using a higher resolution (but this increases the scan time substantially), and/or a different type of CAT based on radioisotope measurement (PET-scan).

Validity of the biodiffusion model

Modelling of particle tracer profiles, and the issue as to whether biodiffusion can appropriately model tracer profiles already have a relatively long history in sediment reworking research (Boudreau 1986a, Meysman et al. 2003, Reed et al. 2006). There are 2 basic aspects

to the problem: (1) is the biodiffusion equation (Eq. 3) applicable? (2) Are the assumptions (constant tracer flux, constant parameters, etc.) in the typical application of Eq. (3) justified?

The validity of the biodiffusion model has been the subject of a number of theoretical studies (Boudreau 1986a, Boudreau & Imboden 1987, Meysman et al. 2003). The picture that emerges from these is that validity of the biodiffusion model rests on a comparison of 2 different types of scales: (1) the inherent time and length scales of sediment reworking (i.e. the distance over which particles are displaced and the frequency of these displacement events); (2) the length scale and time scale of observation. For radioisotopes, this observational length scale can be interpreted as the depth of tracer penetration, and the observational time scale is the half-life of the radioisotope (5 times the half-life determines the time window of experimental observation). Meysman et al. (2003) concluded that the biodiffusion analogy can be theoretically justified when the intrinsic time and length scales of sediment reworking are much smaller than their observational counterparts. Yet, when scrutinizing natural sediment reworking activity, these authors conclude that these conditions are often not satisfied, particularly for experiments over short time scales (e.g. short-lived radioisotopes, chl *a* studies, pulse-tracer experiments with luminophores). This is because particles can be displaced over the same centimetre scale distance as the tracer penetration depth; moreover, the time between particle displacements becomes large when compared to the observational time scale. Therefore, Meysman et al. (2003) concluded that in many cases, the application of the biodiffusion model is questionable from a theoretical point of view. Still, in practice, tracer profiles often look diffusive, and the biodiffusion analogy is widely employed to analyze these profiles. Meysman et al. (2003) refer to this apparently contradictory situation as the 'biodiffusion paradox'.

Boudreau & Imboden (1987) have proven that the biodiffusion model can be deduced from the integro-differential equation of the non-local exchange model when particle exchange is symmetric and operates on a small scale (see also Meysman et al. 2003). Consequently, the non-local exchange model emerges as the more general formalism, which covers all modes of biological mixing. The biodiffusion paradox could be resolved if we better understood the exact conditions under which the more general model leads to the biodiffusion model. This is an important topic for future research (see for example Meysman et al. 2008, this Theme Section).

A second puzzling observation is that the biodiffusion coefficient deduced from radioisotope profiles seems to be dependent on the half-life of the tracer. Smith et al. (1993) and Pope et al. (1996) have examined the mixing intensity from radioisotopes with different half-lives. They concluded that, in many deep-sea sediments, the biodiffusion coefficients derived from short-lived tracers are much higher than those derived from long-lived ones. They suggested that this age-dependent mixing results from selective ingestion and, thus, mixing of recently deposited food-rich particles. The occurrence of age-dependent mixing driven by food quality is supported by field measurements (e.g. gut enrichment of short-lived tracers) and particle introduction experiments (Smith et al. 1993, Miller et al. 2000, Fornes et al. 2001). As an alternative to age-dependent mixing, it has also been suggested that tracer dependence of the biodiffusion coefficient can simply result from unjustified assumptions of the biodiffusive model. The biodiffusion analogy indeed requires that the number of mixing events experienced by each sediment particle needs to be >25 (Boudreau 1986a, Meysman et al. 2008). Based on LABS simulation, Reed et al. (2006) confirmed that short-lived radioisotopes are likely to provide biased estimations of the biodiffusion coefficient in sedimentary environments characterized by low sediment reworking. On the other hand, Maire et al. (2007a) experimentally determined the step length and resting time for the deposit-feeding bivalve *Abra ovata* at field densities, and the results suggest that the assumptions of the biodiffusion model can be met in littoral environments where sediment reworking is high. A future challenge, therefore, consists in identifying which part of the observed tracer-dependent mixing is explained by age-dependent mixing and/or by unjustified assumptions of the biodiffusion model.

The above theoretical considerations reveal that the conditions for the biodiffusion analogy to hold *depend on the tracer*: particles must be sufficiently frequently displaced within the time window of the specific tracer. This implies that some forms of sediment reworking can be seen as 'local' with respect to long-lived radioisotopes and considered 'non-local' with respect to short-lived ones. This implies that for the same type of sediment reworking activity, different models may be needed at different time scales. Maire et al. (2007a) showed experimentally that sediment reworking displayed non-local features during the first 48 h of an experiment and subsequently evolved in biodiffusive mixing. This result confirms the theoretical predictions that over short time scales the non-local model should provide a more accurate description of sediment reworking, but as the number of sediment reworking events increases, the non-local model should converge toward the biodiffusion model (Meysman et al. 2008).

In conclusion, the biodiffusion model offers a simple mathematical formalism for the interpretation of tracer

profiles, and, therefore, it constitutes an attractive way to quantify biological mixing. Nonetheless, one should be cautious when applying the biodiffusion model. Non-local models are particularly relevant for short time scale investigations, and also for benthic fauna that display a clear non-local transport activity (e.g. head-down deposit feeders) and thus generate particular tracer profile shapes (e.g. subsurface maxima).

Temporal assessment of sediment reworking

It is important to define the time scale at which sediment reworking is considered, taking into consideration the objectives of the study and the type of particle tracer. For example, the term 'short time scale' is currently used for radionuclide experiments that span from one to several months (Gérino et al. 1998, Schmidt et al. 2007). However, the term 'short time scale' is also used for tracer experiments with luminophores that last <1 d or even <1 h (Solan et al. 2004, Maire et al. 2006, 2007a,b). Each tracer indeed provides information about sediment reworking over a different time scale, depending on its reactivity.

Non-conservative tracers, such as radionuclides and chl *a*, exhibit an exponential decay with time (and thus with depth in undisturbed sediment). In environments with low sedimentation rates, chl *a* (half-life between 3 and 250 d) and radionuclides with short half-lives, such as ^{234}Th (24.1 d) and ^{7}Be (53.4 d), should thus theoretically be present only near the sediment surface. Therefore, their penetration to deeper sediment layers is indicative of vertical sediment reworking. Analysis of steady-state tracer profiles allows the estimation of sediment reworking rates over different periods of time and depends on their decay kinetics. ^{210}Pb (22.3 yr) is particularly appropriate to assess the depth of the reworked sediment layer, and is suitable to estimate the average accumulation rate and sediment reworking rate over the past 100 yr. Therefore, ^{210}Pb has often been used to assess sediment reworking in the deep sea (Peng et al. 1979, Stordal et al. 1985, Thomson et al. 1988, 2000, Soetaert et al. 1996, Hughes et al. 2005). Conversely, chl *a*, ^{234}Th and ^{7}Be are more appropriate to derive information about sediment processes occurring at a seasonal time scale (i.e. 3 to 4 mo) (Aller & Cochran 1976, Fuller et al. 1999, Schmidt et al. 2007). These short time tracers have also been used to assess biogenic sediment reworking in more intensively reworked sediments such as shallow coastal environments (Aller & Cochran 1976, Rice 1986, Lecroart et al. 2005). One disadvantage of chl *a*, compared to radionuclides, is that its degradation rate is highly dependent on environmental conditions (Sun et al. 1993).

Sediment reworking experiments usually involve naturally occurring tracers (radionuclides and chl *a*), based on the assumption that a constant flux of tracer arrives at the sediment surface. This may seem surprising, as many authors have concluded that transient-state regimes are the rule in aquatic sediments rather than the exception. Nonetheless, steady-state conditions form a model approximation. Therefore, the steady-state approximation remains valid when the fluctuations exhibit significantly shorter or longer periodicity than the observational time scale. If this is the case, a sedimentary system can still be described by a steady-state model (Boudreau 1997). The real problem is when the fluctuations have about the same time scale as the observational time scale. When using short-lived radioisotopes like ^{7}Be (half-life 53.4 d) or ^{234}Th (half-life 24.1 d), daily fluctuations of the deposition flux (e.g. resulting from tidal currents) will not be important, as they simply can be considered as noise superimposed on the constant average flux. Similarly, decadal changes in the flux of these tracers (e.g. resulting from climate change) will not hamper the steady-state assumption of the model. However, seasonal fluctuations are on the same time scale as the tracers, and transient effects can occur in the calculation of the reworking rate. Lecroart et al. (2007b) showed that the presence of a seasonally changing flux regime can generate a significant error, up to a factor of 2, in the rate (D_b) calculation. Moreover, radionuclide profiles associated with such a transient flux still adopt the exponential shape of the steady-state profiles. Consequently, transient regime effects are difficult to detect in field data, and, hence, it would be erroneous to justify the steady-state approximation by the simple observation of an exponential profile.

Radionuclides are undoubtedly useful tracers to measure and compare sediment reworking rates from different sites and over a relatively large range of time scales. However, variations in biogenic sediment reworking over very short temporal scales (on the order of hours or minutes), in relation with quick temporal changes of environmental parameters, cannot be evaluated using only radionuclides as particle tracers. This is particularly restricting, since one of the main effects of sediment reworking is precisely its influence on organic matter mineralization, a process that may be affected by short-term sediment reworking events, depending on the type of organic matter. Moreover, several studies have shown that sediment reworking modes depend on the type of activities (e.g. feeding mode) and that these modes can change over short time scales, in phase with environmental factors such as food availability and temperature. It is thus mandatory to obtain information on the time scale of sediment reworking events. Only the use of a pulse of conserva-

tive tracers at the sediment–water interface, together with high-frequency image analysis techniques, can document such rapid mixing events. This approach also allows the identification of modes of sediment reworking and the assessment of rapid temporal changes in sediment reworking rates in relation to environmental parameters. However, care should be taken when analysing tracer profiles, since the tracer particles may initially settle into burrows, tubes, or pits in the sediment column during the spreading procedure. This can generate subsurface peaks, which are usually considered the hallmark of non-local transport.

Temporal variation of biodiffusion D_b

Seasonal changes in environmental conditions are commonly observed in temperate areas, and are especially pronounced in shallow environments such as Mediterranean lagoons, where the yearly amplitude of temperature can reach 25°C. Such seasonal changes can induce a seasonal pattern in the activity of the lagoon's benthic fauna, and hence the reworking rate, as recently suggested by Schmidt et al. (2007). Using a modelling approach, Lecroart et al. (2007a) showed that the biodiffusion model is suitable to quantify the seasonal variability of particle mixing activities, provided that radioisotopes are used that have a half-live lower than the length of the season (e.g. ^{224}Th and ^{7}Be). For such short-lived radioisotopes, the tracer profiles are rapidly adjusted to the new reworking conditions and the classical procedure to estimate D_b can be used. Recently, Maire et al. (2007a) investigated seasonal variations of the mixing activity based on pulse-tracer experiments with luminophores. They concluded that both temperature and food availability have an impact on sediment reworking during summertime, whereas temperature and not food availability controls sediment reworking during wintertime. Conversely, based on 3 yr time series measurements, Wheatcroft (2006) reported no significant control of the temperature on sediment reworking rates at a site where temperature seasonally varies between 7 and 12°C, whereas a significant variation in food availability between seasons was hypothesized. However, Wheatcroft (2006) underlined that temporal changes in sediment reworking rates that result from both biotic (e.g. organism abundance, size) and abiotic parameters (e.g. temperature, food availability) are particularly difficult to assess during *in situ* experiments. These parameters can vary simultaneously and affect sediment reworking in different ways, e.g. decrease of temperature during a time of increasing animal abundance and food availability (Wheatcroft 2006).

Depth variation of porosity, burial velocity and D_b

The conventional procedure to estimate D_b from tracer profiles typically assumes that the parameters (D_b, ω, ϕ) in Eq. (3) do not vary with depth. Note that under the assumption of steady-state compaction, the porosity ϕ and the burial velocity ω will co-vary with depth, as mass conservation requires that the product $(1 - \phi)\omega$ remains constant. Meysman et al. (2007) tested how strongly the constant-porosity assumption could affect the resulting D_b estimates. They showed that the influence of porosity gradients on D_b values was modest. Also note that in most sedimentary environments, sediment reworking rates are much higher than sedimentation rates, and, hence, D_b calculation will not be affected by variations in the burial velocity.

Boudreau (1986a) explored the influence of a depth-dependent D_b on the shape of tracer profiles. This study concluded that for steady-state profile of radio-tracers, depth-dependent D_b and constant D_b models could generate very similar profiles. Differences occur if D_b decreases faster than according to quadratic decay, and only when $\omega L/D_b(0) \leq 1$ and $0.03 \leq \lambda L^2 D_b(0) \leq 3$. In the transient case, when simulating the pulse input of an inert tracer, the depth-dependent D_b and the constant D_b cases could also have similar profiles. Consequently, the depth dependence of the biodiffusion coefficient cannot be constrained from a single tracer profile (Boudreau 1986a). Some biogeochemical sediment models introduce a transition zone between an upper bioturbated layer (with constant D_b) and a deeper burial zone (where $D_b = 0$). In this transition zone, D_b decreases with depth (e.g. Rabouille & Gaillard 1991, van Cappellen & Wang 1996, Berg et al. 2003). This smooth transition is advantageous from a numerical perspective (discontinuities are to be avoided in numerical solution procedures), but the exact mathematical form of this depth dependence is poorly constrained by data.

CONCLUSIONS

Many methods are available to measure sediment reworking, each of them has advantages and drawbacks. Amongst the direct methods, laser telemetry is the most promising, since it allows for an accurate measurement of sediment reworking at the sediment–water interface, with relatively high spatial and temporal resolutions. Moreover, this method can be improved by decreasing the time required to capture successive micro-topography mappings. Amongst the tracer methods, the use of natural radionuclides in combination with classical core slicing techniques is a solid and proven technique that is here to stay. However, attention must be given to the tracer dependence of

reworking rates, and further studies should focus on the exact mechanism behind this tracer dependence. In addition, the use of conservative tracers (e.g. luminophores) supplied at the sediment–water interface under non-steady-state conditions has received a lot of attention. This technique is particularly promising when used in combination with sediment imaging profiling and cutting edge image analysis techniques that allow for a high-resolution assessment of short-term temporal and spatial changes in 2 dimensions. This approach also allows for the simultaneous measurement of biological activity and sediment reworking. Accordingly, it can be used to relate changes in the rate of sediment reworking with specific variations in infaunal activity (Solan et al. 2004, Maire et al. 2007b). Such information is particularly needed for a better conceptualization of sediment reworking models, and thus for a better quantification of sediment reworking.

With regard to the modelling of sediment reworking, several topics can be identified for future research. Particular efforts need to be addressed to better understand the exact conditions under which the different models can be used with the available tracers. Furthermore, a model is by definition a simplified representation of reality, but there is a trend towards the development of more and more complex models. This then brings on the issue of simplicity versus complexity: What is the optimal complexity of a model to explain certain features of tracer concentration patterns? Further breakthrough developments are expected from LABS simulations, when more complex biological behaviour is incorporated, such as particle selectivity. All these topics require close cooperation between modellers and experimental biologists.

Overall, no method can currently be considered as standard. Instead, the selection of a method depends on the problem at hand and the type of environment investigated (deep sea versus coast). It is thus mandatory to first define the scientific objectives and requirements before selecting the most appropriate method, which may itself include several complementary approaches (e.g. laser telemetry, thin aquaria and luminophores; see Maire et al. 2007b) or require a further development of existing methods.

Acknowledgements. We thank 3 anonymous reviewers for their detailed and constructive comments. F.M. was supported by an Odysseus grant from the Research Foundation Flanders.

LITERATURE CITED

Abele-Oeschger D, Theede H (1991) Digestion of algal pigments by the common periwinkle *Littorina littorea* L. (Gastropoda). J Exp Mar Biol Ecol 147:177–184

Aller RC (1982) The effects of macrobenthos on chemical properties of marine sediment and overlying water. In: McCall PL, Tevesz MJS (eds) Animal–sediment relations—the biogenic alteration of sediments. Topics in geobiology, Vol 2. Plenum Press, New York, p 53–102

Aller RC, Cochran JK (1976) $^{234}Th/^{238}U$ disequilibrium in near-shore sediment: particle reworking and diagenetic time scales. Earth Planet Sci Lett 29:37–50

Andersson JH, Middelburg JJ, Soetaert K (2006) Identifiability and uncertainty analysis of bio-irrigation rates. J Mar Res 64:407–429

Bender K, Davis WR (1984) The effect of feeding by *Yoldia limatula* on bioturbation. Ophelia 23:91–100

Berg P, Rysgaard S, Funch P, Sejr MK (2001) Effects of bioturbation on solutes and solids in marine sediments. Aquat Microb Ecol 26:81–94

Berg P, Rysgaard S, Thamdrup B (2003) Dynamic modeling of early diagenesis and nutrient cycling. A case study in an arctic marine sediment. Am J Sci 303:905–955

Berkenbusch K, Rowden AA (1999) Factors influencing sediment turnover by the burrowing ghost shrimp *Callianassa filholi* (Decapoda: Thalassinidea). J Exp Mar Biol Ecol 238: 283–292

Blair NE, Levin LA, DeMaster D, Plaia G (1996) The short term fate of fresh algal carbon in continental slope sediments. Limnol Oceanogr 41:1208–1219

Boudreau BP (1986a) Mathematics of tracer mixing in sediments. I. Spatially-dependent, diffusive mixing. Am J Sci 286:161–198

Boudreau BP (1986b) Mathematics of tracer mixing in sediments. II. Non-local mixing and biological conveyor-belt phenomena. Am J Sci 286:199–238

Boudreau B (1989) The diffusion and telegraph equations in diagenetic modelling. Geochim Cosmochim Acta 53: 1857–1866

Boudreau B (1997) Diagenetic models and their implementation: modelling, transport and reactions in aquatic sediments. Springer Verlag, Berlin

Boudreau BP, Imboden DM (1987) Mathematics of tracer mixing in sediments. III. The theory of nonlocal mixing within sediments. Am J Sci 287:693–719

Boudreau BP, Choi J, Meysman F, Francois-Carcaillet F (2001) Diffusion in a lattice-automaton model of bioturbation by small deposit feeders. J Mar Res 59:749–768

Cadée GC (1976) Sediment reworking by *Arenicola marina* on tidal flats in the Dutch Wadden Sea. Neth J Sea Res 10: 440–460

Callender E, Robbins JA (1993) Transport and accumulation of radionuclides and stable elements in a Missouri River reservoir. Water Resour Res 29:1787–1804

Caradec S, Grossi V, Hulth S, Stora G, Gilbert F (2004) Macrofaunal reworking activities and hydrocarbon redistribution in an experimental sediment system. J Sea Res 52: 199–210

Choi J, François-Carcaillet F, Boudreau BP (2002) Lattice-automaton bioturbation simulator (LABS): implementation for small deposit feeders. Comput Geosci 28:213–222

Ciutat A, Gérino M, Mesmer-Dudons N, Anschutz P, Boudou A (2005) Cadmium bioaccumulation in Tubificidae from the overlying water source and effects on bioturbation. Ecotoxicol Environ Saf 60:237–246

Cochran JK, Aller RC (1979) Particle reworking in sediments from the New York Bight apex: evidence from $^{234}Th/^{238}U$ disequilibrium. Estuar Coast Mar Sci 9:739–747

Crusius J, Kenna TC (2007) Ensuring confidence in radionuclide-based sediment chronologies and bioturbation rates. Estuar Coast Shelf Sci 71:537–544

D'Andrea AF, Lopez GR, Aller RC (2004) Rapid physical and

biological particle mixing on an intertidal sandflat. J Mar Res 62:67–92

Davis RB (1974) Stratigraphic effects of tubificids in profundal lake sediments. Limnol Oceanogr 19:466–488

Davison C (1891) On the amount of sand brought up by lobworms to the surface. Geol Mag 8:489–493

Delmotte S, Meysman FJR, Ciutat A, Boudou A, Sauvage S, Gerino M (2007) Cadmium transport in sediments by tubificid bioturbation: an assessment of model complexity. Geochim Cosmochim Acta 71:844–862

Dobbs FC (1983) Monitoring defecation activity of infaunal deposit feeders. Mar Ecol Prog Ser 12:47–50

Duchêne JC, Nozais C (1994) Light influence on larval emission and vertical swimming in the terebellid worm *Eupolymnia nebulosa* (Montagu, 1818). Mem Mus Natl Hist Nat Ser A Zool 162:405–412

Duchêne JC, Queiroga H (2001) Use of an intelligent CCD camera for the study of endogenous vertical migration rhythms in first zoeae of the crab *Carcinus maenas.* Mar Biol 139:901–909

Dufour SC, Desrosiers G, Long B, Lajeunesse P and others (2005) A new method for three-dimensional visualisation and quantification of biogenic structures in aquatic sediments using axial tomodensitometry. Limnol Oceanogr Methods 3:372–380

Fernandes S, Meysman F, Sobral P (2006) The influence of Cu contamination on *Nereis diversicolor* bioturbation. Mar Chem 102:148–158

Fisher JB, Lick WJ, McCall PL, Robbins JA (1980) Vertical mixing of lake sediments by tubificid oligochaetes. J Geophys Res 85:3997–4006

Fornes WL, DeMaster D, Smith CR (2001) A particle introduction experiment in Santa Catalina Basin sediments: testing the age-dependent mixing hypothesis. J Sea Res 59:97–112

François F, Poggiale JC, Durbec JP, Stora G (1997) A new approach for the modelling of sediment reworking induced by a macrobenthic community. Acta Biotheor 45: 295–319

François F, Dalegre K, Gilbert F, Stora G (1999) Specific variability within functional groups: study of the sediment reworking of two Veneridae bivalves, *Ruditapes decussatus* and *Venerupis aurea.* CR Acad Sci Ser III Sci Vie 322: 339–345

François F, Poggiale JC, Durbec JP, Stora G (2001) A new model of bioturbation for a functional approach to sediment reworking resulting from macrobenthic communities. In: Aller JY, Woodin SA, Aller RC (eds) Organism–sediment interactions. University of South Carolina Press, Columbia, p 73–86

François F, Gérino M, Stora G, Durbec JP, Poggiale JC (2002) Functional approach to sediment reworking by gallery-forming macrobenthic organisms: modeling and application with the polychaete *Nereis diversicolor*. Mar Ecol Prog Ser 229:127–136

Fuller CC, Van Geen A, Baskaran M, Anima R (1999) Sediment chronology in San Francisco Bay, California, defined by ^{210}Pb, ^{234}Th, ^{137}Cs, and ^{239,240}Pu. Mar Chem 64:7–27

Furukawa Y, Bentley SJ, Lavoie DL (2001) Bioirrigation modeling in experimental benthic mesocosms. J Mar Res 59: 417–452

Gérino M (1990) The effects of bioturbation on particle redistribution in Mediterranean coastal sediment. Preliminary result. Hydrobiologia 207:251–258

Gérino M, Stora G, Durbec JP (1994) Quantitative estimation of biodiffusive and bioadvective sediment mixing: *in situ* experimental approach. Oceanol Acta 17:547–554

Gérino M, Aller RC, Lee C, Cochran JK, Aller JY, Green MA, Hirschberg D (1998) Comparison of different tracers and methods used to quantify bioturbation during a spring bloom: 234-Thorium, luminophores and chlorophyll *a*. Estuar Coast Shelf Sci 46:531–547

Gielazyn ML, Stancyk SE, Piegorsch WW (1999) Experimental evidence of subsurface feeding by the burrowing ophiuroid *Amphipholis gracillima* (Echinodermata). Mar Ecol Prog Ser 184:129–138

Gilbert F, Bonin P, Stora G (1995) Effect of bioturbation on denitrification in a marine sediment from the West Mediterranean littoral. Hydrobiologia 304:49–58

Gilbert F, Hulth S, Stroemberg N, Ringdahl K, Poggiale JC (2003) 2-D optical quantification of particle reworking activities in marine surface sediments. J Exp Mar Biol Ecol 285/286:251–263

Gilbert F, Hulth S, Grossi V, Poggiale JC and others (2007) Sediment reworking by marine benthic species from the Gullmer Fjord (western Sweden): importance of faunal biovolume. J Exp Mar Biol Ecol 348:133–144

Glass BP (1969) Reworking of deep-sea sediments as indicated by the vertical dispersion of the Australasian and Ivory Coast microtektite horizons. Earth Planet Sci Lett 6:409–415

Glass BP, Baker RN, Storzer D, Wagner GA (1973) North American microtektites from the Caribbean Sea and their fission track age. Earth Planet Sci Lett 19:184–192

Goldberg ED, Koide M (1962) Geochronological studies of deep sea sediments by the ionium/thorium method. Geochim Cosmochim Acta 26:417–450

Green MA, Aller RC, Cochran JK, Lee C, Aller JY (2002) Bioturbation in shelf/slope sediments off Cape Hatteras, North Carolina: the use of ^{234}Th, chl-*a*, and Br^- to evaluate rates of particle and solute transport. Deep-Sea Res II 49:4627–4644

Grémare A, Amouroux JM, Charles F, Dinet A and others (1997) Temporal changes in the biochemical composition and nutritional value of the particulate organic matter available to surface deposit-feeders: a two year study. Mar Ecol Prog Ser 150:195–206

Guinasso NL, Schink DR (1975) Quantitative estimates of biological mixing in abyssal sediments. J Geophys Res 80:3032–3043

Hansen R, Forbes TL, Westermann P (1999) Importance of bioturbation and feeding by the polychaete *Capitella* sp. I in the degradation of di(2-ethylexyl)phthalate (DEHP). Mar Ecol Prog Ser 182:187–199

Hollertz K, Duchêne JC (2001) Burrowing behaviour and sediment reworking in the heart urchin *Brissopsis lyrifera* Forbes (Spatangoida). Mar Biol 139:951–957

Hughes DJ, Ansell AD, Atkinson RJA (1996) Sediment bioturbation by the echiuran worm *Maxmuelleria lankesteri* (Herdman) and its consequences for radionuclide dispersal in Irish Sea sediments. J Exp Mar Biol Ecol 195: 203–220

Hughes DJ, Brown L, Cook GT, Cowie G and others (2005) The effects of megafaunal burrows on radiotracer profiles and organic composition in deep-sea sediments: preliminary results from two sites in the bathyal north-east Atlantic. Deep-Sea Res I 52:1–13

Josefson AB, Forbes TL, Rosenberg R (2002) Fate of phytodetritus in marine sediments: functional importance of macrofaunal community. Mar Ecol Prog Ser 230:71–85

Jumars PA, Self RFL, Nowell ARM (1982) Mechanics of particle selection by tentaculate deposit-feeders. J Exp Mar Biol Ecol 64:47–70

Krezoski JR, Robbins JA, White DS (1984) Dual radiotracer measurement of zoobenthos-mediated solute and particle

transport in freshwater sediments. J Geophys Res 89: 7937–7947

Kristensen E (2000) Organic matter diagenesis at the oxic/anoxic interface in coastal marine sediments, with emphasis on the role of burrowing animals. Hydrobiologia 426: 1–24

Kudenov JD (1982) Rates of seasonal sediment reworking in *Axiothella rubrocincta* (Polychaeta: Maldanidae). Mar Biol 70:181–186

Lecroart P, Schmidt S, Jouanneau JM, Weber O (2005) Be-7 and Th-234 as tracers of sediment mixing on seasonal time scale at the water–sediment interface of the Thau Lagoon. Radioprotection 40:661–667

Lecroart P, Schmidt S, Anschutz P, Jouanneau JM (2007a) Modeling sensitivity of biodiffusion coefficient to seasonal bioturbation. J Mar Res 65:417–440

Lecroart P, Schmidt S, Jouanneau JM (2007b) Numerical estimation of the error of the biodiffusion coefficient in coastal sediments. Estuar Coast Shelf Sci 72:543–552

Lee H, Swartz RC (1980) Biological processes affecting the distribution of pollutants in marine sediments. II: biodeposition and bioturbation. In: Baker RA (ed) Contaminants and sediments, Vol 2. Analysis, chemistry, biology. Ann Arbor Science Publishers, Ann Arbor, MI, p 555–606

Lohrer AM, Thrush SF, Gibbs MM (2004) Bioturbators enhance ecosystem function through complex biogeochemical interactions. Nature 431:1092–1095

Lohrer AM, Thrush SF, Hunt L, Hancock N, Lundquist C (2005) Rapid reworking of subtidal sediments by burrowing spatangoid urchins. J Exp Mar Biol Ecol 321:155–169

Lopez GR, Levington JS (1987) Ecology of deposit-feeding animals in marine sediments. Q Rev Biol 62:235–260

Madsen S, Forbes TL, Forbes VE (1997) Particle mixing by the polychaete *Capitella* sp. I: coupling fate and effect of a particle-bound organic contaminant (fluoranthene) in a marine sediment. Mar Ecol Prog Ser 147:129–142

Mahaut ML, Graf G (1987) A luminophore tracer technique for bioturbation studies. Oceanol Acta 10:323–328

Mahon HK, Dauer DM (2005) Organic coatings and ontogenetic particle selection in *Streblospio benedicti* Webster (Spionidae: Polychaeta). J Exp Mar Biol Ecol 323:84–92

Maire O, Duchêne JC, Rosenberg R, Braga de Mendonça J Jr, Grémare A (2006) Effects of food availability on sediment reworking in *Abra ovata* and *A. nitida.* Mar Ecol Prog Ser 319:135–153

Maire O, Duchêne JC, Grémare A, Malyuga VS, Meysman FJR (2007a) A comparison of sediment reworking rates by the surface deposit-feeding bivalve *Abra ovata* during summertime and wintertime, with a comparison between two models of sediment reworking. J Exp Mar Biol Ecol 343:21–36

Maire O, Duchêne JC, Bigot L, Grémare A (2007b) Linking feeding activity and sediment reworking in the deposit-feeding bivalve *Abra ovata* with image analysis, laser telemetry, and luminophore tracers. Mar Ecol Prog Ser 351:139–150

Maire O, Duchêne JC, Amouroux JM, Grémare A (2007c) Activity patterns in the terebellid polychaete *Eupolymnia nebulosa* assessed using a new image analysis system. Mar Biol 151:737–749

Meile C, van Cappellen P (2005) Particle age distribution and O_2 exposure time: time scales in bioturbated sediments. Global Biogeochem Cycles 19:GB3013

Mermillod-Blondin F, Marie S, Desrosiers G, Long B, de Montety L, Michaud E, Stora G (2003) Assessment of the spatial variability of intertidal benthic communities by axial tomodensitometry: importance of fine-scale heterogeneity. J Exp Mar Biol Ecol 287:193–208

Mermillod-Blondin F, François-Carcaillet F, Rosenberg R (2005) Biodiversity of benthic invertebrates and organic matter processing in shallow marine sediments: an experimental study. J Exp Mar Biol Ecol 315:187–209

Meysman FJR, Boudreau BP, Middelburg JJ (2003) Relations between local, nonlocal, discrete and continuous models of bioturbation. J Mar Res 61:391–410

Meysman FJR, Galaktionov OS, Gribsholt B, Middelburg JJ (2006) Bio-irrigation in permeable sediments: an assessment of model complexity. J Mar Res 64:589–627

Meysman FJR, Malyuga VS, Boudreau BP, Middelburg JJ (2007) The influence of porosity gradients on mixing coefficients in sediments. Geochim Cosmochim Acta 71: 961–973

Meysman FJR, Malyuga VS, Boudreau BP, Middelburg JJ (2008) Quantifying particle dispersal in aquatic sediments at short time scales: model selection. Aquat Biol 2:239–254

Miller RJ, Smith CR, DeMaster DJ, Fornes WL (2000) Feeding selectivity and rapid particle processing by deep-sea megafaunal deposit feeders: a ^{234}Th tracer approach. J Mar Res 58:653–673

Mugnai C, Gérino M, Frignani M, Sauvage S, Bellucci LG (2003) Bioturbation experiments in the Venice Lagoon. Hydrobiologia 494:245–250

Mulsow S, Landrum PF, Robbins JA (2002) Biological mixing responses to sublethal concentrations of DDT in sediments by *Heteromastus filiformis* using a ^{137}Cs marker layer technique. Mar Ecol Prog Ser 239:181–191

Nichols FH (1974) Sediment turnover by a deposit-feeding polychaete. Limnol Oceanogr 19:945–950

Olmez I, Pink FX, Wheatcroft RA (1994) New particle-labelling technique for use in biological and physical sediment transport studies. Environ Sci Technol 28: 1487–1490

Ouellette D, Desrosiers G, Gagne JP, Gilbert F, Poggiale JC, Blier PU, Stora G (2004) Effects of temperature on *in vitro* sediment reworking processes by a gallery biodiffusor, the polychaete *Neanthes virens.* Mar Ecol Prog Ser 266: 185–193

Peng TH, Broecker WS, Berger WH (1979) Rates of benthic mixing in deep sea sediments as determined by radioactive tracers. Quat Res 11:141–149

Pope RH, Demaster DJ, Smith CR, Seltman HJ (1996) Rapid bioturbation in equatorial Pacific sediments: evidence from excess ^{234}Th measurements. Deep-Sea Res II 43: 1339–1364

Rabouille C, Gaillard JF (1991) A coupled model representing the deep-sea organic carbon mineralization and oxygen consumption in surficial sediments. J Geophys Res 96: 2761–2776

Reed DC, Huang K, Boudreau BP, Meysman FJR (2006) Steady-state tracer dynamics in a lattice-automaton model of bioturbation. Geochim Cosmochim Acta 70:5855–5867

Rhoads DC (1963) Rates of sediment reworking by *Yoldia limatula* in Buzzards Bay, Massachusetts, and Long Island Sound. J Sediment Petrol 33:723–727

Rhoads DC (1967) Biogenic reworking of intertidal and subtidal sediments in Barnstable Harbor and Buzzards Bay, Massachusetts. J Geol 75:461–476

Rhoads DC (1974) Organism-sediment relations on the muddy sea floor. Oceanogr Mar Biol Annu Rev 12:263–300

Rice DL (1986) Early diagenesis in bioadvective sediments: relationships between the diagenesis of beryllium-7, sediment reworking rates, and the abundance of conveyor-belt deposit-feeders. J Mar Res 44:149–184

Robbins JA (1986) A model for particle-selective transport of

tracers in sediments with conveyor-belt deposit feeders. J Geophys Res 91:8542–8558

Rosenberg R, Davey E, Gunnarsson J, Norling K, Frank M (2007) Application of computer-aided tomography to visualize and quantify biogenic structures in marine sediments. Mar Ecol Prog Ser 331:23–34

Rosenberg R, Grémare A, Duchême JC, Davey E, Frank M (2008) 3D visualization and quantification of marine benthic biogenic structures and particle transport utilizing computer-aided tomography. Mar Ecol Prog Ser (in press)

Rowden AA, Jago CF, Jones SE (1998) Influence of benthic macrofauna on the geotechnical and geophysical properties of surficial sediment, North Sea. Cont Shelf Res 18: 1347–1363

Roy H, Huettel M, Jorgensen BB (2002) The role of small-scale sediment topography for oxygen flux across the diffusive boundary layer. Limnol Oceanogr 47:837–847

Roy H, Huettel M, Jorgensen BB (2005) The influence of topography on the functional exchange surface of marine soft sediments, assessed from sediment topography measured *in situ*. Limnol Oceanogr 50:106–112

Sandnes J, Forbes T, Hansen R, Sandnes B, Rygg B (2000a) Bioturbation and irrigation in natural sediments, described by animal-community parameters. Mar Ecol Prog Ser 197:169–179

Sandnes J, Forbes T, Hansen R, Sandnes B (2000b) Influence of particle type and faunal activity on mixing of di(2-ethylhexyl)phthalate (DEHP) in natural sediments. Mar Ecol Prog Ser 197:151–167

Schmidt S, Gonzales JL, Lecroart P, Tronczynski J, Billy I, Jouanneau JM (2007) Bioturbation at the water–sediment interface of the Thau Lagoon: impact of shellfish farming. Aquat Living Resour 20:163–169

Sharma P, Gardner LR, Moore WS, Bollinger MS (1987) Sedimentation and bioturbation in a salt marsh as revealed by ^{210}Pb, ^{137}Cs, and ^{7}Be studies. Limnol Oceanogr 32:313–326

Shull DH (2001) Transition-matrix model of bioturbation and radionuclide diagenesis. Limnol Oceanogr 46:905–916

Shull DH, Yasuda M (2001) Size-selective downward particle transport by cirratulid polychaetes. J Sea Res 59:453–473

Smith JN, Boudreau BP, Noshkin V (1986) Plutonium and ^{210}Pb distribution in northeast Atlantic sediments: subsurface anomalies caused by non-local mixing. Earth Planet Sci Lett 81:15–28

Smith CR, Pope RH, DeMaster DJ, Magaard L (1993) Age-dependent mixing of deep-sea sediments. Geochim Cosmochim Acta 57:1473–1488

Soetaert K, Herman PMJ, Middelburg JJ, Heip C and others (1996) Modelling ^{210}Pb-derived mixing activity in ocean margin sediments: diffusive versus non local mixing. J Mar Res 54:1207–1227

Solan M, Wigham BD (2005) Biogenic particle reworking and bacterial–invertebrate interactions in marine sediments. In: Kristensen E, Haese RR, Kostka JE (eds) Interactions between macro- and microorganisms in marine sediments. Coastal and Estuarine Studies 60, American Geophysical Union, Washington, DC, p 105–124

Solan M, Wigham BD, Hudson IR, Kennedy R and others (2004) *In situ* quantification of bioturbation using time-lapse fluorescent sediment profile imaging (f-SPI), luminophore tracers and model simulation. Mar Ecol Prog Ser 271:1–12

Stephens MP, Kadko DC, Smith CR, Latasa M (1997) Chlorophyll-*a* and pheopigments as tracers of labile organic carbon at the central equatorial Pacific seafloor. Geochim Cosmochim Acta 61:4605–4619

Stordal MC, Johnson JW, Guinasso NL, Schink DR (1985) Quantitative evaluation of bioturbation rates in deep ocean sediments. II. Comparison of rates determined by ^{210}Pb and ^{239,240}Pu. Mar Chem 17:99–114

Suchanek TH, Colin PL, McMurty GM, Suchanek CS (1986) Bioturbation and redistribution of sediment radionuclides in Enewetak Atoll lagoon by callianassid shrimp: biological aspects. Bull Mar Sci 38:144–154

Sun M, Aller RC, Lee C (1991) Early diagenesis of chlorophyll-*a* in Long Island Sound sediments: a measure of carbon flux and particle reworking. J Mar Res 49:379–401

Sun MY, Lee C, Aller RC (1993) Laboratory studies of oxic and anoxic degradation of chlorophyll *a* in Long Island Sound sediments. Geochim Cosmochim Acta 57:147–157

Taghon GL (1982) Optimal foraging by deposit-feeding invertebrates: roles of particle size and organic coating. Oecologia 52:295–304

Thomson J, Colley S, Weaver PPE (1988) Bioturbation into a recently emplaced deep-sea turbidite surface as revealed by $^{210}Pb_{excess}$, $^{230}Th_{excess}$ and planktonic foraminifera distributions. Earth Planet Sci Lett 90:157–173

Thomson J, Brown L, Nixon S, Cook GT, MacKenzie AB (2000) Bioturbation and Holocene sediment accumulation fluxes in the north-east Atlantic Ocean (benthic boundary layer experiment sites). Mar Geol 169:21–39

Turnewitsch R, Witte U, Graf G (2000) Bioturbation in the abyssal Arabian Sea: influence of fauna and food supply. Deep-Sea Res II 47:2877–2911

van Cappellen P, Wang Y (1996) Cycling of iron and manganese in surface sediments: a general theory for the coupled transport and reaction of carbon, oxygen, nitrogen, sulfur, iron, and manganese. Am J Sci 296:197–243

Wheatcroft RA (1991) Conservative tracer study of horizontal sediment mixing rates in a bathyal basin, California borderland. J Mar Res 49:565–588

Wheatcroft RA (2006) Time-series measurements of macrobenthos abundance and sediment bioturbation intensity on a flood-dominated shelf. Prog Oceanogr 71:88–122

Wheatcroft RA, Jumars PA, Smith CR, Nowell ARM (1990) A mechanistic view of the particulate biodiffusion coefficient: step lengths, rest periods and transport directions. J Mar Res 48:177–207

Wheatcroft RA, Olmez I, Pink FX (1994) Particle bioturbation in Massachusetts Bay: preliminary results using a new deliberate tracer technique. J Mar Res 52:1129–1150

White DS, Klahr PC, Robbins JA (1987) Effects of temperature and density on sediment reworking by *Stylodrilus heringianus* (Oligochaeta: Lumbriculidae). J Gt Lakes Res 13: 147–156

Submitted: October 1, 2007; Accepted: March 12, 2008

Proofs received from author(s): May 26, 2008

Vol. 2: 239–254, 2008
doi: 10.3354/ab00054

AQUATIC BIOLOGY
Aquat Biol

Printed June 2008
Published online June 19, 2008

Contribution to the Theme Section 'Bioturbation in aquatic environments: linking past and present'

OPEN ACCESS

Quantifying particle dispersal in aquatic sediments at short time scales: model selection

Filip J. R. Meysman[1,2,*], Volodymyr S. Malyuga[1], Bernard P. Boudreau[3], Jack J. Middelburg[1]

[1]The Netherlands Institute of Ecology (NIOO-KNAW), Centre for Estuarine and Marine Ecology, PO Box 140, 4400 AC Yerseke, The Netherlands

[2]Department of Analytical and Environmental Chemistry, Vrije Universiteit Brussel (VUB), Pleinlaan 2, 1050 Brussel, Belgium

[3]Department of Oceanography, Dalhousie University, Halifax, Nova Scotia B3H 4J1, Canada

ABSTRACT: In a pulse-tracer experiment, a layer of tracer particles is added to the sediment–water interface, and the down-mixing of these particles is followed over a short time scale. Here, we compared different models (biodiffusion, telegraph, CTRW) to analyse the resulting tracer depth profiles. The biodiffusion model is widely applied, but entails 2 problems: (1) infinite propagation speed—the infinitely fast propagation of tracer to depth, and (2) infinitely short waiting times—mixing events follow each other infinitely fast. We show that the problem of waiting times is far more relevant to tracer studies than the problem of propagation speed. The key issue in pulse-tracer experiments is that models should explicitly account for a finite waiting time between mixing events. The telegraph equation has a finite propagation speed, but it still assumes infinitely short waiting times, and, hence, it does not form a suitable alternative to the biodiffusion model. Therefore, we advance the continuous-time random walk (CTRW), which explicitly accounts for finite waiting times between mixing events, as a suitable description of bioturbation. CTRW models are able to cope with lateral spatial heterogeneity in reworking, which is a crucial feature of bioturbation at short time scales. We show how existing bioturbation models (biodiffusion model, telegraph equation, non-local exchange model) can be considered as special cases of the CTRW model. Accordingly, the CTRW model is not a new bioturbation model, but a generalization of existing models.

KEY WORDS: Bioturbation · Diffusion · Luminophores · Modelling · Continuous-time random walk

INTRODUCTION

Aquatic sediments are continuously reworked due to the activity of local infauna, a process typically referred to as bioturbation (Richter 1952). Bioturbation results from a wide range of animal behaviours, such as burrow and tube excavation (including the ultimate collapse and refilling of these tubes), feeding and defecation, crawling and ploughing through the sediment, the building of mounds and the digging of craters (Rhoads 1974, Cadée 2001, Solan & Wigham 2005). Bioturbation also forms the driving force for the dispersal of various solid particles, which can be both mineral (e.g. organic matter, metal oxides and contaminants) as well as biological (e.g. bacteria, viruses, cysts and resting stages of plankton) in nature. As a consequence, bioturbation plays a crucial role in the geochemistry and ecology of aquatic sediments (Aller & Yingst 1978, Aller 1988, Meysman et al. 2006). To further our understanding of these subsurface environments, it is of prime interest to quantitatively describe the particle dispersal induced by bioturbation.

To date, the most commonly employed bioturbation model is the biodiffusion analogy, which assumes that Fick's laws of diffusion are applicable to macrofauna-induced particle dispersal (Goldberg & Koide 1962, Guinasso & Schink 1975, Boudreau 1986). By fitting suitable solutions of the biodiffusion model to tracer

*Email: filip.meysman@vub.ac.be

depth profiles, the mixing intensity is quantified by a single parameter, the diffusion coefficient D_b. In recent years, the validity and accuracy of the biodiffusion model has, however, been questioned for different reasons (Boudreau 1989, Meysman et al. 2003, Reed et al. 2006). A first issue was brought up by Boudreau (1989), who noted that the biodiffusion model inherently has an infinite speed of signal propagation. Immediately after releasing a tracer pulse, the biodiffusion model will predict that the tracer is already present far away from the source, which is physically unrealistic. This means that the biodiffusion model will generate biased predictions at short time spans. Okubo (1971) illustrated this problem for oceanic turbulence: if one releases 2 kg of salt off the coast of California, a diffusive model of turbulence would predict to find 1 molecule in 500 l of water off the coast of Japan in 15 mo. This molecule then would have travelled with a mean velocity of 25 cm s^{-1}, which is highly unrealistic. Accordingly, to describe natural mixing processes at short time scales, models with a finite signal propagation velocity are preferential from a theoretical point of view. In this light, Boudreau (1989) suggested that the telegraph equation (see below Eq. 33) could be an alternative to the diffusion equation. The telegraph equation has indeed a finite velocity of signal propagation (Monin 1959, Okubo 1971), and, hence, it would resolve the problem of unphysical fast penetration of tracer at depth. Yet up to present, the telegraph equation has not been applied in bioturbation studies.

A second objection to the biodiffusion model was advanced by Meysman et al. (2003): its assumptions are violated at short time scales. But how 'short' is a short time scale? Based on a theoretical analysis of random-walk models, it was argued that the biodiffusion model requires that the inherent time scale of the mixing process should be considerably smaller than the observational time scale. The inherent time scale of the mixing process then refers to the average time interval between 2 displacements of a particle. In contrast, the observational time scale denotes the period over which bioturbation is studied. In other words, Meysman et al. (2003) argued that the biodiffusion model can only be used when the observational period is long enough so that it 'captures' a sufficiently large number of mixing events. This 'frequency' constraint is illustrated by the following hypothetical example. Suppose that bioturbation is studied at a given site with the common radiotracer methods ^{234}Th and ^{210}Pb, which have respective half-lives of 24.1 d and 22.3 yr. The observational time scale is proportional to the half-life of the tracer, because the characteristic period over which radiotracer-coated particles still can be followed is about 5 times the half-life. Constraining the time scale of the mixing is more difficult, because at present we do not have accurate estimates of the time interval between displacements in natural environments (this is one of the major challenges in bioturbation research—see Maire et al. 2007). But let us assume that particles are moved once every day on average. Accordingly, the 'captured' number of particle displacement events greatly differs between the 2 methods: 8140 events for ^{210}Pb, but only 24 events for ^{234}Th. Accordingly, compared to the mixing time scale of 1 d, ^{234}Th is qualified as a short time scale method, while the ^{210}Pb method classifies as a long time scale method. This emphasizes the relative nature of the term 'short': short means short with respect to the inherent time scale of the mixing, which may drastically vary between environments (e.g. deep sea versus coastal sediments).

So why would the biodiffusion model in the example above be more suited to analyse the ^{210}Pb activity profile as opposed to the ^{234}Th profile? The prime reason is that the biodiffusion model implicitly assumes that mixing events follow each other infinitely fast, so that infinitely many mixing events are thought to take place within the observational period. When particle dispersal is observed over sufficiently long time scales (e.g. with long-lived radiotracers such as ^{210}Pb), the time between 2 mixing events is small compared to the period of observation, and so the idealization of infinitely frequent mixing may be justified. However, when particle dispersal is observed over shorter time scales (e.g. with short-lived radiotracers such as ^{234}Th), the observed number of mixing events is reduced, and so the biodiffusion model may no longer be applicable. Recently, Reed et al. (2006) convincingly demonstrated this breakdown of the biodiffusion model at short time scales using a lattice-automaton model environment (this is basically a virtual sediment environment in which bioturbation experiments can be simulated). These simulations revealed that biodiffusion coefficients estimated from steady-state profiles of short-lived isotopes showed a conspicuous tracer dependence. Overall, biodiffusion coefficients based on short-lived isotopes were strongly biased towards larger values and had large standard deviations.

As in the case of methods based on steady-state profiles of short-lived isotopes, pulse-tracer experiments typically have short observation windows. Because the time scale of experiments is tuned to the expected time scale of mixing, observation times range from 1 d in coastal areas (e.g. Fornes et al. 1999, Solan et al. 2004) over 1 mo in laboratory microcosms (e.g. Fernandes et al. 2006) to 1 yr in the deep sea (Wheatcroft 1991). In the pulse-tracer method, a layer of tracer particles is deposited onto the sediment–water interface (SWI), and its subsequent down-mixing into the sediment is followed. Typical tracer particles are inert particles, such as glass beads (e.g. Shull & Yasuda 2001) and

fluorescent luminophores (Mahaut & Graf 1987), or particles tagged with short-lived radionuclides (Fornes et al. 1999, 2001). The final output of a tracer-pulse experiment is a set of tracer-depth profiles, collected at different time intervals. Our principal aim here is to examine what model is most appropriate for analyzing such tracer profiles. Is the biodiffusion model applicable, or should we search for alternative model formulations?

To examine this, we compared the performance of the biodiffusion model to 2 alternative models: (1) the telegraph equation, which was proposed by Boudreau (1989) on theoretical grounds, but the applicability of which as a bioturbation model has not been examined yet; (2) the continuous-time random-walk (CTRW) model, which has recently received substantial attention in the field of statistical physics (Metzler & Klafter 2000). We examined the CTRW model as a new alternative to the biodiffusion model. The CTRW bioturbation model, which is presented in detail here, has been applied by Maire et al. (2007) to analyse luminophore data obtained via a high-resolution imaging technique. This work revealed that the CTRW model provided better and more robust fits to the data than the biodiffusion model, particularly at short time scales. Here, our main ambition is to provide a theoretical framework for these results: Why does the CTRW perform better at short time scales and how does it relate to classical bioturbation models such as the biodiffusion and non-local exchange models? In a first step, we detail the model formulation and numerical solution of the CTRW model. In a second step, we show how the biodiffusion and telegraph models can be obtained as limiting cases of the CTRW model, and how the assumptions of an infinite signal propagation speed and infinite mixing frequency are linked to these limiting conditions. In a final step, we perform simulations of a pulse-tracer experiment and compare the simulation output of the biodiffusion, telegraph and general CTRW models.

MODEL FORMULATION

Modelling approach

Many different organisms are present in the sediment, and each organism displays a range of different particle displacement activities, thus providing an insurmountable number of possibilities for the movement of a given particle. Because of this complexity, we cannot deterministically describe the motion of each single particle in the sediment. A convenient solution to this problem is to assume that the interplay between particles and biological activity is sufficiently erratic, so that a particle's motion can be described as a random process (Boudreau 1986, Wheatcroft et al. 1990, Meysman et al. 2003). Adopting a stochastic perspective, particle dispersal due to bioturbation can be regarded as a random walk, which is essentially a mathematical formalization of the intuitive idea of taking successive steps, each in a random direction (Hughes 1995). The consecutive movement of a bioturbated particle is principally governed by 3 quantities: (1) the jump direction, (2) the jump distance and (3) the waiting time between jumps or bioturbation events. Each of these quantities can be modelled in either a deterministic or a stochastic way, and, depending on these choices, one will obtain different random-walk models. When all variables (jump direction, jump distance and waiting time) are true stochastic variables, each modelled by a suitable probability distribution, the resulting description of particle dispersal is referred to as a continuous-time random walk (CTRW).

General CTRW formulation

From a stochastic perspective, one can regard particle displacement as a random sequence of bioturbation events, e.g. the infilling of a burrow or the passage of a crawling organism. In this view, a bioturbated particle displays 2 types of 'behaviour': (1) 'jumping' to a new location during a given bioturbation event and (2) 'waiting' at a given location until the next bioturbation event occurs (Fig. 1). When casting this into a mathematical model, 2 basic parameters need specification: (1) the jump vector **J**, i.e. the direction and distance a particle travels in a given jump, and (2) the waiting time T, i.e. the time a particle waits between 2 jumps. In the analogy of the wandering drunkard, the vector **J**

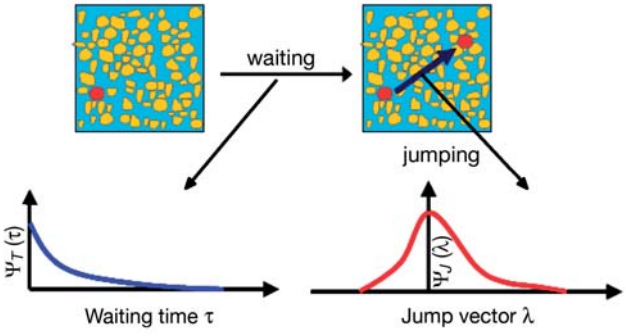

Fig. 1. Idealization of particle displacement as a position jump process. Particles display 2 behavioural modes: long waits (waiting time T) and fast jumps (jump vector **J**, which in 1 dimension becomes the jump length λ). In a continuous-time random-walk model, these 2 quantities are described by a probability distribution function termed the waiting time and jump vector distribution, respectively

models the actual steps that are taken, while T represents the time the drunkard hesitates between steps. The CTRW model (Montroll & Weiss 1965, Hughes 1995, Metzler & Klafter 2000) assumes that both the jump vector $\mathbf{J}$ and the waiting time T are drawn from a joint probability distribution function (PDF). When a particle is located at point $\mathbf{x}'$ at time t', the probability of finding this particle at the new location $\mathbf{x}$ at a later time t is given by the so-called jump distribution (Metzler & Klafter 2000) such that:

$$\Psi(\mathbf{x},t;\mathbf{x}',t')\mathrm{d}t\,\mathrm{d}\mathbf{x} = \Pr\{t-t' < T < t+\mathrm{d}t-t';\ \mathbf{x}-\mathbf{x}' < \mathbf{J} < \mathbf{x}+\mathrm{d}\mathbf{x}-\mathbf{x}'\} \quad (1)$$

The notation Pr{…} refers to the probability that a certain 'event' takes place (see general texts on stochastic processes and multivariate distributions, e.g. Gardiner 2002). The actual form of the jump vector $\mathbf{J}$ will depend on the dimensionality of the problem and the coordinate system in use. In the general 3-dimensional case, the position jump model will incorporate 4 degrees of freedom, i.e. 3 spatial (the 3 components of $\mathbf{J}$) and 1 temporal (T). In 3D Cartesian coordinates, the jump vector is then given by $\mathbf{J} = \mathbf{J}(L_x,L_y,L_z)$, where L_x, L_y and L_z denote the jump lengths along the x-, y- and z-axis, respectively, each having a range $-\infty \le L \le +\infty$.

Simplifying assumptions

The idea is now to develop the general CTRW description (Eq. 1) into an actual bioturbation model. In doing so, we adopt some suitable simplifications (see Meysman et al. 2008) for an in-depth discussion of these idealizations. Firstly, the probability distribution Ψ remains invariant with time (temporal homogeneity) and does not vary over the spatial domain (spatial homogeneity). Secondly, the jump vector $\mathbf{J}$ and the waiting time T are considered independent variables, and, as a result, the joint probability distribution Ψ can be decomposed into 2 separate units such that:

$$\Psi(\mathbf{x},t;\mathbf{x}',t')\mathrm{d}t\mathrm{d}\mathbf{x} = \Psi_T(t;t')\Psi_{\mathbf{J}}(\mathbf{x};\mathbf{x}')\mathrm{d}t\mathrm{d}\mathbf{x} \quad (2)$$

where $\Psi_{\mathbf{J}}$ is referred to as the jump vector distribution and Ψ_T is the waiting time distribution. Thirdly, our bioturbation models are restricted to 1 dimension, a constraint that results from the type of data that are normally available (tracer depth profiles). We use a single coordinate x that represents the depth into the sediment. As particles can only travel in 1 dimension, the jump vector $\mathbf{J}$ is represented in the Euclidean form $\mathbf{J}(L,0,0)$, where the scalar quantity L is usually referred to as the jump length (Metzler & Klafter 2000). Note that the jump length L can be either positive or negative, and, hence, it also accounts for the direction of particle movement. The value of L is positive when the direction of the jump coincides with the direction of the x-axis (particles move downwards into the sediment) and is negative otherwise (particles move upwards). When a given particle is located at point x' at time t', the probability of finding a particle within the interval $(x, x+\mathrm{d}x)$ at some time from $(t, t+\mathrm{d}t)$ can be written as:

$$\Psi(x,t;x',t')\mathrm{d}t\mathrm{d}x = \Psi_T(t-t')\Psi_L(x-x')\mathrm{d}t\mathrm{d}x = \Psi_T(\tau)\Psi_L(\lambda)\mathrm{d}\tau\mathrm{d}\lambda \quad (3)$$

Eq. (3) is the implementation of the general model (Eq. 2) in 1 dimension. The first factor on the right is again the waiting time distribution with $\tau \equiv t - t'$. The second factor is the jump length distribution with $\lambda \equiv x - x'$. Both the waiting time and jump length distributions are now of the convolutive form. Note that Eq. (3) still allows for drift. This can occur when the jump length distribution is non-symmetric, i.e. $\Psi_L(-\lambda) \neq \Psi_L(\lambda)$, although here we will mainly consider symmetric distributions.

Governing equations

The jump distribution (Eq. 3) describes the effect of a single bioturbation event on the location of a single particle. To quantify the effect of many bioturbation events on a single particle, we can release a certain particle at the origin and analyse the evolution of position. The probability $P(x,t|0,0)$ of finding such a particle at depth x after some time t is given (Othmer et al. 1988, Meysman et al. 2008) as:

$$P(x,t\,|\,0,0) = \delta(x)\left[1-\int_0^t \Psi_T(\tau)\mathrm{d}\tau\right] + \int_0^t\int_{-\infty}^{\infty} \Psi_T(\tau)\Psi_L(\lambda)P(x-\lambda,t-\tau|0,0)\mathrm{d}\lambda\mathrm{d}\tau \quad (4)$$

where $\delta(x)$ is the Dirac delta function. Eq. (4) is termed a renewal equation, and describes the stochastic behaviour of a single particle after many bioturbation events (Othmer et al. 1988). The first term on the right-hand side of Eq. (4) expresses the probability that a particle remains 'unmoved' at the origin. The second (integral) term accounts for the 'behaviour' of the particle when it effectively leaves its initial position. The renewal equation (Eq. 4) thus represents a *stochastic* model for the position of a *single* particle. However, the goal of any bioturbation model is to *deterministically* describe the effect of many bioturbation events on the location of *many* particles. To go from the 'stochastic/single particle' level to the 'deterministic/many particles' level, we can invoke the law of large numbers (Feller 1968). This law basically implies that the average of a random sample from a large population is likely to be close to the mean of the whole population. Invoking the law of large numbers, the concentration

of particles at an arbitrary location and time can be expressed as:

$$C(x,t) = C_0(x)\left[1-\int_0^t \Psi_T(\tau)\mathrm{d}\tau\right] + \int_0^t \int_{-\infty}^{\infty} \Psi_T(\tau)\Psi_L(\lambda)C(x-\lambda,t-\tau)\mathrm{d}\lambda\mathrm{d}\tau \quad (5)$$

where the initial concentration distribution of particles is given by:

$$C_0(x) = C(x,0) \quad (6)$$

The initial value problem as specified by Eqs. (5) & (6) forms the complete statement of our CTRW model of bioturbation. Given a particular waiting time PDF $\Psi_T(\tau)$ and a step length PDF $\Psi_L(\lambda)$, Eq. (5) will predict how the initial tracer profile $C_0(x)$ will evolve with time. Together, the distributions $\Psi_T(\tau)$ and $\Psi_L(\lambda)$ may be regarded as the 'bioturbation fingerprint' for a given macrofaunal community. Obviously, this fingerprint will depend on the organisms that are present (species composition, size, abundance) and on the specific activities involved (e.g. deposit-feeding, burrowing).

Reflection at the sediment–water interface (SWI)

Until now, we have implicitly assumed that the jump distribution (Eq. 3) applies to the infinite domain $-\infty < x < \infty$, and we will refer to the associated jump length distribution as Ψ_L^{inf}. In reality, however, the sediment is bounded by the SWI, and so particle dispersal only occurs within the semi-infinite domain $0 < x < \infty$. Here, we do not consider the removal of particles due to resuspension or erosion, nor the increase of particles due to sedimentation. So, any particle that is transported across the SWI must return to the bioturbated zone. Particles ejected from the sediment will settle in a random fashion at the SWI. A realistic description of this process would, however, drastically increase the mathematical complexity of the model. To avoid such complexity, we adopt the most parsimonious boundary condition: the SWI acts as a perfectly reflective barrier. Moreover, this idealization does not influence the discussion and conclusions arrived upon below. Mathematically, this reflection implies that the original jump length distribution Ψ_L^{inf} is mirrored around the origin, and that the mirrored 'tail' is added to the original jump length distribution (Fig. 2). The probability that a particle starts at x' and arrives within the interval $(x,\ x+\mathrm{d}x)$ is now composed of 2 parts: the chance that it moves to this interval directly, and the chance that it moves indirectly to $(x,\ x+\mathrm{d}x)$ after reflection at the SWI. The latter probability is the same as that it would start at x' and arrive within the neighbourhood of $-x$:

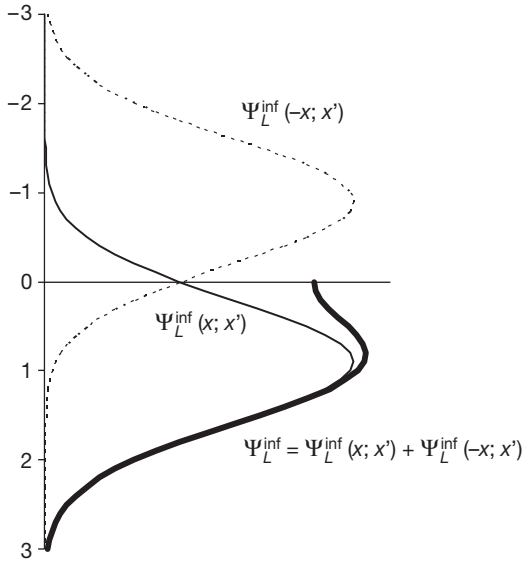

Fig. 2. Reflection of particles at the sediment–water interface. The jump length distribution consists of the sum of 2 components: one part accounts for direct travel, the other part accounts for reflected particles

$$\Psi_L(x;x') = \Psi_L^{\mathrm{inf}}(x;x') + \Psi_L^{\mathrm{inf}}(-x;x') \quad (7)$$

Using the convolutive form of Eq. (3) and implementing the coordinate change $\lambda \equiv x - x'$, we directly obtain:

$$\Psi_L(\lambda) = \Psi_L^{\mathrm{inf}}(\lambda) + \Psi_L^{\mathrm{inf}}(-2x+\lambda) \quad (8)$$

This new jump length distribution Ψ_L must only be implemented over the semi-infinite domain $0 \le x < \infty$. Accordingly, the initial conditions (Eq. 6) only apply to the semi-infinite domain, and the upper boundary of integration in Eq. (5) should be adapted, so that the variable λ starts at $-\infty$ and only runs to x:

$$C(x,t) = C_0(x)\left[1-\int_0^t \Psi_T(\tau)\mathrm{d}\tau\right] + \int_0^t \int_{-\infty}^{x} \Psi_T(\tau)[\Psi_L^{\mathrm{inf}}(\lambda) + \Psi_L^{\mathrm{inf}}(-2x+\lambda)]C(x-\lambda,t-\tau)\mathrm{d}\lambda\mathrm{d}\tau \quad (9)$$

This integral equation forms the statement of our CTRW model of bioturbation. In the general case, Eq. (9) should be solved numerically. However, under the special condition that the jump length time distribution Ψ_L^{inf} is symmetrical (as we assume here), one can transform Eq. (9) into a form that allows a simplified numerical solution. To see this, we first introduce the coordinate $z = x - \lambda$, so that Eq. (9) becomes:

$$C(x,t) = C_0(x)\left[1-\int_0^t \Psi_T(\tau)\mathrm{d}\tau\right] + \int_0^t \int_0^{\infty} \Psi_T(\tau)\Psi_L^{\mathrm{inf}}(x-z)C(z,t-\tau)\mathrm{d}z\mathrm{d}\tau + \int_0^t \int_0^{\infty} \Psi_T(\tau)\Psi_L^{\mathrm{inf}}(-x-z)C(z,t-\tau)\mathrm{d}z\mathrm{d}\tau \quad (10)$$

Using the symmetry of the jump length distribution $\Psi_L^{\inf}(-x-z) = \Psi_L^{\inf}(x+z)$, and changing the integration variable from z to $(-z)$ in the second integral, this expression is re-arranged to:

$$C(x,t) = C_0(x)\left[1-\int_0^t \Psi_T(\tau)\mathrm{d}\tau\right] + \int_0^t\int_0^\infty \Psi_T(\tau)\Psi_L^{\inf}(x-z)C(z,t-\tau)\mathrm{d}z\mathrm{d}\tau + \int_0^t\int_{-\infty}^0 \Psi_T(\tau)\Psi_L^{\inf}(x-z)C(-z,t-\tau)\mathrm{d}z\mathrm{d}\tau \quad (11)$$

In Eq. (11), the concentration $C(x,t)$ is still only defined over the semi-infinite domain $0 \le x < \infty$. We now introduce a new concentration $\overline{C}$ over the whole infinite domain:

$$\overline{C}(x,t) = \begin{cases} C(x,t) & \text{when } x \ge 0 \\ C(-x,t) & \text{when } x < 0 \end{cases} \quad (12)$$

Reversing the coordinate definition $z = x - \lambda$ from above, Eq. (11) can be rewritten as:

$$\overline{C}(x,t) = \overline{C}_0(x)\left[1-\int_0^t \Psi_T(\tau)\mathrm{d}\tau\right] + \int_0^t\int_{-\infty}^\infty \Psi_T(\tau)\Psi_L^{\inf}(\tau)\overline{C}(x-\lambda,t-\tau)\mathrm{d}\lambda\mathrm{d}\tau \quad (13)$$

Remarkably, the integral Eq. (13), stated in terms of $\overline{C}$, is identical to the original form (Eq. 5), stated in terms of C, which, however, did not account for the SWI. Nonetheless, the solution is not the same. The difference is that the original initial conditions C_0 (as defined in Eq. 6) should be mirrored around the origin to arrive at the new initial conditions $\overline{C}_0$:

$$\overline{C}_0(x) = \begin{cases} C_0(x) & \text{when } x \ge 0 \\ C_0(-x) & \text{when } x < 0 \end{cases} \quad (14)$$

Accordingly, by a simple reflection of the initial conditions C_0 around the origin, we are able to explicitly account for the presence of the SWI. This is the way the CTRW problem is solved here. For notational simplicity, we will from now on drop the bar symbols above the concentrations, and drop the 'inf' superscript for the jump length distribution.

MODEL SOLUTION

The solution of the initial value problem (Eqs. 13 & 14) is obtained via a semi-analytical solution procedure, which involves a Fourier transformation to the spatial coordinate and a Laplace transformation to the time coordinate. In the transformed plane, the problem is then solved analytically. To arrive at the final solution in the original (x,t) plane, the resulting Fourier and Laplace integrals need to be evaluated numerically.

Fourier and Laplace transforms

In a first step, we can apply the Fourier transform to Eq. (13) with respect to spatial coordinates. Using the convolution theorem, we thus obtain:

$$\hat{C}(k,t) = \hat{C}_0(k)\left[1-\int_0^t \Psi_T(\tau)\mathrm{d}\tau\right] + \int_0^t \Psi_T(\tau)\hat{\Psi}_L(k)\hat{C}(k,t-\tau)\mathrm{d}\tau \quad (15)$$

where the hat notation is used to denote the Fourier transform. In a second step, we apply the Laplace transform to Eq. (15) with respect to time. Again using the convolution theorem, we arrive at:

$$\hat{\tilde{C}}(k,s) = \frac{1}{s}\left[1-\tilde{\Psi}_T(s)\right]\hat{C}_0(k) + \tilde{\Psi}_T(s)\hat{\Psi}_L(k)\hat{\tilde{C}}(k,s) \quad (16)$$

where the tilde notation denotes the Laplace transform. By solving the algebraic equation (Eq. 16), we directly obtain the transform of the unknown concentration profile as:

$$\hat{\tilde{C}}(k,s) = \frac{1-\tilde{\Psi}_T(s)}{s\left[1-\tilde{\Psi}_T(s)\hat{\Psi}_L(k)\right]}\hat{C}_0(k) \quad (17)$$

Upon back transformation of Eq. (17), the concentration profile thus becomes:

$$C(x,t) = \frac{1}{4\pi^2 i}\int_{-\infty}^{\infty}\hat{C}_0(k)\exp(-ikx) \int_{\gamma-j\infty}^{\gamma+j\infty}\frac{1-\tilde{\Psi}_T(s)}{s\left[1-\tilde{\Psi}_T(s)\hat{\Psi}_L(k)\right]}\exp(st)\mathrm{d}s\mathrm{d}k \quad (18)$$

where γ is a real number so that the contour path of integration is in the region of convergence of the Laplace transform.

Numerical evaluation of integrals

Eq. (18) is not solved as such, but is first reformulated in terms of real integrals before numerical integration. This procedure is detailed in Appendix 1, and eventually leads to the integral equation (Eq. A3), which only contains integrals that consist of sums of real Fourier sine and cosine functions. For the evaluation of these integrals, we employed the DQDAWF routine from the IMSL Fortran 90 MP Library Version 4.01. This routine approximates the Fourier integrals by repeated calls to the IMSL routine DQDAWO, which integrates functions $f(x)\sin(\omega x)$ or $f(x)\cos(\omega x)$ over a finite interval, followed by extrapolation. Depending on the length of the subinterval in relation to the value of ω, either a modified Clenshaw-Curtis procedure or a Gauss-Kronrod 7/15 rule is employed by the DQDAWO routine to approximate the integral on a subinterval. In addition, this routine uses the ε-algorithm for the extrapolation. The routines DQDAWF and DQDAWO are implementations of the subroutines QAWF and QAWO, respectively, fully documented by Piessens et al. (1983).

BENCHMARK SOLUTION: BIODIFFUSION

In order to check the accuracy and consistency of the numerical solution procedure, it is useful to compare the numerical solution to a corresponding analytical model solution (model verification). To achieve this, we use a result from random-walk theory with regard to the long-time behaviour of the CTRW model (Eq. 5). Effectively, one can prove (Hughes 1995, Metzler & Klafter 2000) that if the waiting time distribution Ψ_T has a finite mean:

$$\tau_c = \int_0^\infty \tau \Psi_T(\tau) d\tau \quad (19)$$

and the jump length distribution Ψ_L is symmetrical, i.e. $\Psi_L(\lambda) = \Psi_L(-\lambda)$, and has a finite variance:

$$\sigma^2 = \int_{-\infty}^{\infty} \lambda^2 \Psi_L(\lambda) d\lambda \quad (20)$$

then, for sufficiently long times, $t \gg \tau_c$, the solution $C(x,t)$ of the CTRW equation (Eq. 5) will approach the solution of the diffusion equation:

$$\frac{\partial C}{\partial t} = \frac{\sigma^2}{2\tau_c} \frac{\partial^2 C}{\partial x^2} \quad (21)$$

In other words, the long-time effect of bioturbation will always look like diffusive mixing irrespective of the actual bioturbation fingerprint Ψ_T and Ψ_L that characterizes the benthic community. The long-time diffusion equation (Eq. 21) provides the following interpretation of the biodiffusion coefficient:

$$D_b = \frac{\sigma^2}{2\tau_c} \quad (22)$$

The root mean square variance σ of the jump length distribution Ψ_L thus serves as a characteristic length scale of mixing (the average displacement of a particle in a bioturbation event), and mean τ_c of the waiting time distribution Ψ_T thus serves as the characteristic time scale of mixing (the average time between 2 displacements of a particle). This scaling result is similar, but not entirely analogous to previous decompositions of the biodiffusion coefficient in Wheatcroft et al. (1990) and Meysman et al. (2003).

Effectively, the relation between the CTRW model and the biodiffusion model has many facets, and a detailed discussion of these is beyond our scope here (see Meysman et al. 2008). For the present purposes 2 points are important: (1) For each CTRW model, we can construct an associated biodiffusion model that has exactly the same mixing intensity; ultimately, at sufficiently long times, the solutions of the CTRW and biodiffusion models should converge. (2) We can take advantage of the 'diffusive' behaviour of the CTRW model at long times to verify the accuracy of our numerical solution procedure. To this end, we proceed as follows. We first calculate the mean waiting time (Eq. 19) and the jump length variance (Eq. 20) for a given bioturbation fingerprint, i.e. a combination of distributions Ψ_T and Ψ_L. Subsequently, we calculate the biodiffusion coefficient via Eq. (22), and we solve the diffusion equation (Eq. 21) for exactly the same initial conditions (Eq. 6). After a sufficiently long time $t \gg \tau_c$, the solution of the CTRW equation (Eq. 18) should match the solution of the 'diffusive' approximation (Eq. 21).

CONNECTION TO EXISTING BIOTURBATION MODELS

The novelty of the CTRW approach lies in the fact that the waiting time between bioturbation events is no longer fixed, but is instead governed by a probability distribution. Yet the CTRW equation (Eq. 5) is not a 'new' bioturbation model, but a generalization or extension from which existing models can be derived. To show this, we can substitute particular forms of the waiting time distribution Ψ_T within the CTRW model (Eq. 5), and see which bioturbation models are obtained. This analysis will also show how the constraints of an 'infinite signal propagation speed' and an 'infinite mixing frequency' are embedded within bioturbation models.

Poisson processes

A first case of interest is a so-called Poisson process, which applies to sequences of events that are 'randomly spaced in time'. Poisson processes have been used to describe the disintegration of radionuclides, incoming telephone calls, or chromosome break-up under irradiation (Feller 1968). The central assumption is that there is no influence of the past events on the present functioning. A Poisson process is thus 'memoryless': the fact that a particle has been displaced, does not affect its chances of being displaced again. In statistical terms, this means that the process becomes a time-homogeneous Markov process (Feller 1968). To investigate the relevance of the Poisson process for bioturbation, we focus on a single sediment particle, start the clock at time 0, and count the number of displacements $N(t)$ within a given time period t. The counter $N(t)$ will increase by 1 for every bioturbation event. Bioturbation will be a Poisson process when the following condition is satisfied: the number of bioturbation events occurring in 2 intervals of the same length must be statistically independent, i.e. the probability of having $N(t)$ bioturbation events must be the same for all intervals of length t, independently from when we actually start the clock. If bioturbation acts as

a Poisson process, the probability that a particle will exactly experience n bioturbation events in the time interval $(0,t)$ is given by the Poisson distribution (Feller 1968, p. 447, Hughes 1995, p. 248):

$$\Pr\{N(t) = n\} = \frac{(t/\tau_c)^n}{n!}\exp(-t/\tau_c) \quad (23)$$

where τ_c represents the expected time interval between 'events'. The average number of particle displacements within a given time period t is indeed given by $\langle N(t)\rangle = t/\tau_c$. From Eq. (23), one can directly derive the waiting time distribution associated with a Poisson process. Upon substitution of $n = 0$ in Eq. (23), one finds the probability that a particle rests for a period of *at least* length t, which is given by:

$$\Pr\{N(t) = 0\} = 1 - \int_0^t \Psi_T(\tau)\mathrm{d}\tau = \exp(-t/\tau_c) \quad (24)$$

This expression features the integral of the waiting time distribution $\Psi_T(\tau)$. Upon differentiation with respect to time, we find that the waiting time between successive events follows the exponential distribution (Hughes 1995):

$$\Psi_T(\tau) = \frac{1}{\tau_c}\exp(-\tau/\tau_c) \quad (25)$$

where τ_c is the average waiting time. Therefore, a CTRW model with an exponential waiting time distribution is typically referred to as a Poisson process. If we insert the exponential waiting time distribution (Eq. 25) into the general CTRW equation (Eq. 5), upon differentiation with respect to time, we obtain the following integro-differential equation (see Othmer et al. 1988 for details of this derivation):

$$\tau_c\frac{\partial C}{\partial t} = -C(x,t) + \int_{-\infty}^{\infty}\Psi_L(\lambda)C(x-\lambda,t)\mathrm{d}\lambda \quad (26)$$

Eq. (26) is identical to the governing equation of the classical non-local exchange model of bioturbation originally proposed by Boudreau & Imboden (1987). Indeed, if we introduce $x' = x - \lambda$ and define the exchange function as:

$$K(x',x) = \frac{1}{\tau_c}\Psi_L(\lambda) = \frac{1}{\tau_c}\Psi_L(x-x') \quad (27)$$

then Eq. (26) can be readily re-arranged to the familiar non-local exchange model (Boudreau & Imboden 1987, Boudreau 1997):

$$\frac{\partial C}{\partial t} = \int_{-\infty}^{\infty}K(x',x)C(x',t)\mathrm{d}x' - \int_{-\infty}^{\infty}K(x,x')C(x,t)\mathrm{d}x' \quad (28)$$

In other words, a central assumption behind the classical non-local exchange model is that the mechanism of bioturbation is a Poisson process.

Note that the left-hand side of Eq. (26) (or equally Eq. 28) contains no higher temporal derivatives of the concentration, apart from the first order one. Strikingly, this is also the case for the diffusion equation (Eq. 21). This absence of such higher order temporal derivatives exemplifies the Markov character of the model. The Poisson process with its exponential waiting time PDF constitutes a Markovian model, in the sense that past bioturbation events do not influence the present probability of jumping. For arbitrary small time intervals, the exponential waiting distribution retains a finite probability of jumping, i.e. $\Psi_T(t) \to 1$ for $\tau \to 0$. Theoretically, this allows for bioturbation events to occur infinitely rapidly one after another, and, hence, there is the finite probability of finding a particle at infinite distances. This property is referred to as the infinite speed of signal propagation. The diffusion equation (Eq. 21) also shows this infinite propagation speed, and because of this it has been criticized as an unrealistic model for bioturbation (Kirwan & Kump 1987, Boudreau 1989).

Non-Markovian processes: the telegraph equation and beyond

Physically, any natural process—hence, also a bioturbation event—requires a finite amount of time to complete. So infinitely small waiting times are unrealistic, and hence one requires that the probability of small waiting times tends to zero, i.e. $\Psi_T(\tau) \to 0$ for $\tau \to 0$. As noted above, the exponential distribution (Eq. 25) violates this constraint, and, because of this, it shows an infinite speed of signal propagation. However, the constraint is satisfied when the waiting time distribution Ψ_T follows the Gamma distribution with parameter $\alpha \geq 1$:

$$\Psi_T(\tau) = \frac{1}{\tau_c}\frac{\alpha^\alpha}{\Gamma(\alpha)}\left(\frac{\tau}{\tau_c}\right)^{\alpha-1}\exp(-\alpha\tau/\tau_c) \quad (29)$$

where $\Gamma(\alpha) = \int_0^\infty s^{\alpha-1}\exp(-s)\mathrm{d}s$ is the gamma function (Abramowitz & Stegun 1964). Each curve has been 'standardized', so that it has the same averaged waiting time τ_c. All curves with $\alpha > 1$ have $\Psi_T(0) = 0$, and so they correspond to a finite speed of signal propagation. When $\alpha = 2$ is substituted into Eq. (29), we obtain the 'telegraph' waiting time distribution:

$$\Psi_T(\tau) = 4\tau_c^{-2}\tau\exp(-2\tau/\tau_c) \quad (30)$$

where the mean waiting time is again τ_c. Fig. 3 illustrates the profiles for $\alpha = 1$ (exponential Eq. 25), and $\alpha = 2$ (telegraph Eq. 30). The implementation of Eq. (30) in Eq. (5) leads to:

$$C(x,t) = (2t/\tau_c + 1)\exp(-2t/\tau_c)C_0(x) + (2/\tau_c)^2\int_0^t\tau\exp(-2\tau/\tau_c)\int_{-\infty}^{\infty}\Psi_L(\lambda)C(x-\lambda,t-\tau)\mathrm{d}\lambda\mathrm{d}\tau \quad (31)$$

Similar to the above, we can re-arrange Eq. (31) into a corresponding integro-differential form. After 2 consecutive differentiations with respect to time, and some rearrangements, the analogue of Eq. (26) thus becomes (Othmer et al. 1988):

$$\left(\frac{\tau_c}{2}\right)^2 \frac{\partial^2 C}{\partial t^2} + \tau_c \frac{\partial C}{\partial t} = -C(x,t) + \int_{-\infty}^{\infty} \Psi_L(\lambda)\, C(x-\lambda,t)\, \mathrm{d}\lambda \quad (32)$$

Eq. (32) bears a strong resemblance with the telegraph equation (Eq. 33), which was proposed by Boudreau (1989) as an alternative to the biodiffusion model, in order to cope with the problem of the infinite propagation speed:

$$\left(\frac{\tau_c}{2}\right)^2 \frac{\partial^2 C}{\partial t^2} + \tau_c \frac{\partial C}{\partial t} = \frac{\sigma^2}{2} \frac{\partial^2 C}{\partial x^2} \quad (33)$$

Note the striking analogy between the diffusion equation (Eq. 21) and the telegraph equation (Eq. 33), on the one hand, and the 'exponential' CTRW equation (Eq. 26) and its 'telegraph extension' (Eq. 32), on the other hand.

MODEL APPLICATION

Simulation of pulse-tracer addition experiments

In a final step, we present simulations that illustrate the relation between the diffusion model (Eq. 21), the telegraph model (Eq. 33) and the general CTRW model (Eq. 5). The aim is to compare how these models simulate bioturbation over 'short' time scales. It is important to point out that 'short' is relative to the mean time interval between 2 consecutive displacements of particles (i.e. mean waiting time τ_c). Different benthic communities will induce particle displacement characterized by a different mean waiting time τ_c, and consequently they will have a different characteristic time scale of mixing. Deep-sea environments are less intensely mixed than coastal environments, and hence the mean waiting time τ_c associated with bioturbation in benthic communities of the deep sea can be far greater than that of coastal communities. Accordingly, the notion 'short time scales' will have a different meaning in different sediment environments.

A widely implemented technique to study bioturbation over short time scales is via a tracer pulse addition experiment (e.g. Gerino 1990, Fornes et al. 1999, 2001, Solan et al. 2004, Fernandes et al. 2006, Duport et al. 2007). A layer of tracer particles is added to the SWI, and its subsequent down-mixing into the sediment is followed. Here, we simulate such a tracer pulse addition for inert particles (e.g. fluorescent luminophores), assuming that the sediment is initially covered by a tracer layer of 5 mm thickness. The tracer concentration is defined as equal to 1 within this initial layer. The 'short time scale' over which the tracer mixing is simulated covers 10 times the mean waiting time τ_c.

Four different bioturbation regimes

We simulated the same pulse-tracer experiment with 6 different models: the biodiffusion model (Eq. 21), the telegraph model (Eq. 33) and 4 different versions of the CTRW model (Eq. 5), which represent 4 different bioturbation regimes. A *bioturbation regime* refers to the particle spreading process within a particular sediment setting. This process will depend on the type and number of organisms that are present, and on the intensity and the mechanism of their activity (e.g. deposit-feeding, burrowing). From the perspective of the CTRW model, a given bioturbation regime is completely characterized by its *bioturbation fingerprint*, i.e. a particular combination of a waiting time distribution Ψ_T and a jump length distribution Ψ_L.

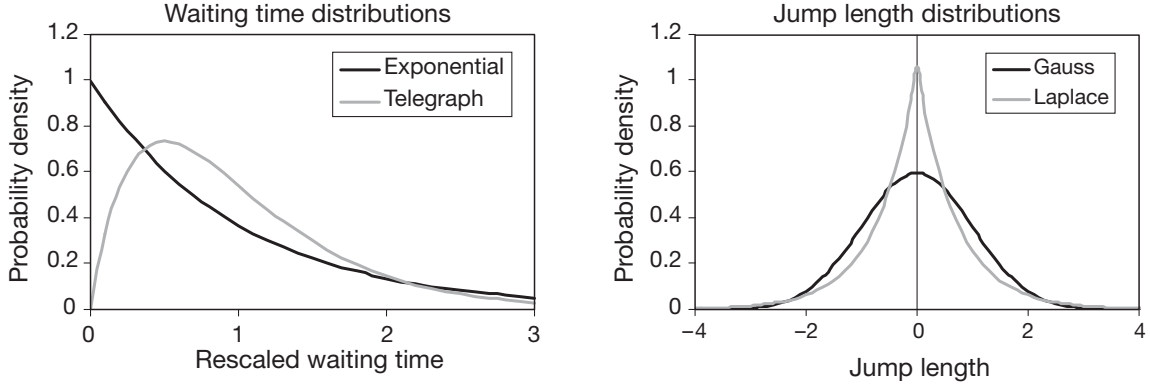

Fig. 3. Four different bioturbation fingerprints are created by the combination of 2 waiting time distributions (left panel) and 2 jump length distributions (right panel). Exponential and telegraph distributions are used for the waiting time probability distribution function (PDF, left panel). Laplacian and Gaussian distributions are used for the jump length PDF (right panel). See 'Model application; Four different bioturbation regimes' for the mathematical formulae that describe these distributions

Once these distributions are known, the CTRW model formulation is complete. Here, 4 different CTRW models were made by combining 2 waiting time distributions Ψ_T and 2 jump length distributions Ψ_L. For the waiting time distribution, we either used the Markovian exponential distribution (Eq. 25) ($\alpha = 1$ in Eq. 29) or the non-Markovian Gamma distribution (Eq. 30) ($\alpha = 2$ in Eq. 29). To construct the jump length distributions Ψ_L, we used the following family of curves:

$$\Psi_L(\lambda) = \frac{1}{2\sigma\ \Gamma(1+1/m)}\sqrt{\frac{\Gamma(1/m)}{\Gamma(3/m)}}\exp\left[-\sqrt{\frac{\Gamma(1/m)}{\Gamma(3/m)}}\left(\frac{\lambda}{\sigma}\right)^m\right] \quad (34)$$

where $\Gamma(x)$ again denotes the Gamma function. The curves (Eq. 34) have a peak at $\lambda = 0$, and the same standard deviation σ^2, and zero skewness. The curves have, however, different kurtosis, depending on the value of m. The values $m = 1$ and $m = 2$ are used here (Fig. 3). When $m = 1$, Eq. (34) becomes the Laplace distribution:

$$\Psi_L(\lambda) = \frac{1}{\sigma\sqrt{2}}\exp\left(-\frac{\sqrt{2}\,|\lambda|}{\sigma}\right) \quad (35)$$

When $m = 2$, Eq. (34) becomes the familiar Gaussian distribution:

$$\Psi_L(\lambda) = \frac{1}{\sigma\sqrt{2\pi}}\exp\left(-\frac{\lambda^2}{2\sigma^2}\right) \quad (36)$$

Combining the 2 waiting time distributions (Eqs. 25 & 30) with the 2 step length distributions (Eqs. 35 & 36) gives rise to 4 different bioturbation fingerprints (Markovian × Gaussian; Markovian × Laplacian; non-Markovian × Gaussian; non-Markovian × Laplacian). Note that all 4 CTRW models, as well as the biodiffusion equation (Eq. 21) and the telegraph equation (Eq. 33), feature the same 2 parameters σ and τ_c. These parameters are given the same values in all 6 simulations.

Simulation results

The 6 model simulations of the same pulse-tracer addition experiment are plotted in Fig. 4. The long-time behaviour of the models is striking: at about 10 times the average waiting time, all 6 solutions coincide. This is exactly what random-walk theory predicts (Hughes 1995, Metzler & Klafter 2000). All models were designed to have the same mixing intensity, as specified by the biodiffusion coefficient (Eq. 22). To this end, the distributions were standardized, so that the mean waiting time τ_c and step length variance σ^2 were the same for all 4 CTRW bioturbation regimes. The same parameter values for τ_c and σ were used in the diffusion equation (Eq. 21) and the telegraph equation (Eq. 33). The merging of the simulated profiles at long times also shows that our numerical solution scheme for the CTRW model is accurate.

At short times, there is a marked difference between the 4 solutions of the CTRW model on the one hand, and the solutions of the biodiffusion and telegraph models on the other hand. The CTRW profiles all consist of 2 parts: (1) a 'blocky' zone corresponding to the initial tracer layer and (2) a 'smooth' zone beneath the initial layer, which shows a gradually decreasing tracer concentration with depth. The 'blocky' zone contains particles that have not yet been moved. Over time, this zone is gradually eroded, as more and more particles are mixed down. The 'smooth' underlying zone contains particles that have been displaced. Neither the diffusion model, nor the telegraph model, shows this characteristic 2-zone pattern. Instead they give rise to a single, more or less homogeneously reworked zone near the sediment surface. As a result, both diffusion and telegraph models predict considerably lower concentrations at the sediment surface during the initial stages of the experiment, when compared to the 4 CTRW models. When comparing the profiles of the 4 CTRW models, the differences are minor. For the same waiting time distribution, the profiles corresponding to the Laplacian and Gaussian step length distributions nearly coincide. For the same step length distribution, the profile corresponding to the Gamma waiting time distribution (Eq. 30) shows slower erosion of the initial tracer layer than the profile obtained from the exponential distribution (Eq. 25).

Finally, there are also 2 marked differences between the tracer profiles generated by the biodiffusion and telegraph models. The concentration profile produced by the telegraph equation at short times takes on an unusual, irregular shape: it shows a marked 'truncation', which abruptly limits the penetration of particles. Just before this truncation, the profiles exhibit a strange accumulation of tracer, which appears like a 'chimney'. Effectively, the chimney appears to sit on the top of a truncated diffusion profile (compare the profiles at $t = 0.5$; the first centimetre of the diffusion profile is very similar to that of the telegraph profile). Okubo (1971) has investigated the mathematical details of the solution of the telegraph equation, and explained the origin of these 2 peculiar features. The solution of the telegraph model actually consists of 2 parts: a wave-like and a diffusive-like component (respectively corresponding to the second-order and first-order temporal derivative in Eq. 33). The truncation then corresponds to the diffusive-like component, where particles can only move downwards with a finite propagation speed $c = \sqrt{2}\sigma/\tau_c$. Accordingly, there are no particles beyond $x = ct$, which is the depth where the tracer profile is truncated. Conversely, the chimney at the front edge is due to the wave-like com-

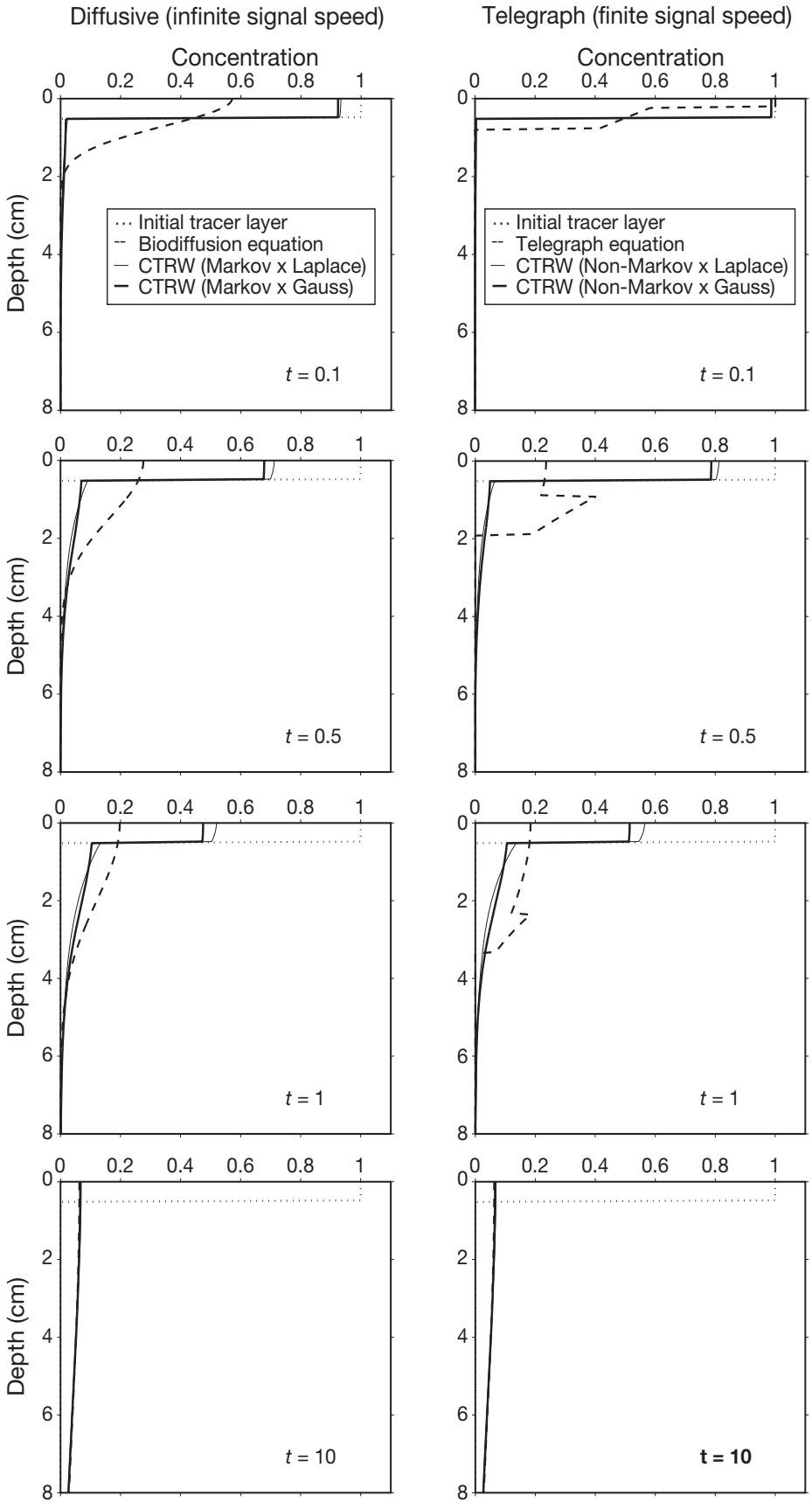

Fig. 4. Transient simulations of the same pulse-tracer addition experiment by 6 different models. The initial tracer layer at the surface is given by the dotted line. Left and right panels each show the output of 3 models at 4 different times. Left panels: thin continuous line: continuous-time random-walk (CTRW) model with exponential waiting time and Laplacian jump length; thick continuous line: CTRW model with exponential waiting time and Gaussian jump length; dashed line: asymptotic biodiffusion model. Right panels: thin continuous line: CTRW model with 'telegraph' waiting time and Laplacian jump length; thick continuous line: CTRW model with 'telegraph' waiting time and Gaussian jump length; dashed line: solution of the associated telegraph equation. In all simulations we used the same characteristic length scale σ = 2 cm. The time elapsed is expressed relative to the mean waiting time between particle displacements (e.g. t = 10 denotes a simulation period of 10 times the mean waiting time)

ponent, and represents a damped wave motion of the initial conditions. The decay of the chimney is on the order of $\sim\tau_c/4$, and therefore the chimney has virtually disappeared when $t > \tau_c$.

DISCUSSION

In bioturbation research, pulse-tracer additions form a popular experimental method. In these methods, a pulse of inert tracer particles is deposited at the sediment surface, and the evolution of the vertical tracer profile is followed over time. These pulse experiments last only a short period compared to the intrinsic mixing time of the environment, typically on the order of hours (e.g. 48 h; Solan et al. 2004) to days (e.g. 22 d in Gerino 1990; 28 d in Fernandes et al. 2006) in nearshore conditions, and years in the deep sea (e.g. Wheatcroft 1991). These observational times should be compared to the inherent time scale of bioturbation, i.e. the mean waiting time τ_c between consecutive displacements of a given particle. At present, we have no accurate estimates of the mean waiting time τ_c between bioturbation events, since we do not have experimental techniques that can track the movement of individual particles. Based on population reworking rates of deposit feeders, Wheatcroft et al. (1990) and Meysman et al. (2003) crudely estimated that τ_c must range on the order of hours to months for natural communities. Recently, Maire et al. (2007) fitted the Markov × Gaussian CTRW to high-resolution luminophore data obtained in microcosm experiments. They found that τ_c ranged between 1 to 10 h in the summertime ($D_b \sim 40$ cm^2 yr^{-1}) and 10 to 30 h in the wintertime ($D_b \sim 5$ cm^2 yr^{-1}) for sediments mixed by the burrowing bivalve *Abra ovata*. In these microcosm experiments, the observational time scale was 48 h. As a result, the observational time scale of the experiment and the intrinsic process time scale of bioturbation are of the same order. In other words, the particles that are observed in pulse-tracer experiments will only experience a limited number of bioturbation events.

Until now, this aspect of short observational time scales has received very little consideration, when interpreting the results of pulse-tracer experiments. In the standard procedure, the biodiffusion model (Eq. 21) is applied, and a biodiffusion coefficient D_b is derived by suitably fitting to the tracer data profiles (with some exceptions: see Shull & Yasuda 2001 and Solan et al. 2004 for the application of non-local models to tracer data). However, it usually is not investigated whether the assumptions underlying the biodiffusion model are valid at such short time scales. Note that the question is not whether the biodiffusion model can be applied to tracer profiles at short time scales (this can always be done), but whether the resulting values for the biodiffusion coefficient are meaningful. Recently, Reed et al. (2006) showed that strong artefacts can arise when the biodiffusion model is applied to steady-state profiles of short-lived radiotracers. Based on lattice-automaton simulations (i.e. synthetic data generated from a virtual sediment), they showed that tracer-derived biodiffusion coefficients, obtained by fitting tracer profiles of short-lived radionuclides, may strongly deviate (by orders of magnitude) from biodiffusion coefficients derived from particle tracking, which represent the true mixing intensity of the sediment (i.e. the D_b obtained from Eq. 22). Our analysis of transient pulse-tracer experiments provides an explanation for these problems with the biodiffusion model at short time scales: the infinite speed of signal propagation and the assumption of infinitely short waiting times.

Infinite signal propagation speed: the telegraph equation as an alternative to the biodiffusion model

One problem with the biodiffusion model is the infinite speed of signal propagation. Shortly after the start of the pulse-tracer experiment, the biodiffusion model will predict that tracer particles penetrate too far down into the sediment (see Fig. 4, left panel $t = 0.1$). To correct this artefact, Boudreau (1989) suggested the telegraph equation (Eq. 33) as an alternative, which has indeed a finite velocity of signal propagation (Monin 1959, Okubo 1971). However, until the present time, no one has actually used the telegraph equation to simulate or analyse a pulse-tracer addition experiment. This is done here, and the results are quite disconcerting for the telegraph model. As shown in Fig. 4, the concentration profile produced by the telegraph equation includes 2 strange and unrealistic features: a truncation of the tracer profile and a strange accumulation of tracer near the truncation depth. In his detailed mathematical investigation of the telegraph equation, Okubo (1971, p. 28) referred to the truncation of the tracer profile as an 'advancing front', while the accumulation was termed a 'heaping of substance near the front edge'. Okubo (1971) noted that the presence of 'an advancing front where substance is heaped' does not match observations in experiments on oceanic diffusion. Nonetheless, Okubo (1971) attributed the 'heaping effect' to unrealistic (Dirac pulse) initial conditions, and he (still) concluded that the telegraph equation could produce realistic tracer patterns. We think that this interpretation of Okubo (1971) is far too merciful for the telegraph equation as a tracer mixing model. In bioturbation studies, neither sharp truncations, nor moving chimneys have been observed in

actual pulse-tracer experiments (see e.g. Fig. 4 in Maire et al. 2007). Unlike Okubo's (1971) assertion, the accumulation of tracer at the front edge does not result from unrealistic initial conditions, but is a fundamental aspect of the telegraph's solution. Given an initial layer of tracer at the sediment surface, the strange accumulation at depth will always be prominently present in the telegraph tracer profile, because a wave-like subcomponent is always present within its solution. In conclusion, the replacement of the diffusion model by the telegraph equation as a bioturbation model solves one minor problem (the infinite propagation speed), but, at the same time, it introduces a far more important bias (the introduction of unrealistic truncation and accumulation features in tracer profiles). Accordingly, the telegraph equation does not form a suitable alternative to the biodiffusion model at short time scales.

The problem of infinitely short waiting times

One can ask whether the infinite speed of signal propagation is the true critical issue when modelling particle mixing at short time scales. Our simulations indicate that it is not. To this end, we compared a CTRW model with an infinite signal propagation speed (exponential waiting time distribution; left column of Fig. 4) and the same model with a finite signal propagation speed (Gamma waiting time distribution; right column of Fig. 4). The differences between the resulting CTRW tracer profiles are very small, and would hardly be distinguishable in the presence of actual data, given the typical error bars associated with such data. In contrast, the crucial dichotomy in Fig. 4 occurs between the differential equation models on the one hand (the diffusion and telegraph solution), and the integral equation models on the other hand (the 4 CTRW solutions). Both categories of models display fundamentally different model behaviour at short time scales. In the CTRW models, the initial tracer layer 'persists' in the model solutions, and only gradually fades with time. In contrast, the initial conditions are immediately wiped out in the differential equation models.

So why do the biodiffusion and telegraph models immediately clear their 'memory' of the initial tracer layer? The answer to this question provides a new insight into the assumptions and applicability of bioturbation models. The difference between integral models such as the CTRW presented here, and differential models such as the biodiffusion (Eq. 21) and telegraph (Eq. 33) models, but also the classical non-local exchange model (Eq. 28), boils down essentially to the underlying assumption about the waiting time between bioturbation events. The integral equation (Eq. 5) of the CTRW model explicitly describes the waiting time between bioturbation events via a probability distribution, and as a consequence the mean waiting time τ_c has a finite value. In contrast, models that feature temporal derivatives implicitly assume an infinitely small τ_c. In the derivations of these models, one performs a series expansion of the concentration about the time, and subsequently one performs a limit operation $\tau_c \rightarrow 0$. This was shown by Wheatcroft et al. (1990) for the biodiffusion model (Eq. 21), by Boudreau (1989) for the telegraph model (Eq. 33), and by Meysman et al. (2003) for the non-local exchange model (Eq. 26). In other words, temporal differentiation implies a limit operation where the mixing time scale τ_c becomes infinitely small. An infinitely small waiting time then implies that all particles are constantly being displaced. In other words, the biodiffusion and other differential models assume that all particles within the initial tracer layer are immediately affected by sediment reworking. This explains why the initial conditions are immediately 'erased' from the tracer profile. In contrast, in the CTRW model, particles are not displaced immediately. Some particles remain undisturbed for a finite time, and this is the reason why the initial tracer layer persists for some time in the tracer profile.

In summary, our analysis brings up a critical and previously unrecognized issue in bioturbation modelling. In a seminal paper on bioturbation modelling, Wheatcroft et al. (1990) introduced the concept of a waiting time between bioturbation events. Here, we elaborate when and why this waiting time becomes important: models should account for a finite waiting time between bioturbation events when modelling tracer behaviour at short observational time scales. The biodiffusion model implicitly assumes an infinitely small waiting time, as does the telegraph equation and any other differential model. Note that even the non-local exchange model of Boudreau & Imboden (1987) also comprises a differential model, and so it also implicitly assumes an infinitely small waiting time. This model has been frequently heralded as a more realistic alternative to the biodiffusion model. Although not explicitly tested here, our analysis questions the usefulness of non-local exchange models at short time scales. When modelling tracers over short time scales, the waiting time between bioturbation events becomes important, and so the waiting time cannot be idealized as infinitely small.

Implications for short-term tracer studies

The discussion in the previous section about the 'persisting' initial layers and importance of finite waiting times was solely based on model analysis (the compari-

son of the CTRW model to other models in Fig. 4). So, are there any empirical data that support these arguments? The relevance of bioturbation models with finite waiting times was recently shown in a tracer study by Maire et al. (2007). The biological reworking of the bivalve *Abra ovata* was followed in thin aquaria over a short time period of 48 h. Particle dispersal was quantified in a classical pulse addition experiment, where a thin layer of luminophores was added on top of the sediment. Images were taken from the side of the aquaria, which then generated 2-dimensional (2D) tracer distributions. It was observed that the bivalve reworking was spatially patchy: some zones were intensively reworked, while, in other zones, the initial tracer layer remained unaltered. Over time, the bivalves relocated, and so gradually more and more of the sediment surface became reworked. When generating 1D tracer profiles from the 2D images, the sediment is laterally averaged, and, hence, 'mixed' and 'unmixed' zones are merged into single tracer depth profiles. This effectively resulted in 1D tracer profiles that are very similar to the CTRW solutions as presented in Fig. 4: the initial tracer layer 'persists' for some time in consecutive tracer profiles (see Fig. 4 in Maire et al. 2007). Only gradually, as the bivalves relocate, is more and more of the 'pristine' sediment (i.e. with intact tracer surface layer) reworked. Maire et al. (2007) showed that the interpretation of such profiles with the standard biodiffusion model leads to significant bias in the mixing intensity. The biodiffusion model assumes that all particles within the initial layer are immediately affected (infinitely frequent bioturbation events), and hence it cannot cope with lateral heterogeneity in bivalve reworking activity. We believe this observation is not specific to *A. ovata*, but applies to bioturbation in general. Over short time scales, lateral heterogeneity in bioturbation activity cannot be ignored in tracer studies. In terms of modelling, this implies that when 1D bioturbation models are applied over short time scales, one should account for differential timing in particle displacements. A tracer layer that is initially deposited at the SWI, should be gradually mixed down, rather than that all particles are displaced immediately and synchronously. The CTRW model presented here allows for such differential timing: lateral spatial heterogeneity in reworking is essentially translated into vertical stochasticity of particle displacement.

CONCLUSIONS

In recent years, new experimental techniques have been developed that generate tracer profiles of a high spatial (~1 mm) and high temporal resolution (~10 min) (Gilbert et al. 2003, Solan et al. 2004, O'Reilly et al. 2006, Maire et al. 2007). Accordingly, one requires suitable tracer models that adequately describe the resulting tracer data at such short time scales. We have identified 2 issues with quantifying bioturbation over short time scales: (1) the infinitely fast propagation of tracer to finite depths and (2) the assumption that bioturbation events occur infinitely frequently. Our model analysis shows that the latter issue is far more relevant to tracer studies than the former. In short-term tracer studies, lateral spatial heterogeneity in reworking becomes important, which translates into vertical particle displacements with finite waiting times. Organisms do not rework the surface layer of sediments and soils in a homogeneous fashion. Rather, bioturbation should be regarded as a process of sediment patches that are individually reworked and that shift with time when organisms relocate. In tracer pulse addition experiments, this lateral heterogeneity in reworking results in conspicuous 1D tracer profiles, where initial conditions 'persist'.

The issue of waiting times has important repercussions for the tracer models that are used in combination with experimental tracer studies. At present, models are used that are stated in a differential form, of which the biodiffusion model (Eq. 21) is by far the most popular. We have shown that such 'differential' models implicitly assume that bioturbation events occur with infinite frequency. At short time scales, the application of such models is problematic, and may lead to biased predictions. When applied to short time scales, bioturbation models should explicitly account for a finite waiting time between bioturbation events. Here, we advance the CTRW model as a suitable description of bioturbation, which is able to cope with lateral spatial heterogeneity in reworking, However, at long time scales, the application of biodiffusion is not a problem. After a sufficient amount of time (i.e. a sufficient amount of bioturbation events), the CTRW model profile becomes identical to that of the biodiffusion model. At this stage, the more complex CTRW model loses its advantage over the much simpler biodiffusion model. So, in conclusion, it is not a good idea to use the biodiffusion model at short time scales, but there seems no reason not to use it at long time scales.

Acknowledgements. This research was supported by grants from the EU (MARBEF, 505446), the Netherlands Organization for Scientific Research (NWO PIONIER, 833.02.2002), and contributes to the Darwin Institute for Biogeology. This is Publication no. 4323 of the Netherlands Institute of Ecology (NIOO-KNAW).

LITERATURE CITED

Abramowitz M, Stegun IA (1964) Handbook of mathematical functions with formulas, graphs, and mathematical tables. Dover, New York

Aller RC (1988) Benthic fauna and biogeochemical processes

in marine sediments: the role of burrow structures. In: Blackburn TH, Sorensen J (eds) Nitrogen cycling in coastal marine sediments. John Wiley & Sons, New York, p 301–338

Aller RC, Yingst JY (1978) Biogeochemistry of tube-dwellings: a study of the sedentary polychaete *Amphitrite ornata* (Leidy). J Mar Res 36:201–254

Boudreau BP (1986) Mathematics of tracer mixing in sediments. I. Spatially dependent, diffusive mixing. Am J Sci 286:161–198

Boudreau BP (1989) The diffusion and telegraph equations in diagenetic modeling. Geochim Cosmochim Acta 53: 1857–1866

Boudreau BP (1997) Diagenetic models and their implementation. Springer, Berlin

Boudreau BP, Imboden DM (1987) Mathematics of tracer mixing in sediments. III. The theory of nonlocal mixing within sediments. Am J Sci 287:693–719

Cadée GC (2001) Sediment dynamics by bioturbating organisms. In: Reise K (ed) Ecological comparisons of sedimentary shores. Springer, Berlin, p 127–148

Duport E, Gilbert F, Poggiale JC, Dedieu K, Rabouille C, Stora G (2007) Benthic macrofauna and sediment reworking quantification in contrasted environments in the Thau Lagoon. Estuar Coast Shelf Sci 72:522–533

Feller W (1968) An introduction to probability theory and its applications. John Wiley & Sons, New York

Fernandes S, Meysman FJR, Sobral P (2006) The influence of Cu contamination on *Nereis diversicolor* bioturbation. Mar Chem 102:148–158

Fornes WL, Demaster DJ, Levin LA, Blair NE (1999) Bioturbation and particle transport in Carolina slope sediments: a radiochemical approach. J Mar Res 57:335–355

Fornes WL, Demaster DJ, Smith CR (2001) A particle introduction experiment in Santa Catalina basin sediments: testing the age-dependent mixing hypothesis. J Mar Res 59:97–112

Gardiner CW (2002) Handbook of stochastic methods for physics, chemistry and the natural sciences. Springer-Verlag, Berlin

Gerino M (1990) The effects of bioturbation on particle redistribution in Mediterranean coastal sediment—preliminary results. Hydrobiologia 207:251–258

Gilbert F, Hulth S, Stromberg N, Ringdahl K, Poggiale JC (2003) 2-D optical quantification of particle reworking activities in marine surface sediments. J Exp Mar Biol Ecol 285-286:251–263

Goldberg ED, Koide M (1962) Geochronological studies of deep-sea sediments by the Io/Th method. Geochim Cosmochim Acta 26:417–450

Guinasso NL, Schink DR (1975) Quantitative estimates of biological mixing rates in abyssal sediments. J Geophys Res 80:3032–3043

Hughes BD (1995) Random walks and random environments, Vol 1. Random walks. Clarendon Press, Oxford

Kirwan AD, Kump LR (1987) Models of geochemical systems for mixture theory: diffusion. Geochim Cosmochim Acta 51:1219–1226

Mahaut ML, Graf G (1987) A luminophore tracer technique for bioturbation studies. Oceanol Acta 10:323–328

Maire O, Duchene JC, Gremare A, Malyuga VS, Meysman FJR (2007) A comparison of sediment reworking rates by the surface deposit-feeding bivalve *Abra ovata* during summertime and wintertime, with a comparison between two models of sediment reworking. J Exp Mar Biol Ecol 343:21–36

Metzler R, Klafter J (2000) The random walk's guide to anomalous diffusion: a fractional dynamics approach. Phys Rep 339:1–77

Meysman FJR, Boudreau BP, Middelburg JJ (2003) Relations between local, nonlocal, discrete and continuous models of bioturbation. J Mar Res 61:391–410

Meysman FJR, Middelburg JJ, Heip CHR (2006) Bioturbation: a fresh look at Darwin's last idea. Trends Ecol Evol 21:688–695

Meysman FJR, Malyuga VS, Boudreau BP, Middelburg JJ (2008) A generalized stochastic approach to particle dispersal in soils and sediments. Geochim Cosmochim Acta (in press)

Monin AS (1959) Smoke propagation in the surface layer of the atmosphere. Adv Geophys 6:331–343

Montroll EW, Weiss GH (1965) Random walks on lattices. II. J Math Phys 6:167–181

Okubo A (1971) Application of the telegraph equation to oceanic diffusion: another mathematical model. Tech Rep 69, Chesapeake Bay Institute, John Hopkins University, Baltimore

O'Reilly R, Kennedy R, Patterson A (2006) Destruction of conspecific bioturbation structures by *Amphiura filiformis* (Ophiuroida): evidence from luminophore tracers and *in situ* time-lapse sediment-profile imagery. Mar Ecol Prog Ser 315:99–111

Othmer HG, Dunbar SR, Alt W (1988) Models of dispersal in biological systems. J Math Biol 26:263–298

Piessens R, de Doncker-Kapenga E, Überhuber C, Kahaner D (1983) QUADPACK: a subroutine package for automatic integration. Springer-Verlag, Berlin

Reed DC, Huang K, Boudreau BP, Meysman FJR (2006) Steady-state tracer dynamics in a lattice-automaton model of bioturbation. Geochim Cosmochim Acta 70:5855–5867

Rhoads DC (1974) Organism–sediment relations on the muddy sea floor. Oceanogr Mar Biol 12:263–300

Richter R (1952) Fluidal-Textur in Sediment-Gesteinen und über Sedifluktion überhaupt. Notizbl Hess Landesamtes Bodenforsch Wiesb 3:67–81

Shull DH, Yasuda M (2001) Size-selective downward particle transport by cirratulid polychaetes. J Mar Res 59:453–473

Solan M, Wigham BD (2005) Biogenic particle reworking and bacterial–invertebrate interactions in marine sediments. In: Kristensen E, Haese RR, Kostka JE (eds) Interactions between macro- and microorganisms in marine sediments. Coastal Estuar Stud 60:105–124

Solan M, Wigham BD, Hudson IR, Kennedy R and others (2004) *In situ* quantification of bioturbation using time-lapse fluorescent sediment profile imaging (f-SPI), luminophore tracers and model simulation. Mar Ecol Prog Ser 271:1–12

Wheatcroft RA (1991) Conservative tracer study of horizontal sediment mixing rates in a bathyal basin, California borderland. J Mar Res 49:565–588

Wheatcroft RA, Jumars PA, Smith CR, Nowell ARM (1990) A mechanistic view of the particulate biodiffusion coefficient—step lengths, rest periods and transport directions. J Mar Res 48:177–207

Appendix 1. Reformulation of Eq. (18) in terms of real integrals

Eq. (18) is not solved as such, but is first reformulated before numerical integration. Taking into account that the Fourier transform $\hat{\Psi}_L(k)$ vanishes as k increases, we can improve the convergence of the integral on the right-hand side as follows:

$$C(x,t) = G(t)C_0(x) + \frac{1}{4\pi^2 i}\int_{-\infty}^{\infty}\exp(-ikx)\int_{\gamma-i\infty}^{\gamma+i\infty}\frac{1-\tilde{\Psi}_T(s)}{s}\left[\frac{1}{1-\tilde{\Psi}_T(s)\hat{\Psi}_L(k)}-1\right]\exp(st)\,\mathrm{d}s\,\mathrm{d}k \quad \text{(A1)}$$

Here, the following auxiliary function $G(t)$ is introduced as:

$$G(t) = 1-\frac{1}{2\pi i}\int_{\sigma-i\infty}^{\sigma+i\infty}\frac{\tilde{\Psi}_T(s)}{s}\exp(st)\,\mathrm{d}s \quad \text{(A2)}$$

The solution of our initial value problem then requires the evaluation of the integrals in Eqs. (A1) & (A2). The contour integrals in Eq. (A1) can be readily represented in terms of real integrals. For this purpose, the variable of integration in the second integral can be rewritten as $s = \gamma + i\xi$. Because the waiting time distribution Ψ_L is an even function, it is evident that its Fourier transform $\hat{\Psi}_L(k)$ is also an even function, which takes real values on the straight line $-\infty < k < \infty$. It is easy to see that the imaginary part of the integrand in Eq. (A1) is an odd function of ξ, and therefore vanishes upon integration. Thus, in order to evaluate the second integral in Eq. (A1), one needs only to integrate the real part of the integrand. In a similar manner, the integral with respect to k requires only the integration of the real part of the integrand. As a result, Eq. (A1) takes the final form:

$$C(x,t) = G(t)C_0(x) + \frac{\exp(\gamma t)}{4\pi^2}\int_{-\infty}^{\infty}\hat{C}_0(k)\cos(kx)\int_{-\infty}^{\infty}H(s,k)\,\mathrm{d}\xi\,\mathrm{d}k \quad \text{(A3)}$$

where $s = \gamma + i\xi$. The auxiliary functions G and H are, respectively:

$$G(t) = 1-\frac{\exp(\gamma t)}{\pi}\int_0^{\infty}\left[\mathrm{Re}\left(\frac{\tilde{\phi}(s)}{s}\right)\cos(\xi t)-\mathrm{Im}\left(\frac{\tilde{\phi}(s)}{s}\right)\sin(\xi t)\right]\mathrm{d}\xi \quad \text{(A4)}$$

$$H(s,k) = \mathrm{Re}\left[\frac{1-\tilde{\Psi}_T(s)}{s}\left(\frac{1}{1-\tilde{\Psi}_T(s)\hat{\Psi}_L(k)}-1\right)\exp(i\gamma t)\right] \quad \text{(A5)}$$

The representation of Eqs. (A3) to (A5) represents the form that was actually used in all numerical simulations.

Submitted: August 21, 2007; Accepted: March 12, 2008

Proofs received from author(s): May 26, 2008

Vol. 2: 255–268, 2008
doi: 10.3354/ab00055

AQUATIC BIOLOGY
Aquat Biol

Printed June 2008
Published online June 19, 2008

Contribution to the Theme Section 'Bioturbation in aquatic environments: linking past and present'

OPEN ACCESS

Biology of shallow marine ichnology: a modern perspective

Murray K. Gingras[1,*], Shahin E. Dashtgard[2], James A. MacEachern[2], S. George Pemberton[1]

[1]**Department of Earth and Atmospheric Sciences, 1-26 Earth Science Building, University of Alberta, Edmonton, Alberta T6G 2E3, Canada**

[2]**Department of Earth Sciences, Simon Fraser University, Burnaby, British Columbia V5A 1S6, Canada**

ABSTRACT: This study considers the construction and functionality of biogenic structures made by marine, vermiform nemerteans, polychaetes and hemichordates; marine crustaceans; motile bivalves; motile echinoderms; and sponges and sea anemones. We report on a range of modern biogenic structures similar to several known ichnogenera. Vermiform animals dominantly occupy vertical burrows that range from simple through helical shafts to Y- and U-shapes. Horizontal traces made by worms range in form, but are dominated by branching and variably sinuous to meandering burrows. Crustaceans primarily excavate open burrow systems that possess a range of architectures that are similar to either *Thalassinoides* or *Psilonichnus*. Smaller crustaceans, such as amphipods, mix the sediment. Bivalve traces vary in form, but generally preserve evidence of vertically oriented filter or interface-deposit feeding from a stationary location, rapid vertical escape, or horizontal grazing. Echinoderms dominantly preserve body impressions and motility traces, such as *Asteriacites*. An important class of biogenic structure, *Scolicia* and *Bichordites*, are made by urchins. Finally, sea anemones can generate large, penetrative, conical biogenic structures. Large, open horizontal networks serve as domiciles and deposit-feeding structures for crustaceans, but with worms similar burrow types are used more for passive carnivory and establishing an interface-feeding network. We report that the trace fossil *Gyrolithes* potentially represents mechanical ramps for shrimp, but is used as a sediment holdfast when made by worms. Finally, Y-shaped burrows are used for filter feeding in shrimp, and interface-deposit feeding in worms. These examples emphasize that inferences of behavior in the rock record are interpretive.

KEY WORDS: Ichnology · Neoichnology · Traces · Crustacea · Vermiforms · Bivalves · Echinoderms · Anemones

INTRODUCTION

Ichnology is the study of trace fossils (or ichnofossils), which primarily constitute the fossilized trails and burrows of animals. Commonly, and inaccurately referred to as 'tracks and trails', these vestiges of animal activity reflect the behavior that animals employed in order to live, feed, move, or hide within their environments. Interpretation of the animal's behavior can lead to better interpretations of the depositional conditions, towards which ichnology is largely applied. Trace fossils are classified morphologically, and are assigned to ichnogenera and ichnospecies on that basis (see Bertling et al. 2006 for a complete review of ichnotaxonomy). As such, trace-fossil names are taxonomically independent of the animal that made them. Below we present several trace-fossil names. These are used so that this summary paper can be linked to the ichnological literature.

Although trace fossils may owe much of their resultant morphology to their tracemaker, this relationship is rarely stressed in the ichnological literature. This is mainly because a large range of tracemakers can generate the same traces if employing broadly similar

*Email: mgingras@ualberta.ca

behaviors to survive comparable environmental conditions (Ekdale et al. 1984). Nevertheless, a better understanding of trace fossils can be obtained if modern animals are studied in the context of their trace-making behaviors. Herein, we explore the more common traces observed in modern environments and associate those traces to groups of animals. This paper particularly focuses on the infaunal behavior of invertebrates in marginal-marine and marine settings. The main groups of animals considered herein are: vermiform nemerteans, polychaetes and hemichordates; a range of marine crustaceans; bivalves; motile echinoderms; and, to a lesser degree, sponges and sea anemones. These groups of animals were chosen on the basis of their abundance in marine environments, the common occurrence of ichnofossils similar to their traces, and the many studies of their trace-making behavior. Animals that bore into hard substrates are not reported, as such studies have been previously performed and are not discussed here (e.g. Kelly & Bromley 1984, Bromley 1994). The aim of the present work is not to suggest limitations to the interpretations of trace fossils, but to increase the range of possible interpretations.

MATERIALS AND METHODS

Most data on modern traces are collected using 1 of 3 methods: (1) manual excavation of sediment in intertidal zones, with careful splitting of the sediment along and perpendicular to bedding planes; (2) resin or plaster casts of burrows, whereby a burrow is flooded with polyester, polyurethane resin, or plaster, and the cast is removed upon hardening of the substance (e.g. Bouma 1969); and (3) collection and slabbing of sediment box-cores followed by X-ray imaging (e.g. Gingras et al. 1999, 2001, Dashtgard & Gingras 2005a). Manual excavation is used in intertidal zones, casting has been conducted in intertidal and shallow subtidal settings, and box-coring is used from intertidal to deep waters. Another means of determining trace morphology is to place burrowing animals in aquaria and study the resultant burrow morphologies (e.g. Dafoe et al. 2008). Aquaria have also been used *in situ* in sedimentary studies and removed after a time for laboratory analysis (Dashtgard & Gingras 2005b).

RESULTS

Vermiform nemerteans, polychaetes and hemichordates

Worm-like animals represent a very important group of macroscopic bioturbators in marine settings. They are diverse and can be exceedingly abundant: >10 000 species of marine polychaetes are known (Rouse & Fauchald 1998). Within the Polychaeta, most reported (ichnological) observations are associated with members of the subclasses Palpata (Glyceridae, Nephtyidae, Nereididae, Serpulidae, Sabellidae, Spionidae, Pectinariidae and Terebellidae) and Scolecida (Arenicolidae, Capitellidae, Maldanidae, Opheliidae and Paraonidae).

Nemerteans are often free swimming, but some are common burrowers (e.g. *Cerebratulus* of the family Lineidae), living infaunally in marginal-marine settings. Although less common, the burrows of vermiform hemichordates (class Enteropneusta or 'acorn worms') are well studied because hemichordates represent the 'evolutionary link' between invertebrates and vertebrates. Two important genera of enteropneusts are *Saccoglossus* and *Balanoglossus*. *Saccoglossus* favors shallow marine waters and *Balanoglossus* appears to be more abundant in deeper waters (Chris Cameron pers. comm.).

The commonest morphology of worm burrows is a simple vertical tube or shaft (Figs. 1A & 2A). From such tubes, worms filter feed in the water column (e.g. sabellariids), gather food from the sediment–water interface (e.g. terebellids, maldanids and glycerids), deposit feed (maldanids and capitellids), or engage in passive carnivory (e.g. *Cerebratulus*). More exotic uses of vertical tubes include gathering stock chemicals for chemobiosis (Romero-Wetzel 1987, Hertweck et al. 2005) or attracting vagile pore-living animals (Minter et al. 2007). The most common modification of the vertical shaft is transformation into a Y-form. This behavior is exemplified by nereid polychaetes, which are observed to extend their burrows laterally with serial Y-branches (Figs. 1C & 2B,C). A second common modification is the establishment of a basal tunnel, which can run horizontally and may be connected to the sediment–water interface laterally (Fig. 1C). The basal tunnel may be observed to branch. Where preserved in the rock record, these structures will generally be assigned to the ichnotaxa *Skolithos* (vertical shaft), *Polykladichnus* (Y-shape), *Planolites* (actively filled, horizontal tube), or *Palaeophycus* (lined tube). To varying degrees, such traces are made by nereids, glycerids, nephtyids, nemerteans and the hemichordate *Balanoglossus* (Gingras et al. 1999, Hertweck et al. 2005, 2007). Burrows that branch basally and possess a single vertical connection to the sediment–water interface, such as those commonly made by nereid and capitellid polychaetes, may produce traces similar to *Chondrites* (Hertweck et al. 2007).

Another common feature of worm-generated tubes is the addition of a lining. Lined vertical burrows are typically unbranched. Linings can be thin and litho-

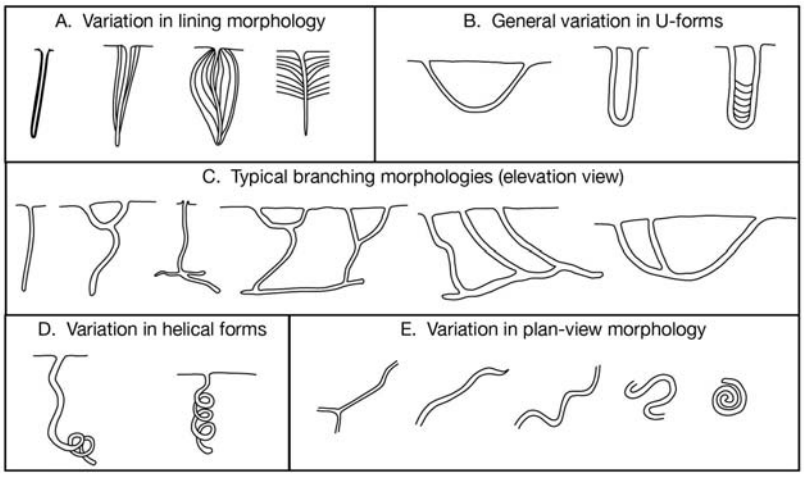

Fig. 1. Variations in worm burrows. (A) Burrow lining types: concentric and thin, through tapered or spindle-shaped. Also, *Tasselia*-like lining is shown on right. (B) Broad, narrow, and *Diplocraterion*-like U-shaped burrows. (C) Morphological variation in Y-shaped burrows. (D) *Helicolithus*- and *Gyrolithes*-type helical burrows. (E) Branching, sinuous, meandering, and coiled forms of intrastratal horizontal burrows

logically distinct, such as the brick-layer style sand tubes of pectinariids, or may comprise mucus-bound sediments, such as those installed by maldanid worms (Fig. 1; Bromley 1996). Although visibly discernible from their unlined counterparts, lined shafts are still assigned to *Skolithos* in the sedimentary record. Tubes with armored linings (i.e. lined with mucus and other material, such as sediment or shell fragments) may be ascribed to *Schaubcylindrichnus*. In some burrows, the lining is observed to be extravagantly over-thickened, typically with fine-grained clastics. This is commonly accompanied by a flaring of the lining, producing the spindle-shaped lining commonly observed in terebellid polychaete burrows (Aller & Yingst 1978, Nara 1995, Gingras et al. 1999), or a drum-shaped morphology (Wetzel & Bromley 1996). Flared or tapered structures in the rock record would be described as *Cylindrichnus* or *Rosselia* (Figs. 1A & 2H). In gravel-dominated sediments, terebellid polychaetes commonly deposit feed within the sediment and do not require a tube opening at the sediment–water interface. In these cases, the resultant burrow is similar in form to *Asterosoma* (Dashtgard et al. 2008).

A morphological advancement of the simple shaft is the U-shaped burrow, resulting in an *Arenicolites*-like trace (left and middle traces, Fig. 1B). Although similar in form to Y-shaped burrows (Fig. 1C), U-shaped burrows serve a fundamentally different feeding strategy. Nereid worms seem to generally employ a Y-morphology and are seldom observed in simple U-burrows, whereas animals that commonly use U-shaped burrows (such as arenicolids) show no predisposition to add a descending Y-branch. This seems to reflect basic functionality: Y-burrows are more commonly used for interface feeding and protection, where access to the detritus-laden surface is enhanced by an extra opening, and extra openings reduce the risk of predation. U-burrows are more commonly dedicated to conveyer-belt feeding strategies (i.e. arenicolids; Swinbanks 1981) or filter feeding (spionids; Gingras et al. 1999). Basic U-form burrows can be modified by extending or shifting the U-structure and, thereby, generating a spreite. U-burrows with spreiten are assigned to the ichnogenus *Diplocraterion*, diminutive examples of which have been observed to be made by spionid polychaetes (Schäfer 1972, Pemberton & Frey 1985, Gingras et al. 2001) and arthropods (Richter 1926, Seilacher 1964, Schäfer 1972). Larger rock-record examples (such as *Diplocraterion habichi*) may well have been produced by nemerteans or nereid polychaetes, but modern examples of large *Diplocraterion* have not been reported.

An important twist on vertical shaft architectures is the imposition of a corkscrew morphology, resulting in the trace fossils *Helicolithus* and *Gyrolithes* (Figs. 1D & 2F,G). Such traces have only been observed in modern settings in association with capitellid polychaetes (Howard & Frey 1975) and decapod shrimp (Dworschak & Rodrigues 1997; discussed in 'Materials and methods—Marine crustaceans'). The morphology is also observed as a component of some enteropneust burrows (*Saccoglossus*; Gingras et al. 1999), but, in those cases, the corkscrew generally resides at the terminal end of the lower burrow (Fig. 2F,G). Although the trace fossil *Gyrolithes* has been linked to salinity-induced stresses in the rock record (MacEachern et al. 1999), modern occurrences seem to be more strongly associated with either anchoring of the worm (e.g. *Saccoglossus*), a response to high-density colonization (e.g. capitellids; M. K. Gingras pers. obs.), or may represent a focused, 3D deposit-feeding structure (M. K. Gingras pers. obs.).

The range of morphologies on the horizontal components of worm burrows are expressed in their planiform configuration. As suggested above, worm burrows may branch near the surface. Such structures facilitate interface feeding, reduce the risk of predation, and possibly allow passive carnivory (all of these general behaviors are discussed in Seilacher 1964). Tubes or burrows may also be sinuous to meandering horizontal tunnels, with or without branches. Nereid polychaetes commonly construct 3D horizontal networks (Fig. 1E), from which branches extend to the

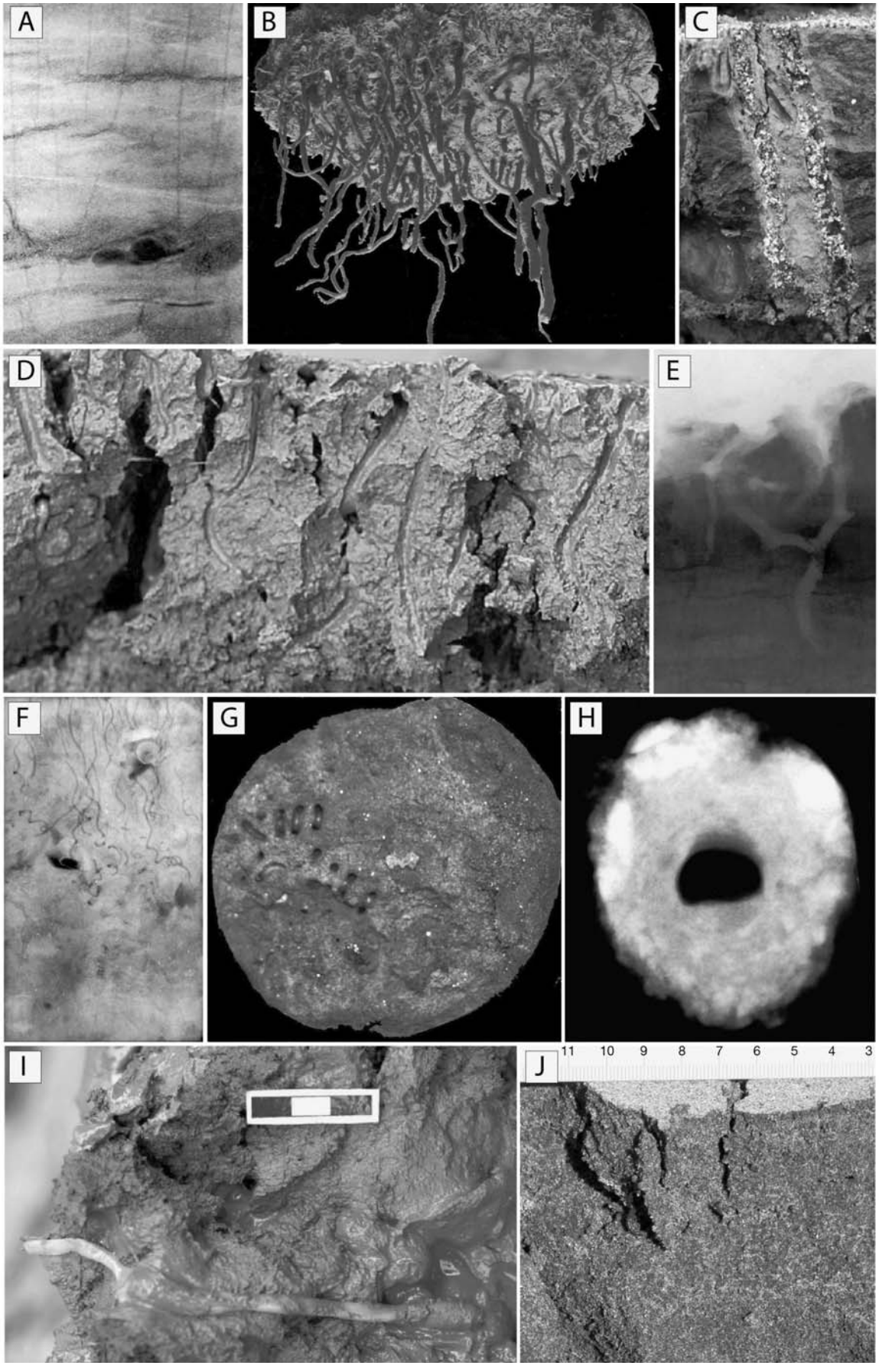
A
B
C
D
E
F
G
H
I
J
11 10 9 8 7 6 5 4 3

Fig. 2. Worm burrows. (A) Incipient *Skolithos* from tidal sands, Ogeechee Estuary (X-ray image); tracemaker not ascertained. Field of view: 12 cm. (B) Resin cast of Y-shaped burrows of *Nereis* from Kouchibouguac Estuary, Canada. Field of view: 34 cm. (C) Reamed vertical tube with concentric lining from Bay of Fundy, Canada. Field of view: 2.5 cm. (D) Nereid polychaetes and incipient *Polykladichnus* from muddy sediments of Shepody Estuary, Canada. Field of view: 15 cm. (E) X-ray image *Polykladichnus*, Bay of Fundy, Canada. Field of view: 14 cm. (F) *Saccoglossus* (enteropneust) burrows, X-ray image from Bay of Fundy, Canada. (G) Exposed parts of *Saccoglossus* burrows from shallow core (Willapa Bay, USA). Field of view: 10.5 cm. (H) Cross section of thickened burrow wall (*Rosselia*) from modern terebellid polychaete (Bay of Fundy, Canada). Field of view: 4 cm. (I) *Palaeophycus*-dwelling nemertean, *Cerebratulus*, Shepody estuary, Canada. Scale bar: 3 cm. (J) *Macaronichnus* made by opheliid polychaete, *Euzonus*. Pachena Beach, Vancouver Island

sediment–water interface. These burrow networks are semi-permanent structures that allow the worm to move quickly through the sediment and deposit feed over a larger area (Hertweck et al. 2007, Gingras et al. 1999, Dashtgard & Gingras 2005a). Opheliid polychaetes also move horizontally though the sediment and backfill their burrows as they relocate. Opheliids are, in part, deposit feeders that are constantly shifting in search of food (Clifton & Thompson 1978, Saunders & Pemberton 1990). As such, a permanent burrow structure would be impractical. Permanent horizontal burrow networks are similar to the trace fossil *Palaeophycus*, whereas temporary burrows of mobile feeders are similar to *Planolites*. Opheliids are also known tracemakers of *Macaronichnus* (Fig. 2G). Unbranched horizontal burrows are difficult to observe in modern settings, but have been inferred from X-rays of box-cores collected from deeper-water deposits (Wetzel 1991, 2002). Such burrow forms probably record deposit-feeding behaviors—such as that interpreted for the trace fossil *Chondrites*—and may be produced by polychaetes (Hertweck et al. 2005). Non-branched horizontal burrows are similar in morphology to the trace fossils *Planolites*, *Helminthopsis*, *Phycosiphon*, and *Cochlichnus*.

In summary, worm burrows from modern settings show a wide range of burrow morphologies that can be directly applied to the rock record. Some of the burrow forms, such as vertical shafts and branched horizontal burrow networks have a wide range of ethological uses. Other forms, such as Y- and U-shaped burrows, and corkscrew-shaped burrows seem to indicate more localized niches. Modifications on planiform morphology are dominantly dedicated to deposit-feeding initiatives.

Marine crustaceans

The range of burrowing marine arthropods is broad. Dominant in this group are isopods, amphipods and decapods, to which we restrict the discussion below. Isopods are a diverse order of crustaceans common to shallow marine waters. Amphipods include >7000 species of small, shrimp-like crustaceans, most of which occupy marine settings. The order Decapoda includes crayfish, crabs, lobsters, prawns, and shrimp. In marine settings, the trace-fossil record is dominated by thalassinid shrimp and amphipods and, to a far lesser degree, the burrows of crabs, stomatopods, and lobsters (Fig. 3).

Isopods are relatively flat, robust animals that scavenge and deposit feed within the intertidal zones of modern sand-dominated shorelines. They excavate shallow burrows in the sediment during high tide, in order to avoid being eaten. As the falling tide exposes the sediment, the isopods move rapidly through water-saturated sediment, processing and extracting organic matter (Griffith & Telford 1985, Hauck et al. 2008). In some cases, the pathways of these small crustaceans are preserved as displaced sedimentary laminae produced by their infaunal, 'sediment-swimming' movement: these traces have no clear taxonomic affinity. The surface trackways constructed by isopods—straight to meandering to chaotically spiraling bedding-plane traces—can be ascribed to *Gordia*. Alternatively, where preservation is exceptional, a bilobate furrow may be evident, and the resulting trace can be classified as *Isopodichnus*.

Amphipods are another major group of burrowing organisms in marginal-marine settings. In sandy backshore settings, talitrid amphipods construct vertical, unlined burrows similar in form to *Skolithos* (Dashtgard & Gingras 2005b). Within the intertidal zone, 2 main burrowing amphipods are commonly found, *Corophium* sp. and *Haustorius* sp. *Corophium volutator* is a mud-loving shrimp, which occurs in population densities up to 63 000 m^{-2} in semi-firm mud substrates (Thurston 1990, Pearson & Gingras 2006). It constructs a U-shaped tube that, during high tide, allows the amphipod to breathe, feed, and evacuate waste material from the safety of its burrow. *C. volutator* burrows are similar to *Arenicolites*. With time, this tube is deepened resulting in the development of *Diplocraterion* (Fig. 4G) (Richter 1926, Seilacher 1964, Schäfer 1972). A second *Corophium* species, *C. arenarium*, is common in sandy substrates within the intertidal zone. *C. arenarium* constructs a single vertical shaft in sand as water flows freely through the burrow walls and does not require an exit shaft. These burrows are similar in

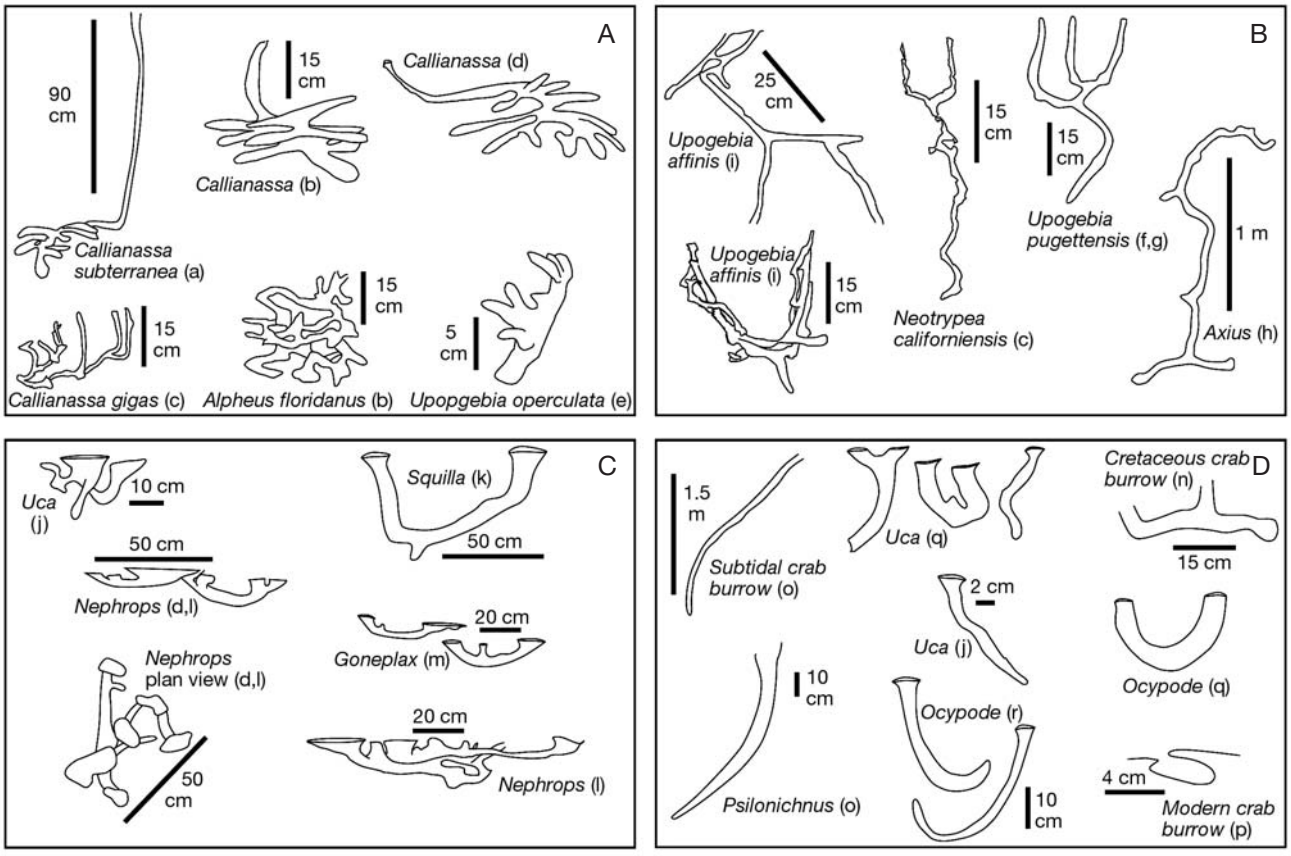

Fig. 3. Variations in crustacean burrows represented by schematic diagrams of resin casts and trace fossils. Thalassinid burrows with (A) a simple subapertural shaft and a complex deposit feeding architecture and (B) with modified U-shaped subaperture and simple or absent basal architectre. (C) Crab, lobster and mantis burrows with complex subaperture and no basal architecture; (D) Crab burrows with a simple J-, U-, or Y-shaped subaperture and no basal architecture. For (A,B) shafts and tubes have a circular cross-section and burrows are (A) commonly lined, or (B) rarely lined. For (C,D) irregular or ovate cross-sections are common and burrows are generally unlined. Note overall higher complexity of basal portion of thalassinid burrows compared to lobster and crab burrows. Lobster burrows demonstrate more complex branching in sub-aperture portion of burrow; crab burrows commonly display simplest architectures. Sources indicated by letters beside burrow schematics are as follows: (a) Atkinson & Nash (1990), (b) Shinn (1968), (c) Griffis & Chavez (1988), (d) Rice & Chapman (1971), (e) Kleeman (1984), (f) Dworschak (1982), (g) Stevens (1929), (h) Pemberton et al. (1976), (i) Frey & Howard (1975), (j) Basan & Frey (1977), (k) Myers (1979), (l) Farmer (1974), (m) Atkinson (1974), (n) Richards (1975), (o) Humphreys & Balson (1988), (p) Savazzi (1982), (q) Farrow (1971), (r) Frey et al. (1984), (s) Fürsich (1981)

form to *Skolithos*. The surface locomotion trackways of *Corophium* and of free-swimming marine amphipods have not been classified.

Haustoriid amphipods—a group of burrowing amphipods—also occur in intertidal settings. Haustoriids are commonly referred to as digger amphipods, as they move through the sediment by excavating and backfilling their burrow as they move. The smaller species of this group of amphipods are only a few millimeters long and tend to contribute to the formation of cryptobioturbation (see 'Biodeformational structures' below). Large specimens, however, disrupt the sediment (Fig. 4F) (Howard & Elders 1970).

Thalassinid shrimp are the best known of crustacean burrowers, producing traces conspicuous in their size and geometry. The basic form of most thalassinid shrimp burrows is a vertical shaft connected to the sediment–water interface, which branches at depth (Shinn 1968, Griffis & Chavez 1988, James et al. 1990). The range of thalassinid traces is summarized in Fig. 3A and Fig. 4A,B. Fossilized, these traces are known collectively as *Thalassinoides*. The upper part of the burrow, referred to as the aperture, may split and narrow, forming a small Y-shape. This is rarely preserved in the rock record. Thalassinid shrimp burrows may display complex basal structures (Fig. 3A) including tiered and box-worked networks (Shinn 1968, Griffis & Chavez 1988, James et al. 1990). In general, thalassinid shrimp use the vertical shaft to maintain a connection to the sediment–water interface, and the basal network for deposit feeding. The large volume of thalassinid burrows also permits shrimp to moderate the burrow

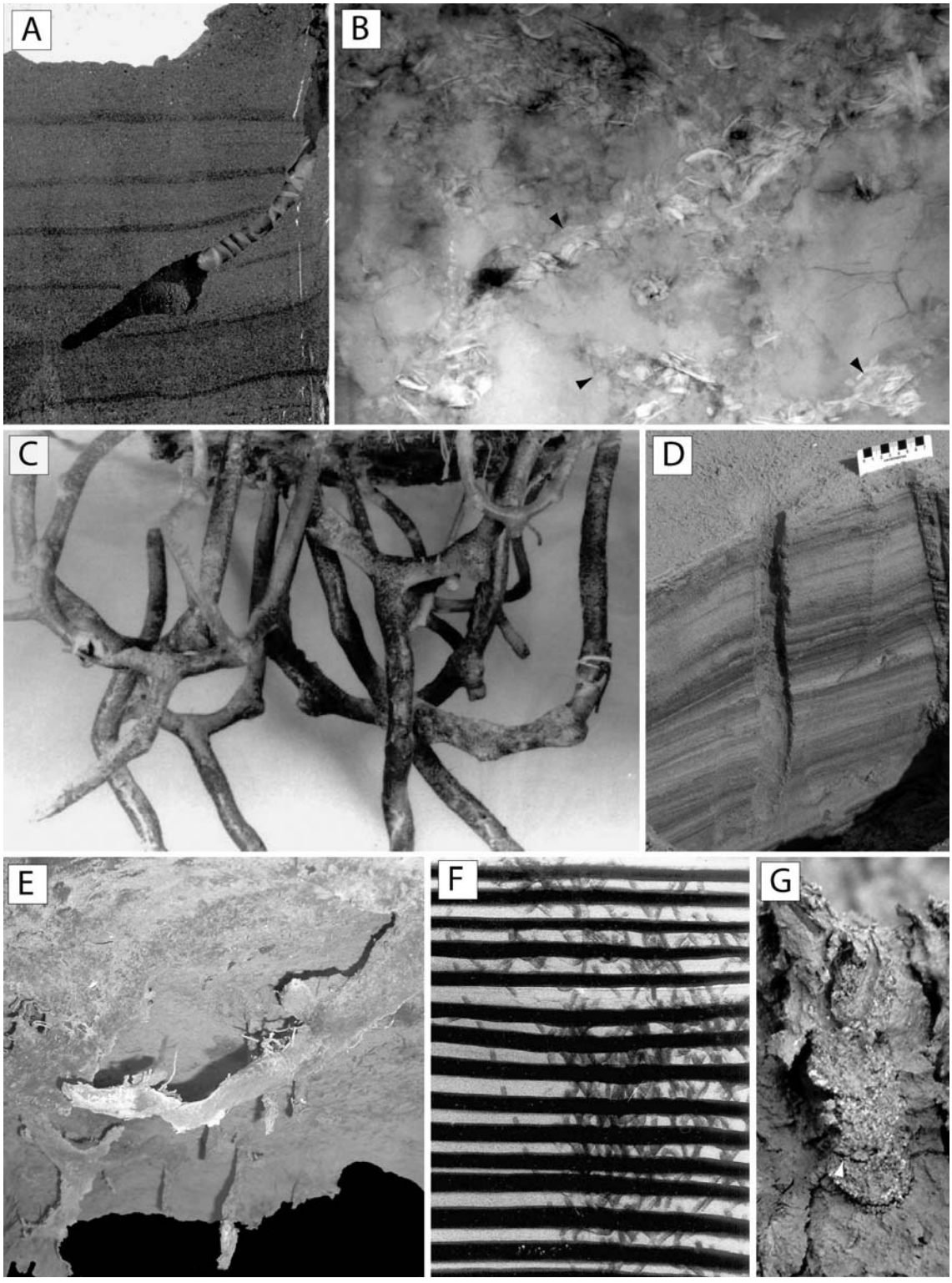

Fig. 4. Crustacean burrows. (A) *Neotrypaea californiensis* (thalassinid) in a laminated aquarium. Image shows swollen turning chamber and typical *Thalassinoides* morphology. Field of view: 14 cm. (B) X-ray of thalassinid burrows filled with shell material (black arrowheads), Ogeechee Estuary, USA. Field of view: 25 cm. (C) Resin cast of burrows of *Upogebia pugettensis* from Willapa Bay, USA. (D) Vertical part of incipient *Psilonichnus* made by crabs, Ogeechee Estuary, USA. (E) Resin cast of *Hemigrapsus oregonensis* from Willapa Bay, USA. Field of view ~20 cm. (F) Sediment mixing by haustoriid amphipods in thin-walled aquarium. (G) Incipient *Diplocraterion* made by amphipod *Corophium volutator*. Field of view: 2 cm

chemistry in intertidal settings and in locales characterized by salinity fluctuation (Thompson & Pritchard 1969). The genus *Upogebia* tends to maintain a Y-shaped burrow (Fig. 4C) (cf. *Polykladichnus*) that the animal employs for filter feeding, using the descending branch as a protective domicile (Stevens 1929, Dworschak 1982). This is a different use of the Y-structures constructed by worms, in that polychaetes activate this strategy for focused interface-feeding activities. Thalassinid shrimp are also known to make large, *Gyrolithes*-style helical burrows (Dworschak & Rodrigues 1997). These burrows are identical to those produced by vermiform animals, except that the trace is much larger and bioglyphs may be imprinted on the burrow wall (Wetzel 2007). It is more likely that the shrimp use such architectures to produce a spiral ramp for the easy maintenance of their domiciles, or that this is a response to high population densities within shrimp species otherwise not known for gregarious behavior.

Shrimp burrows may be pellet-, mud-, and mucus-lined (Pemberton et al. 1976, Frey et al. 1978) but can vary appreciably. These are normally used in shifting substrates and, in the rock record, would be considered stabilized variants of the trace fossil *Thalassinoides*. In general, pellet-walled shrimp burrows would be ascribed to the ichnogenus *Ophiomorpha*.

Modern crab burrows have many characteristics that are not generally seen in burrows made by other crustaceans (Figs. 3C,D & 4D,E). These include comparatively simple architectures (U-, Y-, and J-shaped), open apertures and irregular ovoid cross sections (Fig. 3C,D). Crab burrows are normally unlined (Atkinson 1974, Curran & White 1991, Gringras & Pickerill 2002) and can be interpreted as *Psilonichnus* (Frey & Pemberton 1987, Pemberton et al. 2001). Because crab burrows represent domiciles as opposed to combined feeding structures, complex basal geometries are absent. The architectures of crab and lobster traces are similar, although lobster burrows normally display shallower, sub-apertural branching (Rice & Chapman 1971, Farmer 1974) and possess more irregular burrow diameters (Fig. 3C,D). No widely used ichnogenus resembles the irregular burrows constructed by lobsters; although the term *Decapodichnus* is informally ascribed (Pemberton et al. 1984).

Marine bivalves

There are 3 main types of bivalve traces (Fig. 5): (1) vertically oriented filter- or surface-deposit-feeding from a stationary location, (2) horizontal motility reflecting grazing near the sediment–water interface, and (3) rapid vertical movement through the sediment as an escape mechanism. Additionally, bivalves process reduced sediment-porewater compounds within their burrows.

Stationary, filter- and surface-deposit-feeding bivalves have been observed to produce columnar traces composed of 3 parts: (1) an ovate cavity situated around the bivalve; (2) possible equilibrichnial structures directly below or above the cavity, recording slight upward and downward movement; and (3) a vertical chimney or chimneys demarcating the location of the bivalve's extended siphon or siphons (Figs. 5 & 6A–C) (Gingras et al. 2007). Similar structures in the rock record include *Siphonichnus* (Stanistreet et al. 1980), *Scalichnus*—an equilibrium trace fossil produced by *Panopea* (see Hanken et al. 2001)—and, to a lesser degree, *Conichnus* which normally only possesses Features 1 and 2 of the 3 main bivalve traces above (e.g. Savrda & Uddin 2003). *Conichnus* represents the efforts of the animal to maintain a connection to the sediment–water interface (Fig. 5). In the case of *Siphonichnus*-type traces, the connection is maintained using a prehensile siphon. Notably, many bivalves also have a 'foot' that is capable of moving the organism up and down in the sediment, and producing equilibrichnia (menisci). Together, the siphon and the foot represent the primary means of sediment reworking.

A very common ichnofossil ascribed to bivalves is *Lockeia*. This is a small, almond-shaped depression indented by the foot of the bivalve during resting.

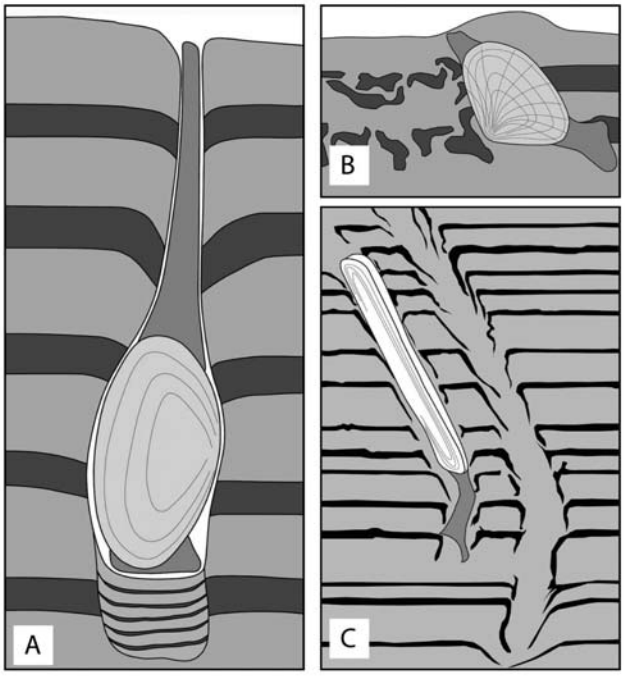

Fig. 5. Bivalve traces. (A) Vertically oriented bivalve produces *Siphonichnus*-type trace. (B) Disruption of sediment produced by horizontal movement of bivalve. (C) Escape structures (fugichnia) produced by upward escape behavior of mobile bivalves

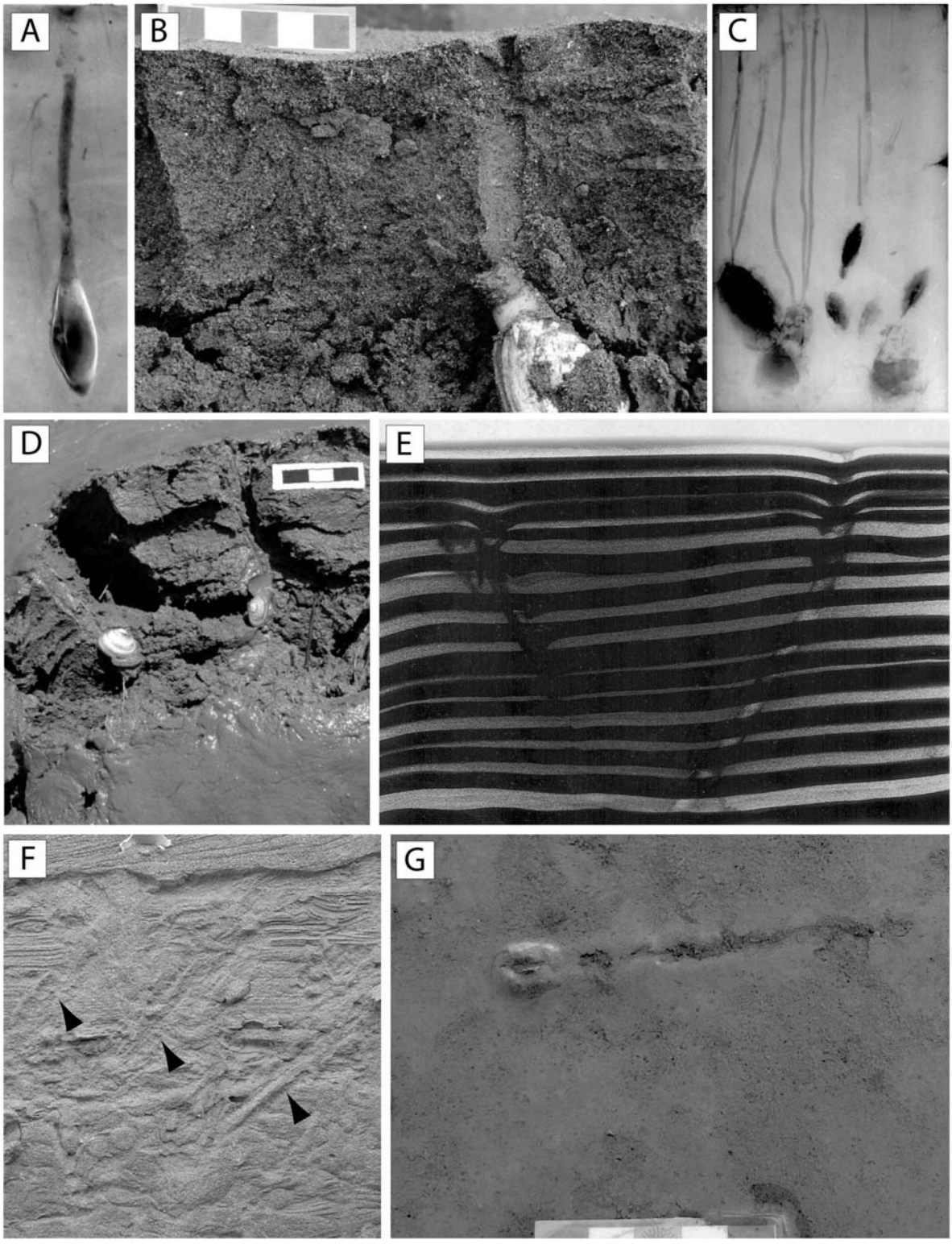

Fig. 6. Bivalve burrows. (A) *Mya arenaria in situ*; X-ray of shallow sediment core from Bay of Fundy, Canada. Field of view: 3.5 cm. (B) *M. arenaria* in sandy sediment, Bay of Fundy, Canada. Scale bar: 5 cm. (C) Split siphon of *Macoma balthica* results in paired connection to sediment–water interface. X-ray image from Kouchibouguac, Canada. Field of view: 14 cm. (D) *M. balthica in situ*, Shepody estuary, Canada. Scale bar: 3 cm (E) Razor clam adjustment structures in thin-walled aquaria. Field of view: 25 cm. (F) Resin peel of shallow box-core showing escape structure (black arrowheads point to escape traces) of modern razor clams. Field of view: 15 cm. Courtesy of B. C. Yang. (G) Horizontal trail of *M. balthica*

These structures are difficult to see in modern deposits, because they are preserved only at interstratal boundaries. They are best seen in bedding-plane views. Inferable structures have been identified in X-ray images, and very well-developed examples (found with preserved *in situ* shells of *Mya arenaria*) have been reported from Recent sediments in the Bay of Fundy (Dashtgard & Gingras 2005b).

Rapid vertical movements by bivalves are preserved almost solely as fugichnia (i.e. upwards-escape tracks). In modern deposits, this is caused by an abrupt sedimentation event and is observed as a wispy, downward deflection of sedimentary laminae. This behavior has been induced in aquaria, and captured in box-core peels (Figs. 5 & 6E,F), but in the rock record it is exceedingly difficult to distinguish such structures from those produced by the escape response of other animals.

Horizontal movements of bivalves leave furrows and produce lateral deformations ascribed to the pushing of the foot (Figs. 5 & 6G). This has been likened to the production of *Protovirgularia* in the rock record (Seilacher & Seilacher 1994). Much more complex (lateral) bivalve movements have been suggested in the case of *Hillichnus loboensis*, which was compared to the traces of modern tellinacean bivalves (Bromley et al. 2003), and in some complex bivalve motility tracks (Werner 2002).

Motile echinoderms

Motile echinoderms are represented by Eleutherozoa, which include the Asteroidea (starfish), Ophiuroidea (brittle stars), Echinoidea (sea urchins and sand dollars), and Holothuroidea (sea cucumbers). All of these animals leave distinctive traces in modern sediments.

Asteroids most commonly leave star-shaped resting traces preserved as the trace fossil *Asteriacites* (Gaillard 1991). It is also recognized that asteroids create motility traces that record their movement across the seafloor. Less well known are the predation traces produced by asteroids digging into shallow sediment to feed on bivalves.

Ophiuroids may move along the seafloor in a manner similar to asteroids, and can leave similar resting traces. Unlike starfish, however, the brittle stars have been observed buried in sediment with their arms stretched above the sediment–water interface (Howard & Frey 1975). This filter-feeding behavior has been reported from various shallow marine settings. The resulting trace is a conical to chevron-shaped disruption of the sediment that has not been reported from the rock record (Fig. 7C), but which could be confused with *Lingulichnus* or *Cylindrichnus* in poorly displayed cross-sections.

Echinoids—such as heart urchins (spatangoids)—can be extremely mobile, especially in sandy substrates. These animals move through the shallow sediment by passing sediment grains under their bodies using their tube feet. The resulting trace, shown from X-ray images of laboratory aquaria and sediment box-cores, can be a very finely and regularly backfilled passage (Fig. 7D,E) (Bromley & Asgaard 1975, Wetzel 1981, Fu & Werner 2000). Not all spatangoids produce a finely back-filled trace, however, with such traces ranging from laminated to crudely backfilled (Bromley & Asgaard 1975, Kanazawa 1995). The backfilled burrows produced by sand dollars (very thin and very shallow: M. K. Gingras pers. obs., Parksville, British Columbia, 2006), sea biscuits, and heart urchins are similar. However, identification of the resultant trace is dependent upon the size and shape of the tracemaker. Backfilled structures constructed by heart urchins are the most conspicuous of these trace fossils, due to their larger cross-sectional width. The very flattened form of sand dollar traces would likely inhibit their identification as trace fossils. Backfilled echinoid tunnels can be broadly classified as *Scolicia* or *Bichordites*, although true *Scolicia* and *Bichordites* should show evidence of a preserved axial canal or canals near the center of the trace fossil. Such details are hard to identify in modern sediments and are, in part, dependant on the grain-size of the sediment (Wetzel 1981). Sand dollars are known to orient themselves vertically within the sediment in a manner similar to brittle stars, such that part of their body is buried and part extends above the sediment–water interface (O'Neill 1978). This behavior is likely to produce small chevron-shaped disruptions virtually identical to the aforementioned brittle star's traces.

Sea cucumbers are probably responsible for a broader range of trace fossils than have been ascribed to them in the ichnological literature. They make crude, sinuous trails at the sediment–water interface and large, also crude, bow-shaped *Arenicolites*-type burrows in intertidal settings (Fig. 7A,B) (Howard 1968). Their ability to burrow infaunally suggests that at least some irregular disruptions of sediment in the rock record could be attributed to the burrowing activity of sea cucumbers.

Sponges and sea anemones

Although sponge traces are widely recognized as borings (e.g. Kelly & Bromley 1984, Bromley 1994, 1996), their traces in soft sediment are limited to cup-shaped resting marks. These traces range in size from

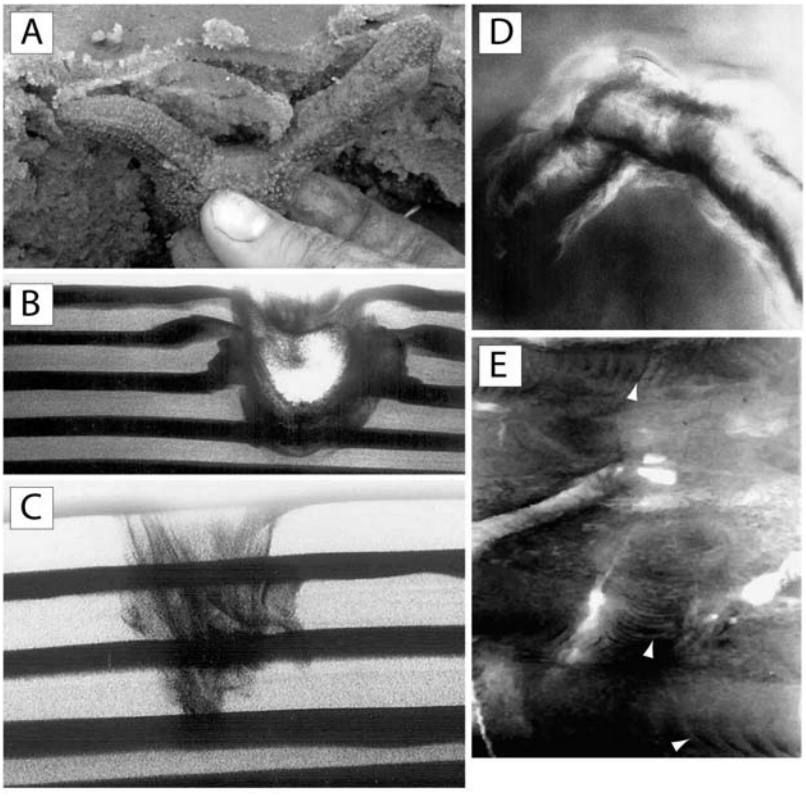

Fig. 7. Echinoderm burrows. (A) Sea cucumber, *Thyone*, living in *Arenicolites*-like burrow, Ogeechee Estuary, USA. (B) X-ray image of *Thyone* in thin-walled aquarium. Field of view: ~20 cm. (C) Typical intrusive structure produced by brittle star. Field of view: 13 cm. (D) X-ray image of sea urchin, *Moira*, from aquarium study. Field of view: 25 cm. (E) Digitized tracing of X-ray image of shallow sediment core bioturbated by heart urchins. Field of view: 14 cm. Arrowheads: mensicate backfill of echinoid passage

centimeter-scale to decimeter-scale, and they generally do not exceed a few centimeters in depth. Sea anemones, in contrast, can produce large, penetrative biogenic structures. The burrowing anemone, *Cerianthus*, for example, may reach 70 cm in length, and can burrow to almost that depth within the sediment (Hargitt 1907). The animal protrudes out of its burrow to hunt, and retracts to nearly full depth to take shelter. Its iterative probing up through the sediment produces a collapsed, chevron-shaped trace fossil that is conical in cross-section (Fig. 8). *Cerianthus* is also very capable of re-establishing its position with respect to the sediment–water interface, such that its dwelling trace can show notable aggradation in response to sedimentation events. Only small anemones have been imaged from X-rays of box-cores, but their traces are nearly identical to the trace fossil *Conichnus*. Buck & Goldring (2003) noted the similarity of conical structures attributed to anemones and various structures produced by dewatering or degassing. This suggests caution should be used when interpreting potential anemone-made structures in the rock record.

Biodeformational structures

Biodeformation structures (sensu Schäfer 1956) include macro-scale deformation, and cryptobioturbation or cryptic bioturbation. Cryptic bioturbation is a common texture in marginal-marine depositional environments. The activities of meiofauna (animals between 0.1 and 1 mm) and very small macrofauna blur or mottle the original sedimentary fabric, resulting in the development of a cryptobioturbate texture (Howard & Frey 1975, Bromley 1996). Whereas the macrofauna discussed above either excavate a penetrative burrow or disrupt the sediment to the point that primary sedimentary structures are destroyed, meiofauna shift grains only slightly as they move and feed between them. In sandy substrates, the mass of meiofauna occupying the sediment may far exceed the macrofaunal population mass. Despite this, meiofaunal disruption of the sediment is commonly ignored, because some primary sedimentary fabrics are still visible even in 100% cryptobioturbated substrates. In tropical environments, complete homogenization of sediments by meiofauna has been reported to occur in as little as a few days (Thayer 1983, Bromley 1996).

Biodeformational structures are features such as 'mantle and swirl' (Schäfer 1956, Lobza & Schieber 1999, Schieber 2003) and sediment-swimming structures. Mantle and swirl structures occur where burrows cross sedimentary layers and obscure the bedding contacts, with the burrow infills displaying an array of complex, convoluted features due to mixing of soupy sediment. Sediment-swimming structures result from an animal passing through fluid-rich substrate. Such structures blur sedimentary laminae, but do not produce a distinct burrow, and develop mainly through the burrowing activity of macrofauna, such as nephtyid polychaetes and isopods. The biosedimentary textures generated are similar to cryptobioturbation.

DISCUSSION

The majority of marine trace fossils can be attributed to invertebrates. Studies from modern settings have revealed tracks and burrows analogous to many trace fossils, including *Arenicolites*, *Asterosoma*, *Cochlichnus*, *Conichnus*, *Cylindrichnus*, *Diplocraterion*, *Gordia*, *Gyrolithes*, *Helminthopsis*, *Isopodichnus*, *Ophiomorpha*, *Lockeia*, *Palaeophycus*, *Planolites*, *Polykladich-*

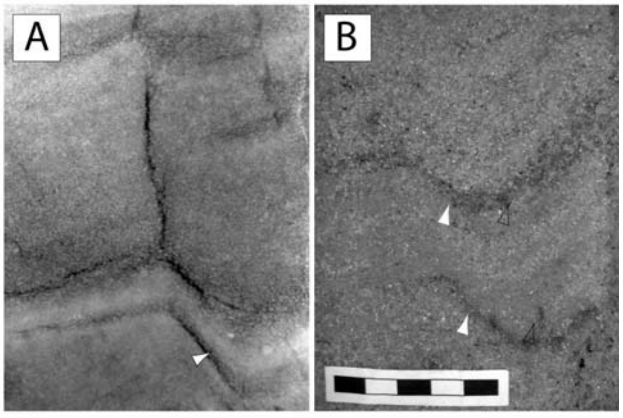

Fig. 8. Anemone burrows. (A) *Conichnus*-like structure from X-ray image, Ogeechee Estuary, USA. Field of view: 10 cm. (B) Slabbed box-core showing sediment disruption around anemone, Ogeechee Estuary, USA. Arrowheads: anemone trace. Scale bar: 5 cm

nus, *Protovirgularia*, *Psilonichnus*, *Rosselia*, *Scolicia*, *Siphonichnus*, *Skolithos*, *Taenidium*, and *Thalassinoides*, as well as biodeformational textures. This is a conservative list. More complex ichnofossils have been interpreted in the context of neoichnological data (e.g. *Neonereites* [Martin & Rindsburgh 2007] and *Hillichnus*). Some traces have been identified (in modern sediments) from deep-water studies, but the tracemakers are not known: *Zoophycos*, *Phycosiphon*, and *Chondrites* are commonly reported from sedimentary core, but without the tracemaker retained (Wetzel 1991). Other deep-water trace fossils (e.g. graphoglyptids or patterned trace fossils) are unknown from modern deposits or are only rarely reported. *Spirorhaphe*, *Cosmorhaphe*, and *Paleodictyon* have been observed as grooves in the tops of washed cores (without their tracemakers; Ekdale 1980), whilst *Paleodictyon* has been reported once from submarine surveys (Rona et al. 2003). Most trace fossils can be associated with a tracemaker only by inference. Analogues of other trace fossils probably will be discovered as studies of deep-marine settings increase.

A fundamental tenet of ichnology is that trace fossils should not be identified or characterized with respect to the inferred tracemaker, because fossil behavior is evolutionarily convergent. In other words, the behavior of a shrimp making a *Skolithos*-type trace is thought to be the same as a worm constructing a similar trace. However, many morphologically similar traces are produced for different reasons by different groups of animals. Large, open horizontal networks serve as domiciles and deposit-feeding structures for crustaceans, but are built by worms mainly for passive carnivory or for expanding an interface-feeding network. The trace fossil *Gyrolithes* potentially represents a mechanical ramp made by a shrimp or a holdfast produced by worms. Similarly, Y-shaped burrows are used for filter feeding by shrimp, and interface deposit feeding by worms. These examples emphasize that inferences of behavior in the rock record are interpretive. Moreover, recurring associations of trace fossils (i.e. ichnofacies) are based upon the most likely (interpreted) behavior linked to a trace fossil. This does not reduce the utility of ichnofacies, but it does suggest that in settings characterized by lower diversities of trace fossils (e.g. brackish-water settings), the application of accepted ichnofacies can be extremely misleading.

Although linking a trace fossil to a tracemaker is not necessarily critical to an ichnological study, we contend that ichnological research can clearly benefit from such efforts. By understanding the life strategies employed by infauna in modern environments and how the traces they produce aid in survival, we can better assess the likely habits represented by individual and groups of trace fossils preserved in the rock record. Infaunal organisms respond to environmental stresses; by assessing organism and community response to various environmental stresses, it is possible to establish relations between ichnofossils, ichnological communities, and sedimentary processes. These links can be used to refine paleoenvironmental interpretations of the rock record and identify or predict spatial changes in the sedimentary environment.

Acknowledgements. Thanks to Dr. Kerrie Bann and Tom Saunders for continued insights into burrowing animals; also to Tyler Hauck and Lynn Dafoe for new insights regarding the distribution and behaviors of marginal-marine bioturbators. This manuscript was substantively improved by the reviews and input provided by Andreas Wetzel and 2 anonymous reviewers. Funding for research in neoichnology was generously provided by a Natural Science and Engineering Research of Canada (NSERC) Discovery Grant to M.K.G.

LITERATURE CITED

Aller RC, Yingst JY (1978) Biogeochemistry of tube-dwellings: a study of the sedentary polychaete *Amphitrite ornata* (Leidy). J Mar Res 36:201–254

Atkinson RJA (1974) Behavioural ecology of the mud-burrowing crab, *Goneplax rhomboides.* Mar Biol 25:239–252

Basan PB, Frey RW (1977) Actual-palaeontology and neoichnology of salt marshes near Sapelo Island, Georgia. In: Crimes TP, Harper JC (eds) Trace fossils. Geol J (Spec Issue 9)2:41–70

Bertling M, Braddy SJ, Bromley RG, Demathieu GR and others (2006) Names for trace fossils: a uniform approach. Lethaia 39:265–286

Bouma AH (1969) Methods for the study of sedimentary structures. John Wiley & Sons, New York

Bromley RG (1994) The palaeoecology of bioerosion. In: Donovan SK (ed) The palaeobiology of trace fossils. Johns Hopkins University Press, Baltimore, MD

Bromley RG (1996) Trace fossils: biology, taphonomy and applications. Chapman & Hall, London

Bromley RG, Asgaard U (1975) Sediment structures produced

by a spatangoid echinoid: a problem of preservation. Bull Geol Soc Den 24:261–281

Bromley RG, Uchman A, Gregory MR, Martin AJ (2003) *Hillichnus lobosensis* igen. et isp. nov., a complex trace fossil produced by tellinacean bivalves, Paleocene, Monterey, California, USA. Palaeogeogr Palaeoclimatol Palaeoecol 192:157–186

Buck SG, Goldring R (2003) Conical sedimentary structures. Trace fossils or not? Observations, experiments, and review. J Sediment Res 73:338–353

Clifton HE, Thompson JK (1978) *Macaronichnus segregatis*: a feeding structure of shallow marine polychaetes. J Sediment Petrol 48:1293–1302

Curran HA, White B (1991) Trace fossils of shallow subtidal to dunal ichnofacies in Bahamian Quaternary carbonates. Palaios 6:498–510

Dafoe LT, Gingras MK, Saunders TDA, Pemberton SG (2008) Determining *Euzonus mucronata* burrowing rates with application to ancient *Macaronichnus segregatis* tracemakers. Ichnos (in press)

Dashtgard SE, Gingras MK (2005a) Facies architecture and ichnology of recent salt-marsh deposits: Waterside Marsh, New Brunswick, Canada. J Sediment Res 75:596–607

Dashtgard SE, Gingras MK (2005b) The temporal significance and distribution of bioturbation in coarse-grained upper foreshore and backshore deposits: Waterside Beach, New Brunswick, Canada. Palaios 20:589–595

Dashtgard SE, Gingras MK, Pemberton SG (2008) Grain-size controls on the occurrence of bioturbation. Palaeogeogr Palaeoclimatol Palaeoecol 257:224–243

Dworschak PC (1982) The biology of *Upogebia pusilla* (Petagna) (Decapoda, Thalassinidae). PSZN I: Mar Ecol 4: 19–43

Dworschak PC, Rodrigues SA (1997) A modern analogue for the trace fossil *Gyrolithes*: the burrows of *Axianassa australis* (Decapoda: Thalassinidea: Laomediidae). Lethaia 30:41–52

Ekdale AA (1980) Graphoglyptid burrows in modern deep-sea sediment. Science 207:304–306

Ekdale AA, Bromley RG, Pemberton SG (1984) Ichnology; the use of trace fossils in sedimentology and stratigraphy. SEPM Short Course 15, Society of Economic Paleontologists and Mineralogists, Tulsa, OK

Farmer ASD (1974) Burrowing behavior of the Norway lobster, *Nephrops norvegicus* (L.) (Decapoda: Nephropidae). Estuar Coast Mar Sci 2:49–58

Farrow GE (1971) Back-reef and lagoonal environments of Aldabra Atoll distinguished by their crustacean burrows. Symp Zool Soc Lond 28:455–500

Frey RW, Howard JD (1975) Endobenthic adaptations of juvenile thalassinid shrimp. Bull Geol Soc Den 24:283–297

Frey RW, Pemberton SG (1987) The *Psilonichnus* ichnocoenose and its relationship to adjacent marine and nonmarine ichnocoenoses along the Georgia coast. Bull Can Petrol Geol 35:333–357

Frey RW, Curran HA, Pemberton SG (1984) Tracemaking activities of crabs and their environmental significance: the ichnogenus *Psilonichnus*. J Paleontol 58:333–350

Fu S, Werner F (2000) Distribution, ecology and taphonomy of the organism trace *Scolicia*, in northeast Atlantic deep-sea sediments. Palaeogeogr Paleoclimatol Palaeoecol 156: 289–300

Fürsich FT (1981) Invertebrate trace fossils from the Upper Jurassic of Portugal. Comunicacoes Servicos Geologicos de Portugal 67:153–168

Gaillard C (1991) Recent organism traces and ichnofacies on the deep-sea floor off New Caledonia, southwestern Pacific. Palaios 6:302–315

Gingras MK, Pickerill R (2002) Resin cast of modern burrows provides analogs for composite trace fossils. Palaios 17: 206–211

Gingras MK, Pemberton SG, Saunders T, Clifton HE (1999) The ichnology of modern and Pleistocene brackish-water deposits at Willapa Bay, Washington: variability in estuarine settings. Palaios 14:352–374

Gingras MK, Pemberton SG, Saunders T (2001) Bathymetry, sediment texture, and substrate cohesiveness: their impact on modern *Glossifungites* trace assemblages at Willapa Bay, Washington. Palaeogeogr Palaeoclimatol Palaeoecol 169:1–21

Gingras MK, Armitage IA, Pemberton SG, Clifton HE (2007) Pleistocene walrus herds in the Olympic peninsula area: trace-fossil evidence of predation by hydraulic jetting. Palaios 22:539–545

Griffis RB, Chavez FL (1988) Effects of sediment type on burrows of *Callianassa californiensis* Dana and *C. gigas* Dana. J Exp Mar Biol Ecol 117:239–253

Griffith H, Telford M (1985) Morphological adaptations to burrowing in *Chiridotea coeca* (Crustacea, Isopoda). Biol Bull 168:296–311

Hanken N, Bromley RG, Thomsen E (2001) Trace fossils of the bivalve *Panopea faujasi*, Pliocene, Rhodes, Greece. Ichnos 8:117–130

Hargitt W (1907) Notes on the behavior of sea-anemones. Biol Bull 12:274–284

Hauck TE, Dashtgard SE, Gingras MK (2008) Relationships between organic carbon and *Fodichnia* morphology. Palaios 23:336–343

Hertweck G, Wehrmann A, Leibezeit G, Steffens M (2005) Ichnofabric zonation in modern tidal flats: paleoenvironmental and paleotrophic implications. Senckenb Marit 35:189–201

Hertweck G, Wehrman A, Liebezeit G (2007) Bioturbation structures of polychaetes in modern shallow marine environments and their analogues to Chondrites group traces. Palaeogeogr Palaeoclimatol Palaeoecol 245:382–389

Howard JD (1968) X-ray radiography for examination of burrowing in sediments by marine invertebrate organisms. Sedimentology 11:249–258

Howard JD, Elders CA (1970) Burrowing patterns of haustoriid amphipods from Sapelo Island, Georgia. Geol J Spec Issues 3:243–262

Howard JD, Frey RW (1975) Regional animal–sediment characteristics of Georgia estuaries. Senckenb Marit 7:33–107

Humphreys B, Balson PS (1988) *Psilonichnus* (Fürsich) in Late Pliocene subtidal marine sands of eastern England. J Paleontol 62:168–17

James R, Atkinson RJA, Nash RDM (1990) Some preliminary observations on the burrows of *Callianassa subterrana* (Montagu) (Decapoda: Thalassinidea) from the west coast of Scotland. J Nat Hist 24:403–413

Kanazawa K (1995) How spatangoids produce their traces: relationship between burrowing mechanism and trace structure. Lethaia 28:211–219

Kelly RA, Bromley RG (1984) Ichnological nomenclature of clavate borings. Palaeontology 27:793–807

Kleeman K (1984) Lebensspuren von *Upogebia operculata* (Crustacea, Decapoda) in karibischen Steinkorallen (Madreporaria, Anthozoa). Beitr Palaeontol Österreich 11:35–57

Lobza V, Schieber J (1999) Biogenic sedimentary structures produced by worms in soupy, soft muds: observations from the Chattanooga Shale (Upper Devonian) and experiments. J Sediment Res 69:1041–1049

MacEachern JA, Stelck CR, Pemberton SG (1999) Marine and marginal marine mudstone deposition: paleoenvironmental interpretations based on the integration of ichnology,

palynology and foraminiferal paleoecology. In: Bergman K (ed) Isolated marine sand bodies: sequence stratigraphic analysis and sedimentological interpretation. Special Publication 64, SEPM, Tulsa, OK

Martin AJ, Rindsburgh AK (2007) Arthropod tracemakers of *Nereites*? Neoichnological observations of juvenile limulids and their paleoichnological applications. In: Miller W (ed) Trace fossils: concepts, problems, prospects. Elsevier, Amsterdam

Minter NJ, Krainer K, Lucas SG, Braddy SJ, Hunt AP (2007) Palaeoecology of an Early Permian playa lake trace fossil assemblage from Castle Peak, Texas, USA. Palaeogeogr Palaeoclimatol Palaeoecol 246:390–423

Myers AC (1979) Summer and winter burrows of a mantis shrimp, *Squilla empusa*, in Narragansett Bay, Rhode Island (USA). Estuar Coast Mar Sci 8:87–98

Nara M (1995) *Rosselia socialis*: a dwelling structure of a probable terebellid polychaete. Lethaia 28:171–178

O'Neill PL (1978) Hydrodynamic analysis of feeding in sand dollars. Oecologia 34:157–174

Pearson NJ, Gingras MK (2006) An ichnological and sedimentological facies model for muddy point-bar deposits. J Sediment Res 76:771–782

Pemberton SG, Frey RW (1985) The *Glossifungites* ichnofacies: modern examples from the Georgia Coast, USA. In: Curran HA (ed) Biogenic structures: their use in interpreting depositional environments. Special Publication 35, SEPM, Tulsa, OK

Pemberton SG, Risk MJ, Buckley DE (1976) Supershrimp: deep bioturbation in the Strait of Canso, Nova Scotia. Science 192:790–791

Pemberton SG, Frey RW, Walker RG (1984) Probable lobster burrows in the Cardium Formation (Upper Cretaceous) of southern Alberta, Canada, and comments on modern burrowing decapods. J Paleontol 58:1422–1435

Pemberton SG, Spila M, Pulham AJ, Saunders T, MacEachern JA, Robbins D, Sinclair IK (2001) Ichnology and sedimentology of shallow to marginal marine systems: Ben Nevis and Avalon Reservoirs, Jeanne d'Arc Basin. Geological Association of Canada Short Course 15, Geological Association of Canada, St. John's

Rice AL, Chapman CJ (1971) Observations on the burrows and burrowing behavior of two mud-dwelling decapod crustaceans, *Nephrops norvegicus* and *Goneplax rhomboides*. Mar Biol 10:330–342

Richards BC (1975) *Longusorbis cuniculosus*: a new genus and species of Upper Cretaceous crab; with comments on Spray Formation at Shelter Point, Vancouver Island, British Columbia. Can J Earth Sci 12:1850–1863

Richter R (1926) Flachseebeobachtungen zur Paläontologie und Geologie, XII–XIV. Senckenbergiana 8:200–224

Romero-Wetzel MB (1987) Sipunculans as inhabitants of very deep, narrow burrows in deep-sea sediments. Mar Biol 96:87–91

Rona PA, Seilacher A, Luginsland H, Seilacher E and others (2003) *Paleodictyon*, a living fossil on the deep sea floor. Fall Meeting 2003, American Geophysical Union, Washington, DC, OS32A-0241 (abstract)

Rouse GW, Fauchald K (1998) Recent views on the status, delineation, and classification of the Annelida. Am Zool 38:953–964

Saunders TDA, Pemberton SG (1990) On the palaeoecological significance of the trace fossil *Macaronichnus*. In: Proc Int Sedimentological Congr 13, p 416

Savazzi E (1982) Burrowing habits and cuticular sculptures in Recent sand-dwelling brachyuran decapods from the Northern Adriatic Sea (Mediterranean): Neues Jahrb Geol Palaeontol Abh 163:369–388

Savrda CE, Uddin A (2003) Behavioral variability preserved in *Conichnus* and *Macaronichnus* in Upper Cretaceous Tombigbee Sand (Eutaw Formation), central Alabama. In: Proceedings of the Annual Meeting, 35, Geological Society of America, Boulder, CO, p 68 (abstract)

Schäfer W (1956) Wirkungen der Benthos Organismen auf den jungen Schichtverband. Senckenb Lethaea 37:183–263

Schäfer W (1972) Ecology and palaeoecology of marine environments. Oliver and Boyd, Edinburgh

Schieber J (2003) Simple gifts and buried treasures—implications of finding bioturbation and erosion surfaces in black shales. The Sedimentary Record 1:4–9

Seilacher A (1964) Biogenic sedimentary structures. In: Imbrie J, Newell N (eds) Approaches to paleoecology. Wiley, New York

Seilacher A, Seilacher E (1994) Bivalvian trace fossils: a lesson from actuopaleontology. Cour Forschinst Senckenb 169: 5–15

Shinn EA (1968) Burrowing in recent lime sediments of Florida and the Bahamas. J Paleontol 42:879–894

Stanistreet IG, Le Blanc Smith G, Cadle AB (1980) Trace fossils as sedimentological and palaeoenvironmental indices in the Ecca Group (Lower Permian) of the Transvaal. Trans Geol Soc South Africa 83:333–344

Stevens BA (1929) Ecological observations on Callianassidae of Puget Sound. Ecology 10:399–405

Swinbanks DD (1981) Sediment reworking and the biogenic formation of clay laminae by *Abarenicola pacifica*. J Sediment Petrol 51:1137–1145

Thayer CW (1983) Sediment-mediated biological disturbance and the evolution of marine benthos. In: Tevesz MJS, McCall PL (eds) Biotic interactions in Recent and fossil benthic communities. Plenum Press, New York

Thompson LD, Pritchard AW (1969) Osmoregulatory capacities of *Callianassa* and *Upogebia* (Crustacea: Thalassinidea). Biol Bull 136:114–129

Thurston H (1990) Tidal life; a natural history of the Bay of Fundy. Nimbus Publishing, Halifax

Werner F (2002) Bioturbation structures in marine Holocene sediments of Kiel Bay, western Baltic. Meyniana 54:41–72

Wetzel A (1981) Ökologische und stratigraphische Bedeutung biogener Gefüge in quartären Sedimenten am NW-afrikanischen Kontinentalrand. Meteor Forschungs-Ergebnisse C 34:1–47

Wetzel A (1991) Ecologic interpretation of deep-sea trace fossil communities. Palaeogeogr Palaeoclimatol Palaeoecol 85:47–69

Wetzel A (2002) Modern *Nereites* in the South China Sea—ecological association with redox conditions in the sediment. Palaios 17:507–515

Wetzel A (2007) Activities. Ichnology Newsletter 27:35

Wetzel A, Bromley RG (1996) The ichnotaxon *Tasselia ordamensis* and its junior synonym *Caudichnus annulatus*. J Paleontol 70:523–526

Submitted: November 6, 2007; Accepted: April 30, 2008

Proofs received from author(s): June 17, 2008

Vol. 2: 269–277, 2008
doi: 10.3354/ab00056

AQUATIC BIOLOGY
Aquat Biol

Printed June 2008
Published online June 19, 2008

Contribution to the Theme Section 'Bioturbation in aquatic environments: linking past and present'

OPEN ACCESS

Benthic invertebrate activity in lakes: linking present and historical bioturbation patterns

David S. White[1,*], Molly F. Miller[2]

[1]Hancock Biological Station, 561 Emma Drive, Murray, Kentucky 42071, USA

[2]Department of Earth and Environmental Sciences, Box 35-0117, 2301 Vanderbilt Place, Vanderbilt University, Nashville, Tennessee 37235, USA

ABSTRACT: Trace fossils of lacustrine benthos are less well known than those of marine benthos, limiting their potential use in interpreting paleo-environmental conditions, including climate change, reconstructing lake ecosystems, and predicting effects of sediment mixing of paleoclimate records. Here, we present a synopsis of limnological controls on the distribution of present day lacustrine benthos, a synopsis of their burrowing and feeding habits, and a summary of the traces they produce. Maximum diversity and density of benthos occur in sublittoral zones and decrease both shoreward and basinward. Common taxa include bivalves (unionids, sphaeriids), snails, oligochaetes, amphipods, and insects (particularly chironomids and ephemeropterans). With a few exceptions, traces produced are morphologically simple, shallowly inscribed, and have low preservation potential. Although lacustrine benthic organisms are widespread, variability within and between lakes causes them and their traces to be patchily distributed. To truly understand the records left in lacustrine sediments and the links between modern and ancient traces, we need comprehensive surveys over a range of lake types and collaborations between ichnologists and benthic ecologists.

KEY WORDS: Lake benthos · Lacustrine fauna · Lake ecology · Paleolimnology · Ichnofacies

INTRODUCTION

Interpretation of marine sedimentary environments has been greatly enhanced by integration of studies of modern traces and their producers with studies of trace fossils and their facies distributions (see examples in W. Miller 2007). In spite of recent work on lacustrine ichnology (e.g. Buatois & Mangano 2007), the contribution of lacustrine biogenic structures to understanding depositional systems lags behind their marine counterparts. One major barrier to ichnologists, who are overwhelmingly marine oriented, is dissimilarity between lacustrine and marine systems and organisms (Miller & White 2007). Because of the small size and isolation of many lakes, important environmental controls, particularly water mixing patterns and distribution of productivity, are highly variable and different from those in the marine realm. As a result, the lacustrine and marine terminologies are not the same, which hinders communication.

A second impediment to lacustrine ichnology is the disconnection between lacustrine trace fossils and the behavior of modern benthic animals in lakes. The large-scale actuo-paleontologic programs, the results of which provided the firm uniformitarian basis for marine ichnology in the 1930s (see Cadée & Goldring 2007), have not been undertaken in lacustrine settings. Coordinated studies must occur before the potential of lacustrine ichnology in elucidating paleoecologic, paleoclimatic, and depositional histories of lakes can be realized. Problem areas include: (1) linking lacustrine benthic animals with the traces produced; (2) correlating modern lacustrine traces typically observed in vertical section and trace fossils commonly preserved on bedding planes; (3) collecting data on the distribution and abundance of infaunal animals in modern lakes and on rates of bioturbation; (4) determining responses of lacustrine benthic fauna to changes in productivity and mixing; and (5) gathering quantitative information on the abundance, type, and facies

*Email: david.white@murraystate.edu

distributions of trace fossils and bioturbation in ancient lakes, including Paleozoic lakes extant prior to vegetative cover.

This paper describes the trace-producing activities of the most abundant lacustrine benthic animals, and summarizes their abundance and distribution. It relates modern traces to lacustrine trace fossils, and identifies barriers and unknowns. Finally, it addresses the extent of disruption of modern and ancient lacustrine sediments by biogenic structures and bioturbation, underscoring the need for data from both modern and ancient deposits in order to reconstruct the Phanerozoic history of lacustrine benthic activity.

DISTRIBUTION OF LACUSTRINE BENTHOS

The benthic environment of any lake is related to combinations of water column productivity (trophic status) and circulation (mixis) and sediment deposition patterns (see Wetzel 2001, Miller & White 2007). Lacustrine sediment deposition varies with proximity to inflowing streams. Clastic sediment deposition from inflowing streams may be on the scale of centimeters per year (e.g. Brinkhurst 1974, Robbins et al. 1989). Sedimentation is greatly reduced away from deltaic areas, where the average rate for natural lakes is about 1 mm yr^{-1} (Miller & White 2007) and may be much less in large oligotrophic lakes. It is under these conditions that typical benthic communities are established.

Limnologically, benthic zones may be thought of as regions of the lake bed that correspond more or less with the depths of light penetration that establish lake stratification, and with lake energy levels (Figs. 1 & 2; Hutchinson 1993, Wetzel 2001). The supralittoral zone occurs at and just above the shoreline and may contain a wide variety of rooted aquatic plants and burrowing invertebrates. The littoral zone extends from the shoreline to the depth where 1% of the surface light reaches the bottom and contains areas of continual wave-induced resuspension nearest the shoreline to occasional storm-induced resuspension nearest the 1% light depth. The sublittoral occurs between the littoral and profundal zones, usually between the 1% light penetration depth and the thermocline. The profundal zone begins where the thermocline impinges the bottom and corresponds with the areal extent of the hypolimnion. Except following extreme events, the summer thermocline depth is expected to remain constant from one year to the next and is established largely by light (heat) penetration (Wetzel 2001). In larger lakes, bottom sediments change from gravel and sand at the lake margin to silt and mud in a basinward direction, reflecting decreasing influence of wave

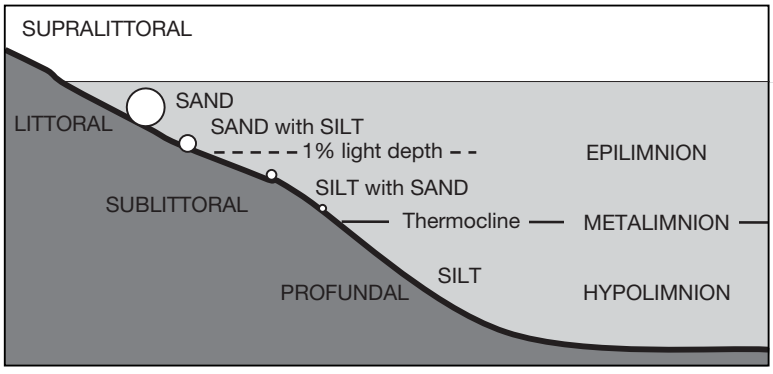

Fig. 1. Benthic and water column zones from shoreline to basin during summer stratification, showing resuspension probabilities (circles) and sediment types. In most lakes, summer stratification periods establish distributions of lacustrine benthos that occur throughout the year (after White et al. 1986, Wetzel 2001)

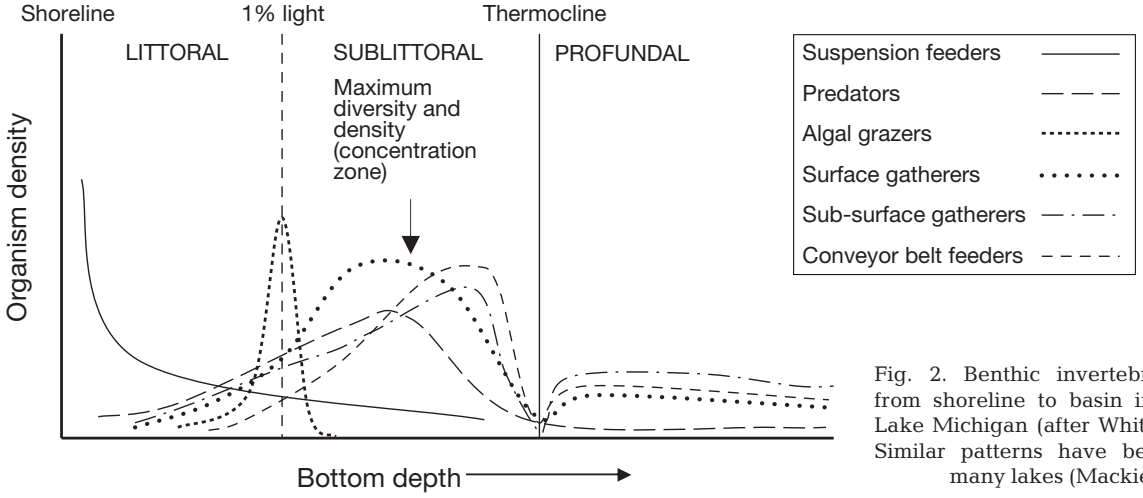

Fig. 2. Benthic invertebrate structure from shoreline to basin in oligotrophic Lake Michigan (after White et al. 1986). Similar patterns have been noted for many lakes (Mackie 2001)

energy and the resulting decrease in resuspension and winnowing (White et al. 1986). Wave-induced resuspension is rare in the profundal zone (Fig. 1), and sediment movement is caused primarily by biological activity and rare physical events such as thermal-bar scouring (Wetzel 2001).

The distribution of benthic invertebrates generally follows the littoral to profundal patterns described above (Fig. 2; White et al. 1986, Wetzel 2001). Maximum benthos density and diversity usually occur in the sublittoral zone in what has been termed the 'concentration zone' (Mackie 2001). Concentration zones often correspond with water column depths that are about 1.5 times the depth of light penetration (White et al. 1986, Mackie 2001). In most lakes, concentration zones (Fig. 2) occur between 2 and 4 m water depth, but may be as deep as 17 to 18 m in large oligotrophic lakes (Mackie 2001, Martin et al. 2005). The benthos is greatly reduced or absent below the thermocline in mesotrophic to eutrophic lakes, but may be found at depths up to 100s of meters in oligotrophic lakes (Fig. 2; Martin et al. 1994, 2005).

BIOGENIC STRUCTURES IN MODERN LAKES

Biogenic structures commonly reflect feeding activities and/or concealment behaviors (Figs. 3 & 4; Thorp & Covich 2001, Merritt et al. 2007). The terminology used for freshwater organisms differs from that used for marine organisms (Bromley 1996). In the broadest sense, collectors feed on deposited or suspended organic matter and associated bacteria. Collector feeding mechanisms include: (1) filter feeding on suspended or resuspended particles; (2) surface gathering of particles at the sediment–water interface; (3) subsurface gathering of buried organic matter, usually in oxidized surficial sediments; and (4) subsurface conveyor-belt feeding that vertically displaces buried particles. Suspension filterers tend to dominate nearshore littoral environments (Figs. 1 & 2), while surface and subsurface gatherers and conveyor-belt feeders dominate where resuspension events rarely occur (White et al. 1986). The distribution of algal grazers corresponds with the maximum abundance of benthic algae, which usually occurs at or just above the depth of the 1% light level (Stevenson & Stoermer 1981).

While there is considerable information on areal distributions, feeding habits, and secondary production of lacustrine benthos (Thorp & Covich 2001), the behavior of most taxa remains poorly known or is inferred from only a few descriptions (e.g. Brinkhurst 1974). This is largely due to the lack of laboratory and *in situ* observations. In general, the 2 main forms of bioturbation in lake sediments are eddy-diffusive and conveyor-belt mixing (Rhoads 1974). Eddy-diffusive mixing, the simple lateral or vertical movement of sediments, is more common and results in most types of traces, particularly those seen on bedding planes. Conveyor-belt mixing, the vertical displacement of sediments through feeding, is limited primarily to deposit-feeding aquatic annelids (e.g. Tubificidae, Lumbriculidae). While 100s of benthic invertebrate species may exist in any lake, the number of phyla is usually small (Hutchinson 1993), particularly those capable of bioturbation or of being preserved as body fossils or trace fossils. The primary groups are Mollusca (Bivalvia, Gastropoda), Annelida (particularly Oligocheata), and Arthropoda (Insecta and Crustacea, particularly Amphipoda and Isopoda).

All bivalves are aquatic and many live buried in the substrate (McMahon & Bogan 2001). With the exception of *Pisidium*, lacustrine bivalves are water-column suspension feeders found in fairly shallow littoral or

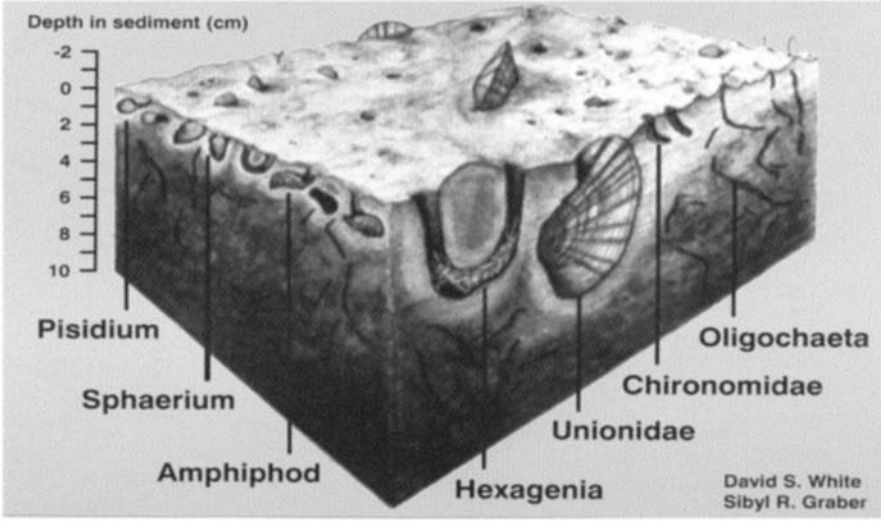

Fig. 3. Idealized drawing of lacustrine benthic community from Lake Michigan showing interactions with sediment (after White et al. 1986). Community components would not be expected to all occur at the same location and might be in much higher or lower densities, depending on lacustrine conditions

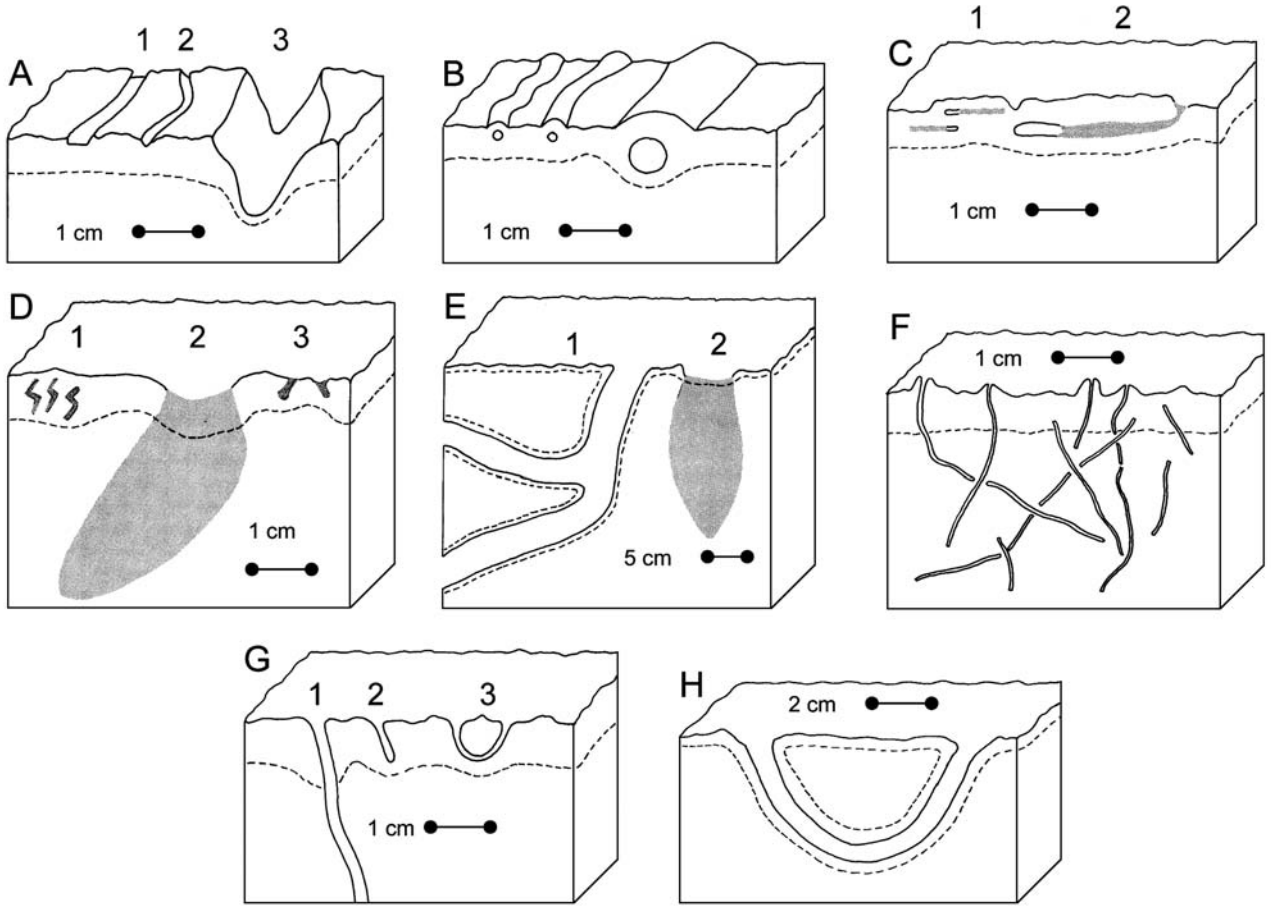

Fig. 4. Tracks and traces left by typical freshwater lacustrine benthos. (A) Surface traces left by (1) gastropods and (2 & 3) bivalves. (B) Subsurface burrows potentially left by burrowing amphipods, bivalves, and aquatic insects. (C) Backfilled burrows of (1) *Pisidium* and (2) amphipods. (D) Backfilled subsurface traces left by (1) *Chaoborus*, (2) small Unionidae and (3) *Sphaerium*. (E) (1) Crayfish burrow and (2) backfilled large Unionidae trace. (F) Tubificidae traces. (G) (1) Large chironomid trace, (2) J-shaped chironomid tube and (3) U-shaped chironomid tube. (H) *Hexagenia* burrow. Dotted lines represent predicted depths of oxidized sediments

sublittoral habitats. Bivalves actively move within or upon sediments (Wu 1987), but the traces produced are often difficult to ascribe to a particular species (Figs. 3 & 4A–E). Bioturbation by bivalves is eddy diffusive (White et al. 1986), and traces of burrows should be recognizable in sediment cores for long periods of time (Fig. 4D,E). *Pisidium*, with its greatly reduced siphon, burrows through sediments (Mackie et al. 1980) (Figs. 3 & 4B,C). *Pisidium* occurs in high densities in sublittoral and profundal sediments of oligotrophic lakes; >20 species and densities of up to 1000 ind. m^{-2} are found in the sublittoral zone of Lake Michigan (Zdeba & White 1985). The constant movements of *Pisidium* result in eddy-diffusive homogenization of surficial sediments (White et al. 1986).

More than 1000 species of lake-dwelling snails are known, and they feed primarily on periphyton and detritus (Harman & Berg 1971, Thorp & Covich 2001). Although some taxa (e.g. Limnaeidae) may burrow temporarily into soft sediments, most graze continually using their muscular foot to glide over surfaces at or above the 1% light level. Traces (Fig. 4A) are generally similar for most freshwater species (shallow and narrow, <1 cm wide), and bioturbation is eddy diffusive.

Annelids, particularly Tubificidae and Lumbriculidae, spend much of their life cycles buried where they feed on sediments and associated bacteria (Brinkhurst & Cook 1980). Oligochaetes feed in a conveyor-belt mode, more or less in a vertical position, with the head downward and the anus at or below the sediment–water interface (Figs. 3 & 4F). Surface defecation may leave small fecal mounds (Figs. 3 & 4F), but most individuals probably defecate below the surface. Densities, species composition, feeding rates, and feeding depths depend on the deposition rate of new organic matter. Where sediment deposition rates are high, such as in embayments and deltas, feeding and mixed depths may exceed 15 cm (Robbins et al. 1989). Popu-

lation densities >10 000 ind. m^{-2} occur in oligotrophic lakes. Several species often occur together, each feeding at a different depth in the sediment and relying on each other's fecal matter as a food resource (Keilty et al. 1988). Endostratal trails produced by oligochaetes are narrow (generally <2.0 mm wide), very irregular, and often appear in seemingly random patterns (Figs. 3 & 4F). Much of the feeding occurs below the oxidized surface layer, and traces tend to remain open in cores for long periods of time because few other benthic organisms venture that deeply into the substrate (Martin et al. 2005). Sediment reworking by oligochaetes can quickly obliterate the traces of other benthic taxa produced at shallower levels; a similar phenomenon has been documented in marine sediments (Bromley 1996). There is often a negative relationship between oligochaete densities and densities of species that build more permanent structures, presumably because oligochaete activities disrupt burrow functions (see Brinkhurst & Jamieson 1971). Few burrowing oligochaetes occur nearshore; they reach maximum diversity in sublittoral bottom sediments and maximum densities in profundal areas of oligotrophic lakes (Brinkhurst & Cook 1980, White et al. 1986).

Several genera and families of amphipods and isopods are known to burrow through surficial sediments feeding on detrital organic matter and associated bacteria. The burrowing patterns of *Euporeia* (= Amphipoda: *Pontoporeia*) and *Caecodotea* (= Isopoda: *Asellus*) appear to be typical of most taxa. *Euporeia* and Gammaridae are the most abundant benthic invertebrates in nearshore environments of the Laurentian Great Lakes, other glacially formed lakes, and deep-rift lakes (Marzolf 1965, Martin et al. 2005), but amphipods and isopods are uncommon in other types of lakes. Amphipods remain buried during the day, feeding on organic particles and bacteria, backfilling their trails as they go (Figs. 3 & 4B,C). *Euporeia* and some Gammaridae occur in the deepest zones of glacial oligotrophic lakes but reach maximum density just above the thermocline (White et al. 1986). Amphipods are often the dominant eddy-diffusive mixers of the sublittoral and profundal zones.

Chironomidae (Diptera, non-biting midges) are the most abundant and diverse aquatic insects, with >20 000 species (Merritt et al. 2007). Chironomid larvae are the most common insects in lakes and have long played a role in lake classification in relation to trophic status (Wetzel 2001). The majority of lacustrine chironomids are small, <1 cm long, and few details are known of their life histories or behavior. Most live either on the sediment surface or buried no more than 1 to 2 cm deep in a wide variety of substrates from sand to silty clays. Chironomids are found in all benthic zones, reaching maximum species diversity in sublittoral areas. *Sergentia koschowi* larvae occur at depths of 1360 m in Lake Baikal (Linevich 1971). Hemoglobin respiratory pigments allow larvae to persist in low-oxygen environments of mesotrophic to eutrophic lakes (Pinder 1995, Gingras et al. 2007). Many taxa create 1 to 2 cm long, silk-lined U- or J-shaped burrows (Figs. 3 & 4G), where they presumably remain for much of their life cycles, often a year, feeding on detritus or algae, or preying on zooplankton or other small invertebrates (Ford 1962, White et al. 1986). Other species, particularly of the genus *Chironomus*, move throughout the sediment creating endostratal trails similar to oligochaete traces (Figs. 3 & 4G). Phantom midge larvae (*Chaoborus*) are planktonic predators that exhibit vertical nightly migrations. During the day, larvae return to the sediments constructing small S-shaped burrows up to a centimeter long (Fig. 4D). Overall, sediment mixing by chironomids is eddy diffusive, but the nature of the bioturbation produced by non-tube-building taxa is unknown.

Ephemerids (burrowing mayflies) are large and perhaps the most spectacular burrowing insects in lakes, particularly the genus *Hexagenia*. *Hexagenia* nymphs build U-shaped burrows, often with many side-chambers that may extend 5 to 10+ cm deep into the fine-grained, firm substrate that they prefer (Figs. 3 & 4H). Nymphal life span for most species is 1 or 2 yr, and an individual may build numerous burrows in a single season. Carr & Hiltunen (1965) reported densities of up to 2000 individuals m^{-2} in western Lake Erie with burrows stacked upon each other in apartment house fashion. Where densities are high, eddy-diffusive bioturbation can be extensive. *Hexagenia* nymphs are most common in littoral and sublittoral zones and are intolerant of dissolved-oxygen concentrations <1 ppm (Madenjian et al. 1998). They are surface-deposit gatherers, but also may filter organic particles brought in by currents through the burrows (Carr & Hiltunen 1965).

Although not as abundant as the taxa mentioned above, a number of other invertebrates may leave traces in or on lake sediments. Among these are crayfish (Decapoda) and larvae of the insect families Tabanidae (Diptera), Sialidae (Neuroptera), Coleoptera (several families), Polycentropodidae (Trichoptera), and Tridactylidae (Orthoptera). Crayfish burrows probably have had the most detailed study of any of the major freshwater taxa (e.g. Hasiotis & Mitchell 1993), with Horwitz & Richardson (1986) providing a general classification scheme. Burrows range from simple tunnels to highly complex structures with numerous branches (Fig. 4G), similar to those described for marine callianassid shrimp (Bromley 1996). Burrowing usually occurs in the upper portions of the

littoral and the supralittoral zones and can play a significant role in bioturbation if densities are high.

Predatory insects, such as Sialidae, Polycentropodidae, and Tabanidae, can be common in shallow, protected lacustrine margins, particularly in association with rooted vegetation, and may also occur occasionally on the open lake floor. Most construct U-, I-, or J-shaped burrows similar to, but usually larger than chironomid burrows (see Fig. 4G). Other aquatic insects burrow just beneath the sediment–water interface, and their traces (Fig. 4B) can be indistinguishable from those made by other benthic organisms. Coleoptera are unique among aquatic insects in that both adults and larvae can share the same habitats and resources. Numerous species occur along the shoreline of both marine and freshwater habitats and are known to burrow just beneath the sediment–water interface (White & Roughley 2007). Coleoptera have been proposed as possible tracemakers for ichnofossils of the *Mermia* ichnofacies (see e.g. Buatois & Mangano 1995).

COMPARING TRACE FOSSILS AND MODERN TRACES

With very few exceptions (e.g. Hasiotis 2007), references to limnological or aquatic biological studies are absent in studies of lacustrine trace fossils. Typically, trace fossils are named and compared morphologically with others in the ichnotaxon and may commonly be assigned to behavioral groups (e.g. Pickerill 1992, Buatois & Mangano 2004, 2007). However, it is less common for a possible tracemaker to be suggested (but see Bromley & Asgaard 1979, Pickerill 1992, Metz 1996). Beyond trace fossil morphology, studies focus typically on documenting the facies distributions and trace fossil assemblages and on comparing them with those in other lacustrine strata.

Three lacustrine ichnofacies have been recognized. The *Mermia* ichnofacies (see e.g. Buatois & Mangano 1995, 2007) is an association of surficial tracks and trails, and shallow endostratal trails, interpreted as feeding and locomotion traces produced in perpetually submerged environments; trace fossils are nonpenetrative and preserved on bedding surfaces. The *Mermia* ichnofacies occurs in shallow to deep lacustrine facies (Buatois & Mangano 2007; reduction in ichnotaxonomic diversity with decreasing depth has been documented; Melchor 2004). Co-occurrence of *Mermia* and *Scoyenia* ichnofacies trace fossils have been interpreted as overprinting of marginal lacustrine bioturbation on biogenic structures produced in permanently submerged sediments (Kim et al. 2005); this corroborates extension of the *Mermia* ichnofacies into very shallow water. Because *Mermia* ichnofacies trace fossils occur in other ichnofacies, modifications in terminology have been suggested to make them more distinctive (Kim et al. 2005).

Broadly, the structures produced by the typical lake benthos described herein resemble the trace fossils of the *Mermia* ichnofacies. Both the modern structures and components of the *Mermia* ichnofacies are morphologically simple and most are produced near the sediment–water interface (see Fig. 4A,B,C,G). Missing from the *Mermia* ichnofacies, however, are the more deeply penetrative traces produced by chironomids, oligochaetes, and ephemerids, along with zones of intensely bioturbated sediment reworked by oligochaetes or amphipods. Trace fossils of the *Mermia* ichnofacies are interpreted generally to have been produced by insects, crustaceans, worms, and fishes (e.g. Pickerill 1992, Buatois & Mangano 1995), but there have been few detailed studies linking the behavior of modern lacustrine animals to the trace fossils.

The *Skolithos* ichnofacies is an association of low-diversity vertical burrows, and has been identified in sandstones deposited in high-energy, lake-margin environments (Buatois & Mangano 2007). However, it has not been widely reported from ancient lacustrine sequences, and no tracemakers have been identified. Insect diversity and abundance are much lower in sands than in other substrate types, and no organism is known that produces deep vertical burrows in mobile, shallow-water, lacustrine sands. Burrowing immature mayflies produce U-shaped burrows, but they are most common in quiet water settings.

The third association, the *Scoyenia* ichnofacies, is indicative of low-energy, lake-margin habitats that experience both subaqueous and subareal conditions (Kim et al. 2005, Buatois & Mangano 2007). The *Scoyenia* ichnofacies includes arthropod tracks and trails, plant traces, and vertebrate tracks (e.g. Frey & Pemberton 1987, Buatois & Mangano 2007). Many of the producers were probably terrestrial or semi-terrestrial rather than fully aquatic: greater diversity of semi-terrestrial burrowers than aquatic infaunal animals is well documented (e.g. Hasiotis 2007). *Scoyenia* itself and other traces that result in pervasive disruption of the sediment (e.g. *Fuersichnus*; Bromley & Asgaard 1979) have not been linked to modern lake-margin burrowers.

Most lacustrine trace fossils are shallowly penetrative and are thus found on bedding planes rather than on vertical surfaces (e.g. Miller et al. 2002). In contrast, most lake sediments are studied in cores, benthic animals are obtained from grab samples, and there is little opportunity to see traces in plain view. Observation and investigation of modern lake traces and sedimentary structures is hampered by the absence of tidal flats, which give easy access to infaunal animals and

surrounding sediment. Extensive studies of the tidal flats of the North Sea (and elsewhere) have provided information on the behavior of modern marine animals that has enhanced interpretation of trace fossils (Schafer 1972, Cadée & Goldring 2007), but similar investigations are not feasible in lacustrine sediments. The water cover and turbid conditions produced by easily re-suspended sediment make even observation of surficial traces difficult. Finally, much of the terminology used in ichnology comes from studies of the marine realm, making it difficult to integrate with limnological terms.

HOW PERVASIVE IS BIOTURBATION IN MODERN AND ANCIENT LAKE DEPOSITS?

Compared with ecological studies of lake benthos, there have been few bioturbation studies, and bioturbation changes over geological time have not been assessed. Further work needs to be carried out because: (1) the extent and style of biologic sediment reworking affects degradation and remineralization of organic matter and, thus, carbon cycling (e.g. Aller 1994, Mermillod-Blondin et al. 2004); (2) the degree of bioturbation affects the resolution of paleoclimate reconstructions from lake sediments; and (3) the depth and facies distribution of bioturbation and biogenic structures in lacustrine deposits through the Phanerozoic is key to reconstructing colonization history of lacustrine benthic habitats. Of particular interest is documenting how bioturbators responded to the post-Silurian increase in detritus from vascular plants and the effect of their activity on global carbon cycling (Park & Gierlowski-Kordesch 2007).

Modern lacustrine sediments

Most lacustrine sediment investigations are based on detailed analysis of only a few cores (e.g. Martin et al. 2005). In one of the few recent studies in which lake sediments were densely sampled (Schiefer 2006: 202 cores taken in a grid pattern every 100 m in a 2 km^2 glacial lake with a maximum depth of 44 m), varved sediments were found to cover 58% of the lake bottom; massive (poorly sorted) shallow water sediments, 13%; deltaic deposits, 10%; and transitional sediments, 19%. Of these, the varved, massive, and deltaic sediments were not affected by animal activity; bioturbation and biogenic structures were restricted to sediments transitional between the varved and massive sediments at depths between 3 and 12 m, depths comparable to the benthos concentration zones of Mackie (2001). The distribution of burrowed sediment in this lake was consistent with the highest density of benthos in sublittoral zones and its paucity in deeper areas. Data from Schiefer (2006) imply that even shallow lakes would have only small areas where sediment reworking by animals would be significant.

Bioturbation in ancient lacustrine stratigraphic sequences

Ichnologic studies of ancient lacustrine deposits often do not provide abundance data (e.g. Buatois & Mangano 1995, Melchor 2004; but see Pickerill 1992), and the abundance of bioturbation is only rarely evaluated (Miller et al. 2002, Melchor 2004). In the absence of such datasets, >50 of the descriptions of lacustrine sequences (Permian to Holocene) were reviewed for records of bioturbation (Gierlowski-Kordesch & Kelts 2000). No study reported extensive and pervasive bioturbation. Similarly, despite its importance as a potential mixing process, bioturbation is typically not mentioned in descriptions of cores from Pleistocene and Holocene lacustrine deposits sampled for high-resolution paleoclimate studies (see e.g. numerous studies published in the Journal of Paleolimnology between 2004 and 2007). Paucity of reported bioturbation in ancient lacustrine deposits may result from the fact that it was not the focus of the studies. The lack of appropriate datasets underscores the need for quantitative or semi-quantitative evaluation of the abundance and distribution of biogenic structures in ancient deposits in order to reconstruct the history of lake benthos through the Phanerozoic.

SUMMARY

In contrast to marine settings, lake systems are strongly affected by local geochemical and climate conditions. These determine nutrient content and mixing processes, which, in turn, control environmental conditions in the water column and substrate and exert a strong influence on the benthic fauna. The most common bottom-dwelling animals in lakes are bivalves, snails, oligochaete worms, crustaceans, and immature insects including chironomids, ephemerids, and chaoborids. The majority are small, soft-bodied shallow burrowers that feed on deposited organic matter. Their distributions are patchy, and are mostly controlled by food resources and water chemistry, including oxygen availability. Although a variety of benthic animals are capable of bioturbation, sensitivities to environmental conditions probably restrict their distribution and abundance in many lake systems. Maximum abundance and diversity generally occur in relatively nar-

row sublittoral concentration zones, but there is little information on the distribution of biogenic structures and bioturbation in modern lake sediments.

Lacustrine ichnology has focused on describing trace fossils, primarily those preserved on bedding planes, documenting their facies distributions and identifying ichnofacies. Rarely are trace fossils interpreted in light of the behavior of modern lacustrine trace producers, and rarely are ichnofacies integrated with what is known about the distributions of modern lacustrine benthic animals. In addition, there is very little information available on abundance of biogenic structures and extent of bioturbation in either modern or ancient lake deposits. As such, the shapes and patterns of traces and tracks produced by extant lacustrine benthos described in this study are a potentially useful ichnological tool.

Lacustrine ichnology can contribute significantly to understanding the flux of materials between the substrate and overlying water, interpreting paleoclimate, unraveling the colonization history of lacustrine substrates, and reconstructing lake histories. However, this potential will be realized only when it is linked to the study of trace fossils and when gaps in the knowledge of the abundance and distribution of bioturbation in both modern and ancient lacustrine deposits are closed.

Acknowledgements. We thank James Ramsey and Brooke Traynham for discussions on *Chironomus* and *Hexagenia* burrows. We thank Sibyl Graber for her patience and skill in helping to capture burrows and traces *in situ*. James Ramsey and a number of reviewers added to the clarity of the manuscript. D.S.W. was supported by the Center for Reservoir Research, Murray State University. M.F.M. was supported by NSF OPP 0126146 and OPP 0940954.

LITERATURE CITED

Aller RC (1994) Bioturbation and remineralization of sedimentary organic matter: effects of redox oscillation. Chem Geol 114:331–345

Brinkhurst RO (1974) The benthos of lakes. St. Martins Press, New York

Brinkhurst RO, Cook DG (eds) (1980) Aquatic oligochaete biology. Plenum Press, New York

Brinkhurst RO, Jamieson BGM (1971) The aquatic Oligochaeta of the world. Oliver & Boyd, Edinburgh

Bromley RG (1996) Trace fossils: biology and taphonomy. Unwin Hyman, London

Bromley R, Asgaard U (1979) Triassic freshwater ichnocoenoses from Carlsberg Fjord, East Greenland. Palaeogeogr Palaeoclimatol Palaeoecol 28:261–281

Buatois LA, Mangano MG (1995) The paleoenvironmental and paleoecological significance of the lacustrine *Mermia* ichnofacies: an archetypical subaqueous nonmarine trace fossil assemblage. Ichnos 4:151–161

Buatois LA, Mangano MG (2004) Animal–substrate interactions in freshwater environments: applications of ichnology in facies and sequence stratigraphic analysis of fluvio-lacustrine successions. In: McIlroy D (ed) The application of ichnology to palaeoenvironmental and stratigraphic analysis. Geol Soc Spec Publ 228:311–334

Buatois LA, Mangano MG (2007) Invertebrate ichnology of continental freshwater environments. In: Miller W III (ed) Trace fossils: concepts, problems, prospects. Elsevier, New York, p 285–323

Cadée C, Goldring R (2007) The Wadden Sea, cradle of invertebrate ichnology. In: Miller W III (ed) Trace fossils: concepts, problems, prospects. Elsevier, New York, p 3–13

Carr JF, Hiltunen JK (1965) Changes in the bottom fauna of western Lake Erie from 1930 to 1961. Limnol Oceanogr 10:551–569

Ford B (1962) The vertical distribution of larval Chironomidae (Dipt.) in the mud of a stream. Hydrobiologia 19:262–272

Frey RW, Pemberton SG (1987) The *Psilonichnus* ichnocoenose, and its relationship to adjacent marine and nonmarine ichnocoenoses along the Georgia coast. Bull Can Petrol Geol 35:333–357

Gierlowski-Kordesch EH, Kelts KR (2000) Lake basin through space and time. AAPG Stud Geol 46, Amer Assoc Petrol Geol, Tulsa

Gingras M, LaLond SV, Amskold L, Konhauser KO (2007) Wintering chironomids mine oxygen. Palaios 22:433–438

Harman WN, Berg CO (1971) The freshwater snails of central New York with illustrated keys to the general and species search. Cornell University, Ithaca, NY

Hasiotis ST (2007) Continental ichnology: fundamental processes and controls on trace fossil distribution. In: Miller W III (ed) Trace fossils: concepts, problems, prospects. Elsevier, New York, p 268–284

Hasiotis ST, Mitchell CE (1993) A comparison of crayfish burrow morphologies: Triassic and Holocene fossil, paleo- and neo-ichnological evidence and the identification of their burrowing signatures. Ichnos 2:291–314

Horwitz PJ, Richardson AMM (1986) An ecological classification of the burrows of Australian freshwater crayfish. Aust J Mar Freshw Res 37:237–242

Hutchinson GE (1993) A treatise on limnology, Vol 4. The zoobenthos. Wiley & Sons, New York

Keilty TJ, White DS, Landru PF (1988) Short term lethality and sediment avoidance assays with endrin-contaminated sediment and two oligochaetes from Lake Michigan: *Stylodrilus heringianus* (Lumbriculidae) and *Limnodrilus hoffmeisteri* (Tubificidae). Arch Environ Contam Toxicol 17:95–101

Kim JY, Keighley DG, Pickerill RK, Hwang W, Kim KS (2005) Trace fossils from marginal lacustrine deposits of the Cretaceous Jinju Formation, southern coast of Korea. Palaeogeogr Palaeoclimatol Palaeoecol 218:105–124

Linevich AA (1971) The Chironomidae of Lake Baikal. Limnologica 8:51–52

Mackie GL (2001) Applied aquatic ecosystem concepts. Kendall/Hunt, Dubuque

Mackie GL, White DS, Zdeba TW (1980) A guide to the freshwater mollusks of the Laurentian Great Lakes with special emphasis on the genus *Pisidium*. EPA-600/3-89-068, US EPA, Duluth

Madenjian CP, Schloesser DW, Kriege KA (1998) Population models of burrowing mayfly recolonization in western Lake Erie. Ecol Appl 8:1206–1212

Martin P, Goddeeris B, Martens K (1994) Depth distribution of oligochaetes in Lake Baikal (Siberia-Russia). Hydrobiologia 278:151–156

Martin P, Boes X, Goddeeris B, Fagel N (2005) A qualitative assessment of the influence of bioturbation in Lake Baikal sediments. Global Planet Change 46:87–99

Marzolf GR (1965) Substrate relations of the burrowing amphipod *Pontoporeia affinis* in Lake Michigan. Ecology 46:579–592

McMahon RF, Bogan AE (2001) Mollusca: Bivalvia. In: Thorp H, Covich AP (eds) Ecology and classification of North American freshwater invertebrates, 2nd edn. Academic Press, New York, p 331–429

Melchor RN (2004) Trace fossil distribution in lacustrine deltas: examples from the Triassic rift lakes of the Ischigualasto-Villa Union Basin, Argentina. In: McIlroy D (ed) The application of ichnology to palaeoenvironmental and stratigraphic analysis. Spec Pub 228, Geological Society, London, p 335–354

Mermillod-Blondin F, Gaudet JP, Gerin M, Desrosiers G, Jose J, Chatelliers MC (2004) Relative influence of bioturbation and predation on organic matter processing in river sediments. Freshw Biol 49:895–912

Merritt RW, Cummins KW, Berg MB (eds) (2007) Aquatic insects of North America, 4th edn. Kendall/Hunt, Dubuque

Metz R (1996) Nonmarine trace fossils from the Late Triassic and Early Jurassic of New Jersey. NJ Acad Sci Bull 41:1–5

Miller MF, White DS (2007) Ecological and evolutionary controls on the composition of marine and lake ichnofacies. In: Miller W III (ed) Trace fossils: concepts, problems, prospects. Elsevier, New York, p 531–544

Miller MF, McDowell TA, Smail SE, Shyr Y, Kem NR (2002) Hardly used habitats: dearth and distribution of bioturbation in Paleozoic and Mesozoic stream and lake deposits. Geology 30:527–530

Miller W III (ed) (2007) Trace fossils: concepts, problems, prospects. Elsevier, New York

Park LE, Gierlowski-Kordesch EH (2007) Paleozoic lake faunas: establishing aquatic life on land. Palaeogeogr Palaeoclimatol Palaeoecol 249:160–179

Pickerill RK (1992) Carboniferous nonmarine invertebrate ichnocoenoses from southern New Brunswick, eastern Canada. Ichnos 2:21–35

Pinder LCV (1995) The habitats of chironomid larvae. In: Armitage PD, Cranston PS, Pinder LCV (eds) The Chironomidae. Chapman & Hall, London, p 107–135

Rhoads DC (1974) Organism sediment relations on the muddy sea floor. Oceanogr Mar Biol Annu Rev 12:263–300

Robbins JA, Keilty TJ, White DS, Edgington DN (1989) Relationships between tubificid abundances, sediment composition, and accumulation rates in Lake Erie. Can J Fish Aquat Sci 46:223–231

Schafer W (1972) Ecology and palaeoecology of marine environments. Oliver & Boyd, Edinburgh

Schiefer E (2006) Contemporary sedimentation rates and depositional structures in a montane lake basin, southern Coast Mountains, British Columbia. Earth Surf Process Landf 31:1311–1324

Stevenson RJ, Stoermer EF (1981) Quantitative differences between benthic algal communities along a depth gradient in Lake Michigan. J Phycol 17:29–36

Thorp JH, Covich AP (eds) (2001) Ecology and classification of North American freshwater invertebrates. Academic Press, New York

Wetzel RG (2001) Limnology, lake and river ecosystems. Academic Press, New York

White DS, Roughley R (2007) Aquatic Coleoptera. In: Merritt R, Cummins K, Berg M (eds) Aquatic insects of North America, 4th edn. Kendall/Hunt, Dubuque, p 399–473

White DS, Winnell M, Zawacki C, LaDronka R, Zdeba T, Mozley S (1986) Ecology of the macrozoobenthos in the vicinity of the Donald C. Cook nuclear plant. In: Rossmann R (ed) Southeastern nearshore Lake Michigan: impact of the Donald C. Cook nuclear plant. Publication 22, Great Lakes Research Division, University of Michigan, Ann Arbor, p 253–283

Wu WI (1987) The burrowing of *Anodonta cygnea* (Linnaeus, 1758) (Bivalvia: Unionidae). Bull Malacol Rep China 13: 29–41

Zdeba TW, White DS (1985) Pisidiidae. Spec Rept 13, Great Lakes Research Division, University of Michigan, Ann Arbor

Submitted: January 4, 2008; Accepted: March 18, 2008

Proofs received from author(s): May 19, 2008

Vol. 2: 279–287, 2008
doi: 10.3354/ab00057

AQUATIC BIOLOGY
Aquat Biol

Printed June 2008
Published online June 19, 2008

Contribution to the Theme Section 'Bioturbation in aquatic environments: linking past and present'

OPEN ACCESS

Bioturbation levels during the end-Ordovician extinction event: a case study of shallow marine strata from the Welsh Basin

Liam G. Herringshaw[1,*], Neil S. Davies[2]

[1]**Geology & Petroleum Geology, School of Geosciences, Meston Building, University of Aberdeen, Aberdeen AB24 3UE, UK**
[2]**Department of Earth Sciences, Dalhousie University, Halifax, Nova Scotia B3H 4J1, Canada**

ABSTRACT: The Ordovician-Silurian succession of the Llandovery area, mid-Wales, preserves shallow marine sediments deposited during the Hirnantian (end-Ordovician) extinction event. Ichnological analysis of the rocks shows that the degree and depth of bioturbation in this part of the Welsh Basin was often low across this interval, both during glacioeustatic sea level fall and the early part of the subsequent transgression. This pattern suggests that stratigraphic dilution was not the primary control on trace fossil abundance: an increase in sediment supply during the regression could explain low abundance in early Hirnantian units, but not in the post-glacial transgressive strata. A significant decrease in oxygen levels during sea level rise might be invoked instead, but this cannot have been the sole cause, as the occurrence of burrows up to 20 mm in diameter in the Bronydd Formation (late Hirnantian–Rhuddanian) shows that seafloor oxygen levels were at least intermittently high. An absence of vertical bioturbation through much of the succession indicates that sessile, suspension-feeding organisms were generally scarce. The overall pattern probably reflects a decline in benthic infauna during the extinction event, but the 2 pulses of extinction described previously in body fossils are not evident ichnologically in this part of the Welsh Basin.

KEY WORDS: Ichnofabrics · Benthos · Infauna · Mass extinctions · Trace fossils

INTRODUCTION

The ecological effects of extinction events have typically been assessed using evidence from the body fossil record. However, the value of ichnology as a tool for measuring environmental stress, ecosystem restructuring and faunal recovery rate during such events is receiving increased recognition. Trace fossils have provided much new information on both the end-Permian (e.g. Twitchett & Wignall 1996, Wignall et al. 1998, Twitchett 1999, Pruss & Bottjer 2004, Pruss et al. 2004, Fraiser & Bottjer 2005) and end-Cretaceous extinctions (e.g. Ekdale & Bromley 1984, Ekdale & Stinnesbeck 1998, Rodríguez-Tovar & Uchman 2004a,b, Rodríguez-Tovar 2005, Uchman et al. 2005). Of the other major Phanerozoic extinctions, however, the end-Ordovician event has seen scant ichnological study. Indeed, in their review of research into ichnological responses to mass extinctions, Twitchett & Barras (2004) were able to cite only 1 published article (McCann 1990) examining trace fossils across the Ordovician-Silurian boundary. This dearth of work is surprising, since the extinction is associated intimately with perturbations of global climate and eustatic sea level and had a particularly severe effect on marine benthos. Ichnological studies, therefore, have the potential to provide greater understanding of ecological changes in the marine realm at that time, and also during extinction events in general.

Around 85% of marine species are estimated to have died out during the Late Ordovician extinction event (Brenchley et al. 2001, Sheehan 2001), which occurred in 2 phases, one at the beginning and one in the middle of the Hirnantian Age (see Fig. 1 in Brenchley et al. 2001). The first extinction pulse is correlated with a glacially forced regression that led to changes

*Email: l.herringshaw@abdn.ac.uk

in nutrient cycling, and the second with post-glacial temperature and sea level rise and the stagnation of oceanic circulation (Sheehan 2001). The rapidity of the climate change is thought to have played a pivotal role in driving the extinctions (Brenchley et al. 1994, 2001). Few fossil groups suffered depletion in both extinction phases (Sheehan 2001), but, using brachiopod diversity as a proxy for ecosystem functioning, Brenchley et al. (2001) argued that, by the end of the second phase, benthic ecosystems had become 'severely disrupted and downgraded in complexity' and that faunal recovery took 4 to 5 million years. Ichnology provides a separate means for testing such hypotheses, using trace fossil diversity, burrow size, depth of bioturbation and ichnofabric index (sensu Droser & Bottjer 1986, 1989) to assess the ecological response of benthic communities.

Ordovician-Silurian boundary strata are preserved in relatively few regions, and complete or near-complete successions through the extinction event are even scarcer. As such, the outcrops of the Welsh Basin are especially significant. The eastern margin of the basin, in the Llandovery area (Fig. 1), preserves a predominantly nearshore succession spanning the end-Ordovician extinction. Its ichnological complexity and diversity has never been examined in detail, and has the potential to provide much new information on the ecological effects of the extinction event. The only previous study of end-Ordovician trace fossils in the Welsh Basin (McCann 1990) focussed on deep marine ichnoassemblages of the *Nereites* ichnofacies rather than on shallow marine assemblages of the *Skolithos* or *Cruziana* ichnofacies. Although such deep marine ichnofaunas had become diverse by the Ordovician (Orr 2001), it is critical to establish the nature of ichnofabrics and trace fossils preserved in shallow marine environments, where the effects of glacioeustatic sea-level change would be more pronounced.

The present study is the first assessment of bioturbation levels and patterns in a nearshore succession from the Welsh Basin and focuses on end-Ordovician shelfal and nearshore deposits in the Llandovery/Llanwrtyd Wells area (Fig. 1). Typically, bioturbation depth and trace fossil diversity is greater in such shallow water settings, so a variation in these is potentially attributable to ecological change. However, a fall in sea level often results in increased sediment supply (see e.g. Einsele 1996). Schofield et al. (2004, p. 13; see also Davies et al. 1997) suggested that this phenomenon might have led to low levels of bioturbation in the Hirnantian strata of the Welsh Basin. To address this, bioturbation levels were examined not only in the sedimentary rocks laid down during the Hirnantian regression, but also in those deposited in the subsequent transgression. Low bioturbation levels in only the regressive part of the succession would support the stratigraphic dilution hypothesis, but their occurrence also in the transgressive strata would imply that other mechanisms were involved.

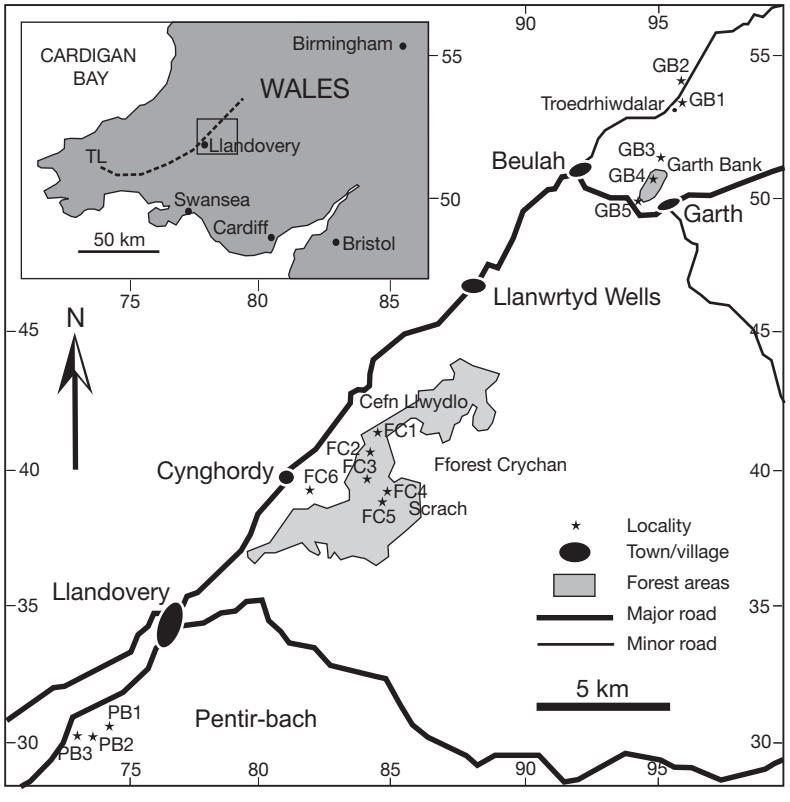

Fig. 1. Llandovery region, mid-Wales, with Garth Bank, Fforest Crychan and Pentir-bâch study areas and localities. Numbered 5 km grid squares are within the Ordnance Survey SN 100 km grid square. Regional map (inset) shows location of study area; dashed line: position of Tywi lineament (TL), a present-day representation of a fault-bounded slope separating shallower and deeper water parts of the Welsh Basin (Woodcock & Smallwood 1987)

LOCALITIES AND STRATIGRAPHY

Following locality information published by Williams & Wright (1981), Cocks et al. (1984), Woodcock & Smallwood (1987) and Temple (1988), field work for the present study focused on 3 areas (Fig. 1): Garth Bank–Troedrhiwdalar, north of the village of Garth; Fforest Crychan, northeast of Llandovery; and Pentir-bâch, southwest of Llandovery.

The geology of the Garth Bank area was described in detail by Williams & Wright (1981), who studied around 450 m of late Ordovician and early Silurian marine mudstones and siltstones. They erected the Wenallt Formation (Rawtheyan-Hirnantian in age, max. 115 m thick); the Cwm Clŷd Formation (11 to 51 m thick), the lower part of which was dated as Hirnantian by the presence of the brachiopod *Eostropheodonta hirnantensis*; and the non-fossiliferous Garth Bank Formation (max. 77 m thick), interpreted as Rhuddanian in age. The transition between the Wenallt and Cwm Clŷd Formations was described as conformable in the northern part of the area, but increasingly unconformable towards the south (Fig. 2).

Cocks et al. (1984) examined the Ordovician-Silurian boundary stratigraphy of the type Llandovery area, including both Fforest Crychan and Pentir-bâch. They erected the Rawtheyan age Tridwr Formation, overlain by the Scrach Formation of Hirnantian age (stratigraphically equivalent to the Cwm Clŷd Formation of Williams & Wright 1981; see also Woodcock & Smallwood 1987) and the Rhuddanian age Bronydd and Crychan Formations. The maximum thickness of the Tridwr Formation was not specified, but the Scrach and Bronydd Formations were illustrated as being up to 150 m thick, and the Crychan Formation was shown to have a maximum thickness of 260 m (Fig. 2). Subsequently, an Hirnantian fauna was identified from mudstones beneath the Scrach Formation in the Pentir-bâch area (Woodcock & Smallwood 1987).

The regional stratigraphy was revised recently by the British Geological Survey (2005a,b; Schofield et al. 2004, Barclay et al. 2005) and is summarized in Fig. 3. The revised stratigraphy is also included in Fig. 2, with the thicknesses and ages of the described strata compared to those published by Williams & Wright (1981) and Cocks et al. (1984). It should be noted, however, that the precise age of many of the formations is uncertain, depending on availability of palaeontological data. The base of the Rhuddanian Stage (i.e. the Ordovician-Silurian boundary), for example, could only be defined as being 'at or near the base of the Bronydd Formation' by Cocks et al. (1984, p. 165).

The British Geological Survey retained the Tridwr Formation of Cocks et al. (1984), but described it as the lateral equivalent of a deeper water unit, the Nantmel Mudstones Formation, above which they erected the Cribarth Formation as the latest Rawtheyan unit. The earliest Hirnantian units are the contemporaneous, interdigitating Ciliau and Yr Allt Formations, representing shallower and deeper water conditions, respectively. As the sea level fell during the Hirnantian, coarser, shallow-water sediments were deposited in the eastern (nearshore) part of the region. Locally, in the Troedrhiwdalar and western Fforest Crychan areas, this is represented by the Cwmcringlyn Formation, which overlies the Ciliau Formation (Fig. 2). Pentir-bâch is part of the Llandovery sheet (E212) and has yet to be revised by the British Geological Survey; their subdivision of the Hirnantian rocks there is not known. The Cwmcringlyn Formation was, however, described by Barclay et al. (2005, p. 3) as equivalent to the lower part of the Scrach Formation of Cocks et al. (1984) and Woodcock & Smallwood (1987). Above the Cwmcringlyn Formation are the Cwm Clŷd Sandstone Forma-

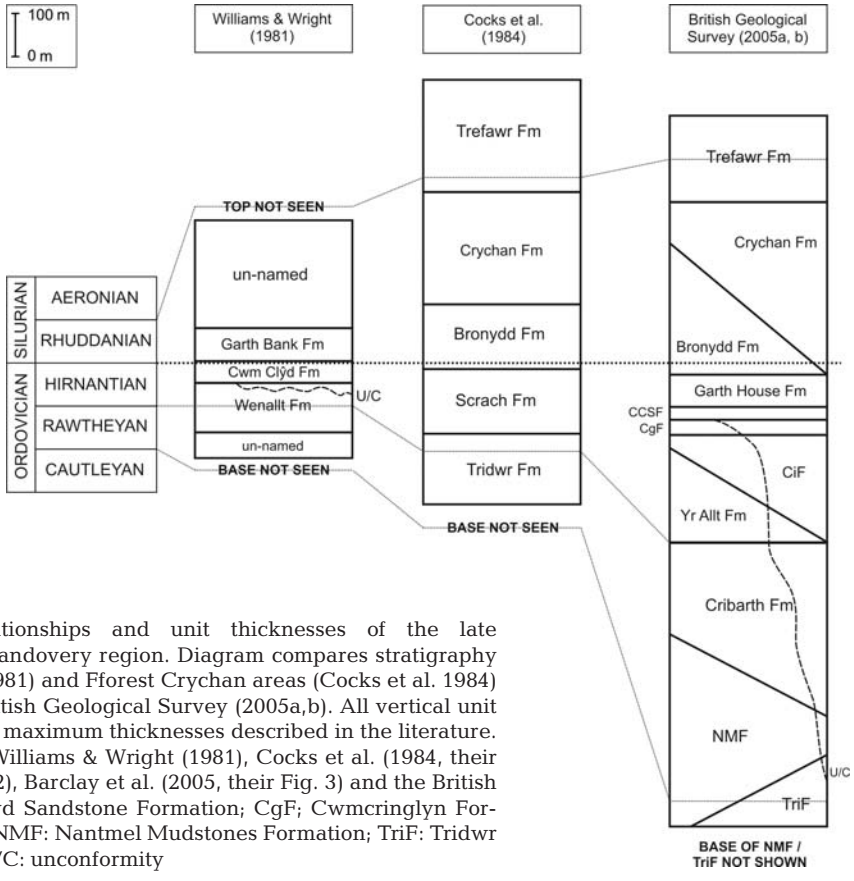

Fig. 2. Stratigraphical nomenclature, relationships and unit thicknesses of the late Ordovician–early Silurian succession of the Llandovery region. Diagram compares stratigraphy of Garth-Troedrhiwdalar (Williams & Wright 1981) and Fforest Crychan areas (Cocks et al. 1984) with regional stratigraphy produced by the British Geological Survey (2005a,b). All vertical unit thicknesses are of the same scale, showing the maximum thicknesses described in the literature. Stratigraphic columns compiled from data of Williams & Wright (1981), Cocks et al. (1984, their Figs. 1, 4, 69), Schofield et al. (2004, their Fig. 2), Barclay et al. (2005, their Fig. 3) and the British Geological Survey (2005a,b). CCSF: Cwm Clŷd Sandstone Formation; CgF; Cwmcringlyn Formation; CiF: Ciliau Formation; Fm: formation; NMF: Nantmel Mudstones Formation; TriF: Tridwr Formation; U/C: unconformity

tion, a shoreface unit of maximum 30 m thickness, which is restricted to the Garth Bank and eastern Fforest Crychan areas, and then the thicker, transgressive Garth House Formation (Figs. 2 & 3). Based on the outcrops mapped by the British Geological Survey (2005a,b), the Garth House Formation encompasses both the upper part of the Scrach Formation and the Garth Bank Formation of Williams & Wright (1981), although this was not stated explicitly. For the uppermost Hirnantian–lower Rhuddanian part of the succession, the Bronydd and Crychan Formations (Cocks et al. 1984) were retained, with deep-water strata to the west being placed in the Tycwtta Mudstones and Chwefri Formations (see Fig. 3). Broadly speaking, the strata form a conformable succession in the northern and western parts of the region, but become unconformable towards the south and east (see Fig. 3 for details).

Given that the present study was concerned with ichnological changes in shelf and nearshore sediments, the distal, basinal units of the succession—Nantmel Mudstones Formation, Yr Allt Formation, Tycwtta Mudstones Formation and Chwefri Formation—were not examined in detail. Outcrops of the more proximal units examined in this study occur mostly in road- or track-side cuttings, particularly in the Forestry Commission-managed areas of Garth Bank and Fforest Crychan. However, many of the localities documented by Williams & Wright (1981), Cocks et al. (1984) and Woodcock & Smallwood (1987) have since degraded considerably. The specific localities/transects studied, shown geographically in Fig. 1 and stratigraphically in Table 1 and Fig. 3, are as follows:

(1) Garth Bank area. GB1, road cutting east of Troedrhiwdalar chapel [SN 953 533]; GB2, road cutting north of Pen-rhiw-dalar farm [SN 956 537]; GB3, roadside outcrop at Dolderwen [SN 949 513]; GB4, disused quarry at Cwm Clŷd, Garth Bank [SN 947 509]; GB5, disused quarry just north of Garth House Farm [SN 943 499].

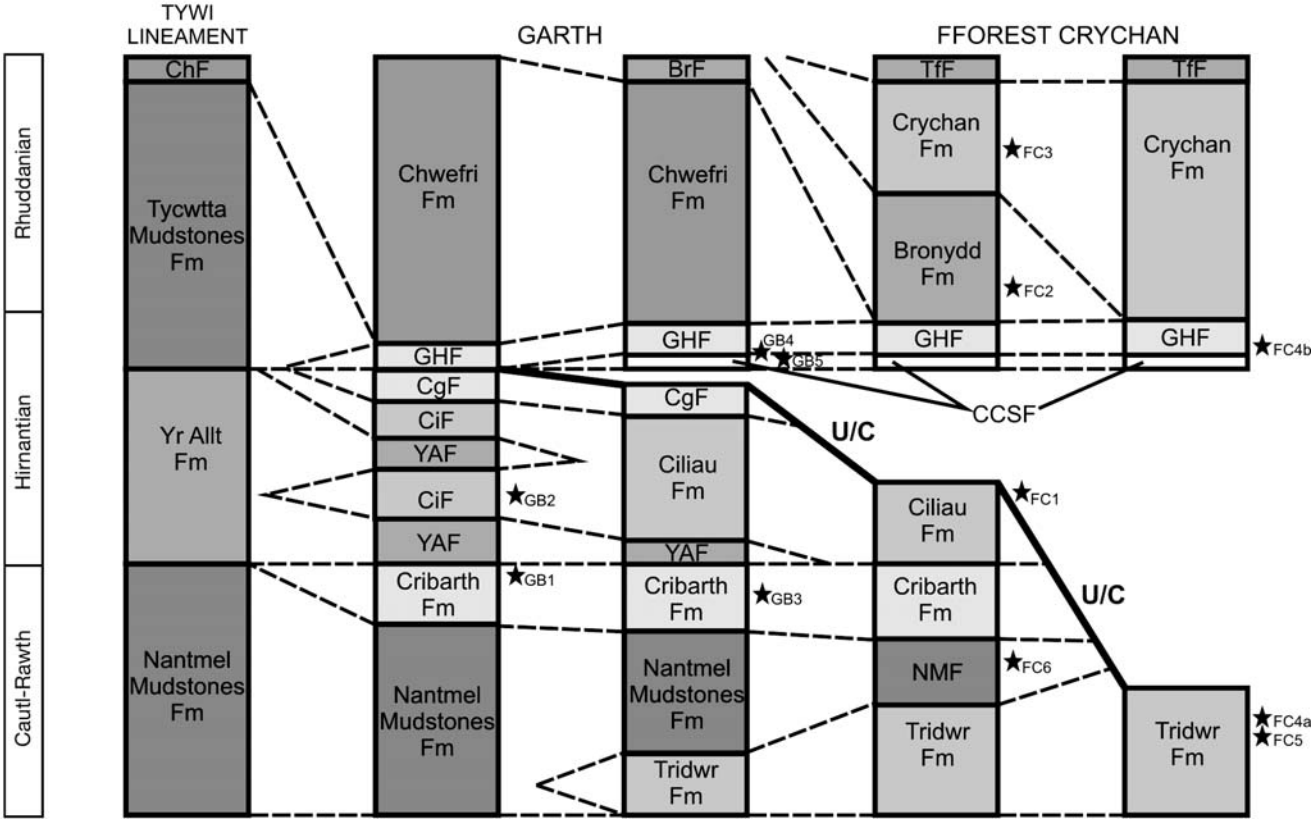

Fig. 3. Stratigraphical relationships of the late Ordovician and early Silurian succession of the Llandovery region, modified from Schofield et al. (2004, their Fig. 2) and Barclay et al. (2005, their Fig. 3). Vertical and lateral changes in unit thicknesses generalized for clarity; spacing between columns does not represent true distances between study areas (see Fig. 1 for locations of Tywi lineament, Garth and Fforest Crychan). Localities in Pentir-bâch are not shown, as revised stratigraphy for the region has not yet been published by the British Geological Survey: see Table 1 for details. BrF: Bronydd Formation; CgF: Cwmcringlyn Formation; ChF: Chwefri Formation; CiF: Ciliau Formation; CCSF: Cwm Clŷd Sandstone Formation; Fm: formation; GHF: Garth House Formation; NMF: Nantmel Mudstones Formation; TfF: Trefawr Formation; YAF: Yr Allt Formation; U/C: unconformity; ★ stratigraphic position of localities shown in Fig. 1

Table 1. Stratigraphical nomenclature and geological ages of localities studied (after Schofield et al. 2004, Barclay et al. 2005). Refer to Fig. 1 for geographical details. Fm: formation

Locality	Unit/s present	Age
FC3	Crychan Fm	Rhuddanian
PB1, FC2	Bronydd Fm	Early Rhuddanian
FC4b	Garth House Fm	Late Hirnantian
GB4	Cwm Clyd Sandstone Fm/ Garth House Fm	Mid- to late Hirnantian
GB5	Cwm Clyd Sandstone Fm	Mid-Hirnantian
PB2, PB3	Scrach Fm (= lower Cwmcringlyn Fm)	Mid-Hirnantian
FC1, GB2	Ciliau Fm	Early Hirnantian
GB1, GB3	Cribarth Fm	Late Rawtheyan
FC4a, FC5	Tridwr Fm	Rawtheyan
FC6	Nantmel Mudstones Fm	Rawtheyan

(2) Fforest Crychan area. FC1, road cutting at junction of main road with track to Cefn Llwydlo [SN 8445 4120]; FC2, small quarry at the junction of 2 forestry tracks [SN 8455 4090]; FC3, small outcrop alongside forestry track at SN 8433 3987; FC4, 2 outcrops northeast of Scrâch farmstead [FC4a at SN 848 394, FC4b at SN 847 393]; FC5, outcrop southwest of Scrâch farmstead at SN 8473 3921; FC6, roadside outcrop SSW of Rhydins farm [SN 8155 3950].

(3) Pentir-bâch area. Transect carried out along public footpath from Lletty-Ifan-Ddu [Locality PB1, SN 7414 3038] via small quarry (PB2) at SN 7356 3019 to small exposure PB3 at SN 7333 3020, east of Glasalltfawr.

RESULTS

At each of the localities, the strata were examined for bioturbation, and the ichnofabric index (ii) was recorded in the field using the semi-quantitative classification scheme of Droser & Bottjer (1986). For any discrete trace fossils present, their width and length were measured, as well as the depth to which they penetrated the substrate. Where bedding surfaces were not visible, the thicknesses of bioturbated intervals were measured. The data are summarized in Table 2. Only in the Ciliau (37 samples) and Bronydd (53 samples) Formations were discrete trace fossils found in sufficient numbers to enable median values of width and length to be calculated meaningfully.

Rawtheyan strata

The Tridwr Formation was examined at Localities FC4a and FC5 and the contemporaneous Nantmel Mudstones Formation at Locality FC6. The Nantmel Mudstones Formation at this locality consisted of finely laminated mudstones devoid of trace fossils (ichnofabric index = 1); bioturbation was present in the interbedded dark grey silts and thin sands of the Tridwr Formation. At Locality FC5, *Chondrites* with a diameter of 1 mm was found with a maximum vertical extent of 14 mm. Simple horizontal traces with a maximum diameter of 12 mm and length of 70 mm (Table 2) were restricted to discrete horizons at the base of thin sandstone beds. The overall ichnofabric index was measured as 2 to 3.

Body fossils from the road cutting east of Troedrhiwdalar Chapel (Locality GB1) are late Rawtheyan in age (Williams & Wright 1981). The rocks were assigned to the Cribarth Formation by the British Geological Survey (2005a), and the formation crops out also at Locality GB3. The mudstone beds are mostly homogeneous and up to 80 mm thick: thin bioturbated sands (<3 mm thick) were seen occasionally, but no discrete trace fossils were found at either GB1 or GB3. Barclay et al. (2005, p. 4) described the unit as 'thoroughly mixed ... by pervasive bioturbation', an interpretation consistent with these observations. As such, an ichnofabric index of 5 is assigned to the unit.

Table 2. Ichnofabric index (ii), bioturbation depth (Max. BD) and trace fossil dimensions (in mm) observed in late Ordovician–early Silurian sediments of the Llandovery region. TrF: Tridwr Formation; CrF: Cribarth Formation; CiF: Ciliau Formation; CgF: Cwmcringlyn Formation; CCSF: Cwm Clŷd Sandstone Formation; GHF: Garth House Formation; BrF: Bronydd Formation; CcF: Crychan Formation

Unit	Age	ii	Max. BD (mm)	Trace fossil width (mm)			Trace fossil length (mm)		
				Min.	Max.	Median	Min.	Max.	Median
CcF	Rhuddanian	2	–	1	7	–	4	14	–
BrF	Rhuddanian	2–3	5	1	20	2	8	50	14.5
GHF	Late Hirnantian	2	5	–	–	–	–	–	–
CCSF	Mid-Hirnantian	2	10	–	5	–	–	–	–
CgF	Mid-Hirnantian	1–2	6	–	–	–	–	–	–
CiF	Early Hirnantian	2–3	9	0.5	15	2	4	60	17
CrF	Late Rawtheyan	5	80	–	–	–	–	–	–
TrF	Rawtheyan	2–3	14	1	12	–	7	70	–

Hirnantian strata

The roadside exposure at Pen-rhiw-dalar (Locality GB2) belongs to the Ciliau Formation (British Geological Survey 2005a). Sand-filled vertical burrows with a diameter of 3 to 5 mm and horizontal burrows up to 50 mm long and 12 mm wide were found (Table 2), but were restricted to discrete layers of sand 2 to 9 mm thick, separated by unbioturbated dark grey silts of 4 to 6 mm thickness. An ichnofabric index of 2 to 3 is assigned to the Ciliau Formation, an observation supported by observations made at a larger exposure of the formation at Locality FC1, where horizontal bioturbation was dominant, consisting of 3 types: tiny chondriform features 0.5 to 1 mm wide and 8 to 12 mm long, arcuate to sub-arcuate burrows 1 to 7 mm wide and 25 to 30 mm long, and rare horn-shaped burrows up to 15 mm wide and 40 mm long (Table 2). No cross-cutting relationships were seen, so it is unclear whether the traces were made simultaneously or sequentially. Very rare vertical to sub-vertical burrows up to 8 mm in diameter were found also, as well as occasional thin bioclastic layers containing crinoid ossicles, bryozoan and possible cephalopod fragments.

The Cwmcringlyn Formation was defined by Barclay et al. (2005, p. 3) as being equivalent to the lower part of the Scrach Formation: based on greater outcrop quality and accessibility, the Scrach Formation at Pentir-bâch was used to assess bioturbation at this stratigraphic level. At Locality PB2, the deposits consisted of very thinly laminated fine sands and organic-rich muds, with some evidence of minor disturbance (<6 mm depth) by tracemakers. In the small exposure of grey sandstones at Locality PB3, bioturbation was not seen, giving the unit an overall ichnofabric index of 1 to 2.

Evidence of bioturbation in the Cwm Clŷd Sandstone Formation was scarce. Rare vertical burrows (diameter <5 mm) were found in the formation at Locality GB5, as well as a single horizontal trace 10 mm in width and 100 mm in length, but the ichnofabric index was never greater than 2. No discrete trace fossils or other signs of bioturbation were found in the formation at Localities GB4 or FC4b. Similarly, no unequivocal bioturbation was seen in the Garth House Formation in the limited exposures accessible on Garth Bank (e.g. Locality GB4). However, at Locality FC4b in Fforest Crychan, a bioturbated, dark-grey mudstone bed 45 mm thick was found, the top of which is a thin, fine-grained sandstone layer in which possible fugichnial trace fossils of limited size (<5 mm vertical depth, 3 to 5 mm width) occur (see Fig. 4A,C). Fugichnia are traces produced by the vertical movement of benthos escaping a rapid inundation of sediment, and, in this case, may be the response to a pulse of sand burying a community that had established itself on or in the seafloor muds.

Rhuddanian strata

Of all the units studied, the greatest ichnological diversity was found in the Bronydd Formation at Localities PB1 and FC2. A variety of trace fossils was present, with relatively short, wide, sinusoidal traces of the ichnogenus *Cochlichnus* (Fig. 4B) and, where more meandering, possibly *Helminthopsis* (see e.g. Buatois et al. 1997 for discussion of morphological differences) and *Planolites*. Long, thin, straight trails were common also, along with short, straight, relatively wide traces, 1 specimen of which (Fig. 4D) has expanded lateral termini, suggesting it might be the basal view of a U-shaped burrow with spreiten, such as *Diplocraterion*. Bioturbation was most abundant in the sandier units of the formation at Locality PB1, where 6 specimens of *Cochlichnus* were found and other horizontal traces are common. The finer grained parts of the Bronydd Formation at PB1 and FC2 were bioturbated also, but, as with many of the older units, the traces were restricted to thin (<2 mm) sand laminae within unbioturbated silts and muds. The ichnofabric index of the unit is classified as 2 to 3.

At Locality FC3, the Crychan Formation consisted of siltstone with bioturbated sandy laminae that yielded occasional cylindrical, horizontal burrows up to 7 mm in diameter and is assigned an ichnofabric index of 2.

DISCUSSION

The low ichnofabric index recorded in most units (Table 2) suggests that, during the late Ordovician and early Silurian, oxygen levels in the Welsh Basin were often reduced at the sea floor. However, an ichnofabric index of 5 in the Cribarth Formation and the presence of burrows >10 mm in diameter in the Tridwr, Ciliau and Bronydd Formations show that, at least periodically, they were sufficiently elevated to support relatively large bioturbators. Of the units with low indexes, the Cwmcringlyn, Cwm Clyd Sandstone and Garth House Formations are noteworthy, as they represent the shallowest water strata studied and, as such, might be expected to be well bioturbated. The lack of bioturbation seen in the Garth House Formation in this study contrasts with the findings of Williams & Wright (1981, p. 15), who stated that the equivalent Garth Bank Formation had 'bedding planes...rich in trace fossils.' However, the bioturbation was not quantified, and the diversity of ichnotaxa was not discussed. Elsewhere, Barclay et al. (2005) described the Nantmel Mudstones Formation as typically mottled by bioturbation, but trace fossils were absent from the exposure at Locality FC6. These patterns may be the result of varying oxygen levels during deposition of the formations, but

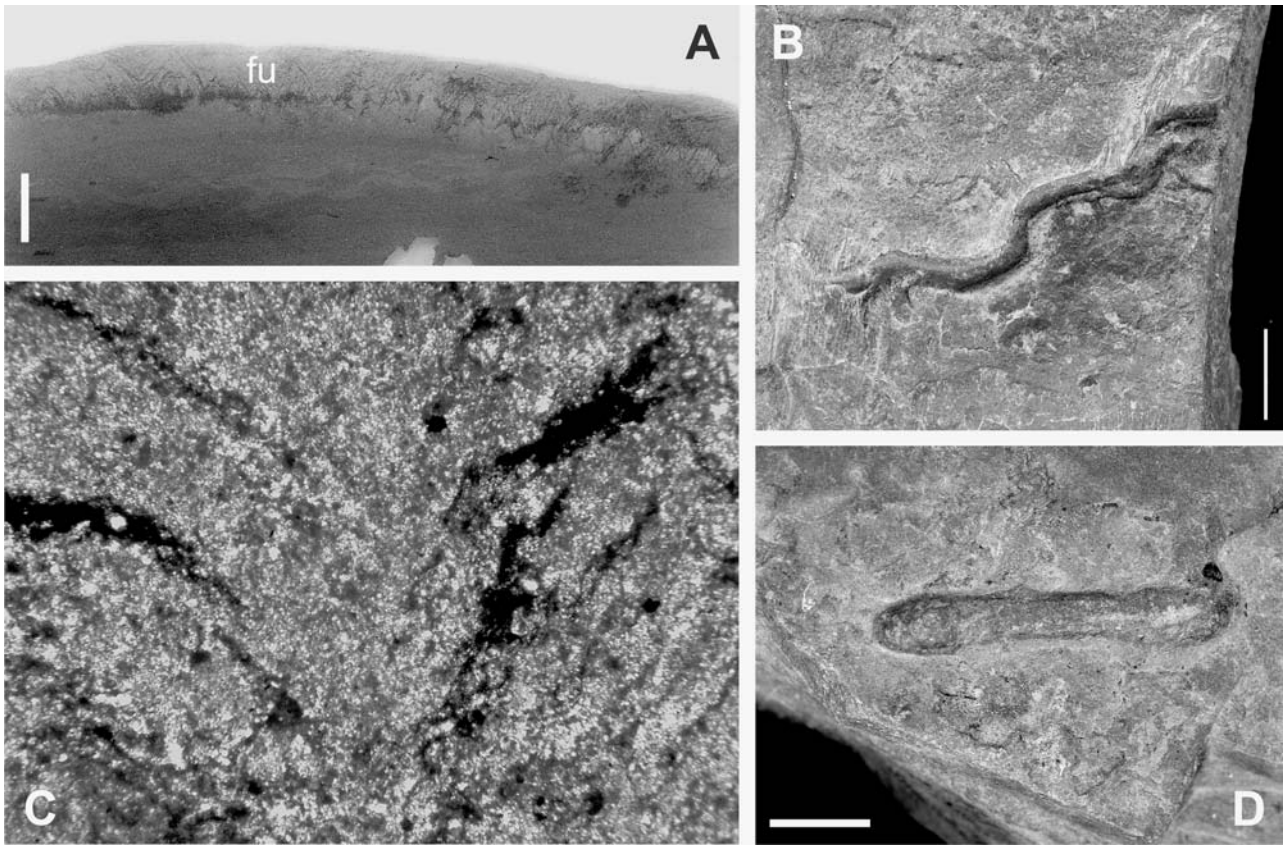

Fig. 4. (A, C) Possible fugichnial bioturbation in thin sand layer deposited on top of dark-grey mudstone, Garth House Formation, Locality FC4b, Fforest Crychan. (A) Thin section showing horizontally bioturbated mudstone overlain by sand layer with possible fugichnia (fu) producing chevron-shaped distortion of laminae; scale bar = 5 mm. (C) Photomicrograph of chevron-shaped laminae within fugichnia; width of field of view = 2 mm. (B, D) Trace fossils from the Bronydd Formation, Locality PB1, Pentir-bâch. (B) *Cochlichnus* isp.; scale bar = 5 mm. (D) A short, straight, trace fossil with expanded lateral terminations; scale bar = 5 mm

could also be an artefact of lateral ichnofabric variability. McIlroy (2004, 2007) demonstrated the patchiness of ichnofabrics within laterally continuous strata and emphasized the problem of correlating bioturbation patterns regionally; examination of end-Ordovician bioturbation across the Welsh Basin is required to determine the significance of this phenomenon.

The low levels of vertical bioturbation observed in the succession are significant. Schofield et al. (2004) described *Skolithos* as abundant in some parts of the Cwm Clŷd Sandstone Formation, indicating conditions suitable to a low-diversity community of suspension-feeding vertical burrow-makers, but they have not been recorded from other nearshore units (Cwmcringlyn and Garth House Formations). Again, this might suggest reduced O_2 levels, but shallow water deposits often accumulate rapidly and may be wave-reworked, reducing the preservation potential of tracemaker activity. Typically though, vertical trace fossils form a significant component of ichnofabrics in shallow marine settings, where higher energy conditions maintain large amounts of nutrients in suspension (Pemberton et al. 2001). When ichnological diversity increases in the Rhuddanian (Bronydd Formation), the trace fossils are exclusively horizontal: their rarity through the succession suggests that conditions in the shallow marine realm of the Welsh Basin were often inimical to suspension-feeding taxa during the end-Ordovician extinction event.

One of the most distinctive aspects of the end-Ordovician extinction is that a high proportion of species and genera disappeared, but few or no groups at ordinal level or above (Brenchley et al. 2001). Given that similar trace fossils can be made by unrelated organisms behaving in the same way (Ekdale et al. 1984, p. 18), correlating ichnological patterns with changes in body fossil diversity is inherently difficult. However, the fact that species and genera became extinct, rather than orders or classes, has led some workers to argue that changes in ecosystem functioning during and after the end-Ordovician extinction were relatively minor (see e.g. Droser et al. 1997). As such, there may not have been major changes in ichnological diversity and complexity.

SUMMARY

(1) In this, the first ichnological study of shallow marine strata spanning the end-Ordovician extinction event, bioturbation levels in a succession from the Welsh Basin are shown to have commonly been low. This is interpreted as being caused primarily by a decline in shallow marine benthic infauna associated with the end-Ordovician extinction event, but the limited nature of the study area necessitates caution in making firm conclusions. Many other factors, biological, environmental and geological, may have contributed to the pattern observed.

(2) The occurrence of low ichnofabric indexes in both Hirnantian and Rhuddanian strata indicates that the bioturbation levels are not artefacts of stratigraphic dilution, and that they may be a consequence of ecological stresses associated with the extinction event. However, due to variations in tectonic activity, a reduction in sedimentation rate during the transgression is not consistent across the Welsh Basin (see e.g. Davies et al. 1997), so this interpretation may not be applicable regionally.

(3) The Welsh Basin is an excellent area for observing ichnological and ecological changes during this time interval, despite variations in the quality and extent of outcrop, and should be studied further to obtain a fuller picture of regional patterns.

(4) Other late Ordovician shallow-water successions should be examined to determine whether their ichnological patterns are comparable with those of the Welsh Basin, and whether the extinction event had a global impact on bioturbation.

Acknowledgements. Andy Rees and Rob Raine (University of Birmingham) are thanked for their assistance with fieldwork and sample measurement, and the critical comments and advice of Paddy Orr and 2 anonymous reviewers are gratefully acknowledged.

LITERATURE CITED

Barclay WJ, Davies JR, Humpage AJ, Waters RA, Wilby PR, Williams M, Wilson D (2005) Geology of the Brecon district—a brief explanation of the geological map. Sheet Explanation of the British Geological Survey, 1:50 000 Sheet 213 Brecon (England and Wales), British Geological Survey, Keyworth, Nottingham

Brenchley PJ, Marshall JD, Carden GAF, Robertson DBR and others (1994) Bathymetric and isotopic evidence for a short-lived Late Ordovician glaciation in a greenhouse period. Geology 22:295–298

Brenchley PJ, Marshall JD, Underwood CJ (2001) Do all mass extinctions represent an ecological crisis? Evidence from the Late Ordovician. Geol J 36:329–340

British Geological Survey (2005a) Builth Wells. England and Wales Sheet 196. Solid and drift geology, 1: 50 000. British Geological Survey, Keyworth, Nottingham

British Geological Survey (2005b) Brecon. England and Wales Sheet 213. Bedrock and superficial deposits, 1:50 000. British Geological Survey, Keyworth, Nottingham

Buatois LA, Jalfin G, Aceñolaza FG (1997) Permian non-marine invertebrate trace fossils from southern Patagonia, Argentina: ichnologic signatures of substrate consolidation and colonization sequences. J Paleontol 71:324–336

Cocks LRM, Woodcock NH, Rickards RB, Temple JT, Lane PD (1984) The Llandovery series of the type area. Bull Br Mus (Nat Hist) Geol 38:131–182

Davies JR, Fletcher CJN, Waters RA, Wilson D, Woodhall DG, Zalasiewicz J (1997) Geology of the country around Llanilar and Rhayader. Memoir of the British Geological Survey, Sheets 178 and 179 (England and Wales). British Geological Survey, Keyworth, Nottingham

Droser ML, Bottjer DJ (1986) A semiquantitative field classification of ichnofabric. J Sediment Petrol 56:558–559

Droser ML, Bottjer DJ (1989) Ichnofabric of sandstones deposited in high-energy nearshore environments: measurement and utilization. Palaios 4:598–604

Droser ML, Bottjer DJ, Sheehan PM (1997) Evaluating the ecological architecture of major events in the Phanerozoic history of marine invertebrate life. Geology 25:167–170

Einsele G (1996) Event deposits: the role of sediment supply and relative sea-level changes—overview. Sediment Geol 104:11–37

Ekdale AA, Bromley RG (1984) Sedimentology and ichnology of the Cretaceous-Tertiary boundary in Denmark: implications for the causes of the terminal Cretaceous extinction. J Sediment Petrol 54:681–703

Ekdale AA, Stinnesbeck W (1998) Trace fossils in Cretaceous-Tertiary (KT) boundary beds in northeastern Mexico: implications for sedimentation during the KT boundary event. Palaios 13:593–602

Ekdale AA, Bromley RG, Pemberton SG (1984) Ichnology: trace fossils in sedimentology and stratigraphy. SEPM Short Course 15, Society of Economic Paleontologists and Mineralogists, Tulsa, OK

Fraiser M, Bottjer DJ (2005) Restructuring in benthic level-bottom shallow marine communities due to prolonged environmental stress following the end-Permian mass extinction. C R Palevol 4:583–591

McCann T (1990) Distribution of Ordovician-Silurian ichnofossil assemblages in Wales—implications for Phanerozoic ichnofaunas. Lethaia 23:243–255

McIlroy D (2004) Some ichnological concepts, methodologies, applications and frontiers. In: McIlroy D (ed) The application of ichnology to palaeoenvironmental and stratigraphic analysis. Spec Pub 228, Geological Society, London, p 3–27

McIlroy D (2007) Lateral variability in shallow marine ichnofabrics: implications for the ichnofabric analysis method. J Geol Soc (Lond) 164:359–369

Orr PJ (2001) Colonization of the deep-marine environment during the early Phanerozoic: the ichnofaunal record. Geol J 36:265–278

Pemberton SG, Spila M, Pulham AJ, Saunders T, MacEachern JA, Robbins D, Sinclair IK (2001) Ichnology and sedimentology of shallow to marginal marine systems: Ben Nevis and Avalon Reservoirs, Jeanne d'Arc Basin. Short Course Notes Vol 15, Geological Association of Canada, St. John's, Newfoundland

Pruss S, Bottjer DJ (2004) Early Triassic trace fossils of the western United States and their implications for prolonged environmental stress from the end-Permian mass extinction. Palaios 19:551–564

Pruss S, Fraiser M, Bottjer DJ (2004) Proliferation of Early

Triassic wrinkle structures: implications for environmental stress following the end-Permian mass extinction. Geology 32:461–464

Rodríguez-Tovar FJ (2005) Fe-oxide spherules infilling *Thalassinoides* burrows at the Cretaceous-Paleogene (K-P) boundary: evidence of a near-contemporaneous macrobenthic colonization during the K-P event. Geology 33: 585–588

Rodríguez-Tovar FJ, Uchman A (2004a) Ichnotaxonomic analysis of the Cretaceous/Palaeogene boundary interval in the Agost section, south-east Spain. Cretac Res 25: 635–647

Rodríguez-Tovar FJ, Uchman A (2004b) Trace fossils after the K-T boundary event from the Agost section, SE Spain. Geol Mag 141:429–440

Schofield DI, Davies JR, Waters RA, Wilby PR, Williams M, Wilson D (2004) Geology of the Builth Wells district—a brief explanation of the geological map. Sheet explanation of the British Geological Survey, 1:50 000 Sheet 196 Builth Wells (England and Wales). British Geological Survey, Keyworth, Nottingham

Sheehan PM (2001) The Late Ordovician mass extinction. Annu Rev Earth Planet Sci 29:331–364

Temple JT (1988) Ordovician-Silurian boundary strata in Wales. Bull Br Mus (Nat Hist) Geol 43:65–71

Twitchett RJ (1999) Palaeoenvironments and faunal recovery after the end-Permian mass extinction. Palaeogeogr Palaeoclimatol Palaeoecol 154:27–37

Twitchett RJ, Barras CG (2004) Trace fossils in the aftermath of mass extinction events. In: McIlroy D (ed) The application of ichnology to palaeoenvironmental and stratigraphic analysis. Spec Pub 228, Geological Society, London, p 397–418

Twitchett RJ, Wignall PB (1996) Trace fossils and the aftermath of the Permo-Triassic mass extinction: evidence from northern Italy. Palaeogeogr Palaeoclimatol Palaeoecol 124:137–151

Uchman A, Bubík M, Mikuláš R (2005) The ichnological record across the Cretaceous/Tertiary boundary in turbiditic sediments at Uzgruň (Moravia, Czech Republic). Geol Carpathica 56:57–65

Wignall PB, Morante R, Newton R (1998) The Permo-Triassic transition in Spitsbergen: $\delta^{13}C_{org}$ chemostratigraphy, Fe and S geochemistry, facies, fauna and trace fossils. Geol Mag 135:47–62

Williams A, Wright AD (1981) The Ordovician-Silurian boundary in the Garth area of southwest Powys, Wales. Geol J 16:1–39

Woodcock NH, Smallwood SD (1987) Late Ordovician shallow marine environments due to glacio-eustatic regression: Scrach Formation, Mid-Wales. J Geol Soc (Lond) 144: 393–400

Submitted: October 8, 2007; Accepted: March 14, 2008

Proofs received from author(s): May 23, 2008

Vol. 2: 289–301, 2008
doi: 10.3354/ab00058

AQUATIC BIOLOGY
Aquat Biol

Printed June 2008
Published online June 19, 2008

Contribution to the Theme Section 'Bioturbation in aquatic environments: linking past and present'

OPEN ACCESS

How biodiversity affects ecosystem processes: implications for ecological revolutions and benthic ecosystem function

Martin Solan[1,*], Paul Batty[2], Mark T. Bulling[1], Jasmin A. Godbold[1]

[1]**Oceanlab, University of Aberdeen, Main Street, Newburgh, Aberdeenshire AB41 6AA, UK**
[2]**The Scottish Association for Marine Science, Dunstaffnage Marine Laboratory, Oban, Argyll PA37 1QA, UK**

ABSTRACT: Current and projected rates of extinction provide impetus to investigate the consequences of biodiversity loss for ecosystem processes. Yet our understanding of present day biodiversity–ecosystem functioning relations contrasts markedly with our understanding of the responses of species to changes that have occurred in the geological record. Of the experiments that have explicitly tested the relationship between biodiversity and ecosystem functioning, few have attempted to reconcile whether the underlying process that gives rise to the observed response is affected by biodiversity in the same way as the observed response. In the present study, we use benthic macrofaunal invertebrates to examine and distinguish the effects of species richness and species identity on bioturbation intensity, a key mechanism that has been important on evolutionary timescales regulating ecosystem functioning in the marine benthos. Our study identifies significant effects of species richness that reflect species-specific impacts on particle reworking that, in turn, lead to elevated levels of nutrient generation. However, our findings also suggest that the consideration of only bioturbation intensity forms an incomplete evaluation of bioturbation effects because the way in which species interact with the benthic environment does not necessarily reflect organism traits only associated with particle transport. Our study emphasises the need for caution when extrapolating from assumed knowledge of organism traits to how changes in species composition associated with ecological crises may impact ecosystem function. Nonetheless, the empirically derived mechanistic effects of bioturbation on ecosystem functioning documented here are sufficiently general to seek correlations between diversity and function in natural systems, including those from the palaeoecological record.

KEY WORDS: Biodiversity · Ecosystem function · Bioturbation · Substrate revolution · Extinction · Marine benthos

INTRODUCTION

One of the most significant events in the history of marine life was the emergence and subsequent diversification of bilaterian invertebrate fauna, approximately 0.5 to 1.0 billion years ago (Wray et al. 1996, Droser et al. 2002). Many morphological features of these fauna suggest that they had a primarily benthic lifestyle (Valentine 1994, Budd & Jensen 2000), and their appearance in the fossil record correlates well with an increase in the depth and intensity of sediment mixing, especially during the Proterozoic–Phanerozoic transition (Droser & Bottjer 1988, McIlroy & Logan 1999). As these early metazoans began to interact with their environment (see, inter alia, Gray 1974, Rhoads 1974, Rhoads et al. 1977, Aller 1982, Rhoads & Boyer 1982, Krantzberg 1985), the sediment–water interface began to change from a distinct and effectively impermeable boundary to a more open and diffuse layer that was more habitable to life. Sequential changes in benthic community structure that coincided with this 'agronomic revolution' (sensu Seilacher & Pflüger 1994) resemble present day conceptual models of benthic macrofaunal succession (Pearson & Rosenberg

*Email: m.solan@abdn.ac.uk

1978, Rhoads et al. 1978, Rumohr et al. 1996); the colonisation of a few opportunistic species paved the way for a greater variety of species and dramatically transformed (i.e. Cambrian substrate revolution, sensu Bottjer et al. 2000) the Precambrian bacterial and algal planar mat systems (e.g. Gehling 1999) into diverse 4-dimensional benthic communities that were sated with complex biogeochemical cycles and novel ecospace (Seilacher 1999, Dornbos et al. 2005, Dornbos 2006). Such changes in community structure and function are expected to be reversible and linked with mass extinction events, a conclusion that corresponds to evolutionary patterns in the fossil record that reveal a close association between extinction forcing agents and the diversification of marine soft-bottom communities (Macleod 1994, Martin 1996, Jacobs & Lindberg 1998, Harper 2006, Pruss et al. 2006, Canfield et al. 2007).

Of relevance to contemporary ecology, the geological record provides confirmation that diversification and extinction events are intimately linked to the provision of ecosystem processes, particularly the biogeochemical cycles of carbon and nutrients (Logan et al. 1995, Martin 1996). Although the ecological impacts of even well-documented ecological revolutions in the geological record have recently been considered (e.g. Jenkins 1992, Dornbos et al. 2005, Seilacher et al. 2005, James & Price 2008), the focus has been on documenting faunal change rather than on examining how changes in biodiversity may have altered species interactions and the functioning of the marine ecosystem (exceptions include Clapham & Narbonne 2002, Vannier et al. 2007, Dornbos & Chen 2008). Many ecosystem processes are mediated by infaunal invertebrates, and concomitant changes in the rates and depths of bioturbation through the Phanerozoic (Thayer 1983) provide compelling evidence that benthic nutrient cycling was necessary to sustain the primary productivity of the marine biosphere (Martin et al. 2008). Given that these early faunal assemblages are ecologically similar to modern communities (Bottjer & Ausich 1986, Clapham et al. 2003, Narbonne 2005 and references therein), and that they appear to have been critical to the provision of ecosystem processes, much can be learnt by performing manipulative experiments with fauna from the present day (e.g. Emmerson et al. 2001, Marinelli & Williams 2003, Mermillod-Blondin et al. 2005, Norling et al. 2007) or by applying modelling approaches (e.g. Solan et al. 2004) to data in order to predict how extinctions have in the past, or will in the future, affect ecosystem processes.

In recent years, spurred by the anticipation that anthropogenic forcing (Worm et al. 2006, Halpern et al. 2008) is likely to have considerable ecological consequences within the next century (Sala et al. 2000), an extensive body of literature has emerged that focuses on the effects of biodiversity loss on key ecological processes (for reviews, see Covich et al. 2004, Hooper et al. 2005, Cardinale et al. 2006, Stachowicz et al. 2007). By adopting an experimental approach (see Raffaelli et al. 2003) that involves measuring pertinent ecosystem processes from simple model communities that differ only in the number of species, it has been possible to identify mechanisms that are important and underpin the biodiversity–ecosystem functioning relationship (e.g. complementarity and selection effects; Cardinale et al. 2002, Loreau & Hector 2001). These reflect how species interact with the environment, such that ecosystem processes can often be predicted from species composition or species traits, but not necessarily from species richness per se (see Stachowicz et al. 2007). Few studies, however, have attempted to reconcile whether the assumed mechanism that mediates the observed response is affected by biodiversity in the same way as the observed response. If the effects of biodiversity alter both the process responsible for generating an ecosystem response (e.g. bioturbation) as well as the response itself (e.g. nutrient generation) then it would be reasonable to assign causality and determine the relative contribution of a given process to the total observed yield.

In the present study, we build on previous empirically derived knowledge (species richness, identity and density effects on benthic nutrient cycling; Ieno et al. 2006) by distinguishing the effects of species richness and species identity on bioturbation intensity, a key process that underpins and regulates ecosystem functioning in the marine benthos. Our aim is: (1) to establish whether strong species richness and identity effects regulate bioturbation intensity and, if so, demonstrate that bioturbation forms the mechanistic link between the infauna and their effect on the benthic environment and (2) to demonstrate the utility of our approach to the palaeoecological research community who hold a valuable repository of information (species richness, evenness, morphological and behavioural information, proxies for ecosystem function; Clapham et al. 2003, Widdicombe et al. 2003) from times of major transitions in the evolutionary past that could be used to inform the biodiversity–ecosystem function agenda.

MATERIALS AND METHODS

Faunal and sediment collection. Sediment and 3 infaunal invertebrates, the deposit-feeding polychaete *Hediste diversicolor* (HD), the surficial grazing bivalve *Hydrobia ulvae* (HU) and the suspension-feeding bivalve *Cerastoderma edule* (CE) were collected from mud flats in the Ythan estuary, Aberdeenshire, Scotland (57° 20.085′ N, 02° 0.206′ W). Sediment was sieved

(0.5 mm mesh) in a seawater bath to remove macrofauna and then allowed to settle for 24 h to retain the fine fraction (<63 µm). The settled sediment was homogenised and added to each mesocosm 48 h prior to species addition. Seawater (UV-sterilised, 10 µm prefiltered, salinity ≈ 33) was replaced after 24 h to allow the removal of excess nutrients associated with disturbance during assembly.

Mesocosms. Replicate (n = 5) macrofaunal communities were assembled in monoculture and in mixtures of 2 and 3 species in Perspex cores (330 mm high, 100 mm internal diameter) containing 10 cm depth of sediment (785 cm^3) and 20 cm of overlying seawater (2.35 l). The mesocosms were maintained in environmental chambers (VC 4100, Vötsch Industrietechnik) that can control temperature (14.0 ± 0.1°C) and light period (12 h light:12 h dark cycle; 2 × 36 W fluorescent tube lights, Arcadia, Model FO-30) for 21 d. To minimise hidden treatment effects (sensu Huston 1997), eliminate pseudoreplication and allow the generality of any diversity effects to be evaluated, species richness treatments containing 1 and 2 species were replicated using unique species permutations (3 × 1 sp. [HD, CE, HU] and 3 × 2 spp. mixtures [CEHU, CEHD, HDHU]; Table 1). This is not possible for the 3-species mixture (CEHDHU) because of the limited available species pool (n = 3). Biomass was fixed at 2.0 g $mesocosm^{-1}$ (≈255 g m^{-2}) in all species richness treatments, a level consistent with that found at the study site. All mesocosms were continually aerated.

Tracers. Sediment particle reworking by benthic fauna was estimated using luminophore tracers (i.e. natural sediments treated with a dye that fluoresces in ultraviolet light; Mahaut & Graf 1987). The luminophores (sand-based, size class 125 to 250 µm diameter; Partrac) were pre-soaked (24 h) and vigorously shaken in seawater prior to addition to the mesocosms to prevent particle aggregation and other hydrophobic effects. For each mesocosm, 0.1 g dry weight of luminophores was added and evenly distributed across the sediment surface. Following experimental incubation (21 d), extruded cores were vertically sectioned at a resolution of 0.5 cm to a depth of 8.0 cm (i.e. 16 slices). Each slice was homogenised, and a subsample (2.5 cm^3) was taken. Each subsample was spread thinly on a 90 mm diameter Petri dish and illuminated by an ultraviolet light source (2 × 8 W tubes; Sylvania Blacklight). Luminophores were viewed via a ⅓ inch CCD colour camera (Genie C8706/240) linked to a television monitor and manually counted. Luminophore counts from each core slice were normalised to the total recovered from the cores.

Bioturbation model. The biodiffusion coefficient (D_b) was determined for the relative concentration of luminophores in each profile using the solution to the 1-dimensional diffusion model presented by Crank (1975):

$$C(z,t) = \frac{M}{\sqrt{\pi D_b t}} \exp\left(\frac{-z^2}{4D_b t}\right) \quad (1)$$

where $C(z,t)$ is the relative tracer (i.e. luminophores) concentration at depth z and time t, and M is the total amount of luminophores applied. D_b was derived by weighted least-squares regression of predicted profiles on observed tracer concentrations (François et al. 2002). This procedure calculates a squared residual between the observed (O) and predicted (P) concentrations for each depth horizon, which is weighted by the corresponding observed concentration + 1 to prevent a null denominator. By summing the residuals, a regression coefficient (r) is calculated as:

$$r = \sum_{i=1}^{n} \frac{(O_i - P_i)^2}{O_i + 1} \quad (2)$$

where the predicted profile forms an identical match with the observed profile, $r = 0$. Model profiles with the lowest r were selected to calculate D_b.

Statistical analyses. Statistical models were developed for the dependent variable bioturbation (D_b), and the independent nominal variables species richness (SR, n = 4) and, separately, species identity (SPID, n = 8) (Table 1). For the latter, the contribution of species mixture to bioturbation was assumed to be synergistic rather than additive (e.g. Ieno et al. 2006) and each species combination was treated as a unique 'species' identity.

Graphical exploratory techniques were used to check for outliers. As a first step we fitted a linear regression. A model validation was applied to check that underlying statistical assumptions were not violated; normality was assessed by plotting theoretical quantiles versus standardised residuals (quantile–quantile plots), homogeneity of variance was evaluated by plotting

Table 1. Summary of species combinations used in the assembled macrofaunal communities. Biomass represents target biomass (realised biomass accuracy, mean ± SE = 2.0082 ± 0.0196 g, n = 35). HD: *Hediste diversicolor*; CE: *Cerastoderma edule*; HU: *Hydrobia ulvae*

Species richness	Species identity	n	Biomass (g $mesocosm^{-1}$) HD	CE	HU	Total biomass (g $mesocosm^{-1}$)
0	0	5	0	0	0	–
1	1	5	2.0	0	0	2.00
1	2	5	0	2.0	0	2.00
1	3	5	0	0	2.0	2.00
2	4	5	0	1.0	1.0	2.00
2	5	5	1.0	1.0	0	2.00
2	6	5	1.0	0	1.0	2.00
3	7	5	0.67	0.67	0.67	2.00

residuals versus fitted values, non-linearity was evaluated by plotting residuals versus explanatory variables, and influential data points were identified using Cook's distance (Quinn & Keough 2002). Where there was evidence of unequal variance in the residuals, we used linear regression with a generalised least-squares (GLS) estimation procedure (Pinheiro & Bates 2000). Use of GLS means that a data transformation to stabilise the variance is not necessary because of the use of variance–covariate terms that allow for unequal variance. This has the added advantage that the original structure of the data can be retained.

To find the minimal adequate model, we adopted the approach outlined by Verbeke & Molenberghs (2000) and Diggle et al. (2002), i.e. the most appropriate structure in terms of random components is determined using a REML (restricted maximum likelihood) estimation; subsequently, the optimal fixed effects structure is determined using an ML (maximum likelihood) estimation. The optimal random structure was determined by starting with a model without any variance–covariate terms (equivalent to linear regression) and comparing this model with subsequent GLS models that contained specific variance structures (i.e. different spread per stratum for each nominal variable; see Table 5.2 in Pinheiro & Bates 2000). Comparisons of these models were made using the AIC (Akaike information criteria) and plots of residuals versus fitted values. The optimal fixed structure was established by applying a backward selection using the likelihood ratio test obtained by ML estimation. The importance of each explanatory factor in the minimum adequate model was assessed by comparing a reduced model (with all terms involving the factor of interest removed) with the full model, using the likelihood ratio test. The numerical output of the optimal model was obtained using REML estimation (West et al. 2007). All analyses were performed using the 'nlme' package (v3.1; Pinheiro et al. 2006) in the R (v2.6.1) statistical and programming environment (R Development Core Team 2005).

In order to assess whether there were any positive effects of species interactions on bioturbation intensity, we compared bioturbation intensity in species mixtures relative to monocultures using D_{max} (Loreau 1998):

$$D_{max} = \frac{D_{b\,mix} - \max(D_{b\,mono})}{\max(D_{b\,mono})} \quad (3)$$

where $D_{b\,mix}$ is the observed bioturbation intensity in the mixture and $\max(D_{b\,mono})$ is the maximum observed bioturbation intensity in the monocultures. When a mixture performs better than the corresponding monocultures (i.e. overyielding), $D_{max} > 0$.

RESULTS

Bioturbation

Use of luminophores allowed quantitative differences in infaunal bioturbation activity to be determined. The mean ± SD relative count in the uppermost layer (0 to 0.5 cm) of mesocosms containing no macrofauna was 99.4 ± 0.01 % (n = 5), indicating that any vertical displacement of particles was not related to the properties of the luminophores or to the method of recovery. The form of the vertical profile differed between species identity treatments, but varied little between replicates (Fig. 1). The maximum vertical displacement of luminophores was 1.0 to 1.5 cm for monocultures of *Hydrobia ulvae*, 1.5 to 2.0 cm when *Cerastoderma edule* was present (alone or in mixture with *H. ulvae*) or >7.5 cm in all treatments containing *Hediste diversicolor*. Despite differences between luminophore profiles (compare panels, Fig. 1), the transport of luminophore particles approximated a biodiffusive profile with depth in all mesocosms (r_{max} = 0.024, n = 40; Fig. 2a). Of the single species treatments, mean D_b ($\times 10^2$ cm^2 yr^{-1}, ±SD, n = 5) was greatest in *H. diversicolor* (4.73 ± 0.89), followed by *C. edule* (3.45 ± 0.86)

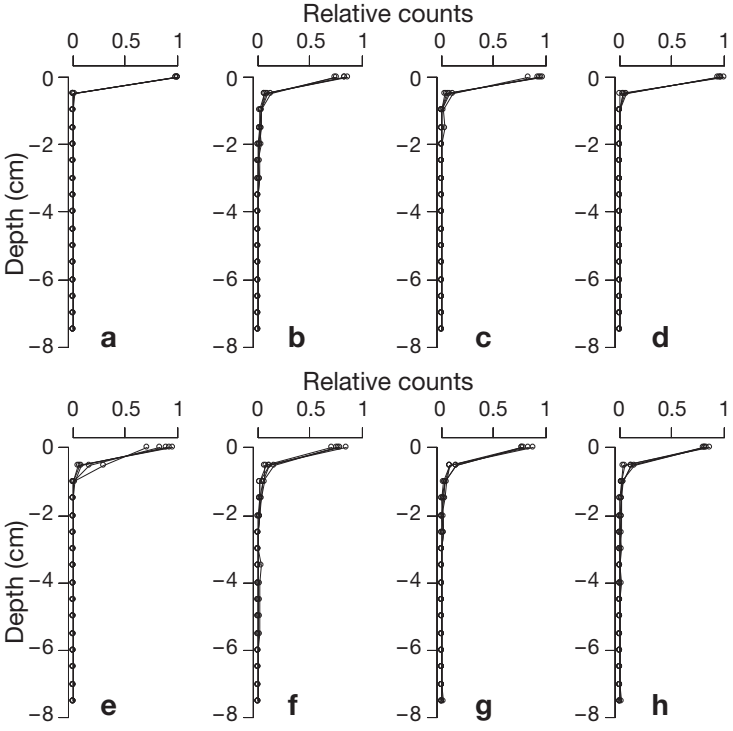

Fig. 1. Vertical distribution of luminophores in each mesocosm for replicate (n = 5) cores containing: (a) no macrofauna, (b) *Hediste diversicolor* (HD), (c) *Cerastoderma edule* (CE), (d) *Hydrobia ulvae* (HU), (e) CEHU, (f) CEHD, (g) HDHU and (h) CEHDHU. The numbers of luminophores from each sediment slice are expressed relative to the total number recovered from each core

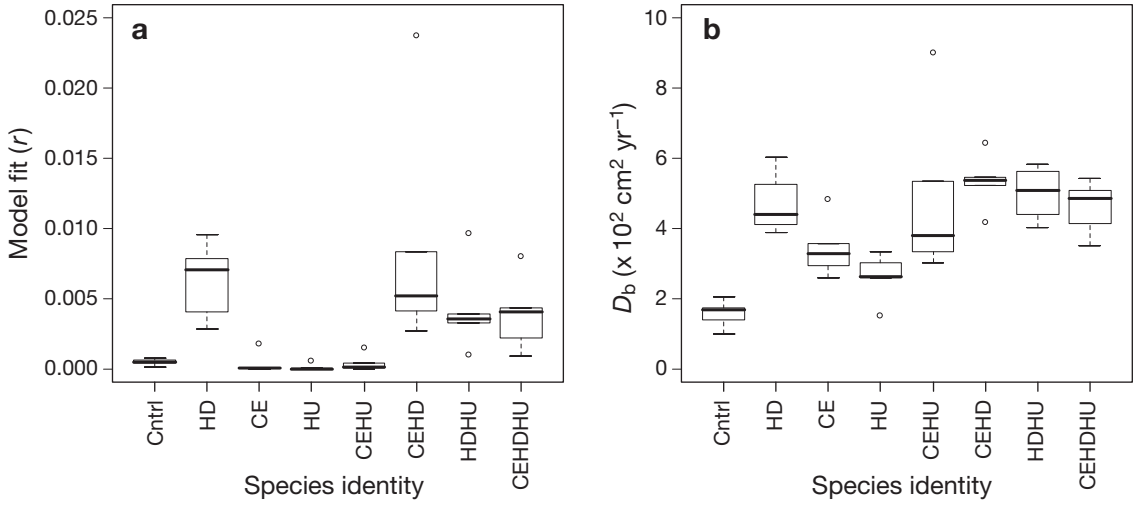

Fig. 2. (a) Weighted least-squares regression of predicted profiles on observed tracer concentrations (r) and (b) bioturbation intensity (D_b) for each species identity treatment (n = 5). In each case, the median is indicated at the midpoint, the upper and lower quartiles are indicated by the hinges, lines represent the spread and open circles indicate outliers. The species composition of each mixture is indicated on the x-axis, where species identity corresponds to: no macrofauna (Cntrl); *Hediste diversicolor* (HD), *Cerastoderma edule* (CE) and *Hydrobia ulvae* (HU)

and *H. ulvae* (2.62 ± 0.69). The mean D_b ($\times 10^2$ cm^2 yr^{-1}, ±SD, n = 5) of the multispecies mixtures tended to be high relative to the monocultures (except *H. diversicolor*), ranging from 4.60 ± 0.78 (3 spp. mixture) to 5.33 ± 0.81 (*C. edule* + *H. diversicolor*) (Fig. 2b).

Species richness effects

There were clear positive effects of species richness on bioturbation intensity (Fig. 3a). The minimal adequate model (Model 1 in Appendix 1) was a linear regression with a GLS extension incorporating species richness as a main term and as a variance–covariate. Although the influence of species richness on bioturbation intensity was significant (L-ratio = 30.14, df = 3, $p < 0.0001$), closer examination of the coefficient tables (Table A1) revealed that bioturbation intensity was greatest in treatments containing 2 species (coefficient = 3.50, $t = 8.42$, $p < 0.0001$) rather than in those containing the highest level of species richness (coefficient = 3.03, $t = 7.78$, $p < 0.0001$). Bioturbation intensity in both the 2-species (coefficient = 3.48, $t = 3.05$, $p = 0.0042$) and 3-species mixtures (coefficient = 1.01, $t = 2.18$, $p = 0.0359$) were greater than the corresponding monocultures (Table A1).

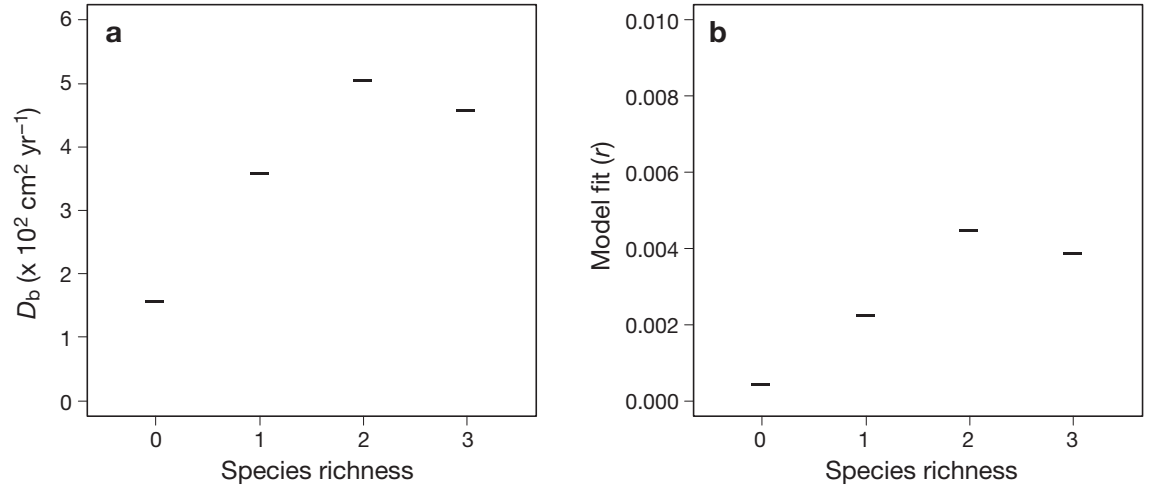

Fig. 3. Effect of species richness on: (a) bioturbation intensity (D_b) and (b) the weighted least-squares regression of predicted profiles on observed tracer concentrations (r). Horizontal bars represent predicted values from the optimal regression model for each species richness treatment. As the generalised least-squares (GLS) framework allows for different spreads in the data, individual data points are omitted to prevent misinterpretation

Although the fit of the biodiffusive model (Fig. 2a) to the observed vertical distribution of luminophores (Fig. 1) was acceptable in all cases, the mean square deviation between the experimental and simulated luminophore counts was affected by species richness (Fig. 3b). The minimal adequate model (Model 2 in Appendix 1), a linear regression with a GLS extension incorporating species richness as a variance–covariate, indicated a negative effect (increasing r) of species richness on model fit (L-ratio = 15.23, df = 3, p = 0.0016). Comparison of the regression model coefficients (Table A2) indicates that the greatest deviation between fitted and observed profile values occurred at intermediate levels of species richness (SR = 2, coefficient = 0.004, t = 2.56, p = 0.0149), followed by the 3-species mixture (coefficient = 0.003, t = 2.85, p = 0.0072) and the monocultures (coefficient = 0.002, t = 2.07, p = 0.0461), although there was no significant difference between the 2-species and 3-species mixtures (coefficient = 0.0006, t = 0.31, p = 0.762).

Species identity effects

The effects of species richness on bioturbation intensity were underpinned by strong effects of species composition (Fig. 4a). The minimal adequate model (Model 3 in Appendix 1), a linear regression, with a GLS extension, species identity as a main term and variance–covariate, highlighted clear differences in bioturbation intensity with species identity (L-ratio = 44.589, df = 7, p < 0.0001; Fig. 4a). Comparison of model coefficients (Table A3) revealed that the effects of *Hediste diversicolor* were greater than those of *Cerastoderma edule* (coefficient = 1.280, t = 2.31, p = 0.0275) and *Hydrobia ulvae* (coefficient = 2.113, t = 4.182, p = 0.0002). Whilst it is clear from the monocultures that the presence of *H. diversicolor* is influential in determining the intensity of bioturbation, the presence of this species did not necessarily dictate polyculture performance as mixtures containing *H. diversicolor* were not significantly higher than mixtures where *H. diversicolor* was absent (compare $SPID_{CEHU}$ to $SPID_{CEHD}$, $SPID_{HDHU}$ and $SPID_{CEHDHU}$ in Table A3; p = 0.7179 to 0.9394). As the lowest bioturbation intensity in monoculture occurred with *H. ulvae*, it is intuitive to assume that the role of *C. edule* is of importance in the mixtures; yet, the contribution of *C. edule* was not significantly higher (coefficient = 0.833, t = 1.691, p = 0.1005) than that of *H. ulvae* when in monoculture. However, when *H. diversicolor* and *C. edule* are in mixture (= $SPID_{CEHD}$), their combined contribution in terms of bioturbation intensity tends to be equivalent to mixtures that contain at least 1 of these species ($SPID_{HD}$, coefficient = –0.596, t = –1.108, p = 0.2763; $SPID_{CEHU}$, coefficient = –0.422, t = –0.364, p = 0.7179; $SPID_{HDHU}$, coefficient = –0.333, t = –0.665, p = 0.5108; $SPID_{CEHDHU}$, coefficient = –0.723, t = –1.446, p = 0.158; Table A3 & Fig. 4a). Thus, the relative contribution to bioturbation from *H. diversicolor* or *C. edule* is so dominant that it masks the contribution of other species present within the same mixture, irrespective of proportional representation.

The relative fit between the experimental and simulated luminophore counts (Fig. 4b) was also influenced by species identity (L-ratio = 29.59, df = 7, p < 0.0001; linear regression with a GLS extension, species identity as a main term and variance–covariate; Model 4 in Appendix 1). Evaluation of the model coefficients

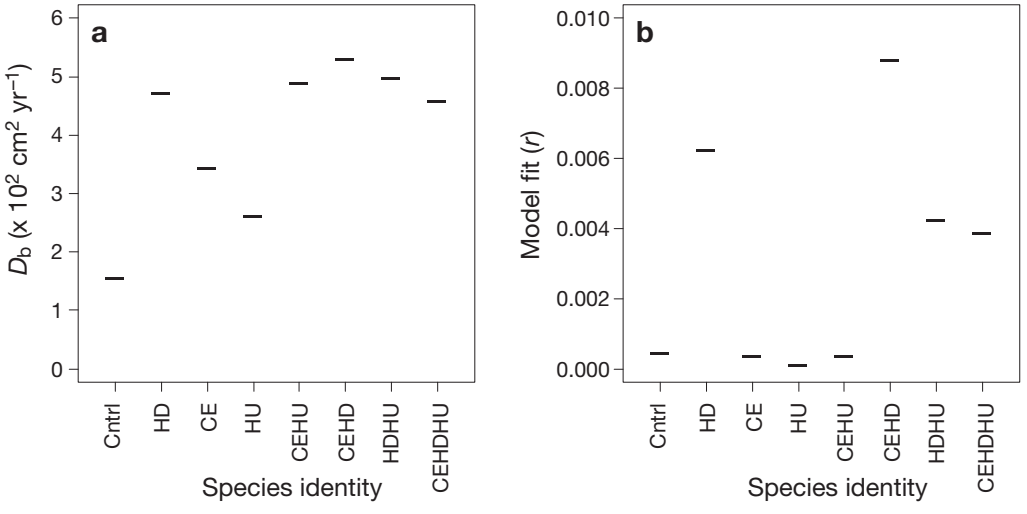

Fig. 4. Effect of species identity on: (a) bioturbation intensity (D_b) and (b) the weighted least-squares regression of predicted profiles on observed tracer concentrations (r). Horizontal bars represent predicted values from the optimal regression model for each species identity treatment. As the GLS framework allows for different spreads in the data, individual data points are omitted to prevent misinterpretation

(Table A4) reveal a marked difference in fit between treatments that contained *Hediste diversicolor* and those where the species was absent. Relative to treatments containing *H. diversicolor* in monoculture, the fit of the biodiffusive model was improved ($r \rightarrow 0$) when *H. diversicolor* was absent ($SPID_0$, coefficient = -5.80×10^{-4}, $t = -4.68$, $p < 0.0001$; $SPID_{CE}$, coefficient = -5.89×10^{-4}, $t = -4.59$, $p < 0.0001$; $SPID_{HU}$, coefficient = -6.16×10^{-4}, $t = -4.96$, $p < 0.0001$; $SPID_{CEHU}$, coefficient = -5.88×10^{-4}, $t = -4.65$, $p < 0.0001$; Table A4). In mixtures where *H. diversicolor* was present, irrespective of the composition of the mixture, the fit of the model was insignificantly different ($SPID_{CEHD}$, coefficient = 2.56×10^{-4}, $t = 0.63$, $p = 0.5317$; $SPID_{HDHU}$, coefficient = -2.01×10^{-4}, $t = -1.06$, $p = 0.2969$; $SPID_{CEHDHU}$, coefficient = 2.40×10^{-4}, $t = -1.38$, $p = 0.1762$; Table A4) to that derived for treatments containing *H. diversicolor* in monoculture. All treatments containing macrofauna, but excluding *H. diversicolor*, showed indistinguishable levels of model fit from one another (compare $SPID_{CE}$ to $SPID_{HU}$ and $SPID_{CEHU}$ in Table A4).

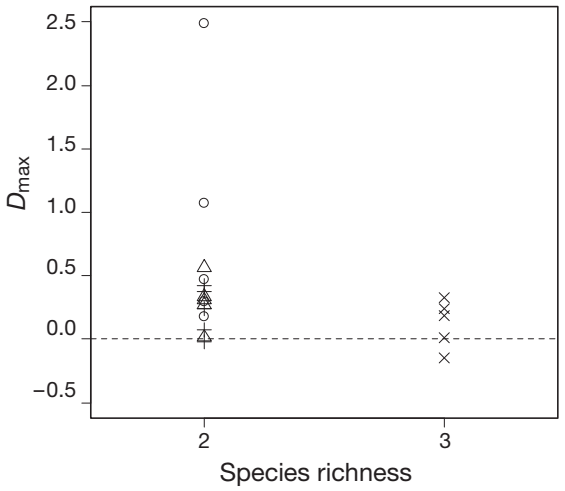

Fig. 5. Observed yield (D_{max}, see Eq. 3) in bioturbation intensity (D_b) relative to monocultures as a function of species richness. Overyielding determines whether a species mixture outperforms the best single species treatment for those species contained in that mixture and is distinguished when $D_{max} > 0$. The species composition of each mixture is indicated by plot symbols (○: CEHU; △: CEHD; +: HDHU; ×: CEHDHU). HD: *Hediste diversicolor*; CE: *Cerastoderma edule*; HU: *Hydrobia ulvae*

Overyielding

Bioturbation intensity in the majority (90%, n = 20) of the species mixtures showed evidence of overyielding ($D_{max} > 0$; Fig. 5), but the degree of overyielding (D_{max}, mean ± SD) reduced with increasing species richness (SR_2, 0.47 ± 0.62, n = 15; SR_3, 0.12 ± 0.19, n = 5). The variability in D_{max} was lower in the 3-species mixtures (range = 0.47, n = 5) relative to the 2-species mixtures (range = 2.51, n = 20), although there were 2 influential points within the $SPID_{CEHU}$ treatment that overemphasised this trend (when removed, range = 0.59, n = 18). Clear effects of species identity underpin the variability in overyielding, with the presence of *Cerastoderma edule* and *Hediste diversicolor* leading to elevated levels of bioturbation intensity.

Linking ecosystem process to ecosystem function

As species richness and species identity have significant effects on both nutrient generation (Ieno et al. 2006) and bioturbation intensity (present study), and as bioturbation forms the mechanistic link between the infauna and their effect on the benthic environment, it is inappropriate to simultaneously regress bioturbation intensity and species richness (or species identity) against nutrient generation, because species richness (or species identity) and bioturbation intensity are collinear. Whilst we recognise that care must be taken in inferring causality from correlation, correlations of bioturbation intensity from the present analysis with all 3 nutrients (NH_4-N, $\rho = 0.429$, $t = 2.93$, df = 38, $p = 0.0057$; NO_x-N, $\rho = -0.337$, $t = -2.21$, df = 38, $p = 0.0333$; PO_4-P, $\rho = 0.447$, $t = 3.08$, df = 38, $p = 0.0038$) previously reported in Ieno et al. (2006) suggest that the effects of biodiversity on nutrient generation are, at least partly, a function of the intensity of particulate bioturbation.

DISCUSSION

When considering the extent to which changes in biodiversity are linked to the provision of ecosystem services, it is important to distinguish between the supply of an ecosystem service (e.g. nutrient availability), the ecosystem function that contributes to that service (e.g. nutrient generation) and the mechanistic processes (e.g. bioturbation intensity) that regulate the observed level of functioning (de Groot 2006). Several studies have recently demonstrated clear effects of species richness (Emmerson et al. 2001, Marinelli & Williams 2003, Mermillod-Blondin et al. 2005, Ieno et al. 2006, Norling et al. 2007) and/or species density (Ieno et al. 2006, Rossi et al. 2008) on several measures of benthic ecosystem function, attributing such effects to inter-specific differences in sediment reworking (bioturbation intensity). Whilst the causal link between changes in biodiversity, bioturbation behaviour and nutrient generation are instinctive (e.g. Gray 1974, Rhoads 1974, Rhoads et al. 1977, Aller 1982, Rhoads & Boyer 1982, Krantzberg 1985) and have even been

implicated as being important over geological timescales (e.g. Martin et al. 2008), the present study is the first to demonstrate positive effects of species richness on the process of bioturbation rather than on ecosystem functions that are a consequence of bioturbation. These effects lead to elevated levels of bioturbation intensity relative to the best performing monocultures for the majority of multi-species treatments, although the proportion of mesocosms exhibiting overyielding declines with increasing species richness as the contributions of individual species become less prominent. The higher levels of bioturbation intensity, in turn, appear to stimulate the release of nutrients from the sediment (Ieno et al. 2006).

Although these findings support the view that nutrient generation is dependent on inter-specific differences in bioturbation intensity, the correlations between bioturbation intensity and nutrient generation were low. This implies that the relationship between ecosystem function and bioturbation is either not so straightforward or, more likely, that the consideration of only bioturbation intensity based on particle movement forms an incomplete evaluation of bioturbation effects (Mermillod-Blondin et al. 2005). Indeed, comparison of the findings from the present study with those of Ieno et al. (2006) reveal differences in the relative contribution of each species to individual response variables (nutrient generation, *Hediste diversicolor* > *Hydrobia ulvae* > *Cerastoderma edule*; bioturbation intensity, *H. diversicolor* > *C. edule* > *H. ulvae*). This observation has important implications for understanding how benthic species influence ecosystem processes, as not all species will interact with the benthic environment in the same way. For example, feeding, burrowing and tube construction tend to influence particle transport, whilst irrigation of burrow structures influences water and solute exchange, yet few studies have assessed the combined relative importance of these activities (Quintana et al. 2007). The results of Ieno et al. (2006), when combined with the present study, are consistent with those of others (e.g. Mermillod-Blondin et al. 2005). They indicate that *H. diversicolor* established deep (>7.5 cm), semi-permanent burrows, which it actively maintained and irrigated; *C. edule* mixed sediments in the upper 2 cm of sediment and actively suspension fed; whilst *H. ulvae* actively grazed the uppermost layers of the sediment–water interface. These differences in lifestyle led to dramatic variations in both particle and solute exchange between species. Whilst all species could be modelled as biodiffusors, the model fit data provided some evidence that the net effect of reworking activity may be more appropriately represented using an alternative bioturbation model when *H. diversicolor* is present. Failure to take into account such species interactions and differing lifestyle traits runs the risk of underestimating both the importance and relevance of individual species in space and in time, and the levels of biodiversity required to maintain multifunctional ecosystems (Hector & Bagchi 2007).

Despite common agreement amongst the biodiversity–function community that there is a need to address the shortcomings of an experimental methodology, little effort has been made to demonstrate and substantiate biodiversity–function relations using data from the real world. The considerable gaps that remain in our understanding of biodiversity–ecosystem functioning relations contrast markedly with our understanding of the responses of species to changes that have occurred in the geological record (e.g. Macleod 1994, Twitchett & Barras 2004, Pruss et al. 2006). The empirically derived mechanistic effects of diversity on ecosystem functioning from the present study are sufficiently general to seek correlations between diversity and function in natural systems (Stachowicz et al. 2007), including those from the palaeoecological record. The latter offers an opportunity to gain vital insights on how strong environmental forcing associated with several major extinction events caused changes in ecosystem function. In many cases, the causes and order of species extinction are well known (Twitchett & Barras 2004, Pruss et al. 2006), the nature of the ichnofabric has been documented, trace fossil preservation and morphological features are sufficient to provide an indication of species lifestyle traits (Dornbos 2006), and community composition can be reconstructed (Clapham et al. 2003, Seilacher et al. 2005). For syntheses attempting to examine biodiversity–ecosystem function relations, the difficulty of obtaining large inventories of species trait data along with suitable measures of ecosystem function is not trivial; however, it is possible to circumvent such problems. For example, trace fossil signatures can be used as surrogates for macrofaunal diversity and community structure (e.g. Widdicombe et al. 2003), and simple models can be parameterised to explore how various drivers of extinction influence infaunal activity in the absence of direct measures of bioturbation given certain circumstances (Solan et al. 2004). Informed by actual events from the palaeoecological record, this approach explicitly recognizes that species are likely to go extinct in a particular order, commensurate with the type of extinction driver and as a function of the susceptibility of each species to extinction. Using approaches such as these, it will be possible to converge current perspectives of biodiversity–ecosystem function relations with longer term evolutionary patterns (diversity gains and losses, functional shifts) that are associated with past ecological crises. In building such an evidence base, ecologists will be better able to

inform and more accurately predict what the likely consequences of future biodiversity change will be for human well-being.

Acknowledgements. We thank O. McPherson and A. Holford for assistance with fieldwork. The support and co-operation received from Forvie National Nature Reserve, Scottish Natural Heritage is gratefully acknowledged. All work was supported by NERC.

LITERATURE CITED

Aller RC (1982) The effects of macrobenthos on chemical properties of marine sediment and overlying water. In: McCall PL, Tevesz MJS (eds) Animal–sediment relations—the biogenic alteration of sediments. Top Geobiol 2:53–102

Bottjer DJ, Ausich WI (1986) Phanerozoic development of tiering in soft substrata suspension-feeding communities. Paleobiology 12:400–420

Bottjer DJ, Hagadorn JW, Dornbos SQ (2000) The Cambrian substrate revolution. GSA Today 10:1–7

Budd GE, Jensen S (2000) A critical reappraisal of the fossil record of the bilaterian phyla. Biol Rev Camb Philos Soc 75:253–295

Canfield DE, Poulton SW, Narbonne GM (2007) Late-Neoproterozoic deep-ocean oxygenation and the rise of animal life. Science 315:92–95

Cardinale BJ, Palmer MA, Collins SL (2002) Species diversity enhances ecosystem functioning through interspecific facilitation. Nature 415:426–429

Cardinale BJ, Srivastava DS, Duffy JE, Wright JP, Downing AL, Sankaran M, Jouseau C (2006) Effects of biodiversity on the functioning of trophic groups and ecosystems. Nature 443:989–992

Clapham ME, Narbonne GM (2002) Ediacaran epifaunal tiering. Geology 30:627–630

Clapham ME, Narbonne GM, Gehling JG (2003) Paleoecology of the oldest known animal communities: Ediacaran assemblages at Mistaken Point, Newfoundland. Paleobiology 29:527–544

Covich AP, Austen MC, Barlocher F, Chauvet E and others (2004) The role of biodiversity in the functioning of freshwater and marine benthic ecosystems. Bioscience 54: 767–775

Crank J (1975) The mathematics of diffusion. Oxford University Press, Oxford

de Groot R (2006) Function-analysis and valuation as a tool to assess land use conflicts in planning for sustainable, multi-functional landscapes. Landsc Urban Plan 75:175–186

Diggle PJ, Heagerty P, Liang KY, Zeger SL (2002) Analysis of longitudinal data. Oxford University Press, New York

Dornbos SQ (2006) Evolutionary palaeoecology of early epifaunal echinoderms: response to increasing bioturbation levels during the Cambrian radiation. Palaeogeogr Palaeoclimatol Palaeoecol 237:225–239

Dornbos SQ, Chen JY (2008) Community palaeoecology of the early Cambrian Maotianshan shale biota: ecological dominance of priapulid worms. Palaeogeogr Palaeoclimatol Palaeoecol 258:200–212

Dornbos SQ, Bottjer DJ, Chen JY (2005) Paleoecology of benthic metazoans in the early Cambrian Maotianshan shale biota and the middle Cambrian Burgess shale biota: evidence for the Cambrian substrate revolution. Palaeogeogr Palaeoclimatol Palaeoecol 220:47–67

Droser ML, Bottjer DJ (1988) Trends in depth and extent of bioturbation in Cambrian carbonate marine environments, western United States. Geology 16:233–236

Droser ML, Jensen S, Gehling JG (2002) Trace fossils and substrates of the terminal Proterozoic–Cambrian transition: implications for the record of early bilaterians and sediment mixing. Proc Natl Acad Sci USA 99:12572–12576

Emmerson MC, Solan M, Emes C, Paterson DM, Raffaelli D (2001) Consistent patterns and the idiosyncratic effects of biodiversity in marine ecosystems. Nature 411:73–77

François F, Gerino M, Stora G, Durbec JP, Poggiale JC (2002) Functional approach to sediment reworking by gallery-forming macrobenthic organisms: modeling and application with the polychaete *Nereis diversicolor*. Mar Ecol Prog Ser 229:127–136

Gehling JG (1999) Microbial mats in terminal Proterozoic siliciclastics: Ediacaran death masks. Palaios 14:40–57

Gray JS (1974) Animal–sediment relationships. Oceanogr Mar Biol Annu Rev 12:223–261

Halpern BS, Walbridge S, Selkoe KA, Kappel CV and others (2008) A global map of human impact on marine ecosystems. Science 319:948–952

Harper DAT (2006) The Ordovician biodiversification: setting an agenda for marine life. Palaeogeogr Palaeoclimatol Palaeoecol 232:148–166

Hector A, Bagchi R (2007) Biodiversity and ecosystem multifunctionality. Nature 448:188–191

Hooper DU, Chapin FS, Ewel JJ, Hector A and others (2005) Effects of biodiversity on ecosystem functioning: a consensus of current knowledge. Ecol Monogr 75:3–35

Huston MA (1997) Hidden treatments in ecological experiments: re-evaluating the ecosystem function of biodiversity. Oecologia 110:449–460

Ieno EN, Solan M, Batty P, Pierce GJ (2006) How biodiversity affects ecosystem functioning: roles of infaunal species richness, identity and density in the marine benthos. Mar Ecol Prog Ser 311:263–271

Jacobs DK, Lindberg DR (1998) Oxygen and evolutionary patterns in the sea: onshore/offshore trends and recent recruitment of deep-sea faunas. Proc Natl Acad Sci USA 95:9396–9401

James HF, Price JP (2008) Integration of palaeontological, historical, and geographical data on the extinction of koa-finches. Divers Distrib 14:441–451

Jenkins RJF (1992) Functional and ecological aspects of Ediacaran assemblages. In: Lipps JH, Signor PW (eds) Origin and early evolution of the Metazoa. Plenum Press, New York, p 131–176

Krantzberg G (1985) The influence of bioturbation on physical, chemical, and biological parameters in aquatic environments: A review. Environ Pollut 39:99–102

Logan GA, Hayes JM, Hieshima GB, Summons RE (1995) Terminal Proterozoic reorganisation of biogeochemical cycles. Nature 376:53–56

Loreau M (1998) Separating sampling and other effects in biodiversity experiments. Oikos 82:600–602

Loreau M, Hector A (2001) Partitioning selection and complementarity in biodiversity experiments. Nature 412:72–76

Macleod KG (1994) Bioturbation, inoceramid extinction and mid-Maastrichtian ecological change. Geology 22:139–142

Mahaut ML, Graf G (1987) A luminophore tracer technique for bioturbation studies. Oceanol Acta 10:323–328

Marinelli RL, Williams TJ (2003) Evidence for density dependent effects of infauna on sediment biogeochemistry and benthic–pelagic coupling in nearshore systems. Estuar Coast Shelf Sci 57:179–192

Martin RE (1996) Secular increase in nutrient levels through

the Phanerozoic: implications for productivity, biomass and diversity of the marine biosphere. Palaios 11:209–219
Martin RE, Quigg A, Podkovyrov V (2008) Marine biodiversification in response to evolving phytoplankton stoichiometry. Palaeogeogr Palaeoclimatol Palaeoecol 258:277–291
McIlroy D, Logan GA (1999) The impact of bioturbation on infaunal ecology and evolution during the Proterozoic–Cambrian transition. Palaios 14:58–72
Mermillod-Blondin F, François-Carcaillet F, Rosenberg R (2005) Biodiversity of benthic invertebrates and organic matter processing in shallow marine sediments: an experimental study. J Exp Mar Biol Ecol 315:187–209
Narbonne GM (2005) The Ediacara biota: Neoproterozoic origin of animals and their ecosystems. Annu Rev Earth Planet Sci 33:421–442
Norling K, Rosenberg R, Hulth S, Gremare A, Bonsdorff E (2007) Importance of functional biodiversity and species-specific traits of benthic fauna for ecosystem functions in marine sediment. Mar Ecol Prog Ser 332:11–23
Pearson TH, Rosenberg R (1978) Macrobenthic succession in relation to organic enrichment and pollution of the marine environment. Oceanogr Mar Biol Annu Rev 16:229–311
Pinheiro JC, Bates DM (2000) Mixed-effects models in S and S-plus. Springer, Heidelberg
Pinheiro J, Bates D, DebRoy S, Sarkar D (2006) nlme: An R package for fitting and comparing Gaussian linear and nonlinear mixed-effects models. Available at www.stats.bris.ac.uk/R/
Pruss SB, Bottjer DJ, Corsetti FA, Baud A (2006) A global marine sedimentary response to the end-Permian mass extinction: examples from southern Turkey and the western United States. Earth Sci Rev 78:193–206
Quinn QP, Keough MJ (2002) Experimental design and data analysis for biologists. Cambridge University Press, Cambridge
Quintana CO, Tang M, Kristensen E (2007) Simultaneous study of particle reworking, irrigation transport and reaction rates in sediment bioturbated by the polychaetes *Heteromastus* and *Marenzelleria.* J Exp Mar Biol Ecol 352:392–406
Raffaelli D, Emmerson M, Solan M, Biles C, Paterson D (2003) Biodiversity and ecosystem functioning in shallow coastal waters: an experimental approach. J Sea Res 49:133–141
R Development Core Team (2005) R: a language and environment for statistical computing. R Foundation for Statistical Computing, Vienna. Available at www.R-project.org
Rhoads DC (1974) Organism–sediment relations on the muddy sea floor. Oceanogr Mar Biol Annu Rev 12: 263–300
Rhoads DC, Boyer LF (1982) The effects of marine benthos on physical properties of sediments. A successional perspective. In: Mc Call PL, Tevesz MJS (eds) Animal–sediment relations—the biogenic alteration of sediments. Top Geobiol 2:3–52
Rhoads DC, Aller RC, Goldhaber MB (1977) The influence of colonising benthos on physical properties and chemical diagenesis of the estuarine seafloor. In: Coull BC (ed) Ecology of marine benthos. Belle W Baruch Libr Mar Sci 6: 113–138
Rhoads DC, McCall PL, Yingst JY (1978) Disturbance and production on the estuarine seafloor. Am Sci 66:577–586
Rossi F, Gribsholt B, Middelburg JJ, Heip C (2008) Context-dependent effects of suspension feeding on intertidal ecosystem functioning. Mar Ecol Prog Ser 354:47–57
Rumohr H, Bonsdorff E, Pearson TH (1996) Zoobenthic succession in Baltic sedimentary habitats. Arch Fish Mar Res 44:179–214
Sala OE, Chapin FS, Armesto JJ, Berlow E and others (2000) Biodiversity—global biodiversity scenarios for the year 2100. Science 287:1770–1774
Seilacher A (1999) Biomat-related lifestyles in the Precambrian. Palaios 14:86–93
Seilacher A, Pflüger F (1994) From biomats to benthic agriculture: a biohistoric revolution. In: Krumbein WE (ed) Biostabiliation of sediments. Bibliothek und Informationsystem der Carl von Ossietky Universität, Oldenburg, p 97–105
Seilacher A, Buatois LA, Mangano MG (2005) Trace fossils in the Ediacaran–Cambrian transition: behavioural diversification, ecological turnover and environmental shift. Palaeogeogr Palaeoclimatol Palaeoecol 227:323–356
Solan M, Cardinale BJ, Downing AL, Engelhardt KAM, Ruesink JL, Srivastava DS (2004) Extinction and ecosystem function in the marine benthos. Science 306: 1177–1180
Stachowicz JJ, Bruno JF, Duffy JE (2007) Understanding the effects of marine biodiversity on communities and ecosystems. Annu Rev Ecol Evol Syst 38:739–766
Thayer CW (1983) Sediment-mediated biological disturbance and the evolution of marine benthos. In: Tevesz MJS, McCall PL (eds) Biotic interactions in recent and fossil benthic communities. Plenum Press, New York, p 479–625
Twitchett RJ, Barras CG (2004) Trace fossils in the aftermath of mass extinction events. In: McIlroy D (ed) The application of ichnology to palaeoenvironmental and stratigraphic analysis. Special Publication 228, Geological Society, London, p 397–418
Valentine JW (1994) Late Precambrian bilaterians: grades and clades. Proc Natl Acad Sci USA 91:6751–6757
Vannier J, Steiner M, Renvoise E, Hu SX, Casanova JP (2007) Early Cambrian origin of modern food webs: evidence from predator arrow worms. Proc R Soc Lond B Biol Sci 274:627–633
Verbeke G, Molenberghs G (2000) Linear mixed models for longitudinal data. Springer-Verlag, New York
West BT, Welch KB, Galecki AT (2007) Linear mixed models: a practical guide using statistical software. Chapman and Hall/CRC, London
Widdicombe S, Kendall MA, Parry DM (2003) Using the surface-features created by bioturbating organisms as surrogates for macrofaunal diversity and community structure. Vie Milieu 53:179–186
Worm B, Barbier EB, Beaumont N, Duffy JE and others (2006) Impacts of biodiversity loss on ecosystem services. Science 314:787–790
Wray GA, Levinton JS, Shapiro LH (1996) Molecular evidence for deep Precambrian divergences among metazoan phyla. Science 274:568–573

Appendix 1. Summary of the statistical analyses for our 4 GLS models (Models A1 to A4). For each model, we list the initial linear regression model, the minimal adequate linear regression model with GLS estimation, and a summary of the coefficient table. The coefficients indicate the relative performance of each treatment level relative to the relevelled baseline (first column of each table)

Model 1. Form of the initial linear regression model (Eq. A1) and the minimal adequate linear regression model with generalised least-squares (GLS) estimation (incorporating species richness as a variance covariate) (Eq. A2) for the effects of species richness (SR) on D_b.

$$D_b \sim \text{as.factor(SR)} \quad \text{(A1)}$$

$$D_b \sim \text{as.factor(SR)}, \text{weights} = \text{varIdent[form} = \sim 1|\text{as.factor(SR)}], \text{method} = \text{'ML'} \quad \text{(A2)}$$

Table A1. Coefficient table for Model 1. Intercept ± SE (when baseline = Cntrl): 1.574187 ± 0.1771883, t = 8.884258, p < 0.0001. Coefficients ± SE and t-values are presented. Significance values are in parentheses

	SR_0	SR_1	SR_2	SR_3
SR_0	–	2.02394 ± 0.351699 5.754744 (<0.0001)	3.49952 ± 0.415631 8.419761 (<0.0001)	3.028525 ± 0.389231 7.780786 (<0.0001)
SR_1	−2.02394 ± 0.351699 −5.754744 (<0.0001)	–	1.475577 ± 0.483374 3.052662 (0.0042)	1.004586 ± 0.460871 2.179756 (0.0359)
SR_2	−3.49952 ± 0.415631 −8.419761 (<0.0001)	−1.47558 ± 0.483374 −3.052662 (0.0042)	–	−0.470991 ± 0.511331 −0.921109 (0.3631)
SR_3	−3.02853 ± 0.389231 −7.780786 (<0.0001)	−1.00459 ± 0.460871 −2.179756 (0.0359)	0.47099 ± 0.511331 0.921109 (0.3631)	–

Model 2. Form of the initial linear regression model (Eq. A3) and the minimal adequate linear regression model with GLS estimation (incorporating species richness as a variance–covariate) (Eq. A4) for the effects of species richness (SR) on the fit of the D_b model to the observed luminophore profile.

$$\text{Fit} \sim \text{as.factor(SR)} \quad \text{(A3)}$$

$$\text{Fit} \sim \text{as.factor(SR)}, \text{weights} = \text{varIdent[form} = \sim 1|\text{as.factor(SR)}], \text{method} = \text{'ML'} \quad \text{(A4)}$$

Table A2. Coefficient table for Model 2. Intercept ± SE (when baseline = Cntrl): 0.000472 ± 0.000103, t = 4.582764, p < 0.0001. Coefficients ± SE and t-values are presented. Significance values are in parentheses

	SR_0	SR_1	SR_2	SR_3
SR_0	–	0.001784 ± 0.000863 2.065994 (<0.0461)	0.004023 ± 0.001573 2.557451 (0.0149)	0.003421 ± 0.001201 2.848089 (0.0072)
SR_1	−0.001784 ± 0.000863 −2.065994 (0.0461)	–	0.002239 ± 0.001789 1.251834 (0.2187)	0.001637 ± 0.001472 1.111813 (0.2736)
SR_2	−0.004023 ± 0.001573 −2.5574515 (0.0149)	−0.002239 ± 0.001789 −1.2518343 (0.2187)	–	−0.000602 ± 0.001974 −0.3051636 (0.762)
SR_3	−0.003421 ± 0.001201 −2.848089 (0.0072)	−0.001637 ± 0.001472 −1.111813 (0.2736)	0.000602 ± 0.001974 0.305164 (0.762)	–

Model 3. Form of the initial linear regression model (Eq. A5) and the minimal adequate linear regression model with GLS estimation (incorporating species identity as a variance covariate) (Eq. A6) for the effects of species identity (SPID) on D_b.

$$D_b \sim \text{as.factor(SPID)} \quad \text{(A5)}$$

$$D_b \sim \text{as.factor(SPID), weights = varIdent[form = } \sim 1|\text{as.factor(SPID)], method = 'ML'} \quad \text{(A6)}$$

Table A3. Coefficient table for Model 3. Intercept ± SE (when baseline = Cntrl): 1.574187 ± 0.1771883, t = 8.884258, p < 0.0001. Coefficients ± SE and t-values are presented. Significance values are in parentheses

	$SPID_0$	$SPID_{HD}$	$SPID_{CE}$	$SPID_{HU}$	$SPID_{CEHU}$	$SPID_{CEHD}$	$SPID_{HDHU}$	$SPID_{CEHDHU}$
$SPID_0$	–	3.155 ± 0.437 7.215 (<0.0001)	1.875 ± 0.423 4.436049 (<0.0001)	1.042 ± 0.356 2.924789 (0.0063)	3.330 ± 1.113 2.990346 (0.0053)	3.751 ± 0.401 9.34410 (<0.0001)	3.418 ± 0.391 8.744099 (<0.0001)	3.029 ± 0.389 7.780786 (<0.0001)
$SPID_{HD}$	−3.155 ± 0.437 −7.214680 (< 0.0001)	–	−1.280 ± 0.554 −2.309957 (0.0275)	−2.113 ± 0.505 −4.182115 (0.0002)	0.175 ± 1.170 0.149210 (0.8823)	0.596 ± 0.538 1.107648 (0.2763)	0.263 ± 0.530 0.495589 (0.6236)	−0.127 ± 0.529 −0.239115 (0.8125)
$SPID_{CE}$	−1.875 ± 0.423 −4.436049 (<0.0001)	1.280 ± 0.554 2.309957 (0.0275)	–	−0.833 ± 0.493 −1.691033 (0.1005)	1.455 ± 1.164 1.249343 (0.2206)	1.876 ± 0.526 3.564703 (0.0012)	1.543 ± 0.518 2.976835 (0.0055)	1.154 ± 0.517 2.230999 (0.0328)
$SPID_{HU}$	−1.042 ± 0.356 −2.924789 (0.0063)	2.113 ± 0.505 4.182115 (0.0002)	0.833 ± 0.493 1.691033 (0.1005)	–	2.288 ± 1.142 2.003537 (0.0536)	2.709 ± 0.475 5.708600 (<0.0001)	2.376 ± 0.466 5.102120 (<0.0001)	1.987 ± 0.464 4.278772 (0.0002)
$SPID_{CEHU}$	−3.330 ± 1.113 −2.990346 (0.0053)	−0.175 ± 1.170 −0.149210 (0.8823)	−1.455 ± 1.164 −1.249343 (0.2206)	−2.288 ± 1.142 −2.003537 (0.0536)	–	0.422 ± 1.157 0.364418 (0.7179)	0.088 ± 1.153 0.076561 (0.9394)	−0.301 ± 1.153 −0.261192 (0.7956)
$SPID_{CEHD}$	−3.751 ± 0.401 −9.344109 (<0.0001)	−0.596 ± 0.538 −1.107648 (0.2763)	−1.876 ± 0.526 −3.564703 (0.0012)	−2.709 ± 0.475 −5.708600 (< 0.0001)	−0.422 ±1.157 −0.364418 (0.7179)	–	−0.333 ± 0.501 −0.664998 (0.5108)	−0.723 ± 0.500 −1.445578 (0.1580)
$SPID_{HDHU}$	−3.418 ± 0.391 −8.744099 (<0.0001)	−0.263 ± 0.530 −0.495589 (0.6236)	−1.543 ± 0.518 −2.976835 (0.0055)	−2.376 ± 0.466 −5.102120 (0.0001)	−0.089 ± 1.153 −0.076561 (0.9394)	0.333 ± 0.501 0.664998 (0.5108)	–	−0.389 ± 0.491 −0.792261 0.4340
$SPID_{CEHDHU}$	−3.029 ± 0.389 −7.780786 (<0.0001)	0.127 ± 0.529 0.239115 (0.8125)	−1.154 ± 0.517 −2.230999 (0.0328)	−1.987 ± 0.464 −4.278772 (0.0002)	0.301 ± 1.153 0.261192 (0.7956)	0.723 ± 0.500 1.445578 (0.1580)	0.389 ± 0.491 0.792261 (0.4340)	–

Model 4. Form of the initial linear regression model (Eq. A7) and the minimal adequate linear regression model with GLS estimation (incorporating species identity as a variance covariate) (Eq. A8) for the effects of species identity (SPID) on the fit of the D_b model to the observed luminophore profile.

Fit ~ as.factor(SPID) (A7)

Fit ~ as.factor(SPID), weights = varIdent[form = ~ 1|as.factor(SPID)], method = 'ML' (A8)

Table A4. Coefficient table for Model 4. Intercept ± SE (when baseline = Cntrl): $0.472 \times 10^{-4} \pm 0.103 \times 10^{-4}$, t = 4.582664, p < 0.0001. [a]Coefficients ± SE ($\times 10^{-4}$); t-values and significance values (in parentheses) are also presented

	$SPID_0$	$SPID_{HD}$	$SPID_{CE}$	$SPID_{HU}$	$SPID_{CEHU}$	$SPID_{CEHD}$	$SPID_{HDHU}$	$SPID_{CEHDHU}$
$SPID_0$	–	5.799 ± 1.239[a] 4.678804 (<0.0001)	−0.092 ± 0.368[a] −0.249746 (0.8044)	−0.355 ± 0.153[a] −2.323676 (0.0267)	−0.08 ± 0.294[a] −0.273502 (0.7862)	8.356 ± 3.852[a] 2.169415 (0.0376)	3.793 ± 1.436[a] 2.640891 (0.0127)	3.421 ± 1.201[a] 2.848068 (0.0076)
$SPID_{HD}$	−5.799 ± 1.239[a] −4.678804 (<0.0001)	–	−5.891 ± 1.285[a] −4.585449 (<0.0001)	−6.155 ± 1.24[a] −4.961955 (<0.0001)	−5.88 ± 1.266[a] −4.646012 (<0.0001)	2.557 ± 4.044[a] 0.63229 (0.5317)	−2.006 ± 1.892[a] −1.060448 (0.2969)	−2.379 ± 1.72[a] −1.383109 (0.1762)
$SPID_{CE}$	0.092 ± 0.368[a] 0.249746 (0.8044)	5.891 ± 1.285[a] 4.585449 (<0.0001)	–	−0.263 ± 0.371[a] −0.709835 (0.4829)	0.012 ± 0.448[a] 0.025674 (0.9797)	8.448 ± 3.866[a] 2.184883 (0.0363)	3.885 ± 1.476[a] 2.632941 (0.0129)	3.513 ± 1.248[a] 2.815198 (0.0083)
$SPID_{HU}$	0.355 ± 0.153[a] 2.323676 (0.0267)	6.155 ± 1.24[a] 4.961955 (<0.0001)	0.263 ± 0.371[a] 0.709835 (0.4829)	–	0.275 ± 0.298[a] 0.92321 (0.3628)	8.711 ± 3.852[a] 2.261501 (0.0307)	4.149 ± 1.437[a] 2.886744 (0.0069)	3.776 ± 1.202[a] 3.141542 (0.0036)
$SPID_{CEHU}$	0.08 ± 0.294[a] 0.273502 (0.7862)	5.88 ± 1.266[a] 4.646012 (<0.0001)	−0.012 ± 0.448[a] −0.025674 (0.9797)	−0.275 ± 0.298[a] −0.92321 (0.3628)	–	8.436 ± 3.86[a] 2.185494 (0.0363)	3.874 ± 1.459[a] 2.655206 (0.0122)	3.501 ± 1.228[a] 2.851232 (0.0076)
$SPID_{CEHD}$	−8.356 ± 3.852[a] −2.1694153 (0.0376)	−2.557 ± 4.044[a] −0.6322899 (0.5317)	−8.448 ± 3.866[a] −2.1848828 (0.0363)	−8.711 ± 3.852[a] −2.2615008 (0.0307)	−8.436 ± 3.86[a] −2.1854938 (0.0363)	–	−4.563 ± 4.108[a] −1.1106207 (0.275)	−4.935 ± 4.032[a] −1.2240458 (0.2299)
$SPID_{HDHU}$	−3.793 ± 1.436[a] −2.6408909 (0.0127)	2.006 ± 1.892[a] 1.0604481 (0.2969)	−3.885 ± 1.476[a] −2.6329414 (0.0129)	−4.149 ± 1.437[a] −2.8867439 (0.0069)	−3.874 ± 1.459[a] −2.6552064 (0.0122)	4.563 ± 4.108[a] 1.1106207 (0.275)	–	−0.373 ± 1.867[a] −0.1996348 (0.843)
$SPID_{CEHDHU}$	−3.421 ± 1.201[a] −2.848068 (0.0076)	2.379 ± 1.72[a] 1.383109 (0.1762)	−3.513 ± 1.248[a] −2.815198 (0.0083)	−3.776 ± 1.202[a] −3.141542 (0.0036)	−3.501 ± 1.228[a] −2.851232 (0.0076)	4.935 ± 4.032[a] 1.224046 (0.2299)	0.373 ± 1.867[a] 0.199635 (0.843)	–

Submitted: January 7, 2008; Accepted: May 29, 2008
Proofs received from author(s): June 17, 2008